UNIVERSITY OF LIVERPOOL

Bacteria-induced Wnt signalling as a mechanism for malignant development in the intestinal epithelium

Thesis submitted in accordance with the requirements of the University of Liverpool for the degree of Doctor in Philosophy

By

Bradley Meehan

June 2017

Declaration

I hereby declare that this thesis is a presentation of my original work. Wherever contributions of others are involved, every effort has been made to indicate this clearly, with due reference to the literature.

Work was performed under the guidance of project supervisors Professor Barry J Campbell[1], Professor Jonathan M Rhodes[1] and Professor Craig Winstanley[2].

[1] Gastroenterology Research Unit, Department of Cellular and Molecular Physiology, Institute of Translational Medicine, University of Liverpool

[2] Clinical Infection, Microbiology and Immunology, Institute of Infection and Global Health, University of Liverpool

Acknowledgements

I would like to express my gratitude to Professor Barry Campbell for his continuous guidance and encouragement throughout my PhD, and would like to say a big thank you to Professor Jonathan Rhodes and Professor Craig Winstanley for their additional support. It has been an absolute pleasure working with you and I have learnt a lot from each of you. I would also like to thank North West Cancer Research. Without their funding, this project would not have been possible.

I would like to extend my thanks to Dr Janelle Arthur, Dr John Jenkins and Dr Carrie Duckworth for providing me with various mouse tissues that were used throughout my *in vivo* work. I would like to thank Professor Julian Marchesi and Dr Matthew Bull for helping with the fosmid sequencing required for this project. I would also like to thank Professor Chris Paraskeva for providing the AA/C1 and AA/C1/SB cell lines.

Additionally, I'd like to say a big thank you to everyone in the Gastroenterology Research Unit, past and present, for their support and friendship throughout my time in the lab. In particular, I would like to thank Professor Barry Campbell and Dr Carrie Duckworth for their support through all aspects of my lab work. Stephanie and Cleberson - thank you for being so obliging during my *in vivo* work, and for making my time in the lab and the office so enjoyable.

To my friends, I'd like to thank you for your sarcastic version of encouragement and for taking my mind away from work whenever necessary. To my hugely supportive family, I'd like thank you for everything you have done for me, both during my studies and over the many years before that to get me to this stage. I wouldn’t have got here without you.

Last but not least, thank you to Victoria. I don't think words are enough to describe how much I appreciate everything you've done for me over the last few years. I can only hope that our many travelling adventures in the years to come are enough to repay you.

Abstract

Colorectal cancer (CRC) is one of the most common cancers worldwide with over a million new cases each year, and evidence implicates chronic inflammation as a risk factor for developing CRC. Inflammatory conditions place stresses on bacteria composing the human gut microbiota and alter the composition of the gut microbiota in favour of pathobiont *Escherichia coli* (*E. coli*), with resultant expansion of these bacteria increasing their interactions with the gut mucosa. Mucosa-associated *E. coli* have been found in high numbers within intestinal tissue taken from IBD and CRC patients.

Pro-inflammatory cytokines such as cyclooxygenase-2 (COX-2) are commonly implicated in inflammatory disease, and can be released upon tissue damage or following infection. COX-2-driven prostaglandin E_2 (PGE_2) increases are believed to activate the cancer-related Wnt signalling pathway, with accumulation and subsequent nuclear translocation of the key Wnt protein β-catenin aiding proliferation, migration and metastasis. With COX-2 implicated in CRC development and progression and a cascade for COX-2 and PGE_2 stimulating cancer cell growth via Wnt activation, mucosa-associated *E. coli* infection could lead to sustained increases in Wnt signalling. In addition, as mucosa-associated *E. coli* strains isolated from CRC patients can survive and replicate within human macrophages and increase COX-2 and PGE_2 secretion, this could enhance their tumourigenic effects.

The aim of this project was to characterise the effects of mucosa-associated *E. coli* isolates from CRC and IBD patients on the activation of the Wnt signalling pathway both *in vitro* and *in vivo*. We first used CRC cell lines and human macrophage cells to assess the effects of mucosa-associated *E. coli* infections. We show consistent increases in total and nuclear localised β-catenin at both the gene and protein level *in vitro*, and have shown that this correlates with increased COX-2 gene and protein levels. Downstream Wnt transcription was shown following infection, and this was inhibited by the addition of a COX-2 inhibitor. We also showed increased release of PGE_2 from macrophages infected with mucosa-associated *E. coli*, which could be a contributing factor in driving the Wnt response in neighbouring intestinal epithelial cells. To investigate these effects *in vivo*, we used colonic tissue from

a germ-free *Il10*$^{-/-}$ mouse model of CRC mucosa-associated *E. coli* infection to determine COX-2 and Wnt pathway activation. Following mono-association of germ-free *Il10*$^{-/-}$ mice with a CRC mucosa-associated *E. coli* isolate, significant increases in COX-2 and β-catenin protein expression and increased levels of β-catenin nuclear localisation were observed.

To further investigate changes in COX-2 and Wnt signalling, we used a fosmid library of 968 clones created from the fragmented DNA of another mucosa-associated *E. coli* isolate from a CRC patient to confirm up-regulation of COX-2 gene expression following infection of CRC cells with fosmid clones. We identified 12 fosmid clones showing confirmed COX-2 gene expression increases, and sequenced the DNA content of all 12 fosmid clones to find common genes or operons that may be contributing towards these expression changes. Sequencing showed similarities in DNA content, with particularly common homology in two fosmids containing genes involved in growth and survival, particularly in high-stress inflammatory conditions. This data may aid identification of genes or operons that contribute to the induction of COX-2 and Wnt signalling observed *in vitro* and *in vivo*.

We were also able to develop a 3D organotypic cell culture using a series of colorectal cell lines at different key stages of malignant transformation in the adenoma-carcinoma pathway. Successful 3D aggregate cultures were achieved, and data obtained from infecting these aggregates would suggest that this method of culture is suitable for studying mucosa-associated *E. coli*-host epithelium interactions, and confirmed data previously obtained by infection of 2D monolayer CRC cell cultures and those responses seen in an *in vivo* gut infection model.

Our study supports the hypothesis that mucosa-associated *E. coli* isolates from CRC and IBD patients can activate the Wnt signalling pathway both *in vitro* and *in vivo*, and provides further evidence towards mucosa-associated *E. coli* isolates upregulating pro-inflammatory COX-2 and PGE_2 release in the gut. This suggests translational effects that might be seen in patients, which indicates a role for mucosa-associated *E. coli*, in the development and progression of colorectal cancer via increased Wnt signalling.

Publications

Papers

In preparation. Meehan B, Rhodes JM & Campbell BJ. Mucosa-associated *E. coli* isolates induce increased cyclooxygenase-2 and Wnt signalling.

Reviews

In preparation. Meehan B & Campbell BJ. Mucosa-associated *E. coli*, inflammation and colorectal cancer: possibilities for therapy.

Abstracts

Meehan B, Winstanley C & Campbell BJ. Investigating bacteria-induced Wnt signalling as a mechanism for malignant development in the colon. Northwest Microbiology 2014, Manchester.

Meehan B, Campbell BJ & Rhodes JM. *Adherent, invasive mucosa-associated E. coli isolates from colorectal cancer patients activate WNT signalling. Gut* 2015*; 64:Suppl 1; A362-A363 (abstract).* DDF 2015, London.

Talks

Meehan B, Campbell BJ & Rhodes JM. Mucosa-associated *E. coli* isolates from inflammatory bowel disease and colorectal cancer patients activate Wnt/beta-catenin signalling *in vitro* and *in vivo*. *Gut* 2016; 65:Suppl 1. doi:10.1136/gutjnl-2016-312388.44. BSG 2016, Liverpool.

Public Engagement Articles

Meehan B. What you can do to reduce the risk of bowel cancer caused by *E. coli* bacteria. The Conversation. June 8, 2016. https://theconversation.com/what-you-can-do-to-reduce-the-risk-of-bowel-cancer-caused-by-e-coli-bacteria-60264.

Abbreviations

2D	Two-dimensional
3D	Three-dimensional
5-FU	5-fluorouracil
Afa	afimbrial adhesin
AIEC	Adherent invasive *E. coli*
AMP	Antimicrobial peptide
ANOVA	Analysis of variance
APC	Adenomatous polyposis coli
ATCC	American Type Culture Collection
BSA	Bovine serum albumin
CD	Crohn's disease
CEACAM	Carcinoembryonic antigen-related cell adhesion molecule
CFU	Colony forming units
CNF	Cytotoxic necrotising factor
COX	Cyclooxygenase
CRC	Colorectal cancer
DAB	Diaminobenzidine
DAPI	4',6-diamidino-2-phenylindole
DEAC	Diffusely adherent *E. coli*
DMEM	Dulbecco's Modified Eagle's Medium
DNA	Deoxyribonucleic acid
DPX	Distyrene, plasticiser, xylene
DSS	Dextran sulphate sodium
DTT	Dithiothreitol
ECACC	European Collection of Authenticated Cell Cultures

ECM	Extracellular matrix
EDTA	Ethylenediaminetetraacetic acid
EGFR	Epidermal growth factor receptor
ELISA	Enzyme-linked immuno-sorbent assay
EPEC	Enteropathogenic *E. coli*
ETBF	Enterotoxigenic *B. fragilis*
ETEC	Enterotoxigenic *E. coli*
FAP	Familial adenomatous polyposis
FBS	Foetal bovine serum
FDA	Food and Drug Administration
FITC	Fluorescein isothiocyanate
GSK	Glycogen synthase kinase
HNPCC	Hereditary nonpolyposis colorectal cancer
HRP	Horseradish peroxidase
IBD	Inflammatory bowel disease
IHC	Immunohistochemistry
IL	Interleukin
ILC	Innate lymphoid cell
Ig	Immunoglobulin
KRAS	V-Ki-ras2 Kirsten rat sarcoma viral oncogene
LB	Luria Burtani
LEF	Lymphoid enhancer-binding factor
LiCl	Lithium chloride
LPS	Lipopolysaccharide
LRP	Lipoprotein receptor-related protein
LV	Leucovorin
MAPK	Mitogen-activated protein kinase

M-cell	Microfold cell
MCS	Multicellular spheroid
Meso-DAP	Meso-diaminopimelic acid
MOI	Multiplicity of infection
MUC	Mucin glycoprotein
MVD	Microvessel density
NF-κβ	Nuclear factor kappa β
NOD	nucleotide-binding oligomerisation domain–containing protein
NSAID	Non-steroidal anti-inflammatory drug
NSCLC	Non-small cell lung cancer
NSP	Non-starch polysaccharide
OD	Optical density
PBS	Phosphate-buffered saline
PFA	Paraformaldehyde
PFGE	Pulsed-field gel electrophoresis
PG	Prostaglandin
PI3K	Phosphoinositide 3-kinase
PMA	Phorbol myristate acetate
RCCS	Rotary cell culture system
RIPA	Radio-immunoprecipitation assay
RNA	Ribonucleic acid
Spp.	Species
SUMO	Small ubiquitin-like modifier
TCF	T cell factor
TLR	Toll-like receptor
TNF	Tumour necrosis factor
TP53	Tumour protein 53

UC	Ulcerative colitis
VEGF	Vascular endothelial growth factor

Contents

List of Figures

List of Tables

Chapter 1:

Introduction

1.1 Introduction to colorectal cancer

Colorectal cancer (CRC) is one of the most common cancers worldwide with over a million new cases each year. Incidence rates differ geographically, with the lowest rates in less developed regions such as Africa and Central America, with the highest in more developed regions such as Australasia, Europe and North America (Gellad and Provenzale, 2010). CRC contributes to approximately 600,000 deaths worldwide each year, making it the fourth most common cause of death from cancer (Ferlay *et al*., 2010), with more than 1.1 million deaths per year expected by 2030 (Arnold *et al*., 2017).

The majority of CRC cases are now known to originate from colonic polyps, masses of hyper-proliferating epithelial cells lining the colon, before progressing into carcinomas (Williams *et al*., 2013). Adenomatous polyps account for half of all colorectal polyps, with the amount and size of polyps present being indicators of increased risk of development of CRC (Williams *et al*., 2013). Some new cases occur in those with a family history of CRC – previous adenomatous polyps or CRC, or inflammatory bowel disease (IBD) that predisposes to CRC (Winawer *et al*., 1997, Fearon, 1995), but at least 70% of all new CRC cases occur with no known predisposing factors, known as sporadic CRC.

Familial adenomatous polyposis (FAP) and hereditary nonpolyposis colorectal cancer (HNPCC) account for the majority of highly penetrant, high-risk hereditary cases. FAP is attributed to *APC* gene mutations, associated with abnormal proliferative Wnt signalling, causing individuals to develop adenomatous polyps throughout the colon. These individuals have an almost 100% chance of developing colorectal cancer (Dunlop *et al*., 2002). HNPCC is a disorder caused by mutations of DNA mismatch repair (MMR) genes causing abnormal functioning, which increases both the risk and penetrance of CRC (Balmana *et al*., 2013). Colectomy is recommended as a form of prophylaxis for those considered high risk for CRC, but this leaves the rectum intact with patients at an increased risk for rectal cancer development (Van Cutsem *et al*., 2009b), so adjuvant therapies are required.

With between 70% and 95% of CRC cases being sporadic – occurring with no known predisposing factors – the approach to chemoprevention and treatment becomes much more convoluted (Butler

and Roberts-Thomson, 2004). Sporadic CRC can involve a number of different genetic alterations caused by mutations and epigenetic changes (Dubois, 2014). The classic examples of genetic alteration are mutations of the *KRAS* oncogene at the early adenoma stage leading to increased MAPK signalling, *p53* tumour suppressor mutations shown to facilitate malignancy, and again mutations of the *APC* gene as an initiating event. *APC* mutations are common to both hereditary and sporadic forms of CRC, causing deregulated Wnt signalling, highlighting a common link.

Due to a lack of known predisposing factors in sporadic cases they are currently treated similar to hereditary cases, where colectomy can be used as a prophylactic or resection treatment followed by suppression of secondary sites using adjuvant therapy. With sporadic forms of CRC accounting for the majority of cases, a lot of effort is going into understanding the molecular events sustaining it as well as the relatively recent implications of chronic inflammation.

Chronic inflammation is a risk factor for developing CRC, with inflammatory bowel diseases (IBD), ulcerative colitis and Crohn's disease, associated with an increased risk of CRC (Renz *et al*., 2013, Eaden *et al*., 2001, Ohman, 1982, Jess *et al*., 2005). The risk associated with IBD is thought to be genetically acquired, but IBD-associated cancers differ from sporadic and hereditary cases in that they typically arise due to lack of proper differentiation of epithelial cells from a flat mucosa (Rhodes and Campbell, 2002). Both *APC* and *p53* mutations are present in both IBD-associated and sporadic CRC cases at different stages of CRC progression, suggesting biological features of IBD-associated and sporadic CRC overlap (see **Figure 1.3**). Altered Wnt signalling due to *APC* mutations occurs late in the sequence from dysplasia to cancer. The genetic alterations seen in common sporadic and IBD-associated CRC cases are widely similar, but these changes have been shown to occur at different stages of carcinogenesis (Rhodes and Campbell, 2002).

1.2 Staging and treatment of colorectal cancer

Current clinically recommended treatments for CRC focus on preventing the hyper-proliferation of intestinal epithelial cells. Advances in the treatment of primary CRC have significantly reduced CRC-

related deaths, and advances in the treatment of advanced and metastatic CRC has significantly improved disease-free survival (Winawer *et al*., 2003, Recondo *et al*., 2014). However, the lack of distinction between treatment of patients at high risk due to hereditary disease, sporadic cases linked to genetic abnormalities and patients at increased risk associated with inflammatory bowel disease (IBD) is concerning. The next step forward for adjuvant therapy for CRC is treatment focussed on smaller patient groups and individualised therapies using a more translational approach, where diagnosis and treatment regimens take into account novel molecular staging as well as traditional pathological and clinical staging.

Current clinical guidelines for CRC treatment are based on associated risk stratification and the effectiveness of current screening techniques (Winawer *et al*., 2003), including colonoscopy, faecal occult blood testing, rectal examination, sigmoidoscopy, barium enemas, virtual colonoscopy and stool DNA. Surveillance guidelines for high-risk patients are also in place aiming to reduce the number of new and recurring CRC cases, with regular colonoscopy being performed in order to identify CRC and any metastases as early as possible (Eaden *et al*., 2002, Newcomb *et al*., 1992, Winawer *et al*., 1997). Diagnosis of colonic adenocarcinoma currently requires confirmation using histopathology of tissue samples taken via colonoscopy/sigmoidoscopy (Van Cutsem *et al*., 2009b). It is also recommended that risk factors including hereditary predisposition and biopsy location should be documented and considered when deciding on treatment (Siriwardana *et al*., 2009). Staging of CRC is done according to the TNM system along with the Dukes' stage using a number of techniques including clinical examination, blood counts, liver and renal function tests, X-ray and CT-scans of the chest, abdomen and pelvis and a colonoscopy of the entire colon (Van Cutsem *et al*., 2009b).

Survival rates for CRC have been steadily increasing, with estimates from the US National Cancer database showing 5-year survival rates of 63.9–93.2% depending on stage of progression (Van Cutsem *et al*., 2009b). Colonoscopy alone is now believed to lower mortality rates due to colorectal cancer by as much as 40% (Bertagnolli *et al*., 2006), and our understanding of the underlying molecular biology of CRC is leading to the development of novel and better-targeted therapies.

Colectomy remains the most effective way of managing CRC, where a wide resection removes the primary tumour site along with any localised lymph nodes (Van Cutsem *et al*., 2009b). Following surgery, adjuvant therapy is dependent on the staging of cancers and treatments have been steadily improving. For more than 40 years, the drug 5-fluorouracil (5-FU) was used to target cell division in hyper-proliferative cells in the treatment of both metastatic and adjuvant colorectal cancers with only a small survival benefit (Arnold and Schmoll, 2005). For primary CRC, options for adjuvant treatment now include 5-FU combinations with leucovorin (5-FU/LV), also known as folinic acid, leucovorin and oxaliplatin (FOLFOX), as well as other chemotherapy agents including irinotecan and capecitabine, all of which act to inhibit DNA replication and enhance the effects of 5-FU (Arnold and Schmoll, 2005, Bauer and Spitz, 1998, Van Cutsem *et al*., 2009b). FOLFOX has been shown to significantly improve disease free survival (DFS) in stage II and III colon cancer and improves also the overall survival in stage III colon cancer, and is now the standard adjuvant treatment for stage III colon cancer, and results suggest patients with stage II colon cancer also see an improved DFS (Van Cutsem *et al*., 2009b). Adjuvant treatment for advanced CRC also includes FOLFOX and a combination of 5-FU/LV and irinotecan or capecitabine.

Additional treatments targeting upregulated pro-metastatic factors, such as vascular endothelial growth factor (VEGF) and epidermal growth factor receptor (EGFR), are now suggested for consideration in patients with metastatic CRC (Van Cutsem *et al*., 2009a). Antibodies for VEGF such as bevacizumab, and for EGFR such as cetuximab and panitumumab are now being successfully investigated as adjuvant therapies (Arnold and Schmoll, 2005, Van Cutsem *et al*., 2009b). Another combination therapy of capecitabine plus oxaliplatin (XELOX) is also fast becoming an effective first-line treatment for metastatic CRC (Cassidy *et al*., 2011, Cassidy *et al*., 2004).

Other treatment regimens now consider non-steroidal anti-inflammatory drugs (NSAIDs) such as sulindac for post-surgery chemoprevention in high-risk patients (Kim *et al*., 2014). This follows earlier studies in human colorectal cancer cell lines suggesting a role for inflammation in disease

development and progression (Liggett *et al*., 2014, Williams *et al*., 1999a, Flis and Splwinski, 2009) and *in vivo* models (Chiu *et al*., 1997).

However, even with survival rates now increasing for both primary and advanced CRC there is a severe lack of more effective treatments, which highlights the need for more innovative approaches for diagnosis and therapy. Development of novel chemopreventative agents are beginning to give promising results (Serafino *et al*., 2014), and further combination therapies will likely lead to improvement in colorectal cancer treatment. However, the variety of current and future treatment options requires translational research to identify those treatments that will be beneficial for specific patient groups and individuals (Arnold and Schmoll, 2005). Specific features and molecular/genetic markers are becoming more of a focus due to our improved understanding of the molecular biology of CRC, and it is hoped this will obtain maximal benefit for each therapeutic option available to smaller patient groups and individualised therapies in the future.

One area of therapeutic potential is to target common changes in molecular biology seen in colorectal cancers. An early study helped to identify adenomas as the starting point for most colorectal carcinomas, and outlined some common genetic alterations and loss of functions at various stages of cancer development (Vogelstein *et al*., 1988). A comprehensive review of gene mutations in CRC revealed many prominent oncogenes and tumour-suppressor genes associated with CRC are the *APC*, *KRAS*, and *TP53* genes, as well as a wider assortment of genes mutated in subsets of CRC cases now being implicated (Fearon, 1995).

We are yet to fully understand the significance of individual and collective genetic and epigenetic defects in CRC (Fearon, 1995). However, gene sequencing, functional genetic studies, and intricate murine models of CRC using mutations in some of these genes, particularly *APC*, have provided further insight into how oncogenes and tumour-suppressors co-operate, with co-existence of mutations found within individual CRC tumours (Jackstadt and Sansom, 2016, Phesse *et al*., 2017). Deletion of *Apc* in mouse models has revealed insights into the mechanism of early tumourigenesis, while

truncations that closely mimic those seen in human CRC have been shown to drive changes in expression of other cell markers, such as Leucine-rich repeat-containing G-protein coupled receptor 5 (Lgr5) and Axin. Some of the more recent findings have been reported to be fundamental changes in concepts on intestinal homeostasis, and have allowed further insights into the impact of deleting genes such as *Apc* (Jackstadt and Sansom, 2016). These developments have allowed a more intricate look at molecular staging of colorectal cancers and better identification of tumour subclasses, progression markers and prediction of disease outcome (Eschrich *et al*., 2005). Molecular staging based on gene expression at the time of diagnosis could predict the behavioural direction of cancers, which has some promise in predicting the long-term outcome of individual cases.

Better characterization of the involvement of oncogenes through to protein expression and post-translational modifications, as well as the epigenetic impact of environmental factors, will be important in furthering the understanding of the biology of CRC progression, particularly in sporadic and IBD-associated CRC. Recent studies showing the complex interactions between diet and environmental agents, the gut flora, and inflammation associated with increased risk of CRC go some way towards improving the treatment of CRC through improving our understanding of the development of carcinomas (Bongers *et al*., 2014, Peterson *et al*., 2008).

1.3 The adenoma-carcinoma sequence

Normal epithelial cells of the gut mucosa progressively transform into a benign state of adenoma, before becoming neoplastic and evolving into invasive carcinoma, eventually leading to metastatic cancer (Hanahan and Weinberg, 2011). This is now stage characterised as the adenoma-carcinoma sequence. CRC can develop from normal colonic tissues, with a single layer of epithelial cells forming the gut mucosal barrier protecting a variety of colonic tissues from the vast contents of the gut (Marshman *et al*., 2002). The colonic mucosa contains deep pockets called the crypts of Lieberkuhn. Highly proliferative pluripotent stem cells are responsible for regeneration of the epithelial layer and can migrate throughout the crypts, differentiating into several specialised functional cell types to form

the mature gut mucosa (Gregorieff and Clevers, 2005, Merlos-Suárez *et al*., van de Wetering *et al*., 2002). Goblet cells are responsible for the production of mucins to protect the epithelium from gut bacteria, whilst colonic enterocytes are absorptive cells allowing nutritional absorption via the colon. Paneth cells produce bactericidal compounds protecting the epithelial barrier from commensal and pathogenic bacteria present in the gut. The entire process of epithelial renewal takes approximately 3–5 days (Hirata *et al*., 2013, Potten and Loeffler, 1990) but depends on a specific order of molecular signalling events to occur normally.

Assuming normal development and proliferation of intestinal stem cells, differentiation and migration occur in a coordinated manner toward the intestinal lumen, forming a complex but conserved arrangement of intestinal cells. However, upon mutation, the normal process of differentiation, proliferation, migration and apoptosis are disrupted. Recently, a 'Big Bang' model has been described. After the initial transformation, colorectal tumours are said to grow predominantly as a single expansion populated by numerous intermixed sub-clones, with alterations arising early during growth. This opens up to increasing numbers of mutations and gene copy numbers over time. Colorectal tumour profiling revealed the absence of intra-tumour heterogeneity in most cases, with most detectable heterogeneity originating from early alterations. This model allows a quantitative framework to interpret tumour growth dynamics and predict early malignant potential with significant clinical implications (Sottoriva *et al*., 2015).

During initial transformation, the epithelial gut mucosa first harbours a small bundle of abnormally proliferating cells creating an adenoma, but these cells remain *in situ*, with no extension into deeper tissues. As the tumour begins to invade deeper into the intestinal tissues of the submucosa, muscular propria and serosa, the tumour extends towards regional lymph nodes and large blood vessels. Once cancerous cells reach the lymph nodes, it becomes much more dangerous, dropping the 5-year survival rate substantially. Cancer cells that move into blood vessels can cause metastasis, which usually leads to death within 5-years of detection (Newcomb *et al*., 1992). Clinical recommendations for treatment of primary CRC following detection concentrate on pathological staging of the adenoma-

carcinoma sequence according to the TNM and modified Dukes' stage systems distinguishing according to the degree of extension of adenomatous polyps from its origin (Van Cutsem *et al*., 2009b, Newcomb *et al*., 1992). As seen in **Figure 1.3**, the adenoma-carcinoma sequence in sporadic and IBD-associated cases is influenced by the molecular biology of CRC, which can be shaped by environmental factors as well as genetic predispositions.

The differences between these two forms of CRC lie in the stage of progression in which common mutations occur. In IBD-associated cases, *p53* mutations occur early in progression with *APC* mutations occurring much later, whereas sporadic cases are commonly associated with much earlier *APC* mutations with *p53* mutations occurring towards the latter stages of progression. It is also interesting that there is a difference in cancer phenotype, where IBD-associated CRC is linked with flat tumours, compared to the polyp-associated tumours in sporadic CRC (Rhodes and Campbell, 2002). These differences may in part be explained by the differing contributions of inflammatory modulators in the development of dysplasia and progression to carcinoma in these two sequences.

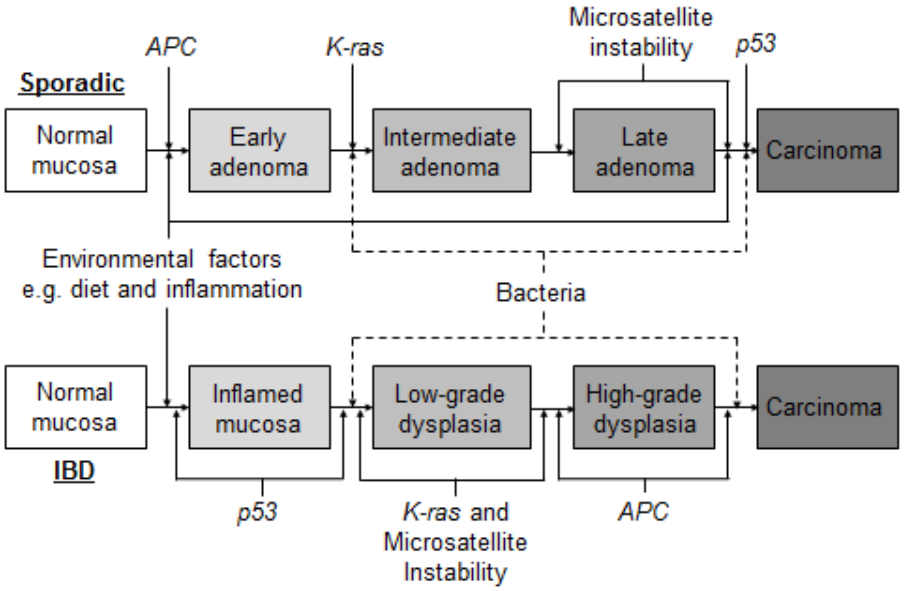

Figure 1.3. The adenoma-carcinoma sequence for sporadic and IBD-associated CRC. Typical mutations of *APC*, *K-ras* and *p53* genes, and microsatellite instability are shown at suggested stages of progression. The impact of environmental factors indicated at the beginning of IBD-associated and throughout sporadic CRC. The potential impact of bacteria (dotted line) is suggested from adenoma (sporadic) or low-grade dysplasia (IBD) to carcinoma. Adapted from (Rhodes and Campbell, 2002).

1.4 The impact of chronic inflammation in the gut

The inflammatory response involves a number of signalling pathways responsible for regulating the expression of inflammatory mediators. Our knowledge of signalling in inflammation has improved considerably, with a particular focus on the study of various interleukin and tumour necrosis factor (TNF) receptor families and the Toll-like microbial pattern recognition receptors (TLRs), which are considered key contributors (Lawrence, 2009). It has been suggested that the effects of inflammatory signalling can depend on the method of cytokine signalling recognition, and the complex processes of cytokine recognition involved in inflammation has been extensively studied.

Pro-inflammatory cytokines such as interleukins, tumour necrosis factor alpha (TNF-α), nitric oxide (NO) and cyclooxygenase-2 (COX-2) are all commonly implicated in inflammatory disease, and can be released upon tissue damage or following infection (Bartchewsky *et al*., 2009, Anderson *et al*., 1996, Laflamme *et al*., 1999, Tak and Firestein, 2001). Both TNF-α and COX-2 have come into focus in recent years as driving forces for the recruitment and activation of inflammatory cells (Karin *et al*., 2006). By blocking key inflammatory mediators associated with TNF-α and COX-2 release, it is possible to attenuate the inflammatory response, so these inflammatory cytokines now established as important therapeutic targets in chronic inflammatory diseases (Karin *et al*., 2006, Nakamura *et al*., 2009).

Chronic inflammatory signalling as a result of tissue damage and/or infection that goes unnoticed or uncorrected can increase risk of chronic inflammatory diseases. Chronic inflammation is often implicated in altering key cancer signalling pathways; one example of this is chronic TNF-α and COX-2 release mediating response via NFκB signalling (Paik *et al*., 2002, Lawrence, 2009). Activation of the canonical NF-κB pathway in response to inflammatory cytokines has shown to be important in the pathogenesis of chronic inflammatory diseases such as rheumatoid arthrtitis (RA) and IBD (Tak and Firestein, 2001). NF-κB activation is thought to play a complex but pivotal role in chronic and acute inflammatory diseases as well as in cancer (Hoesel and Schmid, 2013), and this has led to the development of anti-inflammatory drugs targeting NF-κB (Karin *et al*., 2004).

With an array of inflammatory molecules involved in different pathways linking inflammatory signalling with cancer signalling, the impact of inflammation could be a key factor in the development and progression of a number of cancers. IBD-associated CRC is an excellent example of the influence of chronic inflammation in the increased risk of cancer development.

IBD consists of ulcerative colitis (UC) affecting the colon and rectum, and Crohn's disease (CD) affecting any part of the gastro-intestinal tract. These have many overlapping genetic factors and clinical features, and the risk of developing cancers is equivalent in both conditions when there is a similar extent and duration of colonic disease (Ekbom *et al*., 1990a). Patients with CD-associated colon cancer and UC-associated colon cancer show marked similarity in terms of median duration of IBD before cancer, age at cancer, and presence of dysplasia (features of malignancy without evidence of tissue invasion) (Choi and Zelig, 1994). In both UC and CD, strong associations exist between the duration and extent of mucosal inflammation and the cancer risk.

The association between cancer risk and inflammation is not straightforward, but there are clear associations between cancer risk and disease extent and duration in patients with colitis extending proximal to the rectum (Ekbom *et al*., 1990b). In CD, there is a convincing association between inflammation and cancer at various sites. Small bowel CD comes with an increased risk for small bowel cancer, which is otherwise a rare phenomenon (Collier *et al*., 1985). Murine models have allowed insights into the impact of inflammation on colorectal carcinogenesis. For example, in *Apc*-mutant mice, activation of the cytokine-stimulated pathway mediated by the first member of the class of cytokine receptors, glycoprotein 130 (gp130), associated Janus kinases (Jaks), and the transcription factor Stat3 (signal transducer and activator of transcription 3) was required for tumourigenesis via the Wnt pathway (Phesse *et al*., 2014). Partial genetic and pharmacological inhibition of the gp130-Jak-Stat3 pathway was shown to prevent Wnt–mediated tumour growth.

With many clinical and epidemiological studies suggesting an association between infectious agents and chronic inflammatory disorders and cancer (Karin *et al*., 2006), it is reasonable to assume that the

increased risk of colorectal cancer in IBD patients is a result of the disease rather than an inherited phenomenon, and can be associated with the site, extent and duration of inflammation.

IBD-associated CRC therefore serves as an exemplary model of inflammation-associated cancer, but this correlation also provides important insights into the understanding of sporadic CRC pathogenesis. With chronic inflammation being a strong factor in the risk of development and progression of CRC in IBD patients, it was suggested that other factors may be involved.

A key aspect of CRC pathogenesis is an intestinal epithelial barrier that can be compromised by microbial toxins, environmental factors or genetic predispositions. This point towards another factor in disease risk alluded to in Figure 1, which is the involvement of bacteria. Both IBD-associated and sporadic CRC are now presumed to result in part from an altered host response to the normal intestinal bacterial flora (Shanahan, 2001), known as the gut microbiota. This led to the question of whether this can result in changes of bacterial composition in the gut and whether this can contribute to disease progression.

1.5 The gut microbiota

Bacteria are an important component of the human body, colonising the majority of epithelial surfaces. The community of bacteria and other microorganisms living within the human body are collectively known as the 'microbiota'. There are 10 times more cells comprising the microbiota than the number of cells in the human body, and approximately 70% of these are localised in the intestine (Compare and Nardone, 2011). Most of the microbiota consists of bacteria with much smaller numbers of Archaea, Eukarya and viruses, and we now know that more than 1,000 bacterial species can be found in the human intestine (Qin *et al*., 2010). A symbiotic relationship between the host and microbiota means that intestinal bacteria can be beneficial to intestinal health.

The human microbiota becomes established in stages. From childbirth and subsequent weaning, the increasing diversity of the microbiota occurs over the first couple of years and once established, by

around 3 years old, the microbiota typically remains constant over time (Ursell *et al*., 2012, Albenberg and Wu, 2014). The majority of bacteria in the gut microbiota belong to four common phyla: Bacteroidetes (e.g. *Bacteroides*), Firmicutes (e.g. *Clostridium*, *Enterococcus* and *Streptococcus*), Actinobacteria (e.g. *Bifidobacterium*) and Proteobacteria (e.g. *Escherichia coli*), with approximately 95% Bacteroidetes or Firmicutes (Siezen and Kleerebezem, 2011, Cotillard *et al*., 2013). However, numerous studies have shown that this composition can be altered.

Microbiota transplantation gave insights into the impact of environmental factors on bacterial composition, suggesting that our gut microbial composition reflects the bacteria we are exposed to from birth as well as what is now known as habitat effects, where specific bacteria are able to colonise at different sites of the gut (Rawls *et al*., 2006).

The production of mucus is also indicated as an important factor influencing the pattern of microbial colonization of different regions of the gut (Peterson *et al*., 2008). An important part of the host-bacterial interactions is the limit of interactions between the two, so it is then important that the intestinal microbiota is kept at a distance from intestinal epithelial cells to minimise the likelihood of bacterial invasion (Brown *et al*., 2013). Innate immune strategies are in place to keep much of the microbial community within the lumen of the intestinal tract and limit invasion of pathogenic bacteria. Specialised functional cells such as goblet cells are responsible for the production of mucins and Paneth cells producing bactericidal compounds help protect the epithelial barrier from commensal and pathogenic bacteria (Kamada *et al*., 2013). The mucus layer, antimicrobial peptides (AMPs) and innate lymphoid cells (ILCs) help to avoid bacterial invasion whilst promoting mutualistic interactions (Brown *et al*., 2013). Microbial signals can also induce the production of interleukins such as IL-22, and immunoglobulins such as IgA to aid in barrier function (Brown *et al*., 2013).

Studies focussing on mouse colonic mucus show two distinct layers of mucus with similar protein composition and mucin-2-glycoprotein (MUC2) as the major structural component (Johansson *et al*., 2008). However, proteolytic cleavage of MUC2 affects the shape and density of the mucus. The inner

layer is densely packed and attached to the epithelium, and this layer is devoid of any bacteria. The outer layer contains cleaved MUC2 glycoproteins, making it much less dense and is often colonized by bacteria. This was confirmed using *MUC2*$^{-/-}$ mice, where bacteria are in direct contact with epithelial cells far down in the crypts, which led to inflammation and cancer development (Johansson *et al*., 2008).

Deregulation of mucin production has therefore provided an important link between inflammation and cancer, and mucins have been identified as attractive therapeutic targets (Kufe, 2009). Ulcerative colitis, a form of IBD, is characterised by marked inflammation, superficial mucosal ulceration, infiltration of neutrophils, and depletion of goblet cell mucins. The extent of disease in patients with ulcerative colitis is associated with decreased MUC2 production, which suggests that the mucosal barrier is important in the pathogenesis of this form of IBD. However, the role of MUC2 as a tumour suppressor appears paradoxical, with reports that MUC2 can be expressed at increased levels in gastric (Leteurtre *et al*., 2006), pancreatic (Takikita *et al*., 2009) and ovarian (Hirabayashi *et al*., 2008) carcinoma and can vary depending on progression. A recent study highlighted the fact that DNA methylation and histone modification of MUC2 may play an important role in carcinogenesis, and concluded that further studies of the epigenetics of mucin gene expression are required in order to fully understand the relationship between mucin expression (Yonezawa *et al*., 2008).

Other studies have focussed on the nutrients available to the gut microbiota and how this might affect microbial composition. For example, diets rich in carbohydrates can benefit certain members of the gut microbiota, such as Bacteroides (Hooper *et al*., 1999), where these bacteria can be found assembled on food particles and mucus. These changes in composition can become more pronounced when the diet is also depleted of complex polysaccharides (Sonnenburg *et al*., 2005).

Complex control mechanisms help to ensure the symbiotic relationship, with crosstalk on a cellular level between intestinal epithelial cells, immune cells and the microbiota, representing a fundamental feature of intestinal homeostasis. However, these control mechanisms can fail, leading to a change in

the relationship between bacteria and epithelial cells lining the intestines. Factors including age, genetics, and diet may influence microbiome composition, and of these diet is the easiest to modify and presents the simplest route for therapeutic intervention (Wu *et al*., 2011).

Epigenetic environmental and lifestyle factors are becoming increasingly prominent in research focussing on microbiota composition. Diet has previously been shown to affect cellular processes like apoptosis in colorectal cancer, which can both limit or increase burden and/or progression of colorectal cancer (Bellamy *et al*., 1995).

The symbiotic relationship between microbiota and gut can also be changed pathologically, where obesity, diabetes, atherosclerosis and IBD have all been implicated as factors affecting microbial composition, and the relationship between alterations in the microbiota and development of intestinal disease such as IBD and colorectal cancer is now becoming more of a key focus. Evidence for the preferential localisation of some tumours in specific areas of the intestine suggests that non-genetic factors such as changes in the microbiome play an important role in their development (Bongers *et al*., 2014).

1.6 The human gut microbiota under inflammatory conditions

Development of tumours associated with local changes in epithelial barrier function, bacterial invasion, production of antimicrobials, and increased expression of several inflammatory factors indicate that tumours can be driven by the interplay between genetic and epigenetic changes in the host, chronic inflammatory responses and a host-specific microbiota.

Inflammatory conditions can place abnormal stresses on bacteria in the human gut. Under chronic inflammatory conditions, such as those seen in IBD in both Crohn's disease and ulcerative colitis patients, the faecal microbiota commonly shows reduced bacterial diversity. This is most pronounced in Crohn's disease where a reduction in Firmicutes can be observed alongside an increase in Proteobacteria such as *Escherichia coli* (*E. coli*) (Hold *et al*., 2014).

Animal models of IBD have been found to result in similar changes in the microbiota, particularly reduced diversity. One of the most typical and most used mouse models in these types of studies is the colitis model induced by dextran sodium sulphate (DSS). Use of these models has shown that there is marked disturbance of the mucosal barrier, with a loss of colonic adherent mucus. The faecal microbiota also shows a reduction in bacterial diversity, with increases in numbers of some of the more robust species. One example of this is increased *Enterobacteriaceae*, such as *E. coli* (Nagalingam and Lynch, 2012).

Similar changes were seen in mouse models of infective gastroenteritis, using *Citrobacter rodentium* and *Campylobacter jejuni* infections, as well as chemically and genetically induced models of intestinal inflammation to demonstrate host-mediated inflammation. Bacterial infection, a chemical trigger such as dextran sodium sulphate (DSS), and genetic pre-dispositions such as interleukin-10-(*Il-10*)-deficiency, known to play a key role in defence against infection of epithelial cells and used in many murine models, markedly alters the colonic microbial community (Lupp *et al*., 2007). It therefore seems likely that many alterations in faecal microbiota seen in IBD could be a consequence of inflammation, and that this is indicative of the gut microbiota as a whole.

While IBD could be influenced by the intestinal microbiota, the difficulty in culturing these complex microorganisms has precluded the formal identification of specific bacteria involved in disease. Several studies have attempted to characterise the gut microbiota using molecular 16S metagenomic sequencing, with one study revealing the composition of the human distal intestinal microbiota in both normal and IBD conditions.

In the normal distal intestine, the two predominant phyla, Firmicutes and Bacteroidetes, make up the majority of microbiota with lesser contributions from Proteobacteria and Actinobacteria, and minor contributions from Fusobacteria, Verrucomicrobia, and Cyanobacteria (Arthur and Jobin, 2011). A study of relative abundance of bacterial phyla in the small intestine and colon showed that Proteobacteria and Firmicutes can be found at increased levels in IBD patients (**Figure 1.6**) (Peterson

et al., 2008). Changes in bacterial composition in favour of these bacteria can lead to an increase in opportunistic pathogens.

Studies focussing on the mucosa-associated microbiota have generated more dramatic differences than study of faecal microbiota between health and IBD, particularly in Crohn's disease. This is the case for the mucosa-associated *E. coli* that have been found more commonly in mucosal biopsies from the ileum and colon of patients with Crohn's disease (Darfeuille-Michaud *et al*., 1998, Martin *et al*., 2004). In colonic biopsies, many of these bacteria are present within the adherent mucus (Swidsinski *et al*., 2002), although there is also evidence of intracellular *E. coli* from study of gentamicin-treated and subsequently lysed mucosal samples (Martin *et al*., 2004).

A recent study of both mucosal and faecal samples from newly-diagnosed paediatric cases prior to treatment has given further clarification, showing clear compositional differentiation between Crohn's disease and controls in mucosal samples and faecal samples (Gevers *et al*., 2014), again including increased numbers of *E. coli*, as well as *Veillonella* spp., *Haemophilus* spp. and *Fusobacteria*, alongside reduced numbers of a range of bacteria, including *Faecalibacterium prausnitzii*.

It is now believed that many of the changes in microbiota composition seen in IBD, including an increase in *E. coli*, may be at least in part secondary to chronic inflammation. With development of tumours driven by the interplay between genetic changes in the host, chronic inflammatory responses and a host-specific microbiota, it seemed understandable that studies into the gut microbiota in CRC would suggest bacteria as a contributing factor.

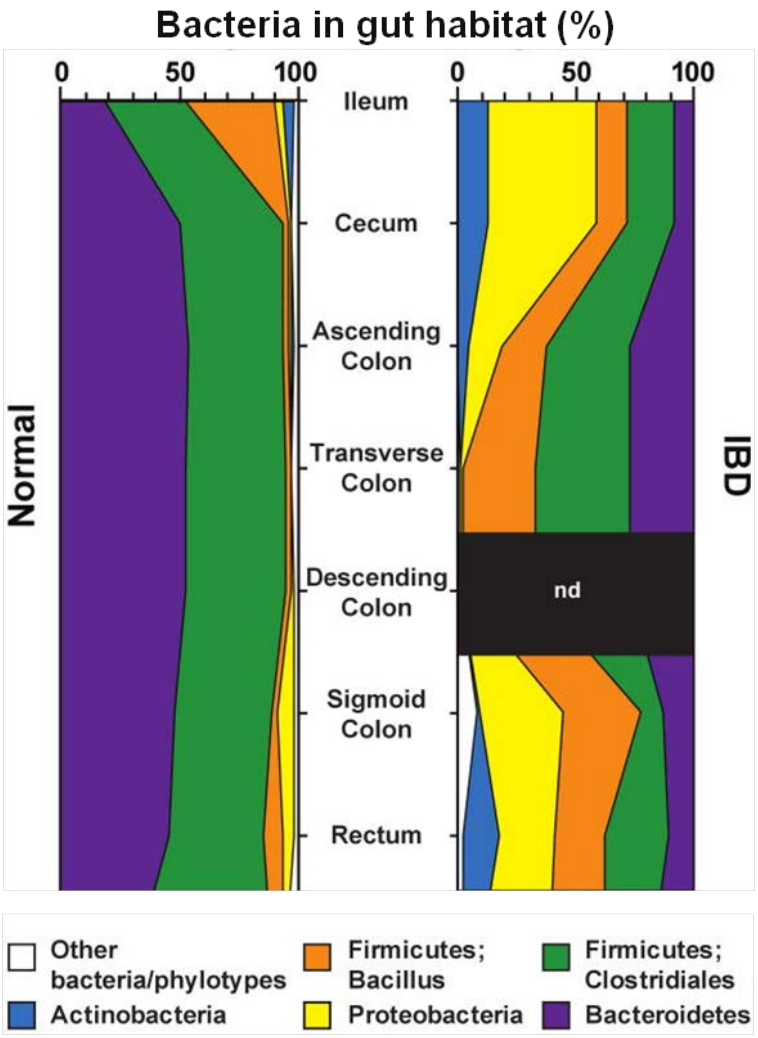

Figure 1.6. IBD Bacterial phyla identified in the human gut microbiota. Under normal conditions, *Firmicutes* and *Bacteroidetes* predominate throughout the gut. In patients with IBD, substantial increases in *Proteobacteria* are shown throughout the small intestine and colon, suggesting chronic gut inflammation can alter the composition of the gut microbiota. No data was provided for the microbiota of the descending colon in IBD. Adapted from (Peterson *et al*., 2008).

1.7 The human gut microbiota in colorectal cancer

Several studies implicate microbial dysbiosis in the development of colorectal adenomas and CRC (Wu *et al*., 2013, Zhu *et al*., 2014, Chen *et al*., 2012, Sobhani *et al*., 2011), with some intriguing similarities between the microbiota in colorectal cancer and in Crohn's disease. In colorectal cancer, and in patients with colonic adenomas, there is tendency for the faecal microbiota to show reduced diversity,

a higher proportion of Proteobacteria and a lower proportion of Bacteroidetes (Dulal and Keku, 2014). Again, study of the mucosa-associated microbiota reveals changes that may be missed by study of faecal microbiota, including increases in mucosa-associated *E. coli* and *Fusobacterium nucleatum*. Mucosa-associated *E. coli* in colon cancers also show some of the adherent, invasive phenotypic features of *E. coli* associated with colorectal disease (Martin *et al*., 2004).

It is becoming increasingly likely that the microbiota plays a significant part in the pathogenesis of colorectal cancer, and a recent study characterising the gut microbiome in healthy, adenoma, and carcinoma patients representing various stages of colorectal cancer development has added extra weight to this theory (Zackular *et al*., 2014). Analysis of stool samples confirmed a similar enrichment/depletion of bacterial populations associated with adenomas and carcinomas to that of previous studies. Inclusion of gut microbiome significantly improved the ability to differentiate between clinical groups in comparison to risk factors such as age and race alone. This demonstrates the feasibility of using the composition of the gut microbiome to determine the necessity to screen for pre-cancerous and cancerous lesions in colorectal disease alongside standard clinical screening. More studies using stool markers along with linkage to dietary data and individual health information could aid the development of more targeted therapies that could be given based on individual screening cases.

The composition and functional stability of the human gut microbiota given the variety of environmental exposures are not well defined. Alterations in bacterial community composition associated with adenomas may be a contributory cause of CRC, and these findings could lead to strategies to manipulate the microbiota to prevent colorectal adenomas and cancer as well as to identify individuals at high risk (Shen *et al*., 2010, Dulal and Keku, 2014). The role of the intestinal microbiota is being studied as a major factor in the impact of innate immune sensors and their associated signalling in protecting or promoting the development of colorectal cancer via inflammation and proliferation.

With the gastrointestinal tract colonised by thousands of bacterial species, this complex microbial community carries a diverse microbial genome with the potential to influence intestinal homeostasis. The relationship between innate sensors, the microbiota and development of colitis-associated colorectal cancer indicate that microbial composition may impact the status of various pathologic conditions including IBD and colorectal cancer (Arthur and Jobin, 2011).

The microbiota has previously been linked to innate (Clarke *et al*., 2010) and adaptive immunity (Chervonsky, 2010), gastrointestinal development (Hooper, 2004), invasion and angiogenesis (Stappenbeck *et al*., 2002). Due to gut bacteria being implicated in a number of steps of disease progression in CRC, it is easy to see the varying ways in which bacteria can influence colorectal disease. The major route in which bacterial infection can aid progression of CRC is via inflammatory pathway.

One important feature of IECs in protection against possible bacterial infection is the expression of Toll-like receptors (TLRs) at the cell surface (Arthur and Jobin, 2011). TLRs can recognise and be activated by specific features of bacterial pathogens, such as cell-surface lipopolysaccharides and proteins, and play an important role in inflammation and tissue regeneration via the myeloid differentiation primary response gene 88 (MyD88).

TLR expression in IECs varies, with low levels of TLR2 and TLR4 expression in colonic tissue, abundant TLR3 expression in the small intestine and colon, and TLR5 expression predominantly in the colon. Activation of TLR signalling results in the expression of antimicrobial peptides and the production of prostaglandins and cytokines as a protective mechanism to stop bacterial colonization of IECs. This includes the induction of cyclooxygenase expression, which can promote epithelial cell proliferation, whilst interleukins are also responsible for regulating TLR signalling by decreasing TLR expression in IECs. These mechanisms help to establish a microorganism-induced programme of epithelial cell homeostasis and aid the repair of the intestinal epithelial barrier. However, TLR signalling can have cancer-promoting effects, which is best established in the colon where there is constant interaction between gut microbiota and intestinal epithelial cells (Arthur and Jobin, 2011, Pradere *et al*., 2014).

Excessive TLR signalling due to the invasion and colonisation of bacteria and the resulting chronic inflammation can lead to over-exuberant repair responses associated with the development of colon cancer. Although inflammation is controlled by numerous mediators and pathways, several systems, such as TLR signalling, can function as key upstream regulators (Pradere *et al*., 2014). Dysregulation of protective mechanisms such as TLR signalling helps to explain how bacterial infections of the gut could promote colorectal cancer. A mouse model of gastric cancer has shown that Stat3 directly up-regulates epithelial expression of TLR2 in gastric tumours, where genetic and therapeutic targeting of TLR2 inhibited gastric tumorigenesis, but didn't affect inflammation (Tye *et al*., 2012). This suggests TLR activation may also regulate cancer growth in an inflammation-independent manner.

Another key protection pathway is the recognition of peptidoglycan by nucleotide-binding oligomerisation domain–containing protein-1 (Nod1), which has been shown to be crucial for maintaining a basal level of immune activation in mouse knock-out studies (Clarke *et al*., 2010). Gram-positive bacteria in the gut microbiota are a rich source of peptidoglycan known to prime the innate immune system, which enhances bacterial killing via neutrophils. Nod1 predominantly recognises meso-diaminopimelic acid (mesoDAP)-containing peptidoglycan found primarily in Gram-negative bacteria. *NOD1* knock-out leads to a reduction in the ability to kill Gram-positive bacteria, allowing better survival and more opportunity to colonise within the gut (Lysenko *et al*., 2007). Genetic polymorphisms in *NOD1* and *NOD2* are associated with increased risk of gastric cancers, particularly in the case of *H. pylori* infection, which suggests they play important roles in promoting the development of gastric cancers (Wang *et al*., 2012a). However, while these changes offer insights into mechanisms of microbial infection control, and demonstrates the importance of Nod1 in neutrophil-mediated clearance of bacteria *in vivo*, there is as yet little evidence convincingly implicating *NOD1* polymorphisms in colorectal cancers.

Any changes in the control of microbial composition can influence the human microbiota, with altered microbiota known to influence our gastrointestinal health as well as our susceptibility to disease (Kamada *et al*., 2013). The final composition and diversity of our microbiota is partially determined by

environmental factors, highlighted by the vast differences of the adult microbiota compared to that at birth (Greer and O'Keefe, 2011). With environmental and lifestyle factors significantly altering microbial function, extensive research now indicates that a westernised diet low in complex carbohydrates and overuse of antibiotics and underuse can lead to an intensified inflammatory potential. Chronic inflammation due to microbial composition can cause increased risk of certain diseases. There has been a rise in cases of inflammatory bowel disease that has been linked to impaired beneficial bacterial exposure and education of the gut immune system (Greer and O'Keefe, 2011), and current research highlights a complicated relationship between the gut microbiota and immunity, inflammation and carcinogenesis.

Recent research has focused on better understanding the interplay between chronic inflammation and development of cancer, with IBD-associated cases at the forefront, with a number of inflammatory, proliferative and immune signalling pathways now linked to the microbiota and development of colorectal cancer (Arthur and Jobin, 2011). TLRs are known to trigger signalling pathways leading to the expression of various genes including growth factors and inflammatory mediators, thus amplifying inflammation and promoting carcinogenesis. Microbial enzymes can also process dietary pro-carcinogens to their biologically active forms (**Figure 1.7**).

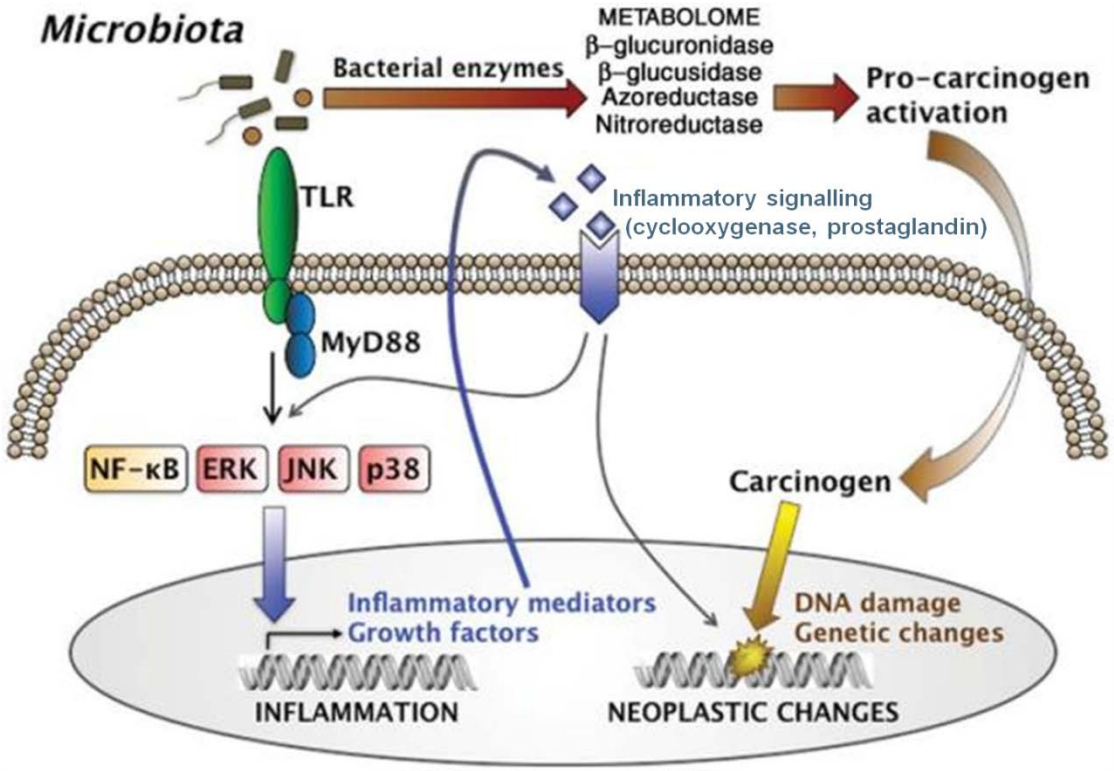

Figure 1.7. Composition of the intestinal microbiota can influence inflammatory signalling and carcinogenesis. The intestinal microbiota promotes inflammation and neoplasia via signatures recognised by TLRs. TLRs trigger downstream signalling pathways leading to the expression of various genes, including inflammatory mediators and growth factors to amplify inflammation and promote neoplasia. Bacterial enzymes can also cause activation of pro-carcinogens to their biologically active form to elicit further neoplastic changes. Adapted from (Arthur and Jobin, 2011).

With carcinogenesis known to be induced via both inflammatory signalling and carcinogenic metabolites of bacteria in the gut, the intricate mechanisms within these pathways could be targeted for novel therapies, reducing the effects brought about by bacterial infection, but for this to be possible more insight into specific bacteria and their associated pathogenic characteristics is necessary. Inflammation has been shown to promote CRC in patients with colitis, and the microbiota has been identified as a target of inflammation affecting the progression of CRC. One study using high throughput sequencing revealed that inflammation modifies composition of the gut microbiota in colitis-susceptible *Il10*$^{-/-}$ mice, and showed the promotion of invasive carcinoma following mono-

association with *E. coli* NC101 expressing the genotoxin-encoding polyketide synthase (pks) pathogenicity island (Arthur *et al*., 2012). These types of studies suggest a contributory and possibly key role played by infection-induced inflammation in colorectal carcinogenesis.

Recent evidence suggests a correlation between Gram-negative *Proteobacteria* found adhered to the adult gut mucosa. A number of bacteria have been implicated as risk factors and causes of gastrointestinal cancers via chronic infection and inflammation. For example, *E. coli* have a higher presence in the gut microbiota under inflammatory conditions and some strains have the arsenal to become opportunistic pathogens, adhering to and invading intestinal epithelial cells (Martin *et al*., 2004). Preventative and adjuvant therapies interfering with inflammatory pathways as well as downstream signalling events, such as Wnt signalling, triggered by infections could help to minimise the risks posed by bacteria such as *E. coli* in colorectal disease. However, our limited understanding of the role of bacteria in colorectal disease meant that more information was required before looking into potential therapies.

1.8 The role of *E. coli* in colorectal disease

In inflammatory bowel diseases (IBD), ulcerative colitis (UC) and Crohn's disease (CD), the composition of the intestinal microbiota can be compromised over a number of years; there is even evidence to suggest that gut bacteria may play a role in the onset of IBD (Chassaing and Darfeuille–Michaud, 2011). In many cases, *E. coli* have been the focus, with independent studies reporting increased numbers of intestinal *E. coli* in patients. Increased numbers of *E. coli* have been found in the ileum of CD patients (Darfeuille-Michaud *et al*., 1998), and data also suggests a preferential increase in the concentration of *Bacteroides*, and in particular *E. coli*, in the gut of IBD patients (Swidsinski *et al*., 1998).

It is therefore believed that the chronic inflammatory conditions in the intestine of CD patients can change bacterial composition to favour those capable of surviving the conditions. This can increase risk of bacterial infection by these bacteria – a phenomenon supported by data showing an increase in mucosa-associated and intra-mucosal bacteria, again primarily *E. coli*, in Crohn's disease as well as

colon cancer patients (Martin *et al*., 2004). These studies support a central role for mucosa-adherent bacteria, in particular *E. coli*, in the pathogenesis of Crohn's disease and colon cancer. However, the mechanisms by which these bacteria are involved in Crohn's disease and colon cancer are not fully understood.

It has also been shown that Crohn's disease-associated *E. coli* can translocate across intestinal M-cells. *E. coli* translocation was shown to be increased across M-cell monolayer cultures, generated by co-culture of Caco-2 and Raji-B cell lines in Ussing chambers, in comparison to using parent Caco-2 monolayer cultures, with electron microscopy also confirming *E. coli* located within M-cells (Roberts *et al*., 2010). Interestingly, the same study also showed how soluble plant fibres and emulsifiers can affect this translocation, highlighting the impact of environmental factors such as diet on potential infection, particularly in those at increased risk. The results suggest that an increase in number of *E. coli* residing within the intestine can increase the risk of infection, inflammation and colon cancers. If this is indeed the case, a better understanding of the role of these bacteria in carcinogenesis, in particular in the case of intestinal epithelial cells, is essential.

A study investigating changes in the gut microbiota that may contribute to colorectal cancer found an altered composition of the colonic-adherent microbiota in Il-10 deficient mice, causing an imbalance in intestinal bacteria, or 'dysbiosis', with a reported 100-fold increase *E. coli* (Arthur *et al*., 2012). The study also reported that mice colonized solely with *E. coli* harbouring the *pks* pathogenicity island developed invasive adenocarcinoma after azoxymethane treatment. The *pks* pathogenicity island is able to synthesise a genotoxin known as colibactin, suggesting that *E. coli* may exert DNA damage independent of inflammation, due to the absence of the anti-inflammatory cytokine Il-10. However, the role of other cytokines, such as tumour necrosis factor (TNF) and Il-12 in these models, were not assessed and may still be involved (Scheinin *et al*., 2003).

The increased abundance of *E. coli* in the gut has long been linked to carcinogenesis. A study detected bacteria in 90% and 93% of adenoma and carcinoma biopsy specimens, respectively. In addition,

partially intracellular *E. coli* were found in 87% of patients with adenoma and carcinoma compared to none in control samples. It was therefore concluded that the colonic mucosa of patients with colorectal carcinoma but not normal colonic mucosa was colonised by intracellular *E. coli* (Swidsinski *et al*., 1998).

Infection-induced hyper-proliferation of epithelial cells, either via inflammatory cytokines or independent of them, seems to be a common theme in most gut-associated cancers. One aspect that seems to stand out is the impact of bacterial composition in carcinogenesis, with dysbiosis being a consistency. If changes in the microbiota are involved in cancer development, the colon should be a major site of action, and inflammation will play a significant role. Therefore, it should not be surprising that the risk of cancer in inflammatory bowel diseases is considerably higher if the disease affects the colon rather than the small intestine (Bienz and Clevers, 2000).

With evidence of *E. coli* found within gut tissues in Crohn's disease and colon cancer, the characteristics responsible for their ability to adhere to and invade these tissues have been recently investigated. A study identifying a number of genes contributing to the adhesive and invasive characteristics of CRC-associated *E. coli* isolates also identified genes that could be involved in colorectal carcinogenesis (Prorok-Hamon *et al*., 2014). Mucosa-associated *E. coli* isolates were found to commonly express lpfA and fimH. These genes are now known to be involved in M-cell translocation, which is likely to be the initial route for invasion *in vivo*. Isolates from Crohn's disease and CRC patients showed increased prevalence of afimbrial adhesion (afa). This increased presence also correlated with increased adherence to and invasion of intestinal epithelial cells, as well as increased VEGF expression known to aid angiogenesis and, therefore, development and progression of cancer.

As mentioned earlier, colonic mucosal *E. coli* from IBD and CRC patients more commonly express the pks pathogenicity island responsible for the formation of colibactin (Arthur *et al*., 2012). Interestingly, *E. coli* expressing both afaC and lpfA were common in Crohn's disease and CRC patients, whereas *E.*

coli expressing both afaC and pks were common in patients with CRC and ulcerative colitis (Prorok-Hamon *et al*., 2014). This suggests that the presence of the pks island isn't the sole determinant of CRC development, and that adherence and invasion characteristics may be contributing to carcinogenesis. All isolates, however, were found to express the htrA gene, encoding the stress protein HtrA, and the dsbA gene, encoding the oxido-reductase enzyme DsbA, both of which have previously been shown to be essential for intracellular replication within macrophages (Bringer *et al*., 2005, Bringer *et al*., 2007). These characteristics are thought to be phenotypic of a collective group of bacteria now termed 'adherent and invasive *E. coli*' (AIEC), associated with IBD and CRC.

1.9 Adherent and invasive *E. coli* (AIEC)

It has been demonstrated that, under IBD and CRC inflammatory conditions, increased numbers of pathogenic *E. coli* are found within the microbiota (Chassaing *et al*., 2011, Hold *et al*., 2014, Rhodes and Campbell, 2002). Martin *et al*. showed these *E. coli* can adhere to and invade the gut mucosa, hence the term AIEC. This effect was shown to be pronounced in IBD and CRC patients, with altered mucosal glycosylation said to affect mucosal bacterial adherence (Martin *et al*., 2004). The mucosa-associated microbiome also shows reduced biodiversity, with *E. coli* dominating (Tawfik *et al*., 2014), which further supports *E. coli* invasion into the mucosa in IBD and CRC patients.

Adhesion and invasion are believed to be dependent, in part, on the expression of type 1 pili (FimH) on the bacterial surface, long polar fimbriae promoting mucosal translocation, and carcinoembryonic antigen-related cell adhesion molecule 6 (CEACAM6) glycoprotein on the apical surface of intestinal epithelial cells (Barnich *et al*., 2007, Prorok-Hamon *et al*., 2014, Tawfik *et al*., 2014). CEACAM6 acts as a receptor for AIEC adhesion and is abnormally expressed by intestinal epithelial cells in CD patients (Darfeuille-Michaud and Colombel, 2008). CEACAM6 has also been a focus for involvement in anoikis, an apoptotic mechanism of cell death, and its contribution in pancreatic carcinogenesis (Duxbury *et al*., 2004). Malignant cells are often able to escape anoikis, contributing to an ability to form metastases. CEACAM6 expression varies between pancreatic cancer cell lines, with over-expression

associated with greater anoikis-resistance and *in vivo* metastasis. CEACAM6 gene silencing promotes anoikis, reversing any acquired anoikis resistance, and was found to inhibit metastasis in pancreatic adenocarcinoma (Duxbury *et al*., 2004).

With both CEACAM glycoproteins associated with adhesion and invasion and overexpressed in many cancers, it has been identified as a therapeutic target. The effects of monoclonal antibodies have been evaluated using migration, invasion and adhesion assays *in vitro* using a panel of human pancreatic, breast, and colonic cancer cell lines, and in the GW-39 human colonic micrometastasis *in vivo* model (Blumenthal *et al*., 2005). These antibodies were effective at inhibiting cell migration, invasion and cell penetration through an extracellular matrix (ECM). Adhesion of tumour cells added to endothelial cells within the *in vivo* micrometastasis model was significantly decreased by up to 58%.

Mucosa-associated *E. coli* strains able to adhere to and invade the intestinal mucosa have been isolated from CRC and IBD patients but not from control patients (without IBD). However, there is still little understanding of the molecular effects of mucosa-associated *E. coli* within the gut mucosa, or whether these are in fact impacting on carcinogenesis. Investigating whether these *E. coli* also possess the ability to activate key cancer-promoting proteins within intestinal epithelial cells will give a better understanding of the development, growth and spread of colonic tumours.

Evidence would suggest these changes may have a significant role in carcinogenesis via inflammatory signalling, meaning it would be important to reduce the inflammatory effects of *E. coli* within the gut mucosa by removing or killing these bacteria. However, AIEC have been shown to be resistant to killing by mucosal macrophages, which has shown to be important in disease pathogenesis (Tawfik *et al*., 2014) and virulence, adherence and invasive factors are believed to be responsible. It has been suggested that further investigation to identify and characterise virulence, adherence and invasive factors supporting AIEC survival could give insights into novel and targeted AIEC treatments (Tawfik *et al*., 2014). Additionally, novel factors may be present that increase their pathogenicity and contribute

to cancer burden. Finding and evaluating other factors expressed by mucosa-associated AIEC that may be potentially contributing to carcinogenesis is an important step.

1.10 Possible mechanisms of colorectal cancer development involving *E. coli*

One of the key factors already shown to contribute to the carcinogenicity of mucosa-associated *E. coli* is the pks pathogenicity island. Several members of the *Enterobacteriaceae* family, including *Escherichia coli*, *Klebsiella pneumonia* and *Enterobacter aerogenes*, are known to harbour the pks pathogenicity island encoding colibactin (Putze *et al*., 2009). Deletion of the pks pathogenicity island from *E. coli* NC101 decreased tumour multiplicity and invasion in AOM-treated *Il10*$^{-/-}$ mice without altering intestinal inflammation (Arthur *et al*., 2012), thus highlighting the importance of this pathogenicity island in carcinogenesis. AIEC containing the pks pathogenicity island were found in a significantly high percentage of inflammatory bowel disease and CRC patients, again suggesting that colitis can promote tumorigenesis by altering microbial composition and induce the expansion of microorganisms with genotoxic capabilities.

The suggested effects of colibactin on the host immune response as well as the impact on cancer development have recently been identified as a therapeutic target. The pks-encoded enzyme ClbP is an atypical peptidase that contributes to the synthesis of colibactin. ClbP has been identified as a therapeutic target, with key features of ClbP analysed using bacterial fractionation and Western-blotting (Cougnoux *et al*., 2012). This revealed the docking of ClbP to the bacterial inner membrane via a C-terminal domain harbouring three transmembrane helices (**Figure 1.10**).

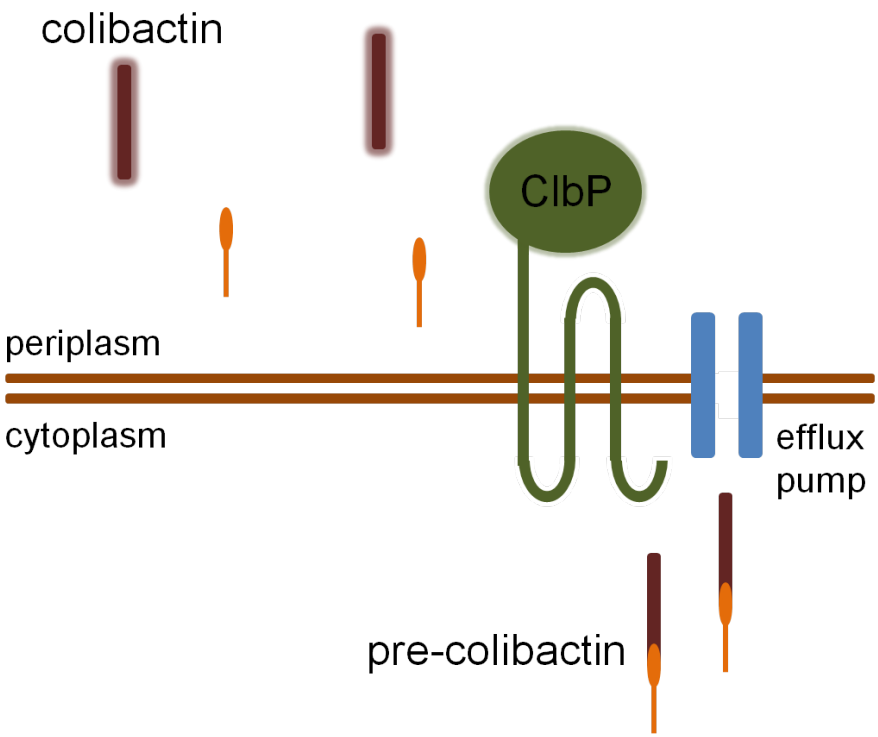

Figure 1.10. The role of the ClbP enzyme in colibactin maturation. Membrane-bound ClbP enzyme activity contributes to the synthesis and maturation of the genotoxin colibactin. Negatively-charged residues in the catalytic domain of ClbP allow docking to the bacterial membrane. The transfer of pre-colibactin into the extracellular matrix (periplasm) via an efflux pump enables its maturation via ClbP into the bioactive form, colibactin. Adapted from (Cougnoux *et al*., 2012)**.**

The complete sequence of the C-terminal domain was found to be necessary for ClbP bioactivity (Cougnoux *et al*., 2012). This study was able to identify key features of ClbP bioactivity, including association with the bacterial inner membrane, the exposition of its enzymatic domain in the bacterial periplasm and key residues of the enzymatic domain. These findings give insights into colibactin synthesis and will aid the design of inhibitors targeting the production of colibactin in bacteria containing pks pathogenicity islands.

The effect of colibactin has also been studied for impact in metastatic CRC, giving a completely different mechanism of carcinogenesis for colibactin. Transient contact of a few malignant cells with colibactin-producing *E. coli* increased tumour growth in a xenograft mouse model, and this growth was sustained by the accompanied production of GM-CSF (granulocyte macrophage colony-

stimulating factor) and fibroblast growth factor (Dalmasso *et al*., 2014). An additional consequence of pks-expressing *E. coli* was the induced alteration of p53 SUMOylation, an essential post-translational modification in eukaryotic cells. Small, ubiquitin-like modifier (SUMO) is believed to be involved in the nuclear export of p53 to allow tumour suppression (Santiago *et al*., 2013), so alterations in the process could be another contributing factor to pathogenicity.

The underlying mechanisms for this process are thought to involve the induction of microRNAs (miRNAs) – a class of highly conserved and endogenous non-coding RNAs regulating the expression of target genes at the post-transcriptional level (Xu *et al*., 2013). For example, expression of one specific miRNA known as miR-20a-5p has been shown to aid production of sentrin/SUMO-specific protease 1 (SENP1) important in the regulation of the SUMOylation process, thus disrupting gene transcription. The expression of SENP1, miR-20a-5p and growth factors have been observed in a CRC mouse model and in human biopsies that are found colonized by pks-expressing *E. coli* (Xu *et al*., 2013). This data reveals a new mechanism of carcinogenesis following infection with pks-expressing *E. coli,* with production of growth factors promoting proliferation of uninfected cells and subsequent tumour growth. This again gives insight into where the pks pathogenicity island shows therapeutic potential, and opens up research into the role of miRNAs in bacterial carcinogenesis.

The many links between bacteria and colonic disease such as CRC is well documented, with the pathogenicity of bacteria such as *E. coli* becoming a key focus. Bacterial invasion has now been linked with a variety of human cancers occurring principally via inflammatory pathways. Understanding the link between chronic inflammatory processes and events that drive carcinogenesis could be important in helping the design of novel strategies to prevent CRC.

Another mechanism affecting gut pathogenicity is disruption of the innate immunity in the gut, with intestinal epithelial cells and underlying macrophages normally able to keep potential pathogens under control, maintaining mucosal homeostasis. One major factor involved in innate immunity of the intestinal mucosa is nuclear factor kappa-light-chain-enhancer of activated B cells (NF-κB; (Jarry *et al*.,

2014). NF-κB, known to be involved in the increased expression of many genes of inflammatory and immune responses, can be upregulated in response to microorganisms and lipopolysaccharides (La Ferla *et al*., 2004), and is known to be involved in inflammatory disease.

NF-κB is considered a crucial factor in maintaining chronic inflammation. Normally, NF-κB-containing complexes are sequestered in the cytosol in the inactive form due to their association with inhibitory proteins. Activation of the canonical pathway causes nuclear translocation of NF-κB (Scheidereit, 2006) where it induces target gene transcription including pro-inflammatory cytokines such as TNF-α (Jarry *et al*., 2014). Release of these inflammatory cytokines have been shown to be associated with increased risk of disease.

A 3D model of human intestinal mucosa explant culture has been used to explore the effects of the mucosa-associated *E. coli* strain LF82, associated with Crohn's disease, on NF-κB signalling. Results showed that LF82 *E. coli* enter and survive within intestinal epithelial cells and macrophages without altering the mucosal architecture. LF82 *E. coli* were able to activate NF-κB signalling in epithelial cells, NF-κB/p65 nuclear translocation, and TNF-α secretion. In addition, NF-κB activation was said to be crucial for the maintenance of epithelial homeostasis upon LF82 infection, with activation of NF-κB also demonstrated *in situ* in macrophages and intestinal epithelial cells in the inflamed mucosa from IBD patients (Rogler *et al*., 1998). With activation of NF-κB also seen in absorptive epithelial enterocytes in response to various *E. coli*, its role in the response of intestinal epithelial cells to bacterial infections, particularly *E. coli*, could be crucial (Savkovic *et al*., 1997, Elewaut *et al*., 1999).

These molecular mechanisms of pathogenicity following *E. coli* adherence and invasion of intestinal epithelial cells such as NF-κB activation are of major interest, with various immune factors, receptors such as TLRs and cytokine receptors thought to be involved. Good examples of these are interleukin-1 receptors and TNF receptors typically associated with the canonical NF-κB pathway (Rahman and McFadden, 2011, May and Ghosh, 1997, Le Negrate, 2012). It has been suggested that enteropathogenic *E. coli* (EPEC) can activate or suppress NF-κB depending on TLR signalling. Increased

TNF-α promoter activity in cells can be stimulated by bacterial isolates from IBD patients, suggesting TNF-α plays an important role in NF-κB-induced inflammation caused by *E. coli* strains associated with inflammatory disease (La Ferla *et al*., 2004, Wang and Hardwidge, 2012).

An experimental murine cancer metastasis model, in which mouse adenocarcinoma cells are injected into the tail vein of BALB/c mice to generate lung metastases, and whose growth is stimulated in response to injection of bacterial lipopolysaccharide (LPS), was used to investigate the role of NF-κB in inflammation-induced tumour growth. Results showed that LPS-induced metastatic growth response depended on both TNF-α production and NF-κB activation in tumour cells. In addition, inhibition of NF-κB in both colon and mammary carcinoma cells converts the LPS-induced growth response to LPS-induced tumour regression (Luo *et al*., 2004).

Molecular mechanisms linking bacterial infections, inflammation and cancer indicate certain strains of *E. coli* as a risk factor for CRC patients following the acquisition of virulence factors. One of these factors is a protein toxin named cytotoxic necrotizing factor 1 (CNF1) (Travaglione *et al*., 2008), which is reported to induce a long-lasting activation of NF-kB, as well as COX-2 expression, to protect epithelial cells from apoptosis and promote cellular motility. As cancer may arise through dysfunction of similar regulatory systems, *E. coli* infections associated with different virulence factors could contribute to tumour development in a similar fashion via other signalling pathways not yet proven in the *E. coli*-influenced colorectal disease.

1.11 Activation of Wnt signalling

Significant increases in COX-2 expression and activity, heavily involved in prostaglandin E_2 (PGE_2) synthesis, have been observed where cancer-associated *E. coli* have been studied in the context of CRC (Raisch *et al*., 2014, Abdallah Hajj Hussein *et al*., 2012, Lew *et al*., 2002). Studies of both CRC animal models and human CRC have shown a long-standing association with increased PGE_2 synthesis, and investigation of PGE_2 synthesis in the gut mucosa using mucosal biopsy specimens obtained during diagnostic colonoscopies show its role in the adenoma-carcinoma sequence (Pugh and Thomas,

1994). Intestinal polyps and adenocarcinomas were found to synthesise more PGE_2 than normal colonic tissues, but there was no difference found between polyps and adenocarcinomas. However, mucosal samples from colorectal cancer patients were found to synthesise more PGE_2 than both control and polyp-associated mucosa. These results suggested colorectal carcinogenesis via the adenoma-carcinoma sequence could be associated with a progressive increase in PGE_2 synthesis.

Canonical Wnt signalling typically begins when a Wnt ligand binds to a cell membrane spanning Frizzled (Fz) family receptor and/or low-density lipoprotein receptor-related proteins 5 or 6 (Flanagan *et al*., 2015a). Upon binding and subsequent activation, the cytoplasmic protein Dishevelled (Dsh) is recruited and activated. Activated Dsh associated with axin, causing inhibition of glycogen synthase kinase 3 (GSK3β). GSK3β normally phosphorylates the tumour suppressor APC, which acts as a negative regulator by phosphorylating β-catenin; GSK3β has also been shown to phosphorylate β-catenin directly. Phosphorylation of β-catenin is normally followed by its degradation within the proteasome. Inhibition of GSK3β or APC activity therefore allows β-catenin to accumulate in the cytoplasm, increasing chances of localisation to the nucleus (Coste *et al*., 2007, Kaler *et al*., 2012, MacDonald *et al*., 2009). The completion of this signalling cascade is dependent on the nuclear localisation of the protein β-catenin. Upon entering the nucleus, β-catenin activates transcription of downstream target genes via the lymphoid enhancer-binding factor 1 (LEF1) and T cell factors (TCF) 1, 3 and 4, with TCF4 reported to be responsible for Wnt-signalling in CRC (Van der Flier *et al*., 2007). Subsequent cellular responses associated with cancer, such as proliferation, adhesion and migration, occur following gene transduction via these TCF/LEF transcription factors.

Cyclooxygenase-2 (COX-2) and PGE_2 have been shown to stimulate colon cancer cell growth via the heterotrimeric guanine nucleotide-binding protein (G protein)–coupled receptor, EP2, by a signalling pathway involving the activation of phosphoinositide 3-kinase (PI3K) and the protein kinase Akt (**Figure 1.11;** Castellone *et al*., 2005). This has since been suggested to lead to the activation of the canonical Wnt signalling pathway, which may provide a new molecular framework for the future evaluation of *E. coli* infection in inflammation-associated colorectal cancer (Castellone *et al*., 2005).

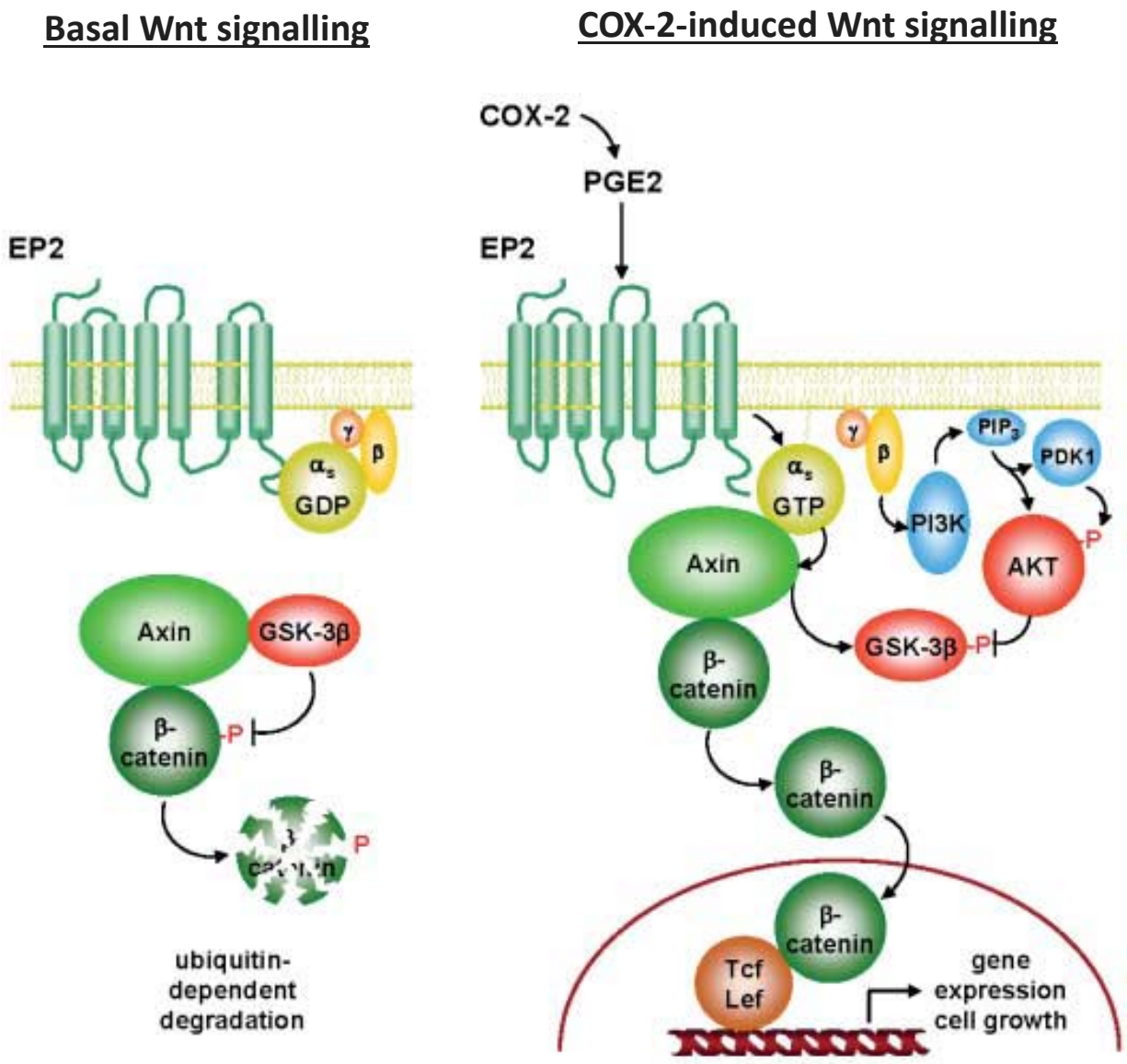

Figure 1.11. Activation of the Wnt signalling pathway by cyclooxygenase-2. In the basal state (left panel), the GSK-3β and axin protein complex promotes b-catenin phosphorylation, leading to ubiquitin-dependent degradation of β-catenin in the proteasome. Overexpression of COX-2 leads to increased production of PGE_2, which can activate EP2 receptors coupled to G proteins of the Gs family (right panel). Activation leads to the exchange of GDP for GTP, causing the alpha subunit of Gs protein to bind to axin. This promotes the release of GSK-3β from the inhibitory complex, with stimulation of the PI3K-Akt signalling route causing phosphorylation and further inactivation of GSK-3β. These events stabilise β-catenin nuclear translocation and lead to the expression of growth-promoting genes regulated by the TCF/LEF transcription factors. Adapted from (Castellone *et al*., 2005).

Wnt signalling through β-catenin is required for homeostasis and regeneration of the adult intestinal epithelium (Phesse *et al*., 2014). However, inappropriate levels of accumulated β-catenin in adult tissues are associated with development of a wide variety of cancers. Most sporadic colorectal cancers as well as familial adenomatous polyposis are linked to Wnt signalling, and in particular the loss of function of APC found in the majority of sporadic colorectal cancers (Kaler *et al*., 2012). β-catenin is frequently mutated in liver cancers and in some gastric adenocarcinomas (Coste *et al*., 2007). *APC* and β-*catenin* mutations both lead to stabilization of β-catenin and constitutive β-catenin/TCF transcriptional activity.

Disrupted Wnt signalling is currently considered as a major risk factor for colorectal cancer, but it is not the only contributor or requirement for tumour initiation and progression (Coste *et al*., 2007). Many studies have since focused on epigenetic changes in colorectal cancer and how environmental factors such as diet can influence colorectal cancer via changes in gene-expression. Epigenetic inactivation of inhibitors of the Wnt/β-catenin pathway is said to be associated with a tumour-favourable phenotypic outcome. Gene silencing through both DNA methylation and histone modification can cause loss of function of Wnt regulators such as SFRPs (Secreted frizzled-related proteins) and Dickkopf Wnt Pathway Inhibitor 3 (DKK3), as well as regulatory Wnt ligands such as Wnt5A, contributing to abberant Wnt signalling (Serman *et al*., 2014, Galamb, *et al*., 2016). Evaluation of the effects of *E. coli* in a similar context could reveal further links between bacteria and Wnt signalling. An interruption of normal Wnt signalling has been confirmed following *H. pylori* infection, with β-catenin identified as a specific host molecule influencing gastric carcinogenesis in conjunction with *H. pylori* infection (Polk and Peek, 2010). Nuclear accumulation of β-catenin has been shown to be increased in gastric adenomas compared with non-transformed gastric mucosa, which suggests that irregular Wnt-signalling precedes the development of gastric cancer.

Increased Wnt signalling has also been identified in intestinal cells following infection with *S. typhimurium*. This *Salmonella* was shown to upregulate several genes implicated in Wnt signalling (Liu *et al*., 2010). A *Salmonella* protein, AvrA, has been identified that modulates Wnt signalling, modifying

β-catenin, increasing total β-catenin expression, and activating Wnt/β-catenin transcriptional activity in intestinal epithelial cells. There is an increase in the number of stem cells and proliferative epithelial cells *in vivo* in intestine infected with *Salmonella* expressing AvrA. An interesting point was made linking Wnt pathway activation and of Notch pathway signalling, with noted modulation of Jagged1. Normally found at the base of crypts in the small intestine, Jagged1 was found distributed diffusely throughout crypts following Salmonella infection (Liu *et al*., 2010).

Enterotoxigenic Bacteroides fragilis (ETBF) has emerged globally as a cause of human diarrheal disease often accompanied by colitis (Housseau and Sears, 2010). Up to 35% of studied populations can carry ETBF without symptoms, which led to a hypothesis towards a secreted toxin. ETBF is now known to secrete the *B. fragilis* toxin (BFT), known to bind to colonic epithelial cells and stimulate cleavage of the tumour suppressor protein, E-cadherin (Rhee *et al*., 2009). E-cadherin cleavage can increase permeability of the intestinal epithelial barrier causing activation of the β-catenin/Wnt pathway and subsequent activation of c-Myc, inducing increased proliferation of colonic epithelial cells (Wu *et al*., 2003). BFT was also reported to be able to activate the NFκB pathway and induce the secretion of inflammatory cytokines, leading to the conclusion that ETBF are pro-inflammatory, oncogenic colonic bacteria. These examples show the influence of bacteria on both stem cells and epithelial cells throughout the gut, and show how bacterial infection can be linked to carcinogenesis. Important mechanisms by which bacterial agents may induce carcinogenesis include chronic infection, immune evasion and immune suppression. Bacterial infections can induce the release of cytokines such as reactive oxygen species, interleukins and cyclooxygenases from inflammatory cells, which can contribute to carcinogenic and mutagenic changes. Chronic stimulation of these substances has been shown to contribute to carcinogenesis (Mager, 2006).

Fusobacterium nucleatum infection, associated with colorectal cancer (CRC), is linked to adherence and invasion and induction of oncogenic and inflammatory responses to stimulate growth of CRC cells. *Fusobacterium nucleatum* infection is believed to occur through its unique FadA adhesin, which has been shown to bind to the protein E-cadherin, which can activate β-catenin signalling (Rubinstein *et*

al., 2013). The FadA gene levels in the colon tissue from patients with adenomas and adenocarcinomas are 10–100 times higher compared to normal individuals and this increased FadA expression in CRC correlates with increased expression of oncogenic and inflammatory genes. With similar traits to AIEC, it is possible that AIEC virulence factors could influence Wnt signalling in a similar manner. This suggests a mechanism by which bacteria can drive Wnt signalling and CRC, and these virulence factors could be a potential diagnostic and therapeutic target in CRC.

Recently, Frizzled receptors have been established as physiologically relevant receptors for colonic epithelial damage following *in vivo* infection with *Clostridium difficile* (*C. difficile*). The *C. difficile* toxin B (TcdB) is a critical virulence factor that causes diseases associated with *C. difficile* infection. TcdB has been shown to bind to a conserved binding site known as the cysteine-rich domain, with the highest affinity towards Frizzled receptors 1, 2 and 7 (Tao, et al., 2016). Interestingly, rather than activate these receptors, TcdB was shown to compete with Wnt ligands for binding, thus blocking Wnt signalling. Frizzled receptor knock-out in both *in vitro* and *in vivo* disease models showed less susceptibility to TcdB-induced tissue damage, suggesting that some bacteria can also negatively regulate the Wnt pathway (Tao, et al., 2016).

With a substantial body of evidence supporting the role of bacteria, particularly with a strong role for *E. coli*, in inflammation and intestinal disease, the inclusion of standard IBD and cancer therapies based on bacterial infections seems almost inevitable. Mucosa-associated *E. coli* have been shown to be able to produce an array of effects associated with many inflammatory and cancer pathways. Further investigation into these abilities, and potential involvement of additional cancer-promoting effects, may allow targeted treatment of bacterial contributors, or even combination therapies. This could be a reasonable approach to targeting this phenomenon, even solely based on current knowledge, in order to minimise the cancer risk now associated with *E. coli* infections.

1.12 Minimising the effects of mucosa-associated *E. coli* in colorectal disease

With several possible pathways available for *E. coli* to impact inflammation of the gut and increase the risk of colorectal disease, there is a strong need to understand and prevent this potential impact. This means that further studies are required to assess these pathways in order to understand where novel therapies could be introduced.

Limiting potentially pathogenic host-bacterial interactions is an important step. If the intestinal microbiota is kept at a distance from intestinal epithelial cells, it may be possible to minimise the likelihood of bacterial invasion (Brown *et al*., 2013). The mucus layer, antimicrobial peptides (AMPs) and innate lymphoid cells (ILCs) are just some factors helping gut tissue to avoid bacterial invasion whilst promoting mutualistic interactions with bacteria (Brown *et al*., 2013). However, it is possible that additional therapies focussing on bacterial interactions would be beneficial, and could prevent invasion of bacteria such as *E. coli*, and these studies are now being conducted.

One particular focus has been on antibiotic treatment of mucosa-associated *E. coli* in Crohn's disease. There is evidence of metronidazole with azathioprine and ornidazole treatment as prophylaxis limiting the postoperative recurrence of Crohn's disease, which could be beneficial in preventing IBD progression into CRC (D'Haens *et al*., 2008, Rutgeerts *et al*., 2005). Quinolone-based antibiotic regimens have also been effective in targeting intra-macrophage AIEC isolates *in vitro* (Subramanian *et al*., 2008), and antibiotic combination therapies such as ciprofloxacin, tetracycline, and trimethoprim could prove clinically relevant and reduce the risk of drug resistance, a problem that has been previously highlighted using Crohn's AIEC isolates (Dogan *et al*., 2013). However, drug-drug interactions could be a problem with combination antibiotics, meaning that alternative strategies maybe be necessary. Nitroimidazole compounds have shown efficacy in Crohn's disease, decreasing recurrence rates in operated patients. The use of metronidazole and ciprofloxacin is now also recommended in perianal disease. A major problem has been the appearance of adverse systemic effects limiting the long-term use of antibiotics as a preventative Crohn's disease therapy. However,

rifaximin, a semi-synthetic derivative of rifamycin, has given some promising results in inducing remission of CD with an excellent safety profile (Scribano and Prantera, 2013).

Studies suggest that targeting prostaglandin production can reduce the incidence of colorectal adenomas, colorectal cancer, and deaths from colorectal cancer. Recent studies are now being used to help explain the beneficial effects of non-steroidal anti-inflammatory drugs (NSAIDs) in animal models and human disease. With bacterial infections associated with increased inflammation and cyclooxygenase/prostaglandin production, the impact of infections in CRC, in particular IBD-associated CRC could be minimised by preventing inflammatory signalling.

COX-2 is overexpressed in early and advanced CRC tissues and indicates a poor prognosis (Brown and DuBois, 2005). Long-term intake of compounds inhibiting cyclooxygenases has been shown to reduce the overall relative risk for developing colorectal cancer (Gupta and Dubois, 2001), with selective COX-2 inhibitors now approved for use as therapy in patients with familial polyposis (Brown and DuBois, 2005). Their role is currently being evaluated for use in wider populations. Importantly, some selective COX-2 inhibitors appear to be relatively safe, which is important to allow large-scale clinical testing in healthy people (Dannenberg *et al*., 2001). Initial clinical trials using selective COX-2 inhibitors such as celecoxib have shown anti-tumour activity in patients with familial adenomatous polyposis and in preventing sporadic colorectal adenomas (Bertagnolli *et al*., 2006). Another study showed that use of celecoxib by patients at high risk for CRC was shown to significantly reduce adenoma burden detected, thus confirming that celecoxib can be used to prevent pre-malignant adenomas (Bertagnolli *et al*., 2006). Rofecoxib, another selective COX-2 inhibitor, was also found to reduce adenoma recurrence as well as the risk of advanced adenomas (Baron *et al*., 2006). Rofecoxib treatment was, however, associated with significant upper gastrointestinal events and serious thrombotic cardiovascular events; therefore, rofecoxib would unlikely be an attractive therapy.

Clinical studies suggest that regular use of aspirin may also decrease the risk of colorectal adenomas, the precursors to most colorectal cancers (Baron *et al*., 2003). A randomized trial of aspirin using

patients with previous colorectal cancer aimed to reduce recurrence of colorectal adenomas. The study was terminated early when statistically significant results were reported during interim analysis where adenomas were found in 17% of patients receiving aspirin and 27% of patients in the placebo group; the number of adenomas was also lower in the aspirin group, as was the time to the detection of a first adenoma was. Daily use of aspirin is associated with significant reduction in the incidence of colorectal adenomas in patients with previous colorectal cancer (Sandler *et al*., 2003).

Another method of reducing the downstream effects of prostaglandins would be to limit interactions with receptors. The predominant prostaglandin species in benign and malignant colorectal tumours is PGE_2, which is known to acts via four EP receptors, termed EP1 to EP4 (Hull *et al*., 2004). EP receptors have been identified as potential targets for prevention of a variety of cancers, including skin (Rundhaug *et al*., 2011), breast (Reader *et al*., 2011) and non-small cell lung cancer (NSCLC) (Gray *et al*., 2009).

Signalling through EP receptors has been linked to several cancer signalling pathways. EP2 receptor activation leads to GSK-3 phosphorylation, and subsequent inactivation (Fang *et al*., 2000), which has been linked to increased β-catenin/TCF transcriptional activity, however the relevance of EP2/EP4 receptor–induced β-catenin up-regulation in colorectal epithelial cells, which already contain only mutant APC, remains to be determined (Hull *et al*., 2004). EP4 receptor signalling can also lead to ERK signalling, with EP1 receptor activation and signalling also shown to activate ERK signalling in human colorectal cancer cells. With several studies showing that PGE_2 levels significantly increased in benign and malignant human and rodent colorectal tumours (Yang *et al*., 1998, Pugh and Thomas, 1994, Chiu *et al*., 1997) it would be beneficial to look at these receptors as a therapeutic target for colorectal cancers.

1.13 The important role of COX-2 and VEGF in colorectal disease

The role of COX-2 in CRC development and progression has been widely reported, with expression now an independent predictor of poor prognosis (Ogino *et al*., 2008). Recently, cancer-associated *E.*

coli strains have been shown to increase cyclooxygenase-2 (COX-2) expression and subsequent prostaglandin-E2 (PGE2) secretion from human macrophages due to their ability to survive and replicate within macrophages (Raisch *et al*., 2015). As previously described, COX-2 and PGE2 have the ability to stimulate colon cancer cell growth via activation of the G protein–coupled receptor EP2, which leads to activation of the Wnt signalling pathway via the inactivation of glycogen synthase kinase 3β (GSK3β), thus allowing the accumulation and increased nuclear localisation of β-catenin (Castellone *et al*., 2005). Alongside adherence and invasion factors, COX-2 induction associated with strains taken from CRC patients could be another important factor in determining the role of these bacteria in the development and progression of CRC.

Prostaglandin production is fast becoming a key focus in CRC diagnosis and treatment. Increased expression of prostaglandin-endoperoxide synthase 2 (PTGS2), also known as COX-2, leads to an increase in prostaglandin E2 (PGE2) production, promoting cancer cell growth via EP2 receptor-mediated signalling (Castellone *et al*., 2005). COX-2 targeted inhibition using NSAIDs such as aspirin reduces CRC incidence and improves clinical outcome following CRC surgery (Tougeron *et al*., 2014).

There is now evidence suggesting that inhibition of COX-2 using NSAIDs can down-regulate phosphatidylinositol 3-kinase (PI3K) signalling activity (Liao *et al*., 2012), which plays a major role in cell proliferation, adhesion, survival, and motility in many human cancers (Samuels *et al*., 2004). Activating mutations in the PI3K signalling pathway are now believed to be potential biomarkers for CRC, meaning that regular use of aspirin following CRC diagnosis is only associated with longer survival among CRC patients with aberrant PI3K signalling (Liao *et al*., 2012).

Another key modulator appears to be vascular endothelial growth factor (VEGF). Increases in VEGF gene and protein expression are widely conserved across most cancers, and is considered to be involved in metastasis and angiogenesis of colorectal cancer. Increases in *VEGFA* gene expression following mucosa-associated *E. coli* infection has been previously confirmed using real-time PCR (Prorok-Hamon *et al*., 2014), whilst citing previous links between inflammation and *E. coli* infections

leading to increases in VEGF and cancer progression (Cane *et al*., 2010, Waldner *et al*., 2010). Interestingly, interventions that either reduces the colonisation of gut tissues by these bacteria or block their interaction with the mucosa may have preventive or therapeutic effects in colon cancer and CD were suggested following this study. This further implicates the importance of the mucosa-association of these *E. coli* strains in the development and progression of CRC.

With antibodies against VEGF now being successfully investigated in advanced and metastatic colorectal cancer trials as adjuvant therapies, and with VEGF being induced by *E. coli* invasion in epithelial cells (Prorok-Hamon *et al*., 2014) this could reduce the impact of bacteria-induced CRC pathogenesis. Both VEGF and increased microvessel density (MVD) have been associated with greater incidence of CRC metastases and decreased survival, with meta-analysis performed on twenty studies focussing on VEGF and MVD. Increased levels of VEGF were associated with unfavourable survival, with a 4-fold increase in the rate of distant metastases. Similar analysis on studies for MVD showed that patients with high MVD expression in tumours again had poorer overall survival and disease prognosis. Results from this study demonstrate a strong indication of using VEGF and MVD as future prognostic biomarkers for CRC patients (Wang *et al*., 2014). Increased VEGF expression has recently been associated with the presence of the afimbrial adhesin operon in mucosa-associated *E. coli* in CD and colon cancer, correlating with diffuse adherence to and invasion of intestinal epithelial cells (Prorok-Hamon *et al*., 2014). The specific identification of VEGF expression in this case further supports the inclusion of VEGF as a future biomarker and a potential target for reducing the effects of mucosa-associated *E. coli* in CD and colon cancer.

Given the wider implications of COX-2 and VEGF in CRC, and the conserved nature of their increases following mucosa-associated *E. coli* infections, this became a clear focus for our project going forwards.

1.14 Modelling bacterial infections *in vitro* and *in vivo*

New models are currently being explored for the diagnosis of primary and metastatic colorectal cancer, which has represented one of the big challenges in the clinical management of patients. For example, the detection of circulating tumour cells is becoming a promising addition to current detection techniques, and testing this model experimentally as well as clinically has demonstrated its use as a relatively reliable prognosis tool to determine progression-free survival in metastatic CRC patients (Barbazan *et al*., 2012). If bacteria are shown to impact the development and progression of CRC, it would be beneficial to be able to model these effects in a similar way before trying to implement then clinically.

When choosing *in vivo* models for investigating the effects of bacterial infections in the development and progression of CRC, it is beneficial to consider the typical microbial composition given its implications in promoting and progressing intestinal disease. The murine microbiota is remarkably similar to that of the human gut, so studies performed in murine models *in vivo* will likely have translational implications relevant to the human disease (Arthur and Jobin, 2011).

There is also a necessary requirement to use better *in vitro* models to improve the translational approach to CRC treatment, with a number of advanced *in vitro* models now being pursued. The multicellular spheroid (MCS) model is an *in vitro* model highly representative of the avascular region of solid tumours, which reflects the micro-environmental conditions of tumours *in vivo*. This model is considered the most appropriate model for studying drug resistance, and has been used to compare the chemo-sensitivity of CRC cell line DLD-1 to 5-fluorouracil (5-FU) and differential protein expression in the 3D MCS model and 2D monolayers. The expression levels of several proteins such as p-mTOR decreased upon 5-FU exposure in 2D monolayers, while its level was higher in the 3D MCS model. The differential expression between the 3D MCS model and 2D monolayers suggests differences in signalling mechanisms in solid tumour microenvironments compared to traditional cell culture

methods for CRC cells, and this has been shown to be important in the modelling of existing CRC treatments (Lee *et al*., 2014).

A recent study developed a novel tumour model that permitted direct *in situ* visualization of *E. coli* in a 3D environment with epithelial-like B16.F10 melanoma cells (Elliott *et al*., 2011) to study proliferation and transport behaviours of *E. coli* in three-dimensional (3D) tumour environment. The findings from studies such as this will become increasingly useful for developing novel strategies to study the effect of bacteria in 3D tumour environments, and the impact of pathogenic bacteria in progressing CRC.

1.15 The potential impact of mucosa-associated *E. coli* on Wnt signalling

Increasing evidence suggests that constituents in the gut microbiota and chronic inflammation are involved in colorectal cancer (CRC) development. Gut inflammation creates an environment that supports tumour development by altering microbial composition. The dysbiotic microbiota is thought to contribute to the initiation and progression of CRC and our understanding of the microbiota could be essential for the management of colorectal disease (Perez-Chanona and Jobin, 2014). The contrast between the beneficial and detrimental roles of the microbiota during initiation, progression, and treatment of cancer further highlight the link between bacteria and cancer, and suggests that the microbiota could be considered as a key factor in the development and progression of colorectal disease.

With resultant expansion of, and contact with, specific bacteria such as *E. coli*, CRC has been associated with increased numbers of mucosal bacteria, particularly adherent and invasive mucosa-associated *E. coli*. A convincing body of evidence supports the influence of these *E. coli* in development and progression of CRC, with chronic infections highly likely to lead to the typical repercussions of chronic inflammatory disease. This promotion and progression of cancer is likely to be aided by pathogenicity and virulence factors. Disruption of cellular signalling pathways controlling inflammation and

tumorigenesis may also be involved, with preliminary data showing that AIEC can upregulate epithelial pro-inflammatory COX-2 and PGE_2 release.

The correlation between AIEC infection and cytokine production, particularly COX-2, in CRC patients suggests the need for additional investigation in order for therapeutic interventions to be better implemented, and the use of anti-inflammatory agents similar to those tested in clinical trials could limit the inflammatory driving force of COX-2 and prostaglandin production, thus potentially reducing proliferative and angiogenic effects, as well as risk of metastases.

High numbers of *E. coli* have been shown in the microbiota and within gut tissue in IBD and CRC patients. The impact of a number of factors are indicated for the progression of IBD-associated and sporadic CRC, and the potential impact of bacteria is suggested from as early as adenoma (sporadic) or low-grade dysplasia (IBD) through to carcinoma (see **Figure 1.3**). Our focus on the impact of *E. coli* in the development and progression of colorectal carcinogenesis stems from the accumulated data implicating *E. coli* in disease. With a number of pathogenic and virulence factors already highlighted as a potential link between *E. coli* and carcinogenesis, we wanted to be able to investigate this further, with a particular focus on pathways already heavily implicated in colorectal disease.

Due to the promising link between COX-2 and colorectal disease, and the suggested link between COX-2 and Wnt signalling, we chose to focus our efforts on this relationship, particularly looking at any impact on β-catenin activity. Wnt signalling helps regulate cell cycle and cell growth, whilst also playing a crucial role in colorectal tumorigenesis, so investigating whether AIEC possess ability to activate key cancer-promoting proteins within epithelial cells lining the bowel may allow further insight into the development, growth and spread of colorectal tumours. We therefore look to characterise Wnt signalling as a mechanism for malignant development in the intestinal epithelium following AIEC infection.

It is already evident that preventative measures limiting the availability of *E. coli* surface adhesion molecules could be achieved by targeting adherence factors; if pathogenic *E. coli* strains are unable to

adhere to epithelial cells in the gut, virulence and invasive factors are effectively nullified. However, to be able to target specific pathogenic factors carried by AIEC would require a better understanding of the factors involved specifically in development and progression of CRC. By using a combination of *in vitro* and *in vivo* techniques, including the introduction and implementation of novel three-dimensional colorectal cultures, further research into the impact of *E. coli* in CRC could add a more definitive insight into the translational effects of chronic infection, and where we could look to prevent these effects in the future.

Chapter 2:

Hypothesis

2.1 Hypothesis

Wnt signalling is a mechanism for malignant development in the intestinal epithelium following mucosa-associated *E. coli* infection.

Chapter 3:

Aims

3.1 Aims

1. To characterise the effects of mucosa-associated *E. coli* isolates from CRC and IBD patients on the activation of the Wnt signalling pathway *in vitro* using human CRC cell lines.
2. To evaluate the inflammatory response of human macrophage cells following treatment with mucosa-associated *E. coli* isolates from IBD and CRC patients.
3. To investigate the effects of mucosa-associated *E. coli* isolates from CRC and IBD patients on the activation of the Wnt signalling pathway *in vivo* using a germ-free *Il10*$^{-/-}$ mouse model of CRC mucosa-associated *E. coli* infection.
4. To sequence and analyse the DNA content of fosmid clones confirmed to up-regulate *PTGS2* (*COX-2*) gene expression *in vitro* in order to find common genes or operons responsible for or contributing towards expression changes.
5. To develop a 3D organotypic cell culture using a series of colorectal cell-lines at different stages of malignant transformation in the adenoma-carcinoma pathway.
6. To investigate the effects of mucosa-associated *E. coli* infection of 3D organotypic cell cultures on COX-2 expression and Wnt pathway activation.

Chapter 4:

Materials and Methods

4.1 Mammalian Cell Culture and Cell Line Maintenance

4.1.1 Cell Line Propagation and Maintenance

All cells were propagated from liquid nitrogen-stored stocks. Vials of frozen cells were thawed for 2 minutes at 37°C in a water bath before being added to the appropriate cell media as recommended by the European Collection of Animal Cell Cultures (ECACC) at the Public Health Laboratory Service (Wiltshire, UK). Cell suspensions were then centrifuged (300 x g) for 5 minutes forming a pellet to remove the 10% v/v dimethyl sulfoxide (DMSO, Sigma Aldrich; Poole, UK) used in cell freezing media. Cell pellets were resuspended in cell media and added to 25 cm^2 cell culture flasks and incubated at 37°C in a humidified atmosphere of 5% CO_2, 95% air.

For cell passage, media was removed and cells were washed with sterile 1X phosphate-buffered saline (PBS; Sigma Aldrich) at pH 7.4 pre-warmed to 37°C in a water bath. Cells were then detached by treatment with 1X trypsin-ethylenediaminetetraacetic acid (EDTA) solution, containing 0.25% (v/v) trypsin and 0.02% (w/v) EDTA (both Sigma Aldrich) in PBS pre-warmed to 37°C. Following detachment, trypsin was removed and washed out by the addition of an equal volume of foetal bovine serum (FBS)-containing cell media (10% FBS). The cell suspension was then mixed thoroughly and split at an appropriate ratio (between 1:3 and 1:20 depending on the cell type) into new cell culture flasks with fresh cell media.

4.1.2 Monolayer Culture of SW480 Colonocytes

The adherent human colonic epithelial cell line SW480 was derived from a Duke's type B colorectal adenocarcinoma removed from a 50-year-old male patient (Leibovitz *et al*., 1976). SW480 is one of the best characterized of the large number of established colorectal cancer cell lines, with numerous biochemical and genetic properties of this cell line previously reported (Yang *et al.,* 2006). This cell line was selected for use due to high basal Wnt signalling activity driven by an APC protein truncated at residue 1338 and therefore lacking the Axin binding domains (Yang *et al.,* 2006), as well as c-Myc

amplification and point mutations of the *KRAS* and *TP53* genes (Rochette *et al.,* 2005, Ahmed *et al.,* 2013).

The SW480 cell line (#87092801, ECACC) was maintained at 20-90% confluence in complete Dulbecco's Modified Eagle's Medium (DMEM, Sigma Aldrich) supplemented with 10% (v/v) FBS (Invitrogen; Paisley, UK), 100 U/mL penicillin and 100 µg/mL streptomycin (Sigma Aldrich). Cells were maintained at 37°C in a humidified atmosphere of 5% CO_2, 95% air.

4.1.3 Monolayer Culture of DLD-1 Colonocytes

The adherent human colonic epithelial cancer cell line DLD-1 was derived from a Dukes' type C colorectal adenocarcinoma removed from a 45-year-old male patient (Dexter *et al.,* 1981). Again, this cell line was selected for use due to high basal Wnt signalling activity driven by APC truncated at residue 1427 in DLD-1 cells, again resulting in loss of axin binding domains (Yang *et al.,* 2006). DLD-1 cells also present with point mutations of the *KRAS* and *TP53* genes, as well as *PIK3CA* gene mutation (Ahmed *et al.,* 2013).

The DLD-1 cell line (#90102540, ECACC) was maintained at 20-90% confluence in complete DMEM supplemented with 10% (v/v) FBS (Invitrogen), 100 U/mL penicillin and 100 µg/mL streptomycin (Sigma Aldrich). Cells were maintained at 37°C in a humidified atmosphere of 5% CO_2, 95% air.

4.1.4 Monolayer Culture of Stably Transfected HeLa TCF/LEF Luciferase Reporter Cells

The Human cervix epitheloid carcinoma HeLa cell line (Lucey *et al.,* 2009) stably transfected with pTA-TCF/LEF-luciferase reporter vector (which contains 6 repeats of TCF/LEF binding sites, a minimal promoter upstream of the firefly luciferase coding region firefly luciferase) was bought commercially (#SL-0022-FP; Signosis, USA). This was used as a reporter system to monitor TCF/LEF transcription downstream of β-catenin nuclear translocation. Cells were maintained at 20-90% confluence in DMEM supplemented with 10% (v/v) FBS (Invitrogen), 100 U/mL penicillin and 100 µg/mL streptomycin (Sigma Aldrich) at 37°C in a humidified atmosphere of 5% CO_2, 95% air.

4.1.5 Monolayer Culture of AA/C1 and AA/C1/SB Colonocytes

The premalignant human colonic epithelial cell line PC/AA and experimentally-transformed AA/C1 and AA/C1/SB cells were kindly donated by Professor Chris Paraskeva (University of Bristol, UK). The PC/AA cell line, established from a premalignant adenoma taken from a patient with familial adenomatous polyposis, was immortalised following *in vitro* passaging in combination with mouse NIH-3T3 fibroblast cells grown in collagen-coated flasks and used to produce clonogenic variants AA/C1 and AA/C1/SB (Williams *et al.,* 1990, Paraskeva *et al.,* 1988). Briefly, PC/AA cells were transformed into AA/C1 under standard culture conditions but in the absence of NIH-3T3 feeder cells and collagen-coating, with AA/C1 cells then transformed into AA/C1/SB cells following continued treatment with 1 mM sodium butyrate. AA/C1 cells remained non-tumourigenic, whereas AA/C1/SB cells showed tumourigenicity in nude mice, showing similar traits to adenoma and carcinoma cells, respectively (Williams *et al.,* 1990).

Both AA/C1 and AA/C1/SB cells required DMEM supplemented with 20% v/v FBS (Invitrogen), 2 mM L-glutamine (Sigma Aldrich), 100 U/mL penicillin and 100 µg/mL streptomycin (Sigma Aldrich), 1 µg/mL hydrocortisone sodium succinate (Sigma Aldrich) and 0.2 units/mL human insulin (Sigma Aldrich). Cells were maintained at 20-90% confluence in 25 cm^2 plastic tissue culture flasks at 37°C in a humidified atmosphere of 5% CO_2, 95% air.

4.1.6 Monolayer Culture of THP-1 Blood Monocytes

The human peripheral blood monocyte suspension cell line THP-1 (#88081201, ECACC) was originally derived from the peripheral blood of a 1 year old male with acute monocytic leukaemia (Tsuchiya *et al.,* 1980). THP-1 cells were maintained at approximately 20-80% density suspended in RPMI-1640 (Sigma Aldrich) supplemented with 10% (v/v) FBS (Invitrogen), 50 µM 2-mercaptoethanol, 100 U/mL penicillin and 100 µg/mL streptomycin (Sigma Aldrich) at 37°C in a humidified atmosphere of 5% CO_2, 95% air.

THP-1 monocytes can be differentiated into macrophage-like cells. THP-1 monocytes were differentiated into macrophages by treatment with 20 ng/mL phorbol myristate acetate (PMA) for 3 days. Enhanced differentiation of PMA-treated cells was also tested by removing the PMA-containing media and incubating the cells in fresh media for a further 5 days (Daigneault *et al.,* 2010). These cells were used to investigate the interactions between macrophage cells and mucosa-associated *E. coli* isolated from patients with IBD and CRC using a PGE_2 enzyme-linked immuno-sorbent assay (ELISA) similar to that used in a previous study (Raisch *et al.,* 2015).

4.2 Three Dimensional Organotypic Cell Culture

The development of a three-dimensional (3D) organotypic colonic tissue model using cells grown *in vitro* was established to mimic that of the host colonic tissue. This model was developed using the Rotary Cell Culture System (RCCS; Synthecon, US) as shown in **Figure 4.2.1**, and was used to develop colonic organotypic tissue cultures to investigate the adenoma-carcinoma sequence, as well as to assess the effect of *E. coli* infection on Wnt signalling.

Figure 4.2.1 Rotary cell culture system (RCCS) setup. The annotated image shows a typical RCCS setup using a 50 mL disposable culture vessels. The RCCS culture system (left) would be placed inside the incubator, with the control box (right) placed outside and linked via cable.

Briefly, colonocytes were added directly into 10 ml or 50 ml disposable vessels, or seeded onto diethylaminoethyl (DEAE) cellulose (Cytodex-1; C0646, Sigma-Aldrich) and collagen (Cytodex-3; C3275, Sigma-Aldrich) micro-carrier beads before being added to a rotary cell culture vessel, or were and attached to the RCCS before initiating rotation. SW480 colonocytes were used for initial testing, before also using the DLD-1 cell line and AA/C1/SB colonocytes. SW480 and DLD-1 cells were maintained in complete DMEM supplemented with 10% (v/v) FBS and 100 U/mL penicillin and 100 µg/mL streptomycin at 37°C in a humidified atmosphere of 5% CO_2 and 95% air, with AA/C1/SB also requiring 2 mM L-glutamine, 1 µg/ml hydrocortisone sodium succinate and 0.2 units/ml human insulin as used in monolayer culture.

Media was changed 72-96 hours after seeding, and then every 48 hours until cell aggregates were harvested. Periodic sampling following media changes allowed monitoring of cell aggregation, viability and morphology, as well as cell interaction with Cytodex-1 and Cytodex-3 coated cross-linked dextran micro-carrier beads using light microscopy (**Figure 4.2.2**). These micro-carriers were selected due to the high surface area to volume ratio and the specific bead coatings, which mimic the surface tension and adhesive surface for epithelial colonocytes *in vivo* (Goh *et al.,* 2013).

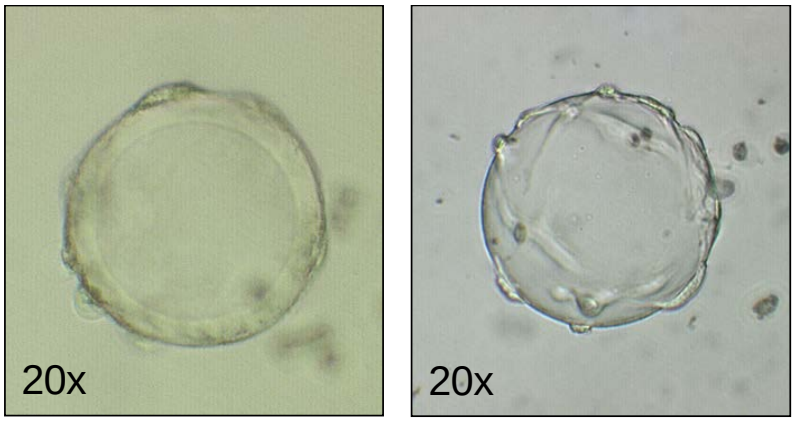

Figure 4.2.2 SW480 cells adhered to Cytodex-1 and Cytodex-3 microcarrier beads. Images show SW480 colonocytes adhered to Cytodex-1 (left) and Cytodex-3 (right) cross-linked dextran micro-carrier beads as viewed under light microscopy at 20x magnification.

Following cell culture using the RCCS, harvested cell aggregates were plated for *E. coli* treatment experiments or used to assess aggregate structure using haematoxylin and eosin (H&E) staining and immunohistochemistry (IHC). The use of this system for infection assays have been previously reported (Carvalho *et al.,* 2005, Barrila *et al.,* 2010).

4.3 Histological Processing

Organotypic 3D cell aggregates were washed and stored in sterile phosphate buffered saline (PBS; pH7.4) overnight to allow the aggregates to settle; this helped to avoid loss of harvested aggregates from processing cassettes. Cell aggregates were then suspended in 500 µL sterile Histogel (Thermo; Paisley, UK) heated until liquid, and left to cool until set solid. The Histogel cell suspension was then placed in histological processing cassettes. Cell aggregates were then processed overnight (see **Table 4.3**) using a Shandon 2LE tissue processor (Thermo Shandon; Runcorn, UK).

Table 4.3. Histological processing schedule for Histogel-suspended cell aggregates.

Step	Reagent	Temp	Time
1	70% ethanol	Room temp.	120 min
2	90% ethanol	Room temp.	120 min
3	100% ethanol	Room temp.	30 min
4	100% ethanol	Room temp.	30 min
5	100% ethanol	Room temp.	90 min
6	Xylene	Room temp.	30 min
7	Xylene	Room temp.	30 min
8	Xylene	Room temp.	40 min
9	Xylene	Room temp.	90 min
10	Wax	60°C	120 min
11	Wax	60°C	180 min

Cell aggregates were embedded within the histological processing cassettes using Surgipath Formula R paraffin wax (Leica; Milton Keynes, UK) in a Shandon Histocentre embedding system (Thermo Shandon; Runcorn, UK). For sectioning of the cell aggregates, the paraffin wax blocks containing the aggregates were cooled on ice for 30 minutes. Blocks were then sectioned by microtome at a thickness of 4 μm and floated in a heated water bath before adhering to glass slides; for immunohistochemistry, 3-aminoprpyltriethoxylsilane (APTS; 98-100%) coated slides were used (Fisher Scientific; Loughborough, UK). Slide-mounted sections were then dried in an oven at 37°C overnight.

4.4 Bacterial Cell Culture

4.4.1 Bacterial Strains

E. coli strains used were previously isolated from the colorectal mucosa of patients with CD, UC and CRC (Martin *et al.,* 2004). Briefly, this study had used human colorectal biopsy specimens washed in sterile saline and treated with dithiothreitol (DTT) solution to remove the overlying mucus layer. The resultant DTT solution was plated onto MacConkey agar and incubated at 37°C for 24 hours, with bacterial growth designated as mucus-associated. Following DTT treatment, biopsy specimens were then either treated with sterile saline or gentamicin (50 μg/mL) – the latter to kill any extracellular bacteria. Supernatant from the saline-treated biopsies were plated, with growth designated as mucosa-associated bacteria. Those biopsy specimens treated with gentamicin were lysed with sterile distilled water and plated onto MacConkey agar, with bacterial growth on these plates designated as being intracellular. Selected colonies were Gram stained; Gram-negative rods were further characterised using API bacterial identification tests (Bio-Merieux; Marcy L'Etoile, France) and pulsed-field gel electrophoresis (PFGE). Individual isolates (including those identified as *E. coli*) were stored as frozen cultures at -80 °C on Protect beads (#D535; Lab M, Manchester, UK). For the *E. coli* isolates used in this project, a number of relevant adhesion and invasion characteristics/virulence factors have been previously identified (Martin *et al.,* 2004, Prorok-Hamon *et al.,* 2014, Arthur *et al.,* 2012); these are summarised in **Table 4.4.1**. Strains were selected in order to cover different characteristics

associated with intestinal disease. The non-pathogenic *E. coli* K12 (#10798; ATCC), isolated from a stool sample of a patient convalescent from diphtheria (Bachmann, 1972), was used as a negative control throughout the project as a negative control, with no reported implications in intestinal inflammation or carcinogenesis.

Table 4.4.1. Summary of adhesion and invasion characteristics and virulence factors associated with *E. coli* strains isolated from patients. Adapted from Martin *et al*. 2004; Subramanian *et al*. 2008; Arthur *et al*. 2012; Prorok-Hamon *et al*. 2014.

E. coli strain	Patient	Mammalian cell interactions		Virulence genes/operons		
		I407 cells	HT29 cells	pks	afa	Other
HM44	Colon cancer	Adherence, invasion	Adherence	-	-	*fimH, lpfA*
HM95	Crohn's disease	Adherence, invasion	Adherence, invasion	-	-	*fimH*
HM250	Ulcerative colitis	*Data not available*	*Data not available*	-	-	*fimH*
HM251	Ulcerative colitis	Adherence, invasion	Adherence	+	-	*fimH, lpfA*
HM358	Colon cancer	Adherence, invasion	Adherence, invasion	+	+	*papC, fimH, lpfA*
HM545	Colon cancer	Adherence, invasion	Adherence	-	-	*papC, fimH, lpfA*
HM605	Crohn's disease	Adherence, invasion	Adherence	+	+	*papC, fimH, lpfA*
K12	Diphtheria convalescent	None identified	None identified	-	-	*fimH*
LF82	Crohn's disease	Adherence, invasion	Adherence, invasion	+	-	*fimH, lpfA*

4.4.2 Bacterial Growth and Culture

Individual *E. coli* strains were grown on solid culture on Luria Bertoni (LB) agar (5.0 g tryptone, 2.5 g yeast extract, 5.0 g sodium chloride, 7.5 g agar, 0.5 L Elga purified water) and incubated at 37°C overnight. Bacto™ agar, Bacto™ tryptone and Bacto™ yeast extract were supplied by BD Biosciences (Oxford, UK), with sodium chloride supplied by Sigma Aldrich. Following incubation, single colonies were removed from solid agar culture and suspended in sterile phosphate buffered saline (PBS, pH 7.4). The bacterial culture was centrifuged at 1,000 x g for 5 minutes and washed before being resuspended in sterile PBS or the appropriate assay culture medium before measuring absorbance (OD_{600nm}); average absorbance from 3 readings of suspension culture was used to estimate bacterial numbers in liquid cultures (OD_{600nm} = 0.6 equivalent to approx. 3 x 10^8 bacteria).

4.4.3 Fragmented *E. coli* HM358 DNA fosmid library of clones

A fosmid library of clones was previously created using the fragmented DNA from *E. coli* HM358 by Professor J. Marchesi at University College Cork (see (Prorok-Hamon *et al*., 2014). Fosmid clones were grown from frozen stocks in liquid-phase culture using LB broth (5.0 g tryptone, 2.5 g yeast extract, 5.0 g sodium chloride, 0.5 L Elga purified water) at 37°C overnight.

Briefly, LB broth was added to deep-well 96 well plates (500 µL per well), with one clone grown in each well. Plates were sealed using a slotted 96-well rubber seal to allow aerobic growth while eliminating the risk of cross-contamination and incubated at 37°C overnight. Following incubation, 200 µL samples were taken from 3 wells of each plate and diluted in 1800 µL PBS before measuring absorbance (OD_{600nm}). Average absorbance was used to estimate bacterial numbers in liquid cultures. These fosmid clones were used to screen for changes in cyclooxygenase-2 (*PTGS2*) gene expression in response to infection.

4.4.4 Bacterial Fosmid DNA Extraction and Purification

Fosmid DNA was extracted and purified from clones of the fragmented *E. coli* HM358 fosmid library showing >2-fold up-regulation of *PTGS2*. Extraction and purification of fosmid DNA was completed using the Plasmid Midi kit (Qiagen; Manchester, UK) following manufacturer guidelines.

This purification protocol uses a modified alkaline lysis procedure followed by the binding of DNA to resin under appropriate salt and pH conditions, with RNA, proteins and other impurities removed and DNA eluted. Briefly, selected clones were grown in a starter culture of LB broth under vigorous shaking conditions overnight at 37°C. The starter culture was then diluted 1/500 and left overnight under the same conditions. Cells were then pelleted by centrifugation at 1,000 x g for 15 minutes and lysed using Buffer P1 in combination with RNase A to remove and RNA contamination. Cell lysate was washed before precipitation of genomic DNA, proteins and cell debris. The precipitate was centrifuged at 1,000 x g for 30 minutes and supernatant containing plasmid DNA removed. Supernatant containing

plasmid DNA was bound to a pre-treated resin by gravity flow and washed with Buffer QC to remove any contaminants. The DNA was then eluted using Buffer QF, precipitated using isopropanol and centrifuged at 1,000 x g for 30 minutes. After removing the supernatant, the DNA pellet was washed in 70% ethanol and centrifuged at 1,000 x g for 10 minutes. The pellet was then air-dried for 10 minutes and DNA dissolved in Tris-EDTA buffer at pH 8.0 (10 mM Tris and 1 mM EDTA in distilled water; Sigma Aldrich).

4.5 Mammalian Cell Infections

In order to ensure consistent and accurate determinations of numbers of bacteria cells to use in mammalian cell infections, optical density curves were generated in order to estimate multiplicity of infection (MOI; **Figure 4.5**). Prior to cell infection, bacteria were removed from solid phase cultures, washed 3 times and re-suspended using sterile phosphate-buffered saline (PBS, pH 7.4). Cultures were then measured for absorbance (OD_{600nm}) to determine volumes of bacterial suspension to achieve the required MOI for the assay.

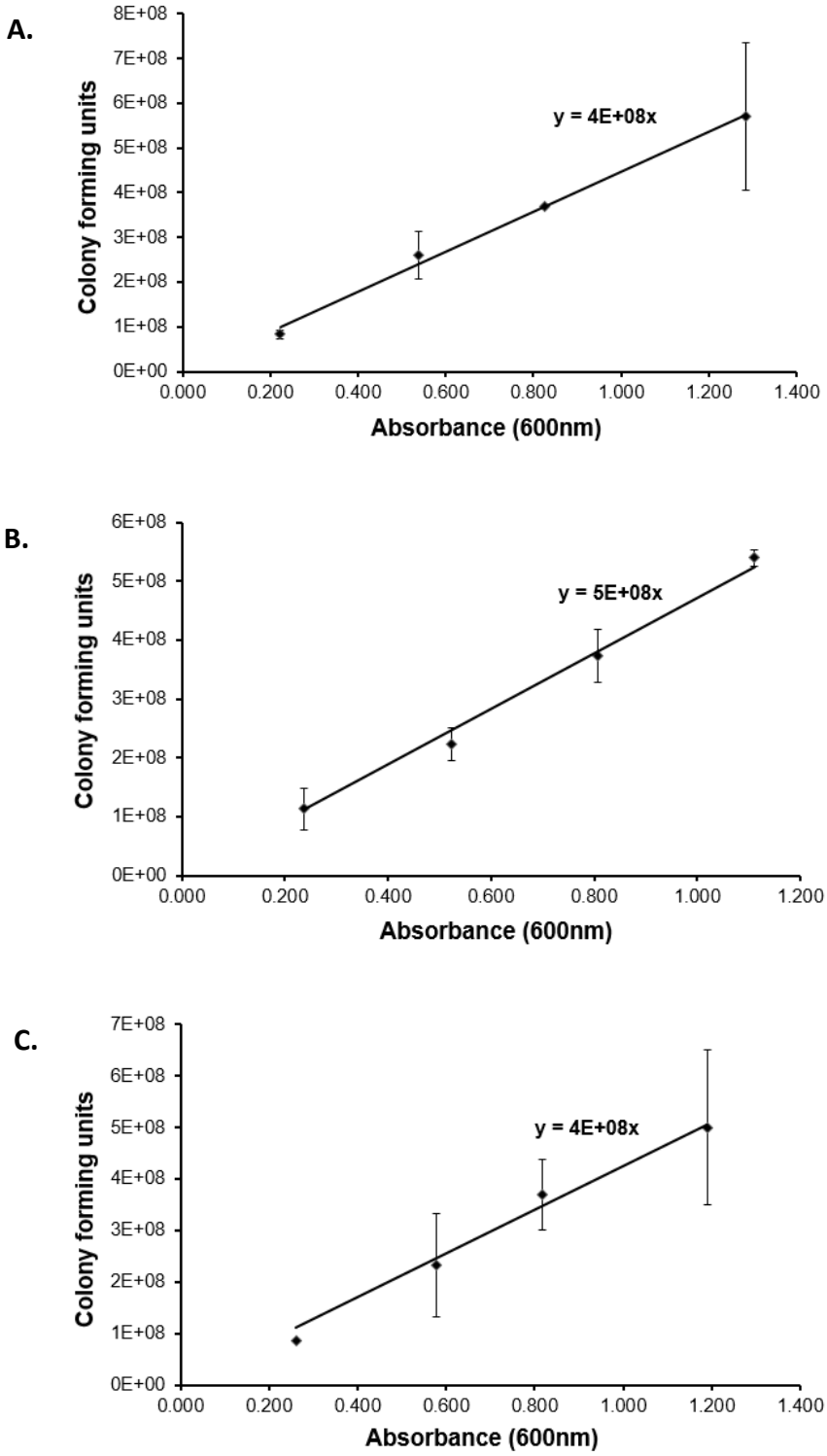

Figure 4.5. **Optical density curves for mucosa-associated and non-pathogenic *E. coli* isolates.** Dilutions of mucosa-associated *E. coli* isolates HM358 (A) and HM605 (B) and non-pathogenic *E. coli* K12 (C) were measured for absorbance (OD_{600nm}) and used to calculate colony forming units (N=1, n=3).

4.6 Quantitative PCR (qPCR)

4.6.1 RNA Extraction

SW-480, DLD-1 and AA/C1/SB cells were treated with *E. coli* isolates (MOI: 10) for up to 4 hours before lysis using Buffer RLT (Qiagen). RNA was extracted and purified using the RNeasy Kit (Qiagen). Briefly, lysed cell samples were homogenised using QIAshredder spin columns (Qiagen) and centrifuged for 2 minutes (13,000 x g) and transferred into spin columns. The homogenised samples were mixed with 70% ethanol and centrifuged for 15 seconds (13,000 x g). The sample then undergoes a series of additions that are applied to the spin column to bind RNA to the membrane and wash away any contaminants. High-quality RNA was then eluted in 50 µL RNase-free water and stored at -80°C. Before use, the concentration of RNA in each sample was quantified by absorbance spectrophotometry at a wavelength of 260nm using a Nanodrop Lite (Thermo Scientific; Loughborough, UK); RNA purity was also assessed by the 260/280 nm absorbance ratio, where an absorbance of ≥1.8 was considered adequate for use in qPCR.

4.6.2 Complementary DNA (cDNA) Synthesis

Random Hexamer cDNA synthesis was performed with 400 ng purified RNA from individual samples using a Transcriptor First Strand Kit (Roche; Welwyn Garden City, UK) as per the manufacturer's instructions. Briefly, RNA was incubated with random hexamer primers for 10 minutes at 65°C in a heat block before cooling on ice. Samples were then incubated with reverse transcriptase component mixture at 25°C for 10 minutes then 50°C for 60 minutes; the reaction was then stopped by incubation at 85°C for 5 minutes, with resulting cDNA stored at -20°C overnight.

4.6.3 RT^2 Wnt Signalling Target Gene PCR Array

cDNA (400 ng) was added to a 96-well Human Wnt Signaling Targets RT^2 Profiler PCR Array plate (SABiosciences; Manchester, UK) containing primers, specific to 84 Wnt target genes and 5 house-

keeping genes, and SYBR Green Mastermix. Real-time PCR (RT-PCR) assay was run using the LightCycler 480 (Roche) with the program outlined in **Table 4.6.3**, and absolute quantification completed using LightCycler 480 software (version 1.5). Analysis was then completed using the RT^2 Profiler PCR Array Data Analysis software (version 3.5, SABiosciences; http://pcrdataanalysis.sabiosciences.com/pcr/arrayanalysis.php).

Table 4.6.3. RT-PCR program for quantification using LightCycler 480.

Procedure	Cycles	Duration	Temp. (°C)	Analysis
Pre-incubation	1	10 minutes	95	None
Amplification	45	15 seconds	95	Quantification
		1 minute	60	
		1 second	72	
Melt Curve	1		95	None
Cooling	1	1 minute	30	None

4.6.4 Taqman qPCR

Real-time PCR (RT-PCR) was run with primers designed using the ProbeFinder system (Roche) and matched to the correct probe in the Human Universal ProbeLibrary (Roche). The concentration of each primer and probe was normalised (**Table 4.6.4**) for use in routine assays following optimisation. RT-PCR was run in 96-well format using TaqMan detection (LightCycler 480 Probes Master; #04902343001, Roche) and absolute quantification completed using the LightCycler 480 (Roche). Analysis was completed in Microsoft Excel (version Excel 2013), with target genes normalised to levels of beta-Actin (*ACTB*) or glyceraldehyde 3-phosphate dehydrogenase (*GAPDH*) house-keeping genes.

Table 4.6.4. Primer, probe and LightCycler 480 Probes Master assay conditions.

Reagent	Stock	Assay conditions
Forward primer	100 µM	300 nM
Reverse primer	100 µM	300 nM
UPL probe	10 µM	200 nM
LC480 Probes Master	2x	1x

Gene	Probe	Oligonucleotide sequence (5'-3')
ACTB	#64	fp: CCAACCGCGAGAAGATGA rp: CCAGAGGCGTACAGGGATAG
GAPDH	#75	fp: CCCCGGTTTCTATAAATTGAGC rp: CGAACAGGAGGAGCAGAGAG
PTGS2	#5	fp: GGATCTGTGGATGCTTCGTT rp: ACCCACAGTGCTTGACACAG
CTNNB1	#8	fp: TGTTAAATTCTTGGCTATTACGACA rp: CCACCACTAGCCAGTATGATGA

4.7 Protein determination using the Bradford Assay

Protein concentration of cell lysate was determined for use in immunoblots using the Bradford assay. Bovine serum albumin (BSA; Sigma Aldrich) protein was diluted in distilled water to create a standard curve from 0-2 mg/mL. BSA standards were then added in triplicate to a clear-bottomed 96-well plate alongside samples of cell lysate of unknown protein concentration diluted 1:10 (e.g. 2 µL in 18 µL distilled water), also in triplicate. After warming to room temperature, 250 µL Bradford reagent (Sigma Aldrich) was added to each well and incubated at room temperature for 30 minutes on a shaker. Following incubation, light absorbance at 595 nm was measured using the Tecan Sunrise plate reader (Tecan Group, Switzerland). A standard curve was plotted in Microsoft Excel using mean absorbance of known BSA standards. A linear trend line was added and line equation obtained, with the y-axis

intercept set as the mean absorbance for wells containing water only (0 mg/mL BSA). The standard curve line equation was then used to calculate unknown protein concentrations.

4.8 Immunoblotting

SW-480 and DLD-1 cells were treated with *E. coli* isolates (MOI:10) for up to 4 hours before lysis using radio-immunoprecipitation assay (RIPA) buffer containing 50mM Tris-HCl, pH 7.4, 150mM NaCl, 1mM EDTA, 1mM phenylmethylsulfonyl fluoride (PMSF), 1mM sodium fluoride, 1mM sodium orthovanadate, 1 µg/mL protease inhibitor cocktail (#P8340); all were obtained from Sigma Aldrich. Protein concentrations for lysate samples were determined by Bradford assay. Protein samples of known concentration were then loaded onto SDS-polyacrylamide gels (**Table 4.8**) alongside the Precision Plus Protein Kaleidoscope marker (#1610375, BioRad, UK).

Gels were run using a Mini-PROTEAN® Tetra Vertical Electrophoresis system (#1658005, BioRad) for 30 minutes at 50 V, then another 90 minutes at 100 V, with protein transferred using electroblotting for 60 minutes at 100 V onto nitrocellulose membrane. Membranes were incubated in blocking buffer (1% w/v BSA in PBS) before incubation with primary antibodies; monoclonal mouse anti-human β-catenin E-5 (#sc-7963, Santa Cruz via Insight Bio; Wembley, UK), monoclonal mouse anti-human cyclooxygenase-2 D-5 (#sc-514489, Santa Cruz) and monoclonal mouse anti-human pan-actin Ab-5 (#MS1295, Thermo) were used. Membranes were developed using SuperSignal West Dura solution (#34075, Thermo) and measured for luminescent signal using a ChemiDoc system (BioRad).

Densitometry was performed using ImageLab software (version 4.1, BioRad) measuring band intensities and normalising to the untreated control. Results were calculated as fold-change relative to untreated controls (designated as 1.0 fold-change). Immunoblot band intensities for COX-2 and β-catenin protein were then normalised to levels of pan-actin.

Table 4.8. Ingredients for polyacrylamide running and stacking gels.

Reagent	Running gel	Stacking gel
distilled water	7900 µl	6000
30% acrylamide:bis-acrylamide (29:1)	6700 µl	1330 µl
TRIS buffer (pH 8.8)	5000 µl	-
TRIS buffer (pH 6.8)	-	2500 µl
SDS (10%)	200 µl	100 µl
APS (10%)	200 µl	100 µl
TEMED	10 µl	10 µl

4.9 Cellular immunofluorescence studies to examine β-catenin nuclear localisation

SW480 and DLD-1 cells were fixed to 13 mm glass coverslips in a 12-well plate tissue culture plate (Corning, UK) at a cell density of 10,000 cells per well in 2 mL growth medium. After 48 hours, cells were gently washed with sterile PBS (pH 7.4). Cells were then cultured overnight in serum-free medium before being treated with *E. coli* isolates for 4 hours.

Following *E. coli* treatment, cells were washed with sterile PBS and incubated overnight in serum-free DMEM containing 50 µg/mL gentamicin (Sigma Aldrich) to enable visualisation of the β-catenin nuclear localisation effect of intracellular isolates, with prostaglandin E_2 (1 µM) treatment also left overnight as a positive control for β-catenin nuclear localisation. Cells were fixed using 100% methanol at -20˚C for 15 minutes before washing using sterile PBS. Cells were then permeabilised using PBS containing 5% w/v BSA and 1% v/v triton X-100 for 30 min, followed by three washes using sterile PBS. Blocking was then completed using PBS containing 5% w/v BSA overnight at 4 °C. Cells were incubated with primary mouse monoclonal IgG antibody for human β-catenin E-5 (#sc-7963, Santa Cruz) for 1 hour. Secondary fluorescein isothiocyanate (FITC) conjugated anti-mouse IgG antibody was then applied to slides in the dark for 1 hour before coverslips were mounted using Vectashield (VectorLabs, Peterborough) containing 4',6-diamidino-2-phenylindole (DAPI) to stain cell nuclei. After mounting, images were captured using AQM Advance software (version 6.0, Kinetic Imaging, UK) using a

fluorescence microscope (DAPI, excitation 405nm, emission 460nm; FITC, excitation 450nm, emission 535nm) and quantified using ImageJ 1.48v (NIH, USA; https://imagej.nih.gov/ij/download.html).

4.9.1 Using ImageJ to examine β-catenin nuclear localization

A user protocol was developed to be able to use ImageJ to quantify nuclear and cytoplasmic FITC staining indicating β-catenin localisation within each cell (for full user protocol, see **Appendix 1**). Briefly, each image containing DAPI and FITC overlay capture was opened in ImageJ, with colour channels split into red, green and blue channels. The channel images are transformed into greyscale, with the blue (DAPI) and green (FITC) channels retained and red channel discarded. Background fluorescence was then removed for both image channels. A pixel radius was set for each image as 50.0 pixels.

4.9.2 Defining nuclear and cytoplasmic regions of interest within ImageJ

In order to define nuclear regions of interest (ROIs), an untreated control image was used. Following channel splitting and removal of background fluorescence, the DAPI image was duplicated and used to define the 'max/min' greyscale thresholds. Image masks were then created to define nuclear ROIs, with dark pixel outliers removed (pixel radius of 2.0, and threshold of 10.0 used to remove dark pixel outliers). Following outlier removal, the mask particles were analysed; for dark stained nuclei, a maximum pixel size (250.0) minus 'infinity' (250-Infinity) was used, with any measure of circularity (0.00-1.00) included. This nuclear ROI was then added to the ROI manager, with the image mask shown to contain numbered nuclear ROIs. To define cytoplasmic ROIs, the green FITC image channel was duplicated and masked in the same way in order to define 'max/min' greyscale thresholds, this time using an inverted image showing FITC-staining as white pixels. The duplicated greyscale image was then matched to the FITC-staining of the unaltered image. Once matched, this threshold was then set for every subsequent image, including images of cell treated with *E. coli*. Nuclear staining was then removed using the thresholds set for nuclear ROIs, creating a new masked pixel image showing only

greyscale cytoplasmic staining. Image masks for nuclear and cytoplasmic staining were then saved and used to quantify ROIs.

4.9.3 Quantification of nuclear and cytoplasmic ROIs

The ROIs were quantified using the within the analysis section of ImageJ. This produces a 'Mean gray value', plus other measurements such as standard deviation, with labels for cytoplasmic and nuclear ROIs also displayed alongside the result. The results are then automatically exported as a table, which was used to quantify cytoplasmic and nuclear β-catenin staining. Cytoplasmic and nuclear ROI results were used to calculate a mean cytoplasmic and nuclear stain for all cells within each image, which was then used to give a ratio for 'nuclear:cytoplasmic' staining by dividing your mean nuclear stain by the mean cytoplasmic stain. These ratios were then used to compare β-catenin nuclear localisation in untreated control and cells treated with *E. coli* isolates (normalised to untreated controls). The ratios for nuclear:cytoplasmic staining for SW480 and DLD-1 cells were then plotted using Microsoft Excel.

4.10 HeLa cell TCF/LEF luciferase reporter assay

The established and commercially-available TCF/LEF luciferase reporter HeLa cell line stably transfected with a pTA-TCF/LEF-luciferase reporter vector contains 6 repeats of the TCF/LEF binding sites upstream of the firefly luciferase coding region (#SL-0022-NP-SIG; Signosis via Stratech Scientific, UK). These cells were used as a reporter system, monitoring the activation of β-catenin activity triggered by mucosa-associated *E. coli* infection.

Briefly, cells were seeded at a cell density of 10,000 cells/well in a clear bottom 96-well plate and incubated in serum-free DMEM overnight. Cells were then treated with *E. coli* isolates (MOI:10) for 4 hours. Following treatment, cells were incubated overnight in serum-free DMEM containing 50 µg/mL gentamicin (Sigma Aldrich) to allow any β-catenin nuclear localisation and subsequent transcription caused by intracellular bacteria before lysis using Passive Lysis Buffer (#E-1941, Promega; Southampton, UK); light microscopy was used to confirm complete cell lysis before transferring the

cell lysate to a white-walled 96-well plate (#3917, Corning). The lysate was then incubated with luciferase substrate (LUC100; Signosis, US), and the plate read immediately for luminescence at 550 nm using a luminometer (Tecan Infinite 200 Pro; Tecan UK Ltd, Reading, UK). Analysis was completed to give fold change data, with 10 mM lithium chloride (LiCl) used as a positive control (as recommended by the manufacturers), and 100 mM LiCl to induce cell death as a negative background luminescence control.

4.11 Prostaglandin E_2 enzyme-linked immuno-sorbent assay (ELISA)

The Prostaglandin E_2 (PGE_2) Express ELISA (#500141, Cayman Chemicals via Cambridge Bioscience; Cambridge, UK) was used to measure levels of PGE_2 in cell supernatant from human THP-1 monocyte-derived macrophage cells treated with *E. coli* isolates. This assay is based on competition between PGE_2 and a PGE_2-acetylcholinesterase conjugate (PGE_2 tracer) for a PGE_2 monoclonal antibody; any PGE_2-antibody complex formation is bound to a goat anti-mouse IgG attached to the well of the assay plate. Following washing, 200 µL Ellman's reagent, containing the substrate for acetylcholinesterase, is added to each well, with the product of the enzymatic reaction having a yellow colour that absorbs strongly at 412 nm.

Briefly, THP-1 monocytes at a cell density of $1x10^6$ cells in a 25 cm^2 flask were differentiated into macrophages by treatment with 20 ng/mL phorbol myristate acetate (PMA) overnight before *E. coli* treatment for 4 hours. Following treatment, cell supernatant and bacteria in suspension were removed and cells were incubated in serum-free RPMI-1640 containing 50 µg/mL gentamicin overnight. Cell supernatant was then removed for use in assay. Briefly, samples of cell supernatant were incubated with PGE_2 antibody and a tracer dye (supplied by manufacturer) in a plate coated with goat anti-mouse IgG (all included in the assay kit) for 1 hour. Wells were then washed before signal development using Ellman's reagent for 90 minutes. The plate was then read for absorbance at 405-420 nm using a Tecan Sunrise (Tecan). Absorbance measurements were compared to those obtained using PGE_2 standards (0 pg/mL – 2000 pg/mL; included in the assay kit).

4.12 *In vivo* modelling of mucosa-associated *E. coli* infection

4.12.1 Animal ethics

Animal models of intestinal inflammation and CRC are indispensable for our understanding of the pathogenesis of IBD and CRC in humans. Procedures were performed with ethical approval under appropriate UK Home Office and overseas institutional licences.

Wild-type C57BL/6 mice were maintained under specific pathogen-free conditions in the new Biomedical Services Unit (University of Liverpool), with wild-type controls sourced from either Charles River (Margate, UK) or the Walter and Eliza Hall Institute (WEHI). Dextran sodium sulphate (DSS) colitis-induction studies were performed under Home Office project licence 70/8457 held by Professor Mark Pritchard (Cellular & Molecular Physiology, University of Liverpool). Animals received 2% w/v DSS (MP Biomedicals, UK) in drinking water for 5 days followed by up to 16 days recovery, with body weight and severity of colitis assessed by Dr Carrie Duckworth (Cellular & Molecular Physiology, University of Liverpool) and scored using well established protocols (Wirtz *et al.,* 2007, Burkitt *et al.,* 2015, Williams *et al.,* 2016).

Apc mutant AhCre mouse studies, recommended for modelling CRC, were performed by Dr John Jenkins and Dr Cleberson Quieroz (Gastroenterology Research Unit, University of Liverpool). The *Apc* mutations induced in this model were the removal of the *Apc* gene using a loxP-flanked *Apc* allele ($Apc^{flox/flox}$), causing accumulation and subsequent nuclear localisation of β-catenin (Sansom *et al*., 2004), as well as mice harbouring one wild-type *Apc* allele and one *Apc* allele mutated at codon 850 ($Apc^{min/+}$).

4.12.2 Germ-free *Il10*$^{-/-}$ 129/SvEv mouse mono-association model

Mouse colonic tissue was kindly donated by Dr Janelle Arthur (University of North Carolina-Chapel Hill, USA). Experimental work utilising this tissue was completed with the aim of gaining insights into how *in vitro* changes could translate *in vivo*. Germ-free *Il10*$^{-/-}$ 129SvEv strain mice (n=17) were mono-

associated with *E. coli* HM44 for 6 weeks at the gnotobiotic facility at University of North Carolina (**Table 4.12.2**) with local ethical approval. Mice were colonized using cotton swabs soaked in an overnight culture of HM44 grown in Luria Broth from a glycerol stock. Stool pellets were collected at the conclusion of the experiment and plated on eosin-methylene blue agar plates (a selective stain for Gram-negative bacteria) to demonstrate *E. coli* colonisation (see **Figure 4.12.2**; courtesy of Dr Janelle Arthur). Colonic tissue was obtained from HM44 mono-associated mice (n=15 of 17) and germ-free controls (n=5). Tissue was formalin-fixed and paraffin-embedded before microtome-sectioning and processing. Dr Janelle Arthur (UNC-Chapel Hill, USA), had noted higher levels of inflammation and vascularisation of the colonic tissue of HM44 mono-associated mice (data not shown).

Table 4.12.2. Details of Germ-free *Il10*$^{-/-}$ 129/SvEv mice colonised with *E. coli* HM44.

Isolator	Strain	Cage	Date of Birth	Sex	Mouse #	Comments
New Hampshire	Il10-/- 129SvEv background	1	28/07/2011	F	1	
New Hampshire	Il10-/- 129SvEv background	1	28/07/2011	F	2	Large abscess throughout liver and in peritoneum with adhesions all within peritoneum
New Hampshire	Il10-/- 129SvEv background	3	28/07/2011	F	3	
New Hampshire	Il10-/- 129SvEv background	3	28/07/2011	F	4	
New Hampshire	Il10-/- 129SvEv background	4	08/12/2011	F	5	
New Hampshire	Il10-/- 129SvEv background	4	08/12/2011	F	6	
New Hampshire	Il10-/- 129SvEv background	5	08/12/2011	M	7	
New Hampshire	Il10-/- 129SvEv background	5	08/12/2011	M	8	
New Hampshire	Il10-/- 129SvEv background	5	08/12/2011	M	-	died 16-Mar-12
New Hampshire	Il10-/- 129SvEv background	6	10/11/2011	F	9	
New Hampshire	Il10-/- 129SvEv background	7	10/11/2011	M	10	
New Hampshire	Il10-/- 129SvEv background	7	10/11/2011	M	11	Abscesses found under peritoneum near scrotum
New Hampshire	Il10-/- 129SvEv background	7	10/11/2011	M	12	
New Hampshire	Il10-/- 129SvEv background	7	10/11/2011	M	-	died 16-Mar-12
New Hampshire	Il10-/- 129SvEv background	8	13/11/2011	F	13	
New Hampshire	Il10-/- 129SvEv background	9	13/11/2011	M	14	Abscesses in scrotum and bladder
New Hampshire	Il10-/- 129SvEv background	10	13/11/2011	M	15	

Figure 4.12.2. *E. coli* colonisation of HM44 mono-associated mice. Stool pellets collected at the conclusion of the experiment were plated on eosin-methylene blue agar plates to demonstrate *E. coli* colonisation. Image courtesy of Dr Janelle Arthur.

4.12.3 Haematoxylin and Eosin (H&E) Staining

Microtome-sectioned tissue was mounted on glass slides and placed in a slide rack. Tissue was de-waxed in xylene for 10 minutes before rehydration (2 minutes in 100% ethanol, 2 minutes in 90% ethanol, 2 minutes in 70% ethanol and 2 minutes in water). Slides were then placed in Gill no.1 haematoxylin (Sigma-Aldrich) for 3 minutes before running under tap water for 10 minutes. Slides were then placed in eosin (Sigma-Aldrich) for 3 minutes, then put immediately in water for 2 minutes before dehydration (20 dips in 70%, 90% and 100% ethanol). Slides were then transferred into xylene for 10 minutes and mounted onto glass coverslips (22x50mm) using DPX Mountant (Sigma Aldrich).

4.12.4 Immunohistochemistry

Microtome-sectioned tissue was processed for incubation with primary antibodies. Immunohistochemistry for cyclooxygenase-2 (COX-2) and β-catenin was performed using a 1:400 dilution of the COX-2 antibody (#ab15191, Abcam; Cambridge, UK) and 1:50 dilution of the β-catenin antibody (#610154, BD Biosciences); these dilutions were decided following antibody titration tests using available tissue. Heat-induced antigen retrieval was performed in citric acid buffer (pH 6.4). Images were captured using SPOT Image Capture Software (SPOT Imaging Solutions) on a light microscope (Leica, Germany); 5 images per slide were taken to ensure adequate coverage of the tissue section. Total epithelial and nuclear staining was evaluated using the IHC Profiler and ImmunoRatio plugins for ImageJ 1.48v. Scoring for total epithelial staining was done using the modified HSCORE method.

4.13 Statistics

N indicates number of independent experiments, whilst n indicates assay treatment replicates within an experiment. Tests for normality and equality of variances of control and treatment groups were performed using Shapiro-Wilk test and Levene's test respectively. Where appropriate, statistical analysis for independent two-sample studies was performed using Students' unpaired T test or non-parametric Mann–Whitney U test. For multiple treatment analyses, one way analysis of variance (ANOVA) or non-parametric Kruskal-Wallis ANOVA was performed as appropriate followed by pair-wise comparison of treatment means. All statistical analyses were completed using StatsDirect v2.6.2 software (Sale, UK). Differences were considered significant when $P<0.05$. Data is expressed as mean ± SEM except for *in vivo* scoring data, where median and interquartile ranges are stated.

Chapter 5:

Characterising *in vitro* changes in Wnt signalling following infection with mucosa-associated *E. coli* isolates from inflammatory bowel disease and colorectal cancer patients

5.1 Introduction

A growing body of evidence suggests that a change in the composition of gut bacterial communities in cases of chronic inflammation has a role in inflammatory bowel disease (IBD) and colorectal cancer (CRC) pathogenesis. Among the many changes in bacterial composition associated with colonic disease, an increased abundance of Gram-negative bacteria Enterobacteriaceae has been shown, with high numbers of *E. coli* found in colonic tissue biopsies taken from patients with IBD and CRC (Martin *et al*., 2004, Swidsinski *et al*., 1998, Viljoen *et al*., 2015). Mucosa-associated *E. coli* isolated from IBD and CRC patient biopsy tissue have been found to possess a number of virulence factors that increase their adherence and invasion to, and that enhance their genotoxic and angiogenic potential within, the colonic epithelium (Prorok-Hamon *et al*., 2014).

Similar mucosa associated *E. coli* strains have demonstrated an ability to survive and replicate within macrophages (Raisch *et al*., 2014). Macrophages are believed to be the predominant tumour-infiltrating cells that integrate signals present in the tumour microenvironment, leading to the secretion of molecules that support cancer progression. Elevated levels of cyclooxygenase-2 (COX-2) and prostaglandin E2 (PGE_2) can orchestrate the pro-cancer role of these macrophages, with COX-2 found elevated in the majority of adenomas and adenocarcinomas. Therefore, survival of these *E. coli* within epithelial and macrophage cells has been suggested as a driving factor in the development and progression of CRC.

Several bacteria have strong association with cancer in the gut, with the key example being *Helicobacter pylori* infection and increased risk of gastric cancer development (Polk and Peek, 2010). A number of mechanisms have been suggested to support gastric adenocarcinoma development (Kim *et al*., 2011), one of which is an increase in Wnt signalling via β-catenin accumulation in the epithelial cell nucleus as shown in animal models of gastric cancer (Polk and Peek, 2010). Similarly, other bacteria and bacterial products have been suggested to have an ability to activate the Wnt signalling pathway. In studies where human colonic cells were treated with S*almonella* typhimurium (Liu *et al*.,

2010) or the *Bacteroides fragilis* enterotoxin (Compare and Nardone, 2011), increased Wnt signalling was shown as defined by high levels of β-catenin nuclear localisation.

One suggested mechanism for the increase in Wnt signalling is increased levels of COX-2 enzyme leading to an increase in nuclear localisation of β-catenin (Castellone *et al*., 2005). In this scenario, bacteria with an ability to invade and survive within the gut mucosa cause increased, sustained release of inflammatory cytokines. This cytokine-induced release of cyclooxygenase 2 (COX-2) has been suggested to be an important factor, where high levels of COX-2 causes an increase in prostaglandin E_2 (PGE_2) that binds to the prostaglandin E_2 (EP_2) receptors (Williams *et al*., 1999b). Once activated, the EP_2 receptor causes the release of β-catenin from critical interacting partners axin and adenomatous polyposis coli (APC). With increased, sustained levels of COX-2, β-catenin accumulates in the cytoplasm, and translocates to the nucleus to induce downstream responses such as cell proliferation, invasion and migration.

With a number of bacteria already shown to increase Wnt signalling, it was understandable to predict that mucosa-associated *E. coli*, originally isolated in increased numbers from the mucosa of IBD and CRC patients, may have a similar effect. In this chapter, the role of these bacteria on Wnt signalling *in vitro* was investigated, with a particular focus on characterising the steps involved and the potential impact on the pathogenesis of colorectal cancer.

5.2 Hypothesis

Mucosa-associated *E. coli* play a role in increasing Wnt/β-catenin signalling and this is a key mechanism contributing to the development and progression of colorectal cancer.

5.3 Aims

1. To characterise the effects of mucosa-associated *E. coli* isolates from CRC and IBD patients on the activation of the Wnt signalling pathway *in vitro* using human CRC cell lines.
2. To evaluate the inflammatory response of human macrophage cells following treatment with mucosa-associated *E. coli* isolates from IBD and CRC patients.

5.4 Methods

An initial screen investigating Wnt-related gene expression using a Human Wnt Signalling Targets RT^2 Profiler PCR array containing 84 Wnt-relevant genes was completed using human CRC cell lines, SW480 and DLD-1, treated for 4 hours (MOI:10) with *E. coli* isolates HM44 and HM358 previously isolated from colonic mucosal biopsies from CRC patients, as well as with a non-pathogenic reference *E. coli* strain K12 (see Chapter 4.4.1) used as a negative control (see Chapter 4.6.3). Changes in Wnt-related gene expression found to be common to both cell lines and CRC *E. coli* isolates were then followed up for further evaluation using additional qPCR. Translation of these changes were investigated at protein level by immunoblotting (see Chapter 4.8) and by immunofluorescence detection of β-catenin nuclear localisation (see Chapter 4.9).

The downstream effect of an increase in *E. coli*-induced β–catenin protein changes was assessed using HeLa cells stably transfected with firefly luciferase reporter vector under the control of TCF/LEF transcription factor activity. Briefly, cells were treated with *E. coli* isolates from IBD and CRC patients for 4 hours (MOI:10) before overnight incubation in gentamicin-containing media. Cells were then lysed before addition of a luciferase substrate and luminescent signal measured using a luminometer (550 nm; for full details see Chapter 4.10).

Given that similar CRC mucosa-associated *E. coli* have been shown to survive and replicate within macrophages, increase COX-2 gene (*PTGS2*) expression and cause subsequent PGE_2 release using THP-1 monocyte-differentiated macrophage cells (Raisch *et al.*, 2015), we examined for the ability of our own IBD and CRC *E. coli* isolates to effect PGE_2 release from the same cell-line (see Chapter 4.11).

5.5 Results

5.5.1 Wnt-related gene expression is altered following CRC *E. coli* infection

To begin the study, we sought to identify early Wnt-related targets that could be impacted by intestinal cell infection by mucosa-associated *E. coli* from CRC patients. The Human Wnt Signalling Targets RT^2 Profiler PCR Array plate (SABiosciences) covering 84 Wnt signalling and target genes was used to gain an insight into the effect of CRC mucosa-associated *E. coli* infection on Wnt target gene expression. Significant changes in gene expression were observed following infection of SW-480 and DLD-1 colorectal cancer cells with CRC mucosa-associated *E. coli* isolates, HM44 and HM358, compared to uninfected controls (**Figure 5.5.1.1**).

A total of 12 genes were up-regulated more than 2-fold and 9 genes down-regulated more than 2-fold following infection of SW480 and DLD-1 cells with both CRC *E. coli* isolates (**Figure 5.5.1.2;** N=3 arrays per treatment). These altered genes play roles in proliferation, invasion, angiogenesis and migration. Only 3 genes were found to be commonly upregulated in response to both *E. coli* strains in both cell lines – the inflammatory and cell cycle regulating prostaglandin synthase-2 (*PTGS2*) gene encoding COX2; the *FOSL1* gene encoding Fos-like antigen 1 involved in cell proliferation and linked to bacterial infection; and *VEGF-A* encoding vascular endothelial growth factor-A involved in migration and angiogenesis (see **Table 5.5.1**). Other notable upregulated genes include those encoding transcription factor c-Myc, *MYC*, and connective tissue growth factor Wnt-inducible-signalling pathway protein 1, *WISP1*. Significant down-regulation of inhibitory Wnt genes such as *WISP2* was also shown, but with no common changes in *WISP2* expression observed between cell lines.

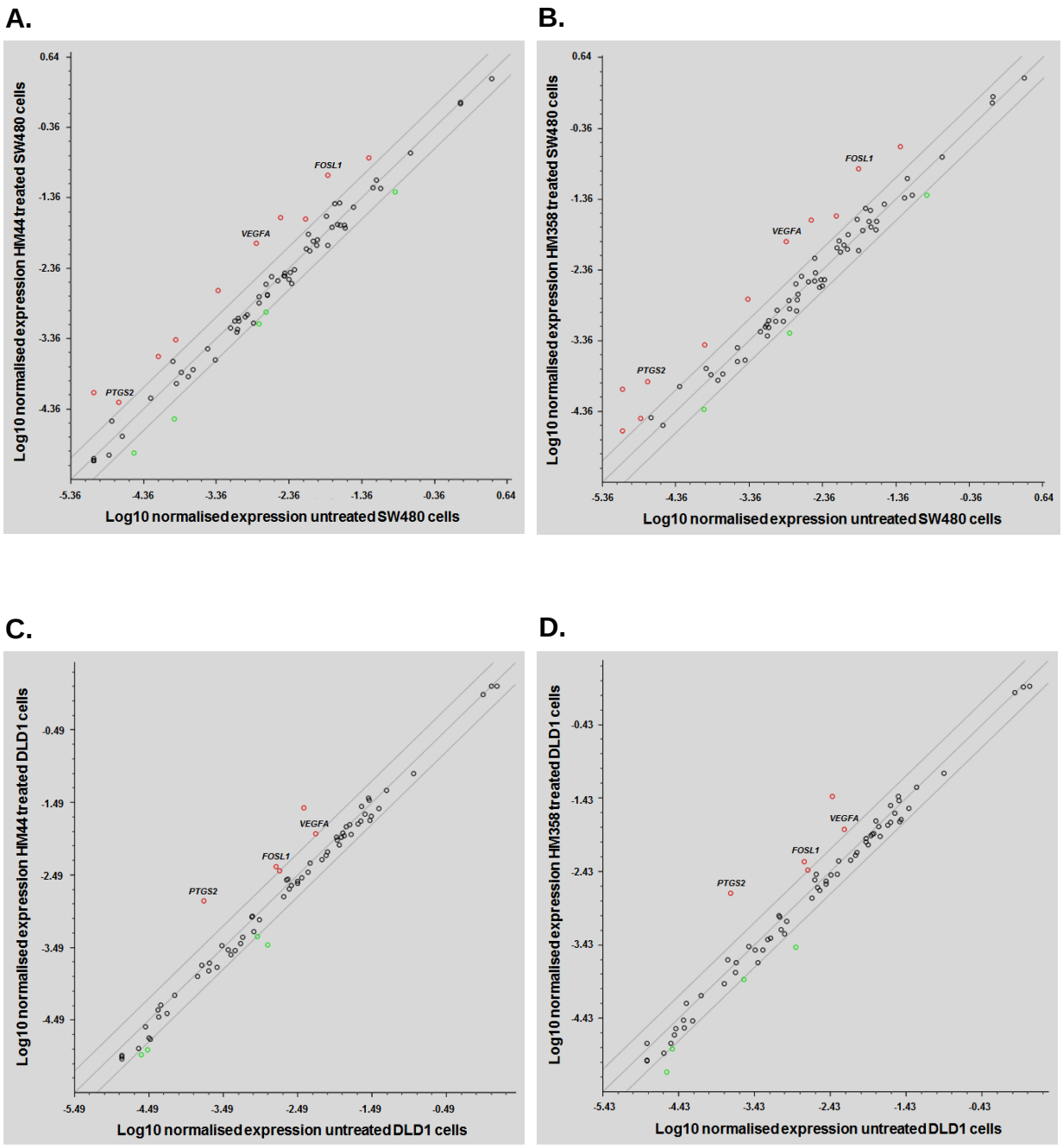

Figure 5.5.1.1. Wnt signalling target gene array profiling: changes in Wnt target gene expression following infection with mucosa-associated *E. coli*. Scatterplots show log10 expression of Wnt signalling target genes normalised to house-keeping gene *GAPDH* for SW480 (A and B) and DLD-1 (C and D) cells infected with *E. coli* HM44 and HM358 for 4 hours (MOI:10) before lysis (N=3 arrays per treatment). A total of 12 genes were up-regulated (red) and 9 genes down-regulated (green) more than 2-fold.

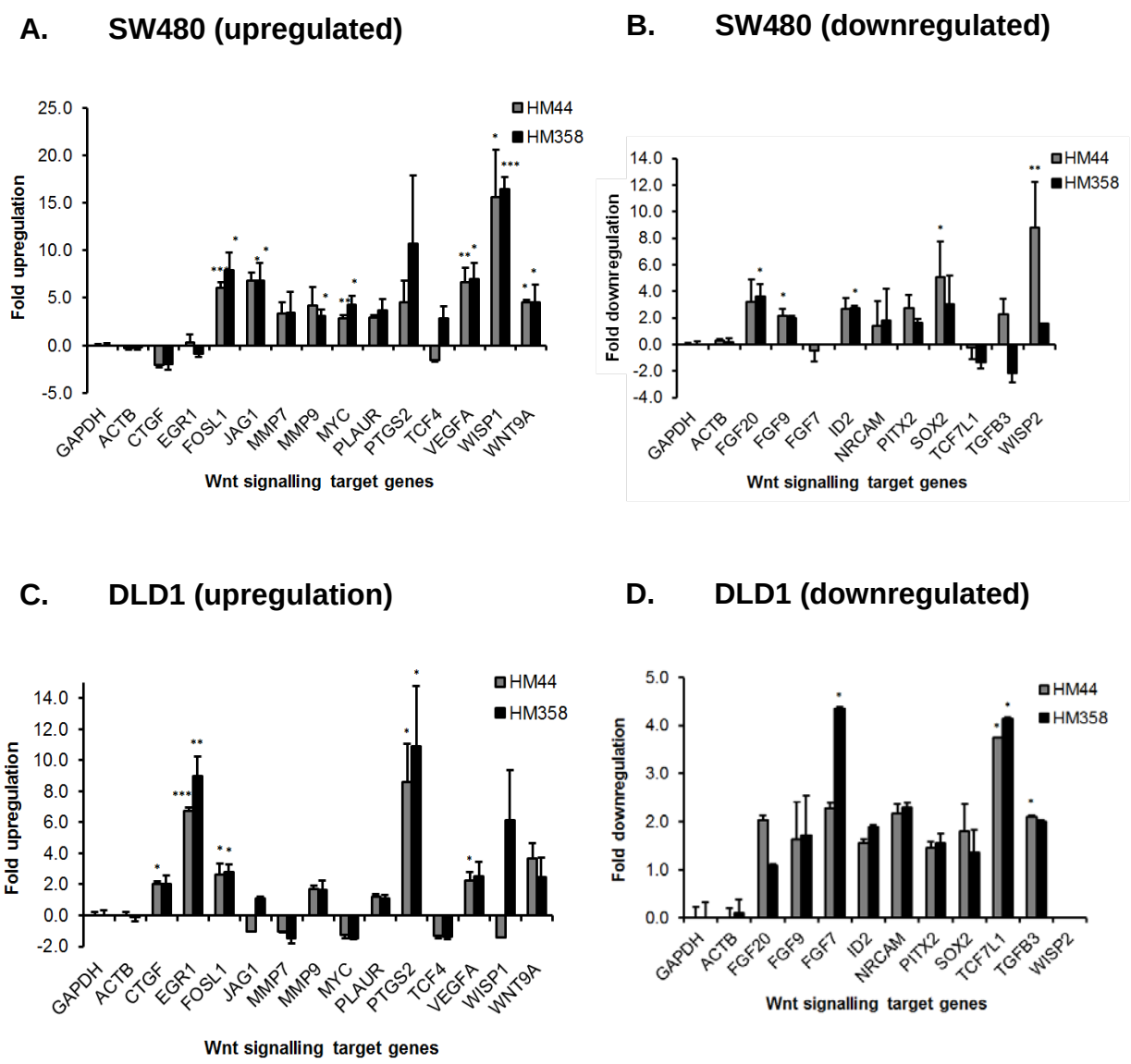

Figure 5.5.1.2. Wnt signalling target gene array profiling: changes in Wnt target gene expression following infection with mucosa-associated *E. coli*. Graphs show Wnt target gene up- and down-regulation following 4h infection with *E. coli* HM44 (grey) and HM358 (black) in comparison to untreated controls, normalised to GAPDH; (A) SW480 genes upregulated, (B) SW480 genes downregulated, (C) DLD1 genes upregulated, (D) DLD1 genes downregulated (N=3 arrays per treatment; Unpaired T-test: *P<0.05, **P<0.01, ***P<0.001). Genes included in graphs showed >2 fold change in one or both of the two cell lines tested. The unpaired T-test was completed using RT2 Profiler PCR Array Data analysis software version 3.5 (available from http://pcrdataanalysis.sabiosciences.com/pcr/arrayanalysis.php).

A.

Gene	Fold regulation (SW480 cells)					
	HM44	P	HM358	P	K12	P
FOSL1	6.08	<0.001	7.87	0.033	0.82	n/s
JAG1	6.81	0.010	6.77	0.047	0.75	n/s
MMP7	3.32	n/s	3.44	n/s	1.71	n/s
MMP9	4.17	n/s	3.11	0.019	0.60	n/s
MYC	2.88	0.003	4.30	0.013	0.71	n/s
PLAUR	2.96	0.001	3.68	0.043	1.09	n/s
PTGS2	4.53	n/s	10.67	n/s	0.49	n/s
VEGFA	6.61	0.033	7.02	0.033	0.86	n/s
WISP1	15.61	0.050	16.43	<0.001	3.19	n/s
WNT9A	4.50	<0.001	4.55	n/s	0.94	n/s
FGF20	-3.21	n/s	-3.61	0.037	2.37	0.045
FGF9	-2.18	0.020	-1.98	n/s	0.65	n/s
ID2	-2.68	n/s	-2.74	0.015	1.83	n/s
SOX2	-5.09	0.020	-3.01	n/s	1.89	n/s
WISP2	-8.82	0.009	-1.59	n/s	0.76	n/s

B.

Gene	Fold regulation (DLD1 cells)			
	HM44	P	HM358	P
CTGF	2.00	0.012	2.00	n/s
EGR1	6.71	<0.001	8.94	0.001
FOSL1	2.61	0.044	2.79	0.014
PTGS2	8.58	0.017	10.89	0.024
VEGFA	2.23	0.049	2.53	n/s
FGF7	-2.28	n/s	-4.36	0.031
NRCAM	-2.17	n/s	-2.29	n/s
TCF7L1	-3.75	0.030	-4.14	0.028
TGFB3	-2.10	0.027	-2.00	n/s

Table 5.5.1. Wnt signalling target gene array profiling: changes in Wnt target gene expression following infection with mucosa-associated *E. coli*. Table shows data for up-regulated (red) and down-regulated (green) expression of Wnt signalling target genes following 4h infection of (A) SW480 and (B) DLD1 cells with *E. coli* HM44, HM358 and K12 (SW480 only) in comparison to untreated controls and normalised to expression of house-keeping gene *GAPDH* (N=3 arrays per treatment). Unpaired T-test completed using RT2 Profiler PCR Array Data analysis software version 3.5 (http://pcrdataanalysis.sabiosciences.com/pcr/arrayanalysis.php).

The Human Wnt Signalling Targets RT2 Profiler PCR array was also conducted for SW480 cells infected with non-pathogenic *E. coli* K12, originally isolated from the stool of a convalescent diphtheria patient. Results showed only one gene to be significantly up-regulated; this was the *FGF20* gene which encodes fibroblast growth factor 20 (P=0.045), which was shown to be down-regulated following infection with the two CRC-associated *E. coli* strains (see **Table 5.5.1A**).

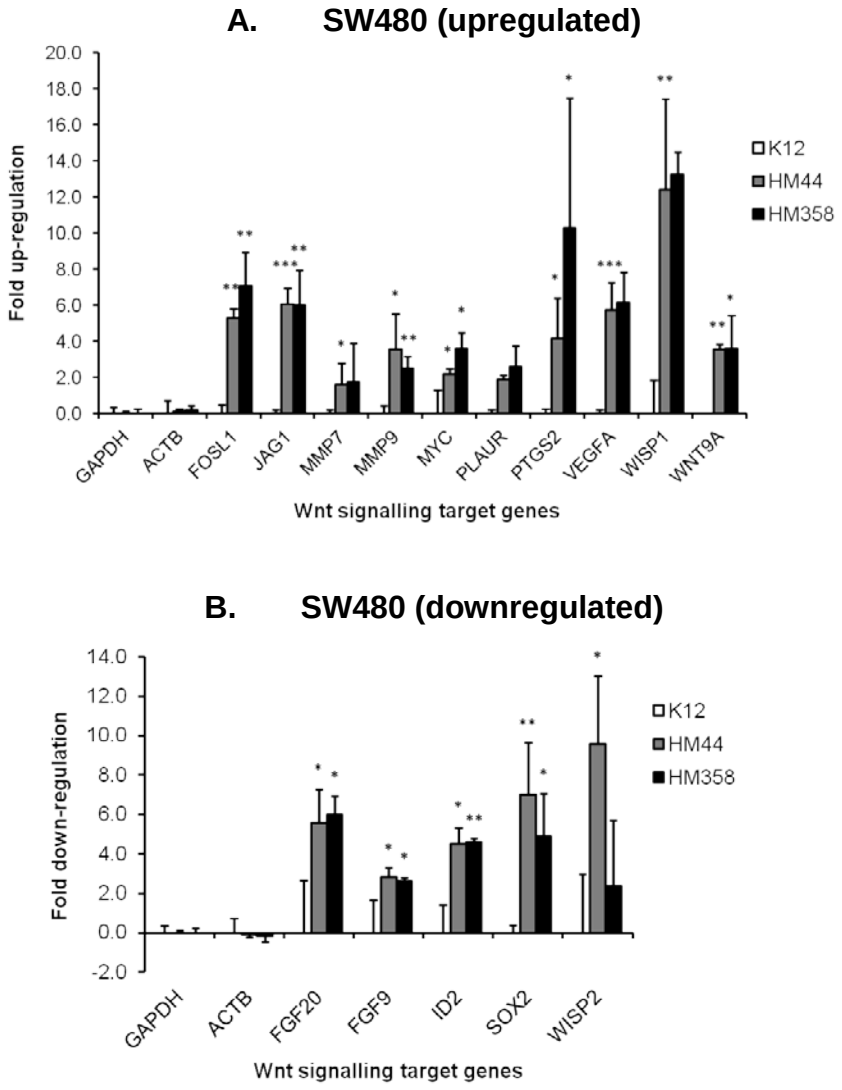

Figure 5.5.1.3. Wnt signalling target gene array profiling: changes in Wnt target gene expression following infection with mucosa-associated CRC *E. coli* isolates HM44 and HM358 and non-pathogenic *E. coli* K12. Graphs show Wnt target gene up-regulation (A) and down-regulation (B) following 4h infection with HM44 (grey) and HM358 (black), with HM44 and HM358 comparison to *E.* coli K12 controls, normalised to GAPDH. Genes included in graphs showed >2 fold change following treatment with *E. coli* HM44 and/or HM358 in one or both of the two cell lines tested (N=3 arrays; Unpaired T-test; *P<0.05 **P<0.01 ***P<0.001).

As the same Wnt gene effects were not shown following *E. coli* K12 infection, gene responses following infection with CRC-associated *E. coli* strains was then compared to those seen following infection with *E. coli* K12 (**Figure 5.5.1.3**). Significant differences in responses to infection suggested that induction of Wnt signalling was likely specific to infection with the CRC mucosa-associated *E. coli* strains. This observation was therefore followed up in later experiments where changes in protein levels were evaluated.

5.5.2 Time-dependent *PTGS2* and *CTNNB1* gene up-regulation assessed by Taqman qPCR

The COX-2 encoding gene, *PTGS2*, was commonly up-regulated in both SW480 and DLD-1 cell lines following infection with both CRC mucosa-associated strains HM44 and HM358. COX-2 up-regulation has been previously linked to increases in Wnt signalling (Castellone *et al*., 2005). These changes were subsequently confirmed by qPCR for *PTGS2* along with increased expression of the gene encoding β-catenin, *CTNNB1*, as a surrogate for Wnt pathway activation (**Figure 5.5.2**; N=3, n=3).

Using an infection time-course, we were able to see significant increase in *PTGS2* and *CTNNB1* expression following 2 hour (2h) and 4 hour (4h) infections of SW480 and DLD-1 cells with CRC mucosa-associated *E. coli* HM44 and HM358 (MOI: 10) compared to untreated controls from the same time-point. SW480 cells infected with *E. coli* HM44 and HM358 for 2h resulted in significant 2.7 ± 0.6 fold ($P<0.05$, Unpaired T-test) and 4.4 ± 0.8 fold ($P<0.01$) *PTGS2* upregulation respectively, whilst infection over 4h produced 8.1 ± 0.8 fold ($P<0.001$) and 9.2 ± 1.0 fold ($P<0.001$) levels of upregulation. Probing for *CTNNB1* expression showed a similar pattern; infection for 2h resulted in 0.9 ± 0.1 fold and 1.7 ± 0.3 fold changes, whilst infections over 4h showed significant 1.5 ± 0.2 fold ($P<0.05$) and 1.7 ± 0.2 fold ($P<0.01$) levels of *CTNNB1* up-regulation.

Similar results for both *PTGS2* and *CTNNB1* expression were also seen in DLD1 cells infected with *E. coli* HM44 and HM358. DLD-1 cells infected for 2h resulted in 4.8 ± 2.0 fold ($P<0.05$) and 4.3 ± 2.1 fold up-regulation of *PTGS2* respectively, whilst infection with the same strains over 4h resulted in 6.7 ± 0.6 fold ($P<0.001$) and 11.4 ± 1.5 fold ($P<0.001$) upregulation of *PTGS2*. *CTNNB1* expression

following 2h infection was not seen to be significant increased (0.8 ± 0.3 fold changes using both strains), but was significantly enhanced following infection for 4h with 3.1 ± 1.0 fold (P<0.05) and 4.0 ± 1.5 fold (P<0.05) upregulation respectively.

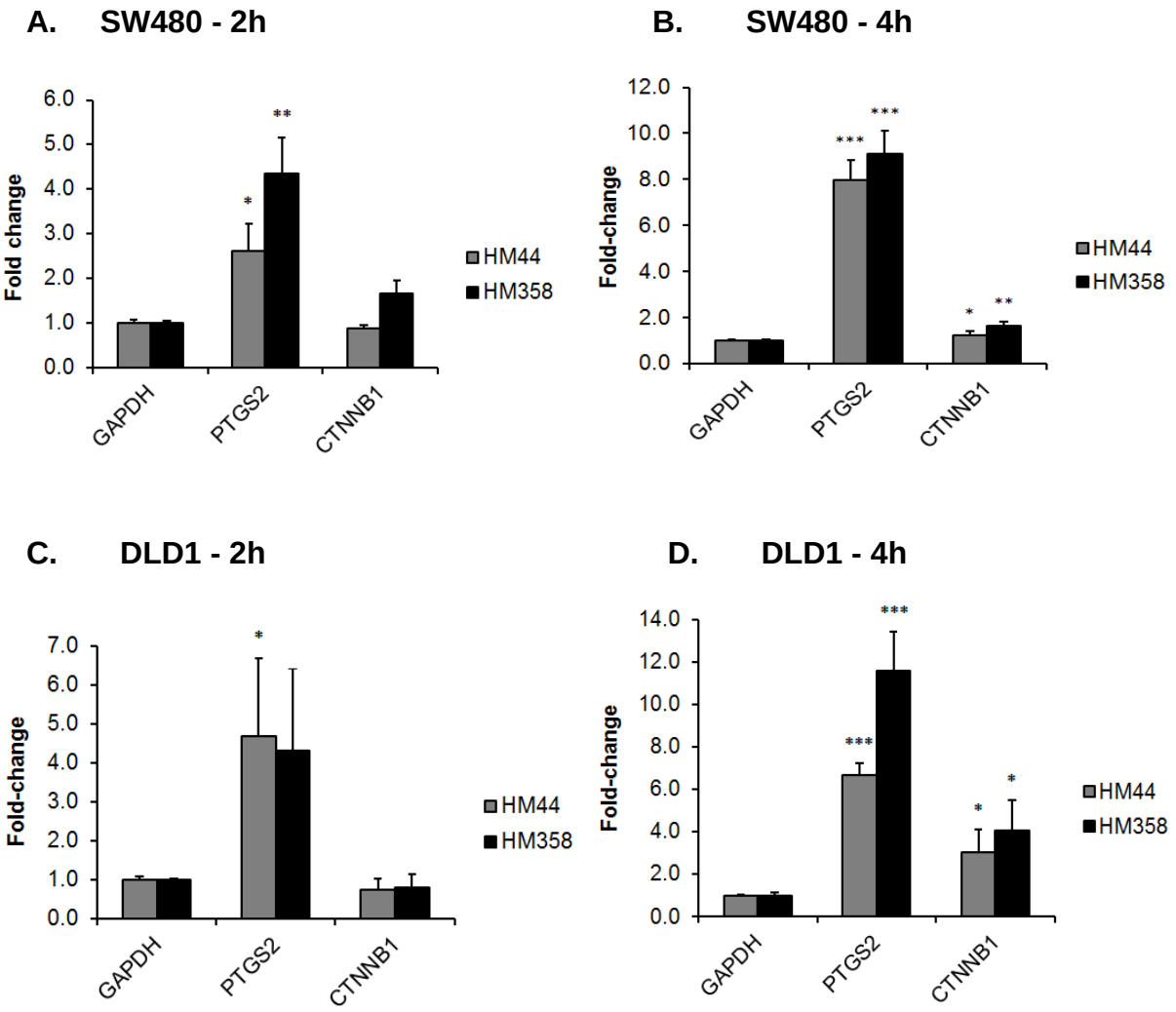

Figure 5.5.2. Time-dependent upregulation of human *PTGS2* and *CTNNB1* genes following mucosa-associated *E. coli* treatment as assessed by Taqman qPCR. Graphs show fold-change data for *PTGS2* (COX-2) and *CTNNB1* (β-catenin) gene expression following *E. coli* HM44 and HM358 infections for 2h and 4h in SW480 (A and B) and DLD1 (C and D) cells. Ct values were originally compared to those of untreated control samples before being normalised to *GAPDH* expression (N=3, n=3; Unpaired T-test; *P<0.05, **P<0.01, ***P<0.001).

5.5.3 Time-dependent increase in COX-2 and β-catenin protein expression in response to CRC mucosa-associated *E. coli* infection

Immunoblots were used to confirm that the increased gene expression of *PTGS2* and *CTNNB1* following CRC mucosa-associated *E. coli* infection translated into changes in protein levels of COX-2 and β-catenin respectively (**Figure 5.5.3.1**). Results show that CRC mucosa-associated *E. coli* infection increases expression of β-catenin in a time-dependent manner, and that this correlated with increased COX-2 protein expression in both SW480 and DLD-1 CRC cell lines.

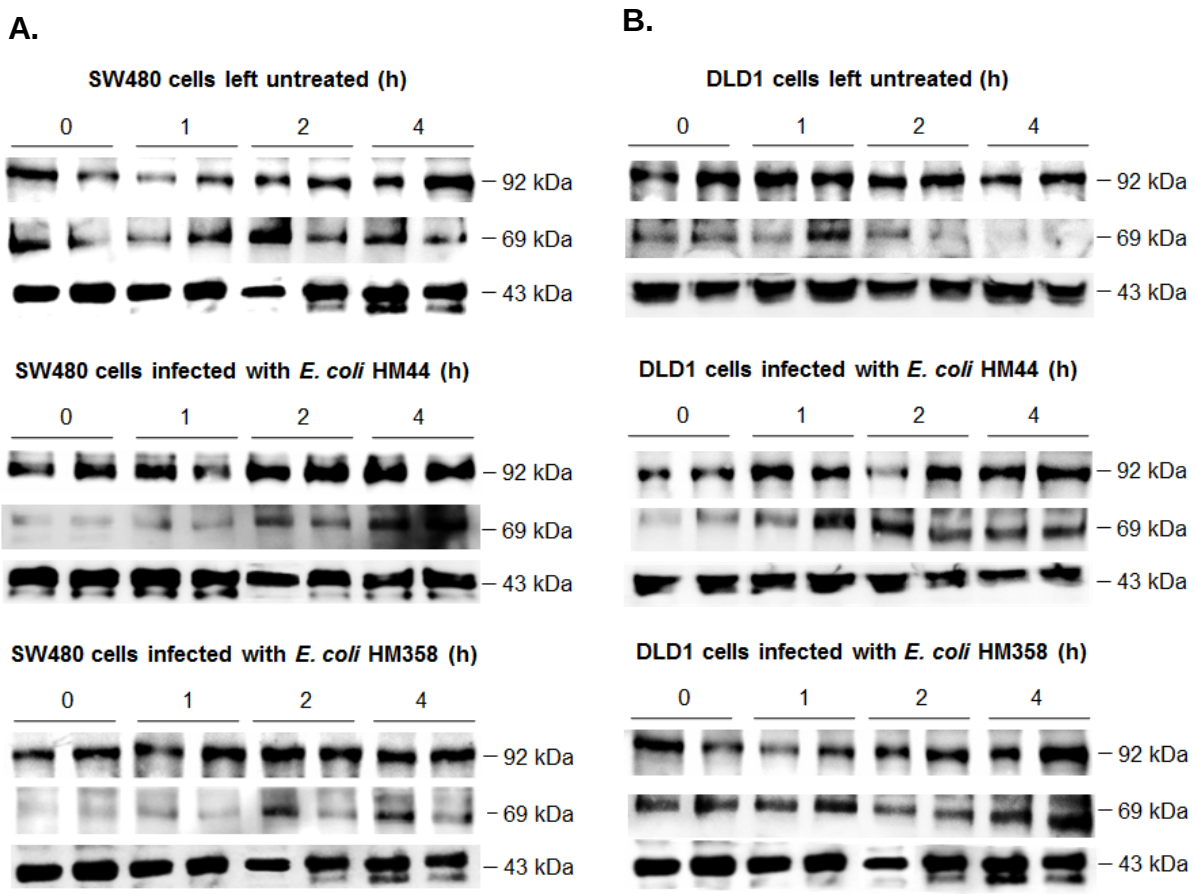

Figure 5.5.3.1. COX2 and β-catenin immunoblots using CRC cells left untreated and following infection with *E. coli* HM44 and HM358. Immunoblots show β-actin control (43 kDa), COX-2 (69 kDa) and β-catenin (92 kDa) protein in (A) SW480 and (B) DLD1 cells untreated and following *E. coli* infection (HM44 and HM358). The infection time-course was carried out over a period of 4 hours (N=2, n=2).

SW480 cells infected with *E. coli* HM44 and HM358 for 4h gave significant 5.7 ± 0.7 fold and 2.8 ± 0.0 fold respective increases in COX-2 protein levels compared to non-infected controls (both P<0.01) (**Figure 5.5.3.2A**). The HM44 and HM358 infections also resulted in significant 2.6 ± 0.1 fold (P<0.001) and 1.8 ± 0.2 fold (P<0.05) increases in β-catenin protein levels respectively (**Figure 5.5.3.2B**). Similar results were observed using DLD-1 cells, where the 4h infection with both *E. coli* strains again resulted in the highest fold-changes in both COX-2 and β-catenin protein expression.

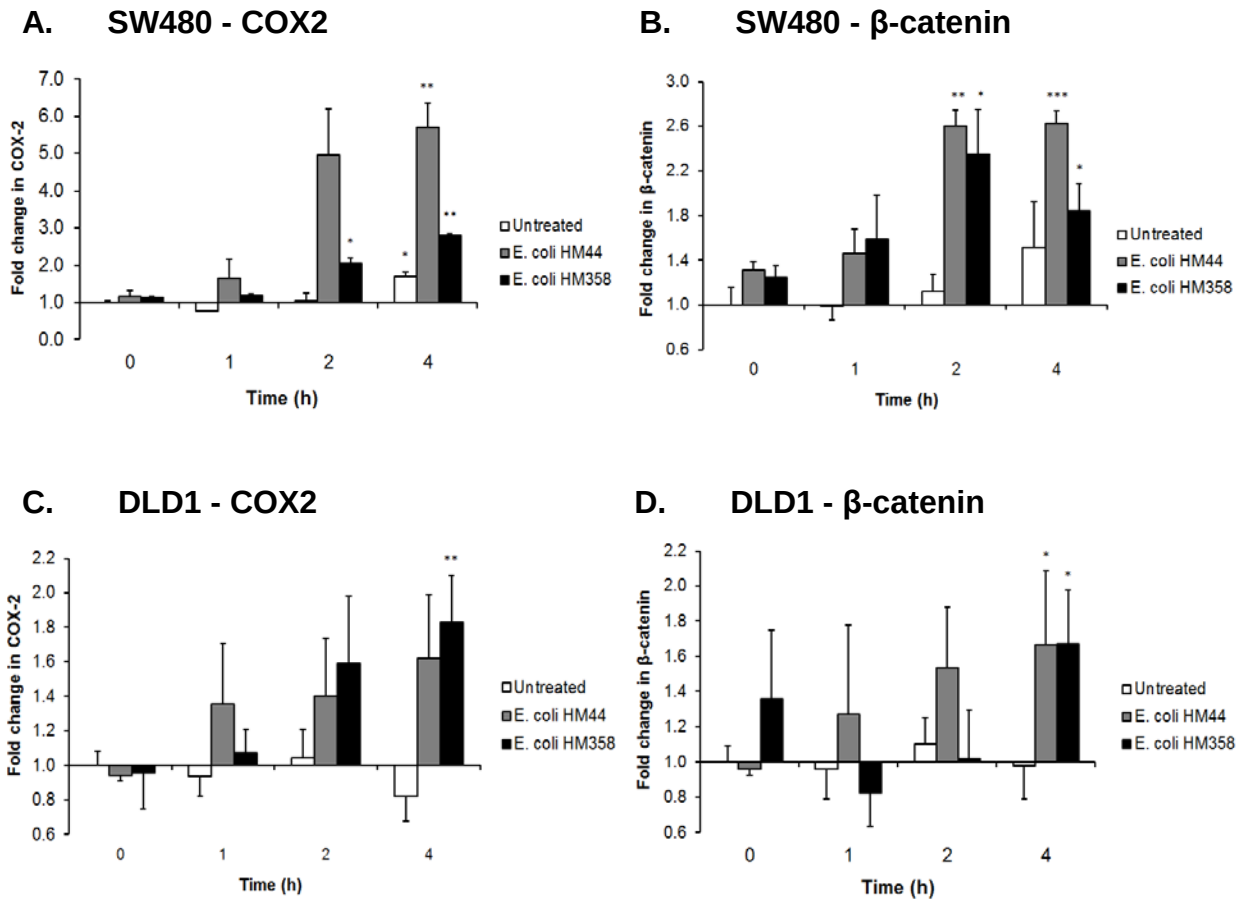

Figure 5.5.3.2. Increased COX2 and β-catenin protein levels in CRC cells following infection with *E. coli* HM44 and HM358. Immunoblots using lysates from SW480 and DLD1 cells left untreated and infected with *E. coli* HM44 and HM358 were analysed by densitometry. Protein levels for COX-2 and β-catenin in SW480 cells (A and B) and DLD1 cells (C and D) were shown to increase in a time-dependent manner following infection. COX-2 and β-catenin densitometry was normalised to changes in β-actin. Fold change was compared to untreated samples at 0h (N=2, n=2) (Unpaired T-test; *P<0.05, **P<0.01, ***P<0.001).

Following the findings that total COX-2 and β-catenin protein levels were significantly increased following CRC-associated *E. coli* HM44 and HM358 infection of colonocytes, the effects of other mucosa-associated *E. coli* strains were investigated. Another CRC mucosa-associated isolate, HM545, an isolate from a CD patient HM605, and the non-pathogenic *E. coli* K12 strain were used to infect SW480 and DLD1 cells in comparison to infection with CRC mucosa-associated isolates HM44 and HM358 (**Figure 5.5.3.3**) (N=2 experiments, n=2 replicates).

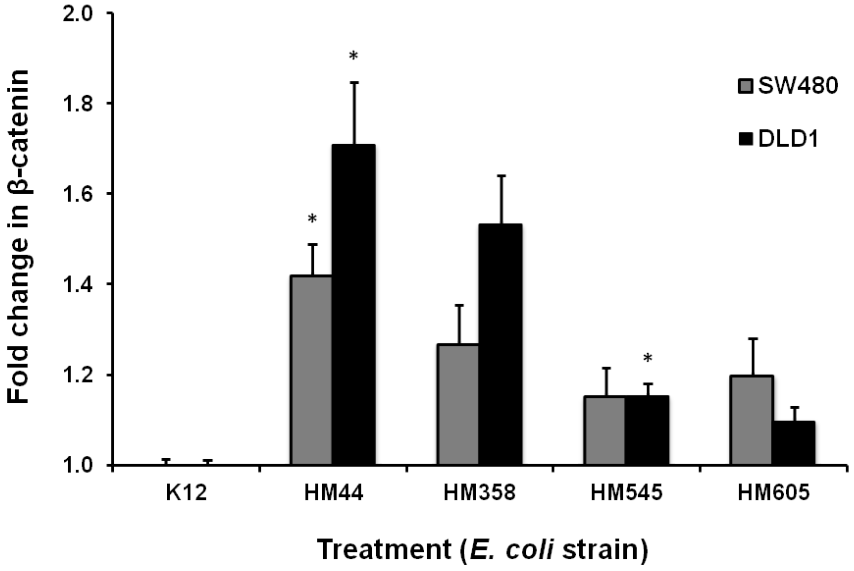

Figure 5.5.3.3. Changes in β-catenin protein levels in CRC cells following infection with CD and CRC mucosa-associated and non-pathogenic *E. coli* isolates. Immunoblots using lysates from SW480 and DLD1 cells and infected with *E. coli* HM44, HM358, HM545, HM605 and K12 for 4h were analysed by densitometry. Densitometry for β-catenin was normalised to β-actin levels. Fold change was statistically compared to *E. coli* K12 infected samples (N=2, n=2; Unpaired T-test, *P<0.05).

Densitometry results indicated that non-pathogenic *E. coli* K12 effected the smallest fold increase in β-catenin in both cell-lines tested (1.15 ± 0.05 fold and 1.14 ± 0.04 fold in SW480 and DLD-1 cells respectively). Results for *E. coli* HM44 and HM358 were similar to those seen previously (see **Figure 5.5.3.2**), with SW480 cells showing a slightly lower fold change in these experiments. CRC mucosa-associated *E. coli* HM545 showed 1.15 ± 0.06 fold (P=0.0670) and 1.15 ± 0.03 fold (0.0474) changes in

SW480 and DLD-1 cells, respectively, with CD-associated *E. coli* HM605 effecting 1.31 ± 0.08 fold (P=0.1296) and 1.19 ± 0.03 fold (P=0.0955) changes. These results would suggest that increases in COX-2 and β-catenin gene expression following CRC-associated *E. coli* infection translate into protein expression. However, the smaller increases in β-catenin protein expression obtained following infection with *E. coli* HM545 and CD-associated *E. coli* HM605 hinted towards a lesser impact on Wnt signalling with some isolates. This suggested that the trait may be shared by other inflamed mucosa-associated *E. coli*, rather than just those strains isolated from CRC patients, but that the extent of the impact on Wnt signalling may show variation. This was followed up by including more CD and UC isolates in later downstream Wnt signalling experiments (see Section 5.5.5).

5.5.4 Mucosa-associated *E. coli* isolates increase nuclear localisation of β-catenin in CRC cell-lines

Development of a Quantitative Immunofluorescent Cell Imaging Assay

Following the increases observed in both *CTNNB1* gene and β-catenin protein expression in response to CRC mucosa-associated *E. coli* infection, it was important to assess the extent of nuclear localisation of β-catenin following infection with these *E. coli*. To do this, SW480 and DLD-1 cells were treated with *E. coli* isolates from CRC patients (HM44, HM358 and HM545), as well as the colonic mucosa-associated *E. coli* isolate from a Crohn's disease patient HM605. Cells infected for 4h were fixed to glass coverslips and assessed for nuclear localisation of β-catenin. DAPI stain was utilised to identify the cell nucleus. Separate high-power field images (5 images per slide) split into FITC (β-catenin) and DAPI (nucleus) channels were then taken and used to produce a DAPI/FITC composite or overlay image. This allowed analysis of each image for both nuclear and cytoplasmic localisation. An automated system of image analysis was developed using the public domain image analysis software Image J (v1.45s, National Institutes of Health, Bethesda, Maryland, USA) as previously published (Noursadeghi *et al*., 2008) in order to remove bias and subjectivity, and negate the impact of using

staining intensity as the sole measure to be quantified. High-quality staining was achieved in both SW480 and DLD-1 cells, which can be seen in **Figures 5.5.4.1 and 5.5.4.2** respectively.

An automated scoring technique was developed and initially employed for DAPI/FITC composite images of both untreated SW-480 and DLD-1 cells. The same thresholds were then applied to cells treated with *E. coli* isolates. The full optimised protocol for scoring can be found in Chapter 4.9 and Appendix 1. Briefly, each composite image was split into channels showing green (FITC) and blue (DAPI). Background fluorescence was the removed using a radius of 50.0 pixels. Regions of interest (ROI's) were then defined for nuclear and cytoplasmic cell regions to measure the extent of β-catenin immunofluorescence in these regions. A ratio of nuclear:cytoplasmic signal was then calculated for each treatment condition and compared to *E. coli* K12 infected controls.

Increased* β*-catenin nuclear localisation in response to mucosa-associated E. coli infection

Localisation of β-catenin was assessed by scoring both nuclear and cytoplasmic FITC-staining, allowing a ratio of nuclear:cytoplasmic β-catenin to be calculated for both SW480 and DLD-1 cells (**Figures 5.5.4.1 and 5.5.4.2**). Importantly, significantly increased nuclear localisation was shown to occur following infection with either CRC or CD mucosa-associated *E. coli* (N=3, n=2).

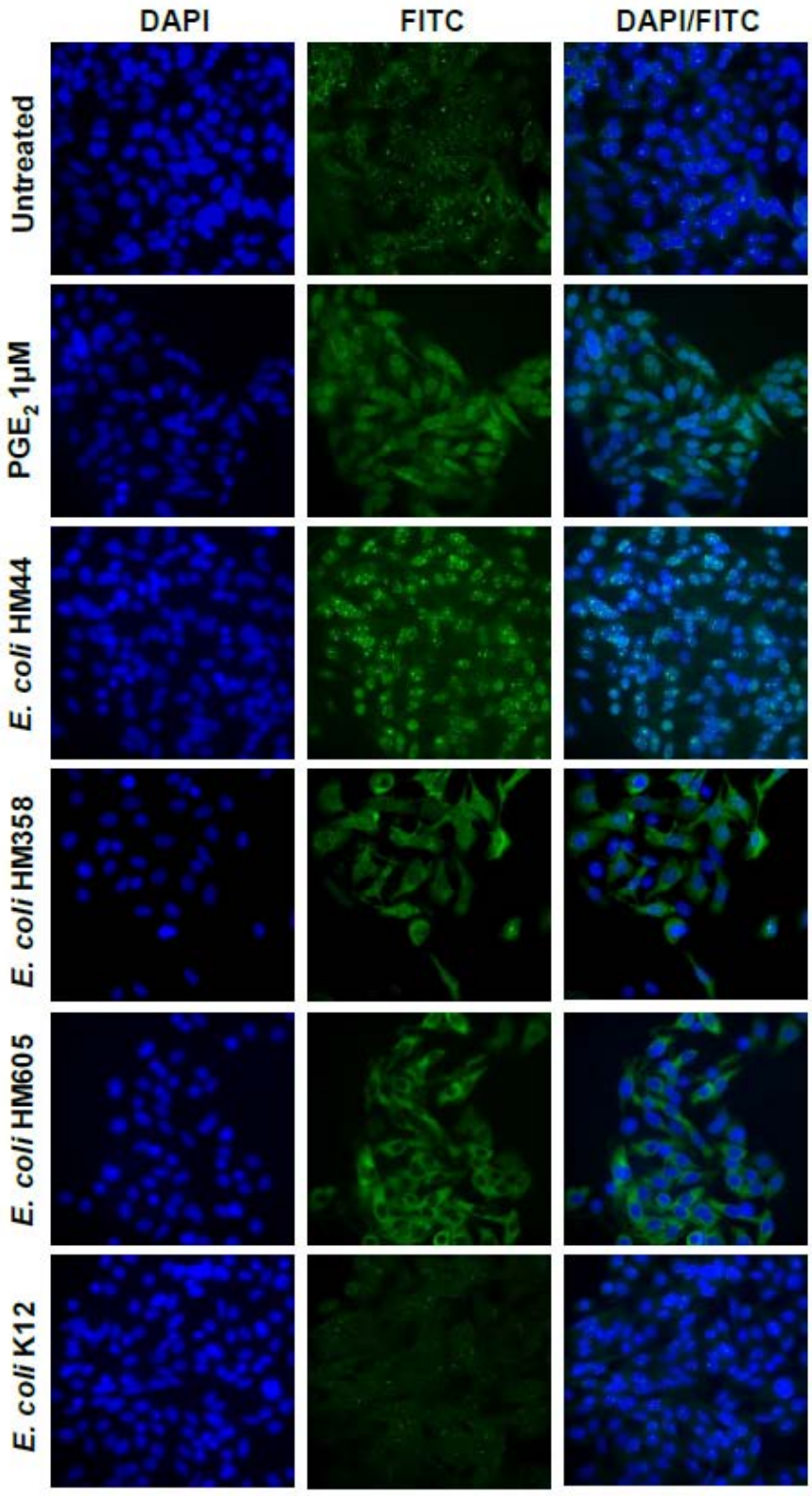

Figure 5.5.4.1. Localisation of β-catenin in SW480 CRC cells following mucosa-associated *E. coli* infection shown by immunofluorescence. DAPI nuclear staining and FITC-labelling of β-catenin in SW480 cells was shown following infection with mucosa-associated E. coli strains associated with CRC (HM44 and HM358) and CD (HM605) and non-pathogenic E. coli K12 (N=3, n=2; 5 images per slide). PGE2 (1µM) known to cause β-catenin nuclear localisation was used as a positive control.

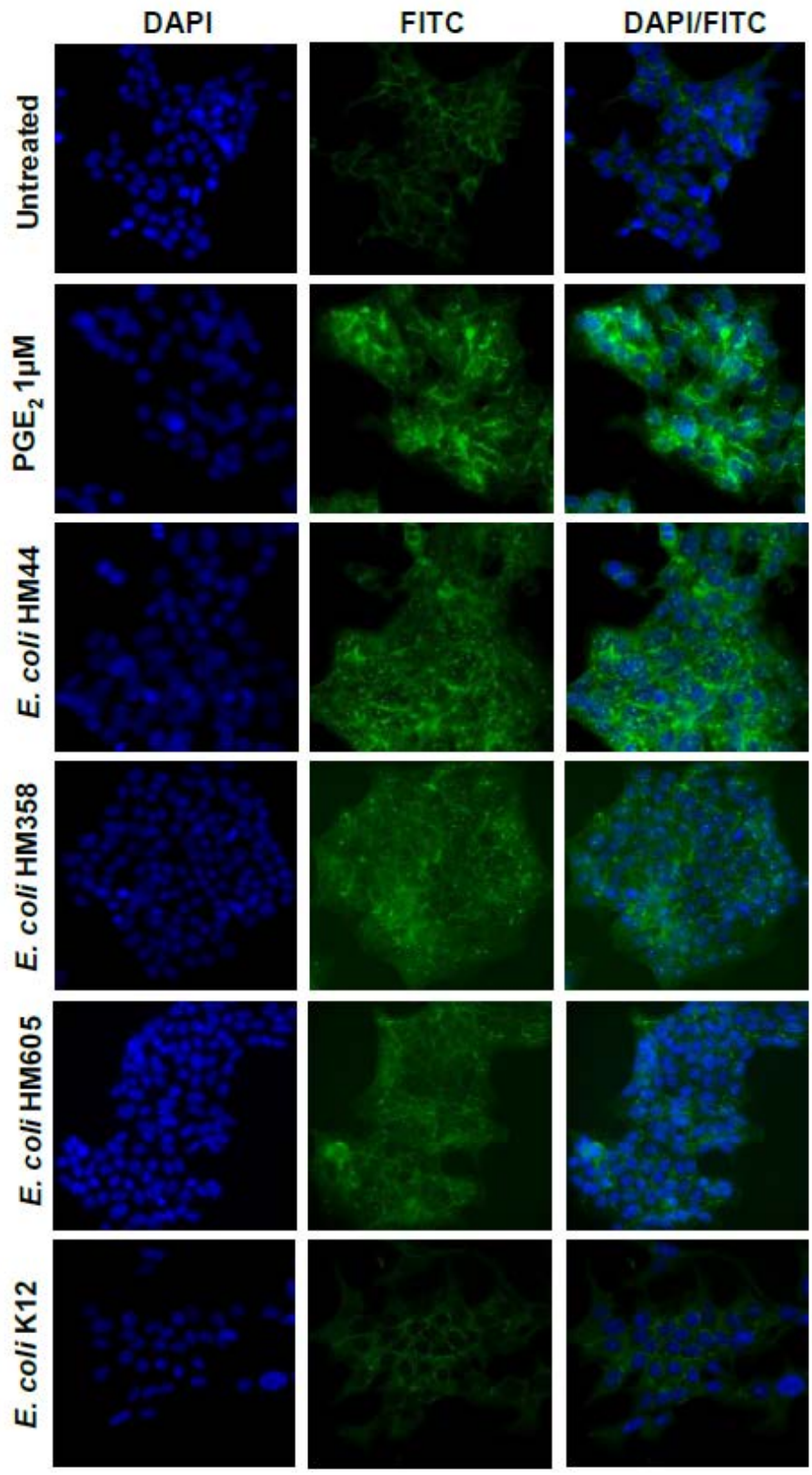

Figure 5.5.4.2. Localisation of β-catenin in DLD1 CRC cells following mucosa-associated *E. coli* infection shown by immunofluorescence. DAPI nuclear staining and FITC-labelling of β-catenin in DLD1 cells was shown following infection with mucosa-associated E. coli strains associated with CRC (HM44 and HM358) and CD (HM605) and non-pathogenic E. coli K12 (N=3, n=2; 5 images per slide). PGE2 (1µM) known to cause β-catenin nuclear localisation was used as a positive control.

Treatment of SW480 cells with CRC mucosa-associated *E. coli* HM44 led to a significant 2.3 ± 0.2 fold increase in β-catenin nuclear localisation (P<0.001; ANOVA), a response similar in magnitude to that seen following treatment with 1μM PGE_2 (2.4 ± 0.3 fold; P<0.001). Likewise, infection of SW480 cells with *E. coli* HM358 also resulted in a significant 1.8 ± 0.2 fold (P<0.01) increase in β-catenin nuclear localisation (**Figure 5.5.4.3**). CD mucosa-associated *E. coli* HM605 also effected a 1.5 ± 0.1 fold (P<0.01) increase nuclear localisation of β-catenin. In addition, *E. coli* K12 did not cause any nuclear localisation of β-catenin (0.9 ± 0.1 fold change) compared to untreated controls. Similar results were seen using DLD-1 cells with significant increases in β-catenin nuclear localisation again observed following infection with mucosa-associated *E. coli* strains HM44, HM358 and HM605.

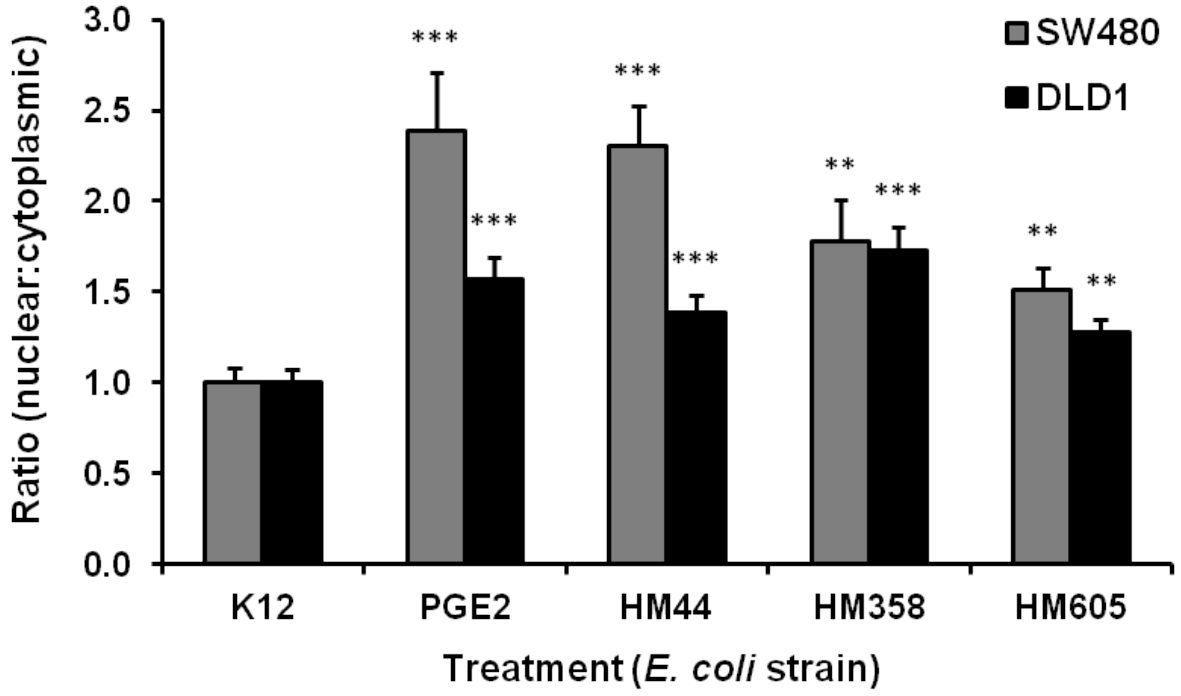

Figure 5.5.4.3. Increased nuclear localisation of β-catenin in CRC cells following mucosa-associated *E. coli* infections shown. A ratio of nuclear:cytoplasmic localisation of FITC-labelled β-catenin was assessed in SW480 and DLD1 cells. Increased nuclear localisation was shown following infection with mucosa-associated *E. coli* strains from CRC (HM44 and HM358) and Crohn's disease (HM605) patient colonic mucosa, compared to non-pathogenic *E. coli* K12 (N=3, n=2; 5 images per slide; *P<0.05, **P<0.01, ***P<0.001; ANOVA). Prostaglandin-E_2 (1 μM) was used as a positive control.

This assessment of nuclear localisation suggests that the observed mucosa-associated *E. coli* infection induced increases in gene and protein expression do indeed translate to increased nuclear translocation of β-catenin. It was then speculated that downstream Wnt transcriptional activity would likely also be increased following infection with mucosa-associated *E. coli* isolates also.

5.5.5 Increased HeLa cell TCF/LEF luciferase activity as a marker for Wnt transcription

The downstream effect of β-catenin nuclear localisation following mucosa-associated *E. coli* infection on Wnt transcription was assessed using an established TCF/LEF luciferase reporter stable HeLa cell line (Signosis, USA). As TCF/LEF transcription factor are the major end point mediators of Wnt signalling, downstream of β-catenin movement into the nucleus, the activity of the luminescent Firefly luciferase protein under the control of TCF/LEF transcription is considered a good reporter of Wnt signalling in the nucleus.

As recommended by the manufacturer, 10 mM lithium chloride (LiCl) was used as a positive control for enhancement of luciferase activity in these cells, as well as use of PGE_2 to be consistent with previous experiments (**Figure 5.5.5A**). In this assay, 10 µM PGE_2 was used as it gave a more consistent and robust signal over 1µM used in previous experiments. A negative control of 100 mM LiCl was also included. This dose was seen to effect cell rounding during optimisation studies allowing only a baseline signal response to be observed.

Overall, we were able to observe significant 1.5 to 2.6 fold increases in luciferase activity following treatment with CRC-associated *E. coli* isolates HM44, HM358 and HM545, CD-associated isolates HM95 and HM605 and UC-associated isolates HM250 and HM251, in comparison to *E. coli* K12 treatment (**Figure 5.5.5B**; all $P<0.001$; ANOVA). A similar 2-fold increase in luciferase activity was observed using 10 µM prostaglandin-E_2 ($P<0.001$), with the non-pathogenic *E. coli* K12 strain only producing a minimal 1.09±0.01 fold change compared to untreated controls ($P<0.05$; all N=2, n=6).

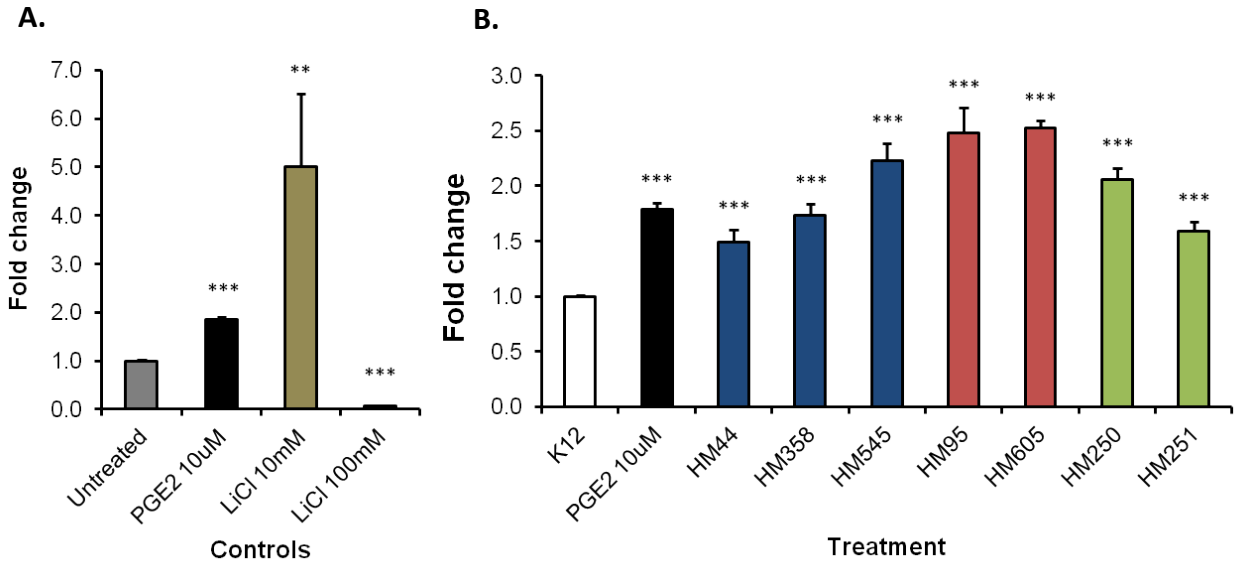

FIGURE 5.5.5. Increased Wnt transcription in cervical HeLa cells following mucosa-associated *E. coli* treatment. Cervical HeLa cell TCF/LEF luciferase reporter assay showed increased TCF/LEF transcription following treatment with mucosa-associated *E. coli* HM44, HM358 and HM545 from CRC, HM95 and HM605 from Crohn's disease (CD), and HM250 and HM251 from ulcerative colitis (UC) patients, compared to *E. coli* K12 (N=2, n=6; *P<0.05, **P<0.01, ***P<0.001; ANOVA).

5.5.6 Inhibition of mucosa-associated *E. coli*-induced Wnt transcription using COX inhibitors

With consistently increased levels of luciferase activity (indicating increased TCF/LEF transcription) following infection with mucosa-associated *E. coli,* and with the ability to screen multiple wells in this assay system, this assay was exploited to assess the impact of COX-2 activity in Wnt transcription. Initially, cyclooxygenase inhibitors aspirin, diclofenac and indomethacin were tested for their ability to block PGE_2-induced Wnt transcriptional activity over 24 hours using the TCF/LEF HeLa cell luciferase reporter assay. Each inhibitor was added at the same time as addition of PGE_2.

Results showed an approximate 3-fold increase in luciferase activity with 10 µM PGE_2 in the presence of no inhibitor (i.e. dH_2O vehicle control only), with lower levels of luciferase activity observed following treatment with increasing concentrations of each inhibitor. The highest level of inhibition observed of the three cyclooxygenase inhibitors selected was using 100 µM diclofenac, showing

95.3 ± 3.3 % inhibition of PGE_2-induced luciferase activity compared to only 22.5 ± 1.4 % and 46.8 ± 4.8 % inhibition with 100 μM aspirin and indomethacin, respectively (**Figure 5.5.6.1B**; N=1, n=3).

Diclofenac at a concentration of 100 μM was then used in combination with *E. coli* HM545 and HM605 treatment for 4 hours; these isolates were chosen to represent mucosa-associated *E. coli* from CRC and IBD patients as they gave the highest increases of luciferase activity. We were able to show consistent, significant inhibition of mucosa-associated *E. coli*-induced TCF/LEF transcription following co-treatment using diclofenac (**Figure 5.5.6.2**). Treatment with *E. coli* HM545 and HM605 along gave 1.5 ± 0.1 fold ($P<0.01$) and 1.7 ± 0.1 fold ($P<0.001$) increases, respectively, reduced to 0.9 ± 0.1 fold ($P<0.01$) and 1.0 ± 0.1 fold ($P<0.001$) changes in combination with diclofenac, respectively. These results were similar to those seen with prostaglandin-E_2 treatment, where a 2.0 ± 0.1 fold ($P<0.001$) increase was reduced to a 1.2 ± 0.1 fold ($P<0.001$) change with diclofenac treatment. Cell phenotype was altered slightly, with cells becoming more rounded under the microscope following treatment with diclofenac (100 μM). Cell growth and cell viability were not quantified.

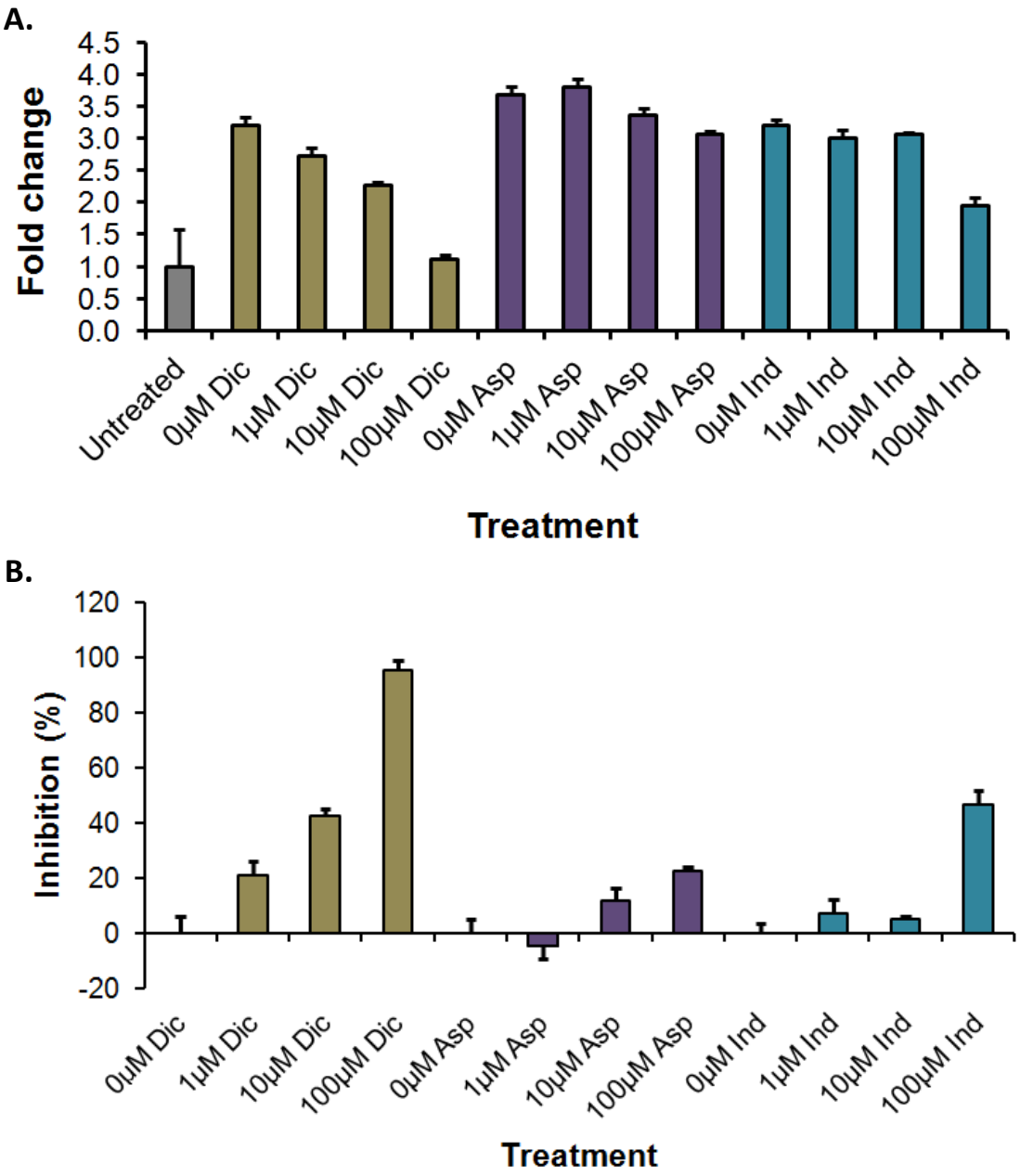

Figure 5.5.6.1. Effect of cyclooxygenase (COX) inhibition on increased Wnt transcription in HeLa TCF/LEF luciferase reporter cells following PGE_2 treatment. Prostaglandin-E2 (10 μM) was used to stimulate Wnt transcription in cervical HeLa cell TCF/LEF luciferase reporter assay in combination with cyclooxygenase inhibitors diclofenac (Dic), aspirin (Asp) and indomethacin (Ind) at 0, 1, 10 and 100 μM. Results show (A) a reduction in PGE_2 induced Wnt transcription with increasing concentrations of COX inhibitor, with (B) the highest % inhibition seen at 100 μM (diclofenac>indomethacin>aspirin; N=1 assays, n=3 wells).

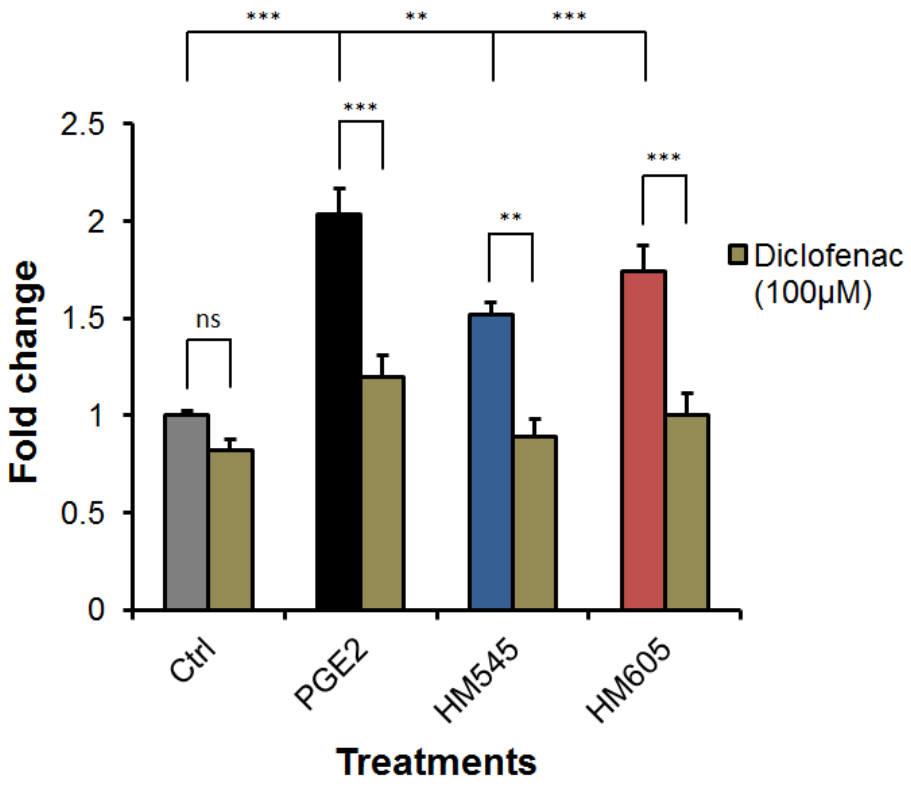

Figure 5.5.6.2. Cyclooxygenase (COX) inhibition significantly reduces Wnt transcription induced following mucosa-associated *E. coli* infection for 4h. COX inhibitor diclofenac (100 μM) showed inhibition of increased TCF/LEF transcription caused by treatment of cells with PGE_2 (10 μM) and mucosa-associated *E. coli* HM545 and HM605 (N=2, n=6; *P<0.05, **P<0.01, ***P<0.001).

Assessment of luciferase activity linked to TCF/LEF transcription using this method would suggest that Wnt transcription induced by mucosa-associated *E. coli* treatment translates from increased nuclear β-catenin localisation. Results also suggest that cyclooxygenase activity contributes significantly to increased Wnt transcription.

5.5.7 Mucosa-associated *E. coli* treatment of THP-1 monocyte-derived macrophage cells results in increased release of prostaglandin-E_2

A recently published study showed CRC *E. coli* promoting COX-2 and PGE_2 expression as well as their survival within human macrophages (Raisch *et al.,* 2015). The authors reported significant changes

only with CRC-associated *E. coli* and not with commensal or non-pathogenic *E. coli* strains, with this induction requiring live bacteria; the changes were not associated with production of the genotoxin colibactin. The study used human THP-1 monocytes differentiated into macrophages with 20 ng/ml phorbol myristate acetate (PMA) treatment for 72 hours. Considering the inhibition of mucosa-associated *E. coli*-induced Wnt transcription following co-treatment with COX inhibitor diclofenac, increased PGE_2 expression and survival within human macrophages, and the involvement of COX-2 in malignant development, we examined the ability of our own mucosa-associated *E. coli* isolates to affect PGE_2 release in the same way.

In addition, another study had shown that removal of PMA over a period of 5 days (termed reduced PMA treatment) produced cells with more macrophage-like morphology (Daigneault *et al*., 2010). Hence, we used this method to confirm the initial differentiation following PMA treatment (**Figure 5.5.7.1**). Using light microscopy, we were able to observe larger macrophage cells showing a wider coverage of the cell culture plate surface, with more pronounced finger-like projections visible following reduced PMA treatment. Cell growth was not quantified.

We assessed the amount of PGE_2 produced following treatment of these monocyte-derived macrophage cells with CRC and IBD mucosa-associated *E. coli* isolates using both PMA and reduced PMA differentiation approach (**Figure 5.5.7.2A and 5.5.7.2B**, respectively). The amount of PGE_2 production was assessed in the same way as the study conducted by Raisch *et al.* (2015) using cell culture supernatant and assay by enzyme-linked immunosorbent (ELISA) assay. *E. coli* LF82, known to persist in macrophage cell lines and increase COX-2 expression (Raisch *et al*., 2015), and *E. coli* K12 were used as positive and negative controls, respectively. The PGE_2 concentration was then assessed for each treatment compared to known standards.

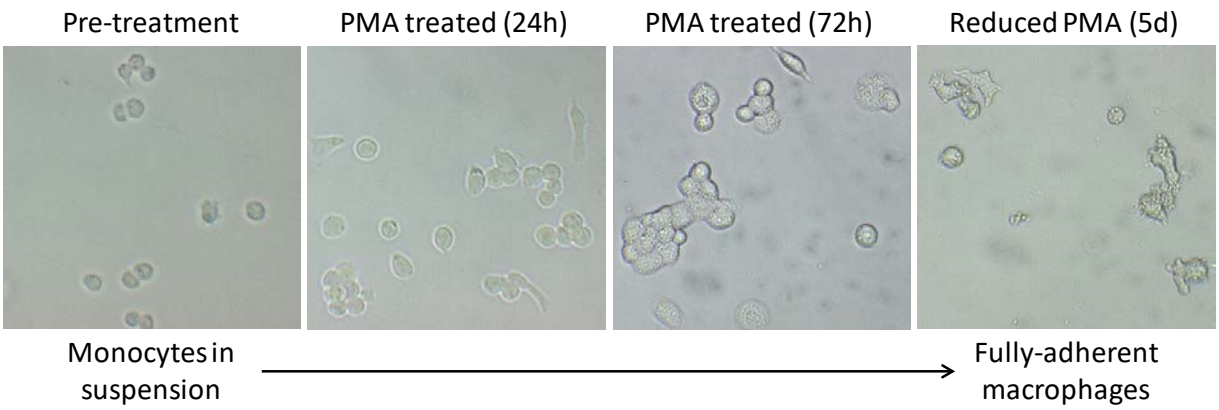

Figure 5.5.7.1. Morphology changes of THP-1 monocytes when differentiated into macrophages. THP-1 monocytes were incubated with 20ng/ml phorbol myristate acetate (PMA) for 72 hours, before removal of PMA and incubation for a further 5 days (reduced PMA). Images from left to right show THP-1 monocytes before PMA treatment, 24 hours and 72 hours after treatment, and 5 days after the removal of PMA. Cells are seen to increase in size 24 hours after PMA treatment and show full adherence after 72 hours. The reduced PMA image shows a more macrophage-like morphology, with larger and more pronounced finger-like projections, whilst remaining fully adherent (N=2, 3 images time point).

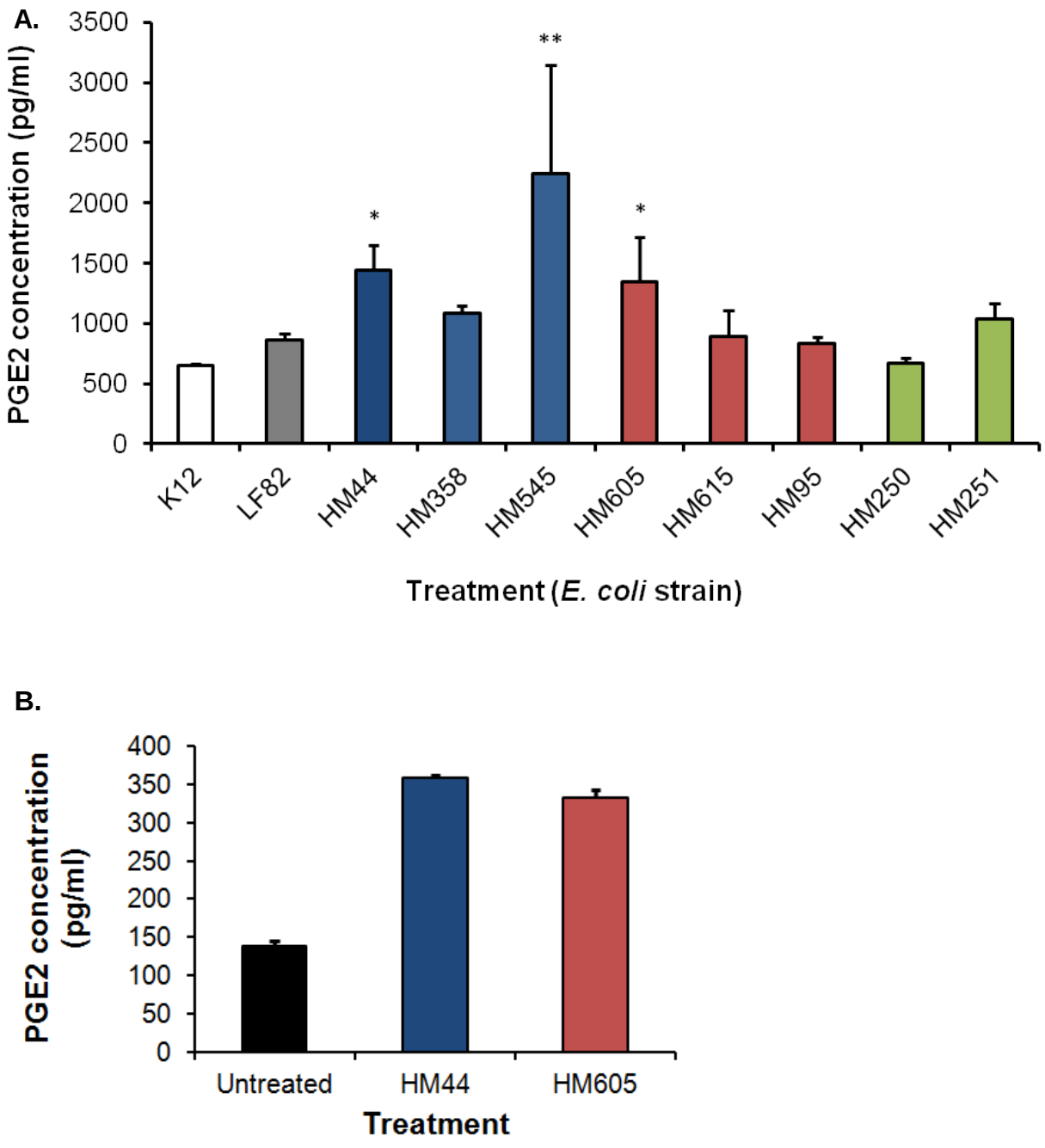

Figure 5.5.7.2. Mucosa-associated *E. coli* induce increases in prostaglandin-E_2 secretion in monocyte-derived macrophage cells. Prostaglandin-E_2 (PGE_2) release was measured using the supernatant of THP-1 monocyte-derived macrophage cells treated with CRC mucosa-associated (HM44, HM358 and HM545), CD mucosa-associated (HM605, HM615, HM95) and UC mucosa-associated (HM250 and HM251) *E. coli* isolates, and *E. coli* K12. PGE_2 release was measured in THP-1 cells differentiated using (A) PMA treatment for 72 hours well (N=2, n=3; *P<0.05, **P<0.01; ANOVA), and (B) following PMA-reduction treatment for another 5 days (N=1, n=3).

We were able to show significantly increased concentrations of PGE_2 in the supernatant of cells infected with both CRC-associated *E. coli* isolates HM44 (2.4 ± 0.4 fold; $P<0.05$) and HM545 (3.8 ± 2.1 fold; $P<0.01$), as well as with the CD-associated isolate HM605 (2.3 ± 0.8 fold; $P<0.001$) in comparison to E. coli K12 treatment. UC-associated isolate HM251 also showed a 1.7 ± 0.2 fold increase, with the positive control LF82 showing a 1.5 ± 0.1 fold increase. Non-pathogenic *E. coli* K12 gave a 1.6 ± 0.1 fold change in comparison to untreated controls.

Both CRC and IBD associated *E. coli* isolates induced high levels of PGE_2 secretion, similar to those previously reported in THP-1 monocyte-differentiated macrophages as per Raisch *et al*. (2015). Lower levels of PGE_2 secretion were shown in cells differentiated using the reduced PMA method; the basal level of PGE_2 secretion in untreated cells and following treatment with HM44 and HM605 isolates was much lower than when using the standard PMA differentiation method. However, treatment with *E. coli* HM44 and HM605 caused similar fold increases in macrophages differentiated using either the standard PMA treatment for 72 hours or following reduction in PMA levels for a further 5 days, showing a 2.5 to 3.5 fold increase in all cases.

5.6 Discussion

Wnt signalling target gene array reveals commonly upregulated genes in response to infection with CRC mucosa-associated *E. coli*

Our first insights into the Wnt-specific effects of mucosa-associated bacteria taken from CRC patients came from the use of a real-time PCR (RT-PCR) array quantifying changes in expression of Wnt target genes following the infection of CRC cell lines SW480 and DLD-1. We observed that a number of key genes associated with Wnt signalling were up-regulated, with many of the gene changes highlighted previously implicated in development, progression and/or spread of CRC.

We observed a significant increase in vascular endothelial growth factor A (*VEGFA*) gene expression in response to infection with CRC-associated *E. coli* strains HM44 and HM358 in both CRC cell lines studied. Increase in *VEGF* gene and VEGF protein expression is widely conserved across most cancers studied, and considered to be a key change promoting angiogenesis and metastasis of colorectal cancer. Increase in *VEGF-A* gene expression following mucosa-associated *E. coli* infection has been previously shown using real-time PCR and correlates to possession of the afimbrial adhesin by these CRC isolates (Prorok-Hamon *et al*., 2014). This also supports previous association between Afa-expressing diffuse adherent *E. coli* (DAEC) infection and inflammation leading to increases in VEGF and induction of epithelial mesenchymal transition (EMT) important in colorectal cancer progression (Cane *et al*., 2010, Waldner *et al*., 2010). Interventions that either reduce colonisation of intestine by these bacteria or block their interaction with the mucosa were suggested following this study as likely having significant preventive or therapeutic benefit in both colon cancer and CD. This further implicates perhaps the importance of the mucosa-association of these *E. coli* strains in the development and progression of CRC.

Another important finding from the Wnt signalling target gene array was the observation that there was significant up-regulation of the COX-2 gene, *PTGS2*, following infection with both CRC-associated *E. coli* strains, again seen in both CRC cell lines used. The role of COX-2 in CRC development and

progression has been widely reported, with expression of COX-2 now an independent predictor of poor prognosis in CRC (Ogino *et al*., 2008). Recently, cancer mucosa-associated *E. coli* strains have been shown to increase COX-2 expression and enhance subsequent PGE_2 secretion from human macrophages, likely due to their ability to survive and replicate within the macrophage phagolysosomes (Raisch *et al*., 2015). As previously described, COX-2 and PGE_2 have the ability to stimulate colon cancer cell growth via activation of the G protein-coupled receptor EP2, which leads to activation of the Wnt signalling pathway via the inactivation of glycogen synthase kinase 3β (GSK3β), thus allowing the accumulation and increased nuclear localisation of β-catenin (Castellone *et al*., 2005). Alongside adherence and invasion factors, COX-2 induction associated with *E. coli* isolated from CRC patient mucosae could be another important fact in establishing a significant role for these bacteria in the development and progression of CRC.

Given the wider implications of COX-2 and VEGF in CRC, and the conserved nature of the observed increases in both following infection of intestinal epithelial cells with CRC and inflamed mucosa-associated *E. coli*, this became a clear focus for the project going forwards. Moreover, other key gene array changes observed in response to both CRC *E. coli* isolates also provide further insight into the molecular events associated with Wnt signal pathway activation following infection.

This includes significant increase in *WISP1* gene expression seen, following infection of SW480 cells with both CRC-associated *E. coli* HM44 and HM358 ($P<0.05$). However, this effect was notably not replicated following infection of DLD-1 cells with these isolates. WNT1 inducible signalling pathway protein 1 (WISP1) is a cysteine rich protein secreted into the extracellular matrix to modulate cellular responses such as cell growth, differentiation and survival (Berschneider and Konigshoff, 2011). The role of WISP1 is inconsistent across different cancers but, importantly, an overexpression of WISP1 has been shown in colorectal cancer patients (Pennica *et al*., 1998, Davies *et al*., 2010). It has been suggested that modulation of WISP1 could represent a novel approach to treating cancers in a tissue specific manner, but that further *in vivo* studies would be necessary to determine the therapeutic potential of WISP1 modulation within these tissues (Berschneider and Konigshoff, 2011). Additionally,

the down-regulation of inhibitory Wnt genes such as *WISP2* suggests a reduction in normal regulation of Wnt signalling. WISP2 protein expression is known to control invasion, with *WISP2* knockout previously been shown to significantly increase Caco-2 CRC cell invasion and motility (Frewer *et al*., 2013). In addition, the same study showed up-regulation of matrix metalloproteinases (MMPs), indicating that WISP2 likely regulates invasion and motility through MMPs. We also showed up-regulation of *MMP7* and *MMP9* in SW480 cells following infection with CRC mucosa-associated *E. coli* isolates. MMP7 protein is known to be highly expressed in advanced colorectal adenomatous polyps showing evidence of severe dysplasia and involved in progressing colorectal adenomas to a malignant stage (Qasim *et al*., 2013). Our findings of *WISP2* gene down-regulation and up-regulation of *MMP* genes in colonocytes following CRC mucosa-associated *E. coli* may add weight to the impact on malignant development in the colon as previously suggested.

Another key finding was the upregulation of the *JAG1* gene encoded Jagged-1 protein in response to infection of colonocytes with the CRC mucosa-associated *E. coli*. Jagged-1 protein is normally found at the base of intestinal crypts and plays an important role in activation of Notch signalling, promoting a cancer stem cell phenotype in CRC cells (Lu *et al*., 2013). Jagged-1 has also previously been found to be distributed diffusely throughout crypts following *Salmonella* Typhimurium infection, a bacterium known to activate Wnt signalling (Liu *et al*., 2010). As also seen for our CRC mucosa-associated *E. coli* strains in this study, upregulated expression of *FOSL1* gene encoding the FOS-like antigen-1 (*FOSL1*) transcription factor, has also previously been associated with intestinal *S.* Typhimurium infection (Hannemann *et al*., 2013). FOS-like antigen-1 plays a key role in enhancing cellular proliferation and migration (key factors in CRC development/progression) by forming dimers with members of the Jun family of proteins to generate the activator protein-1 (AP-1) transcription factor (Verde *et al*., 2007).

The varied roles of these Wnt target genes and their associated proteins could be important in determining the chronic effect of Wnt signalling induced by CRC-associated *E. coli* infections. Taking this a step further, with significant up-regulation of a number of these genes associated with Gram-

negative bacterial infection, it is possible these genes and their associated protein products would likely be of therapeutic interest in limiting the development and progression of CRC.

Following the Wnt signalling target gene array studies, we went on to confirm the observed up-regulation of both COX-2 (*PTGS-2*) gene and β catenin (*CTNNB1*) gene expression by Taqman qPCR using Roche Human Universal Probe Library primers designed specifically to recognise the *PTGS2* and *CTNNB1* gene transcripts. Here we investigated mRNA abundance following 2h and 4 h infection of SW480 and DLD-1 cells with CRC mucosa-associated *E. coli* HM44 and HM358. The results using this technique were consistent with the Wnt RT^2 PCR array, thus further confirming increases observed in expression of these genes. We observed a time-dependent increase of *PTGS-2* gene expression, as well as the expression of the *CTNNB1* gene encoding β-catenin, at both 2 and 4 h, with 4h infection of both cell lines using either HM44 or HM358 *E. coli* strains, resulting in the largest fold increases in comparison to uninfected controls. The observed increases in gene expression also converted to time-dependent increases of both COX-2 and β-catenin protein expression respectively, with the highest levels of protein expression observed following 4h post infection.

Differences observed between CRC cell lines

Results from the Wnt signalling gene profiling array, alongside confirmatory real time qPCR and subsequent analysis of protein level changes, suggested some potential signalling differences between SW480 and DLD-1 cells. Both CRC cell lines are known to have high basal levels of Wnt signalling (Yang *et al*., 2006). One possible explanation for the difference between SW480 and DLD1 cell Wnt/β-catenin signalling pathway activity might be differing levels of β-catenin phosphorylation (Yang *et al*., 2006). It has been suggested that differences in β-catenin phosphorylation may be a consequence of loss in a key phosphatase binding site, likely due to the differences in site of APC truncation across a variety of CRC cell lines (Sadot *et al*., 2002). For example, SW480 colon cancer cells harbour a truncation in APC at position 1338 and show high levels of phospho-β-catenin, whereas HT29 cells harbour truncation in APC at position 1555 and accumulate non-phosphorylated β-catenin. This suggests the

1338-1555 amino acid region of APC is likely involved in the differential regulation of the de-phosphorylation and degradation of phospho-β-catenin. It would be interesting to examine CRC mucosa-associated *E. coli*-infected HT29 cell responses in the same way as we have examined for in SW480 and DLD1 cells so as to check for any differences in these protein levels and associated signalling.

Whilst high basal levels of Wnt signalling makes these cell lines a useful model for this study, larger increases in Wnt signalling could be masked in comparison to other CRC cell lines such as HT-29. CRC mucosa-associated *E. coli* isolates may have a similar if not bigger impact in intestinal epithelial cells with lower levels of basal Wnt activity and those earlier in the intestinal adenoma-carcinoma sequence. On the other hand, lower levels of basal Wnt signalling might also make for difficulty in detection of changes in Wnt signalling target gene and protein expression more difficult.

Nuclear β-catenin translocation in CRC cells

A previously described, validated technique for the quantitative analysis of nuclear translocation of NFκB in primary human macrophages (Noursadeghi *et al*., 2008) was successfully adapted here to quantify cytoplasmic and nuclear localisation of β-catenin. Here we used a monoclonal IgG antibody recognising β-catenin E-5, followed by FITC-conjugated anti-mouse IgG antibody amplification, to show increase in nuclear translocation of β-catenin in colonocytes following infection with CRC mucosa-associated *E. coli* isolates (combined with DAPI to define the cell nucleus). We were also able to show similar increased nuclear translocation of β-catenin with LiCl and PGE_2 treatment. Quantification using ImageJ, as described in the study of Noursadeghi *et al.* (2008), allowed us to differentiate levels of nuclear and cytoplasmic staining to generate a stain localisation ratio. Without this, the results would have relied on staining intensity, which is notoriously difficult to interpret.

The observed increase in nuclear β-catenin localisation in response to CRC mucosa-associated *E. coli* infection was similar in both SW480 and DLD-1 cells but with DLD-1 cells showing a lower level/pattern

of increase. This supports earlier observations where changes in both β-catenin gene and protein expression in DLD-1 cells were also less pronounced than those seen in SW480 cells.

Use of TCF/LEF signalling in HeLa cells as a model for assessing increased Wnt transcription

TCF/LEF activity induces transcription of Wnt target genes by binding promoters of downstream target genes involved in cell proliferation, survival and migration (Morin *et al*., 1997, van de Wetering *et al*., 2002). Results obtained here in this study using the luciferase-reporter HeLa cell line obtained from Signosis show that this phenomenon may occur in cells without high basal Wnt activity. Data obtained suggest that mucosa-associated *E. coli* isolates taken from CRC and IBD (CD and UC) patients all possess ability to increase Wnt transcription via TCF/LEF transcription factors, further confirming the movement of β-catenin to the epithelial cell nucleus. Again, the lack of induction of Wnt transcriptional activity by the non-pathogenic non-invasive *E. coli* K12 suggests this could be specific to CRC/inflamed mucosa-associated *E. coli* known to invade intestinal epithelial cells *in vitro* (Martin *et al*., 2004) and observed to be intraepithelial within CRC tissue (Swidsinski *et al.*, 1998). The results obtained using the luciferase-reporter HeLa cell line supported those observations previously seen in mucosa-associated *E. coli* inoculated CRC cells assessed using the Wnt RT^2 PCR array, qPCR and immunoblot analyses.

COX inhibition reduces mucosa-associated *E. coli*-induced Wnt transcriptional activity

Another key outcome from this study that was obtained using the HeLa TCF/LEF-luciferase reporter cells was that inhibition of Wnt transcription could be seen using several cyclooxygenase (COX) inhibitors. The chemopreventative effects of diclofenac (Kaur and Sanyal, 2010, Kaur Saini and Nath Sanyal, 2010), aspirin (Menzel *et al*., 2002, Tougeron *et al*., 2014) and indomethacin (Xu and Zhang, 2005, Wang and Zhang, 2005) in colorectal cancer have been extensively studied both *in vitro* and *in vivo*. Both diclofenac and aspirin have also been reported to have potential, even proven, chemotherapeutic action in patients (Ng *et al*., 2015). In this study, COX inhibitor treatment resulted

in observed decreases in Wnt transcriptional activity of PGE_2-treated HeLa TCF/LEF-luciferase reporter cells, with diclofenac showing the highest levels of inhibition; diclofenac>indomethacin>aspirin at concentrations selected for initial testing based on previous key studies (Botting, 2006, Din *et al*., 2004). Following this, we tested diclofenac (100μM) in HeLa TCF/LEF-luciferase reporter cells infected with mucosa-associated *E. coli* strains HM545 (CRC) and HM605 (CD), strains which were selected as they gave consistently higher fold changes in activity of Wnt/β-catenin signalling pathway in the cultured cells. Diclofenac (100μM) was shown to significantly inhibit the increased signalling seen in cells infected with HM545 and HM605 in the absence of diclofenac. The high concentration of diclofenac caused some cell rounding (indicative of possible increased cell toxicity) as has also been noted with COX inhibitors in other studies (Din *et al*., 2004, Inoue *et al*., 2013), which might explain the lower levels of luciferase activity seen in uninfected controls treated with diclofenac. However, these apparent changes in cell viability were not significantly impacted with COX inhibitor treatments used in our study, as shown by the lack of significant changes between uninfected controls with and without inhibitor in HeLa TCF/LEF-luciferase reporter cells.

It has been suggested that diclofenac could also attenuate Wnt signalling via the nuclear factor kappa-B (NFκB) pathway (Cho *et al.*, 2005). Indomethacin has also been shown to re-localise β-catenin from the nucleus and cytoplasm to the plasma membrane thus decreasing Wnt/β-catenin signalling (Kapitanovic *et al*., 2006). Our results demonstrating Wnt pathway activation by CRC and IBD mucosa-associated *E. coli* alongside evidence that Wnt pathway attenuation following the use of COX inhibitors suggest that mucosa-associated *E. coli* mono-association/infection studies promoting tumourigenesis *in vivo* (Arthur *et al*., 2012) focussing on the effect of COX-2 inhibitors or Wnt signal pathway inhibitors would be of high scientific interest.

The impact of COX-2 inhibitors here points towards regulation of Wnt activity via reduced signalling by the EP2 receptor, as COX-2 and subsequent PGE_2 increases are believed to increase Wnt activity via binding to the EP2 receptor (Castellone *et al*., 2005). However, although COX-2 inhibitors significantly decreased Wnt transcription, other potential changes in receptor numbers or release of Wnt ligands

has not been assessed, and may contributing to Wnt regulation here. Significant alteration of Wnt ligand release and Frizzled receptors following *E. coli* and/or COX-2 inhibitor treatment could impact Wnt transcription. Therefore, it would be interesting to investigate the impact of Wnt ligand release following these treatments using immunoblotting and ELISA, as well as assessing the impact of Frizzled receptor inhibitors/antibodies, such as OMP-185 used successfully in preclinical models (Zhang and Hao, 2015), alone and in combination with COX-2 inhibitors.

Increased PGE_2 secretion from monocyte-derived macrophages

The recruitment of macrophages following an infection is a key mechanism of protection. Macrophages are a predominant stromal component of both murine and human tumours supporting key processes involved in cancer development and progression via production of key oncogenic factors such as COX-2 (Raisch *et al*., 2015). If tumour-infiltrating macrophages are unable to kill mucosa-associated/invading bacteria this may lead to intraphagolysome residence of these pathogenic bacteria within intestinal tissue, with genotoxic, angiogenic and pro-inflammatory potential (Subramanian *et al*., 2008, Arthur *et al*., 2012, Prorok-Hamon *et al*., 2014). *E. coli* have been isolated from macrophages in CD, and persistence within the macrophage phagolysosome may provide stimulus for inflammation (Bringer *et al*., 2007, Mpofu *et al*., 2007, Subramanian *et al*., 2008). The results from the present study confirm those of similar studies (Raisch *et al*., 2015), with human monocyte-derived macrophages infected with pathogenic *E. coli* showing increased production and release of COX-2. These results would suggest that macrophage activity, or survival of bacteria within macrophages, contributes to increased levels of Wnt signalling in nearby tissues, particularly given the link between COX-2 signalling and Wnt signalling shown throughout.

CD and CRC mucosa-associated *E. coli* appear to be adapted to an intracellular lifestyle within the low pH, low nutrient, high oxidative stress environment of the macrophage phagolysosome (Bringer *et al*., 2005, Bringer *et al*., 2007, Tawfik *et al*., 2014). Intracellular survival and replication of these particular *E. coli* has also been shown to be similar whether phagocytosed by macrophages isolated from CD or

healthy non-inflamed intestine control patients (Flanagan *et al*., 2015b). This study also showed that the macrophage intraphagolysosome alkalinizing drug hydroxychloroquine (HCQ) promoted killing of phagocytosed mucosa-associated *E. coli* and also enhanced the efficacy of antibiotics targeting bacteria with an intracellular lifestyle, such as doxycycline and ciprofloxacin (Flanagan *et al*., 2015b). This study further identified that supplementation with vitamin D, to enhance macrophage function, also supported killing of these *E. coli* strains. This would suggest future animal studies to see whether targeting CRC mucosa-associated *E. coli* with combination HCQ/antibiotics and/or vitamin D supplementation reduced Wnt signal pathway activation and carcinogenesis *in vivo*. Later human preventative trials might then be warranted.

The role of COX-2 in CRC is already supported by its elevated expression found in 50% of adenomas and 85% of adenocarcinomas, its association with worse survival among CRC patients, and the efficiency of nonsteroidal anti-inflammatory drugs (NSAIDs) and selective COX-2 inhibitors (COXIBs) to reduce the occurrence of sporadic CRC. The results obtained in this study and in the Raisch *et al.* (2015) study suggest that bacteria residing within macrophages could contribute to progression of CRC, including proliferation and survival of cancer cells, angiogenesis, immunosuppression, invasion, and metastasis (Raisch *et al*., 2015). The increased release of PGE_2 could be another major contributing factor in driving the Wnt response in neighbouring intestinal epithelial cells.

Summary

We have been able to show increases in total and nuclear localised β-catenin at both the gene protein level *in vitro* following infection with mucosa-associated *E. coli* isolates from IBD and CRC patients, and have shown that this correlates with COX-2 gene and protein levels. While this part of the study does not elude to why this happens, it does suggest an effect that is specific to mucosa-associated *E. coli* strains with the ability to adhere to and invade intestinal epithelial cells.

Chapter 6:

Increased expression of cyclooxygenase-2 and β-catenin *in vivo* following mono-association of *Il10*$^{-/-}$ germ-free mice with CRC *E. coli* HM44 indicates translation of increased Wnt signalling

6.1 Introduction

With a wide role of COX-2 in CRC development and progression reported (Brown and DuBois, 2005, Ogino *et al*., 2008), and a cascade suggested for the role of COX-2 and prostaglandin-E_2 (PGE_2) in stimulating cancer cell growth via Wnt activation (Castellone *et al*., 2005), it is highly possible that COX-2 induction following chronic bacterial infection of colonic cells could lead to sustained increases in Wnt signalling *in vivo*.

COX-2-driven PGE_2 increases are believed to activate the G protein-coupled receptor EP2 leading to phosphoinositide 3-kinase (PI3K) activation of the Wnt signalling pathway via the inactivation of glycogen synthase kinase 3β (GSK3β). The subsequent accumulation of β-catenin in the cytoplasm and nuclear translocation following infection of colonic cells with mucosa-associated *E. coli* could aid proliferation, migration and metastasis. With gut inflammation able to alter the composition of the gut microbiota in favour of pathogenic mucosa-associated *E. coli* (Darfeuille-Michaud *et al.*, 1998, Swidsinski *et al.*, 1998, Martin *et al.*, 2004), this could create an environment that supports tumour development by resultant expansion of, and contact with, these bacteria.

In addition, as CRC-associated *E. coli* strains can survive and replicate within human macrophages, as well as increase COX-2 expression and subsequent PGE_2 secretion (Raisch *et al.*, 2015), the impact of mucosa-associated *E. coli* survival and PGE_2 increases shown in the present study could enhance the tumourigenic effect of these infections *in vivo*.

We have so far been able to characterise upregulation of Wnt signalling target genes alongside increases in COX-2 and β-catenin, at both mRNA and protein level, following *in vitro* infection of CRC cell lines with mucosa-associated *E. coli*. The existing link between COX-2 and β-catenin previously reported (Castellone *et al*., 2005) and shown here using *in vitro* infection models would suggest translation into an *in vivo* infection model.

The *Il10* knock-out ($Il10^{-/-}$) model removes anti-inflammatory Il-10 as an innate defence mechanism, allowing a direct look at the effect of CRC mucosa-associated *E. coli* HM44 infection of an otherwise

germ-free gut. This model has been previously used to show that colitis in mice can promote tumorigenesis by altering microbial composition and inducing the expansion of microorganisms with genotoxic capabilities (Arthur *et al.*, 2012). Similar germ-free studies have revealed a key role for the microbiota in driving CRC, particularly where changes in microbial composition can influence the development of colitis-associated CRC (Arthur and Jobin, 2011). Therefore, we investigated this effect *in vivo* using a germ-free *Il10* knock-out (*Il10*$^{-/-}$) mouse model mono-associated with the mucosa-associated *E. coli* HM44, a clinical isolate from a CRC patient (Martin *et al.*, 2004).

Other *in vivo* model studies assessing the effects of bacteria such as *H. pylori* have also shown links between increased COX-2 and β-catenin expression and tumor development (Oshima and Oshima, 2010). Similarly, *H. felis* infections have shown activation of Wnt signalling through activation of PI3K and AKT, leading to the phosphorylation and inactivation of GSK3β, allowing β-catenin to accumulate in the cytosol and translocate to the nucleus (Oguma *et al*., 2008). This has been attributed to multiple *H. pylori* cancer-associated determinant factors reported to influence β-catenin activation, and is consistent with other reports investigating β-catenin activation caused by infection with bacteria such as *Salmonella* typhimurium and *Bacteroides fragilis* (Polk and Peek, 2010).

Any similar alterations in β-catenin signalling following mono-association with mucosa-associated *E. coli* HM44 would suggest that the effects previously seen *in vitro* could translate into increased risk of cancer development in disease-relevant animal models, further implicating the potential for these bacteria to cause human disease. By investigating the effects of HM44 mono-association on COX-2 protein expression, this could also be important in further establishing the link between increased COX-2 and β-catenin signalling.

6.2 Hypothesis

Increase in COX-2 and Wnt signalling following mucosa-associated *E. coli* infection of human CRC cells observed *in vitro* translates to changes *in vivo* following CRC mucosa-associated *E. coli* HM44 mono-association of a germ-free *Il10*$^{-/-}$ mouse model.

6.3 Aims

- To investigate by immunohistochemistry (IHC) whether COX-2 and Wnt pathway activation are initiated *in vivo* using a germ-free *Il10*$^{-/-}$ mouse model of CRC mucosa-associated *E. coli* infection.

- To confirm the *in vitro* link between COX-2 upregulation and increased Wnt signalling *in vivo* using the same germ-free *Il10*$^{-/-}$ mouse model of mucosa-associated *E. coli* infection.

6.4 Methods

The COX-2 and β-catenin IHC protocols were initially optimised using intestinal tissue obtained from wild-type C57BL/6 mice where colitis had been induced with dextran-sodium sulphate (DSS) (Melgar *et al*., 2005), that results in significant upregulation of COX-2 (Singh *et al*., 2010), and from AhCre+ *Apc*$^{fl/fl}$ mice (a novel inducible Ahcre transgenic line in conjunction with a loxP-flanked Apc allele), where Cre Apcfl/fl induction by β-napthoflavone results in significant nuclear translocation of β-catenin (Sansom *et al*., 2004).

Mono-association studies used gut tissue from germ-free *Il10*$^{-/-}$ 129SvEv strain mice mono-associated with *E. coli* HM44 for 6 weeks (n=15) or those mice uninfected (n=5). Mono-association was carried out at the gnotobiotic facility at NC State University (University of North Carolina Chapel Hill, USA); all animal infection and tissue/bundling/processing work was completed by Dr Janelle Arthur with protocols previously well established (Arthur *et al.*, 2012). Briefly, strain mice were mono-associated for 6 weeks. Germ-free *Il10*$^{-/-}$ 129SvEv mice were colonized using cotton swabs soaked in an overnight culture of CRC mucosa-associated *E. coli* HM44 grown in LB broth from a -80^{o}C glycerol stock – a common colonization procedure used in the NC State gnotobiotic facilities, where mouse health was continuously monitored. Stool pellets were collected at the conclusion of the experiment and plated to demonstrate colonization. Colonic tissue was taken from HM44 mono-associated mice (n=15) and germ-free controls (n=5) before fixing and paraffin wax embedding (see Chapter 4.3).

Paraffin wax embedded tissue was microtome-sectioned and processed for incubation with primary antibodies. Heat-induced antigen retrieval was performed in citric acid buffer (pH 6.4) before bovine serum albumin (BSA) blocking. Immunohistochemistry for COX-2 and β-catenin was performed using a 1:400 dilution of the COX-2 antibody (#ab15191, Abcam) and 1:50 dilution of the β-catenin antibody (#610154, BD Biosciences). Slides were then incubated in haematoxylin before being fixed with DPX mountant – a mixture of distyrene, plasticizer and xylene – to enable visualisation and quantification of cellular localisation.

Images were captured (5 random fields of view) using SPOT Image Capture Software (SPOT Imaging Solutions) on a light microscope (Leica). Total epithelial and nuclear staining was evaluated using the IHC Profiler and ImmunoRatio plugins for ImageJ 1.48v, respectively. Scoring for total epithelial staining, quantified using the IHC Profiler plugin, was done using the Modified HSCORE method (Varghese *et al.*, 2014), with a maximum achievable score of 300 and a minimum score of 0 (arbitrary units). Comparison of nuclear and cytoplasmic β-catenin staining, quantified using ImmunoRatio, was performed calculating ratios of nuclear and total staining in tissue sections following published techniques (Tuominen *et al.*, 2010, Sundara Rajan *et al.*, 2014).

6.5 Results

6.5.1 Optimisation of IHC conditions for detection of COX-2 and β-catenin protein

Before submitting the germ-free *Il10*$^{-/-}$ model tissue slides for IHC, a number of steps were completed in order to optimise the IHC protocol (see Section 4.12.3), for both COX-2 and β-catenin detection, and to validate the scoring technique. The COX-2 IHC protocol was optimised using gut tissue from a wild-type C57BL/6 DSS-induced colitis mouse model (Melgar *et al.*, 2005); this tissue was kindly generated and donated by Dr Carrie Duckworth and Miss Stephanie James (Cellular and Molecular Physiology, University of Liverpool).

The β-catenin IHC protocol was optimised using small intestinal tissue section slides obtained from AhCre+ *Apc*$^{fl/fl}$ and *Apc*$^{Min/+}$ mice, kindly donated by Dr John Jenkins and Dr Cleberson Quieroz (Gastroenterology Research Unit, University of Liverpool), a gift from the late Professor Alan Clarke (University of Cardiff). The mutation induced in the AhCre+ *Apc*$^{fl/fl}$ model was the removal of the *Apc* gene using a loxP-flanked *Apc* allele following β-napthoflavone treatment, causing accumulation and subsequent nuclear localisation of β-catenin (Sansom *et al.*, 2004). Nuclear localisation observed in these tissues were compared to that of colonic sections from tissue of six-month old *Apc*$^{Min/+}$ mice harbouring one wild-type *Apc* allele and one *Apc* allele mutated at codon 850 (Su *et al*., 1992). Images of immuno-stained tissue were used to validate the scoring techniques of Modified HSCORE and ImmunoRatio for use with the germ-free *Il10*$^{-/-}$ mono-association model tissue.

The developed IHC staining protocol used an anti-mouse COX-2 antibody (#ab15191, Abcam) previously used successfully with mouse tissue (Miyoshi *et al.*, 2012, Nilsson *et al.*, 2012). This antibody was recommended for use at 1:200 to 1:1000 by the manufacturer, with an in-house protocol developed for similar mouse model tissue at a 1:400 dilution. To confirm this dilution was suitable for use, a titration was completed using 1:200, 1:400 and 1:800 dilutions on spare small intestinal tissue made available from the DSS-induced colitis mouse model (**Figure 6.5.1.1**).

The tissue was taken from a mouse at day 7 of DSS treatment; at this stage of treatment, a high level of inflammation (Melgar *et al.*, 2005) should allow for detectable COX-2 protein levels. From image analysis of antibody treated tissue sections, it was shown that the 1:400 dilution allowed detection of suitable levels of COX-2 protein for this particular tissue without showing any noticeable non-specific binding.

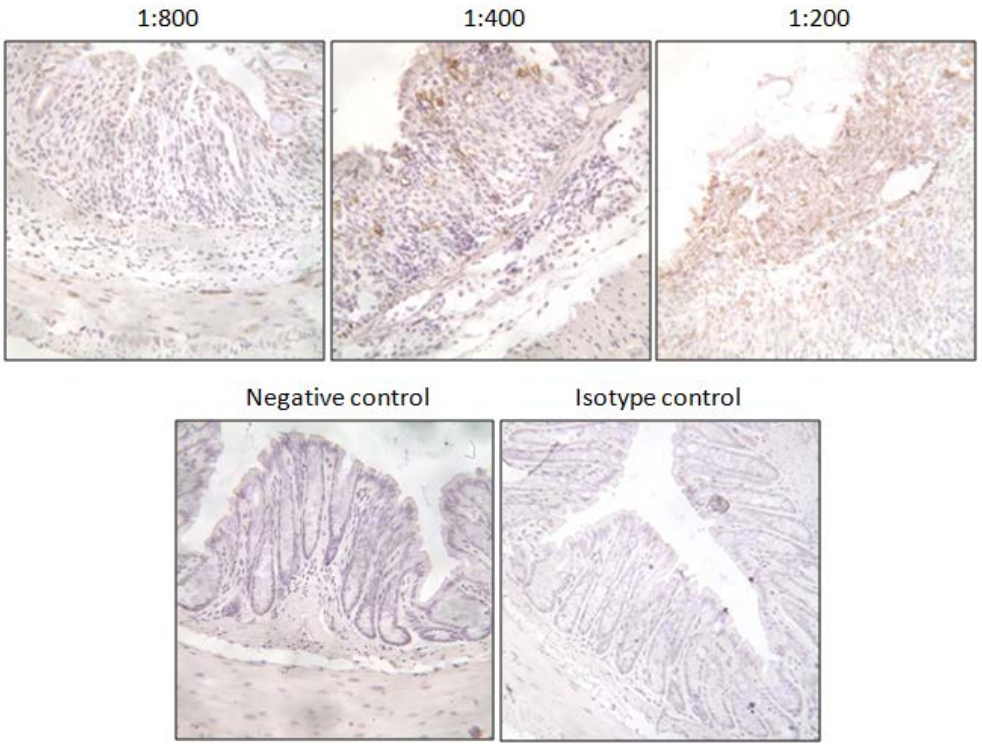

Figure 6.5.1.1 Titration of anti-mouse cyclooxygenase-2 (COX-2) antibody. Images show C57BL/6 mouse small intestinal tissue sections taken from a mouse at day 7 of DSS-induced colitis development, with COX-2 protein and cell nucleus immuno-stained using diaminobenzene (DAB) and haematoxylin, respectively. Tissue sections were incubated with 1:200, 1:400 and 1:800 dilutions of anti-mouse COX-2 antibody, as well as a no-antibody control (Negative control) and a primary IgG control (Isotype control). Sections (n=3) were imaged at 40x magnification (3 random fields per section).

Following the titration of the anti-mouse COX-2 antibody, a 1:400 dilution was used for detection of COX-2 expression in intestinal tissue from mice at different stages of DSS treatment. The aim of this

was to ensure that differences in COX-2 levels could be effectively visualised, with higher levels expected following inflammation caused by DSS treatment.

Tissue isolated from mice at an early stage of DSS-induced colitis, day 1 to day 4, showed minimal levels of COX-2 expression, with expression seen to increase as the model progressed to day 7 through day 9. The tissue taken from mice at day 10 and day 11 following DSS treatment showed decreased expression of COX-2, with levels seen to be similar to that of the earlier stages of DSS-induced colitis; this is believed to be in line with the recovery stage, normally observed around 12 days after DSS treatment in this particular model (Melgar *et al.*, 2005). Example images can be seen in **Figure 6.5.1.2**.

The expression of β-catenin in intestinal tissues of *Apc* mutant AhCre+ $Apc^{fl/fl}$ and $Apc^{Min/+}$ mice were assessed using conditions pre-defined by Dr John Jenkins and Dr Cleberson Quieroz (University of Liverpool; unpublished data); an antibody dilution of 1:50 was used solely. Due to the nature of the mutations in both the $Apc^{fl/fl}$ and $Apc^{Min/+}$ models, it was expected that the total expression and nuclear localisation of β-catenin would be observed to be higher in the $Apc^{fl/fl}$ tissue; this was confirmed by DAB staining these antibody-treated tissues (**Figure 6.5.1.3**).

COX-2 staining in the *Apc* mutant mouse intestines was much less evident when compared to β-catenin, which is indicative of the lower expression levels these gut tissues. However, the detection levels were deemed acceptable to submit these tissues for validation of the automated scoring system that was to be used for the germ-free $Il10^{-/-}$ model tissue imaging.

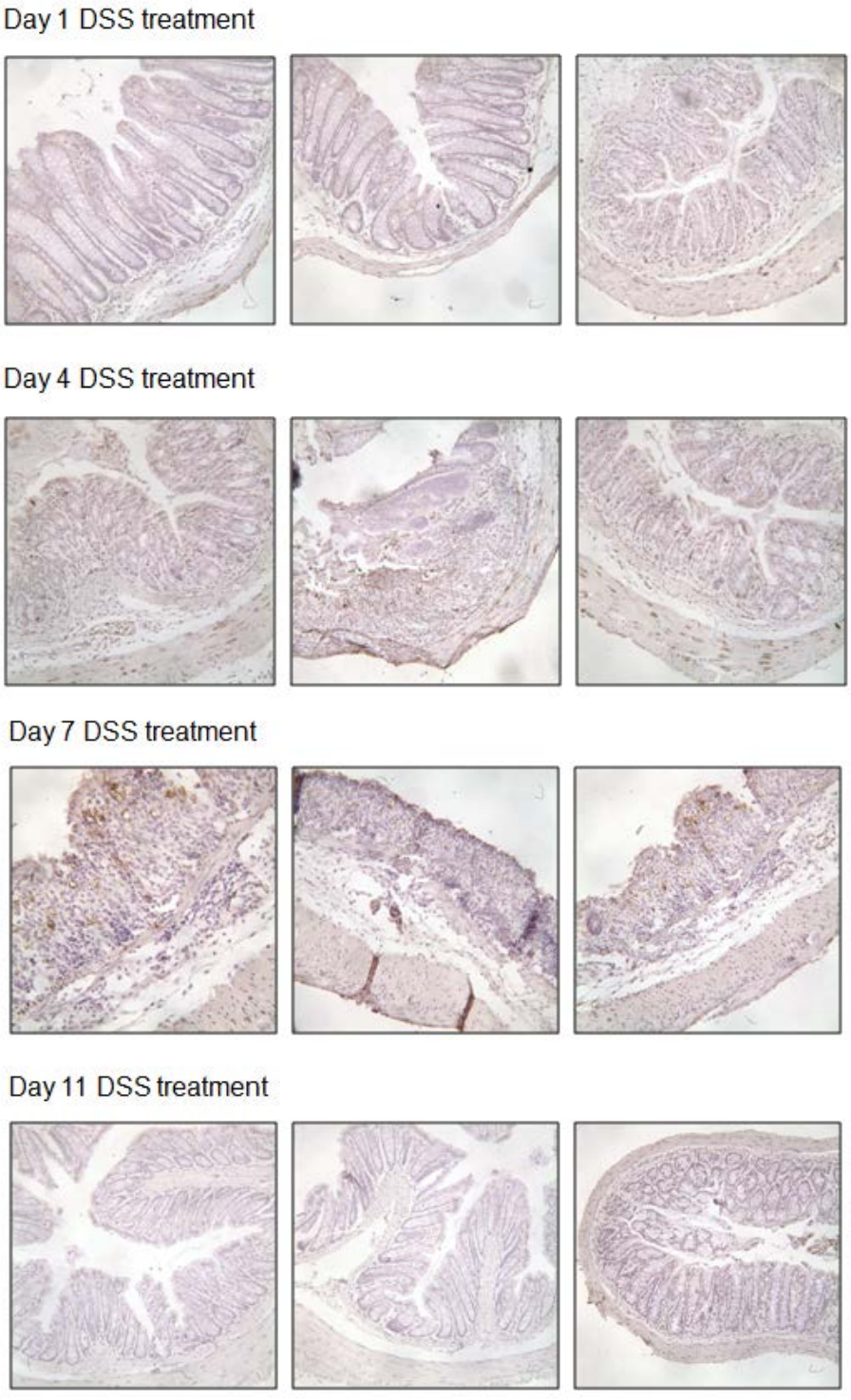

Figure 6.5.1.2. Cyclooxygenase-2 (COX-2) levels in DSS-induced colitis. Images show small intestinal tissue sections taken from C57BL/6 mice following 1, 4, 7 and 11 days of 2% w/v DSS treatment (N=1), with COX-2 protein antibody immuno-histochemical staining using diaminobenzene (DAB) and cell nucleus staining with haematoxylin, respectively. Tissue sections were incubated with a 1:400 dilution of anti-mouse COX-2 antibody, with sections (n=3) imaged at 25x magnification (3 random fields per section).

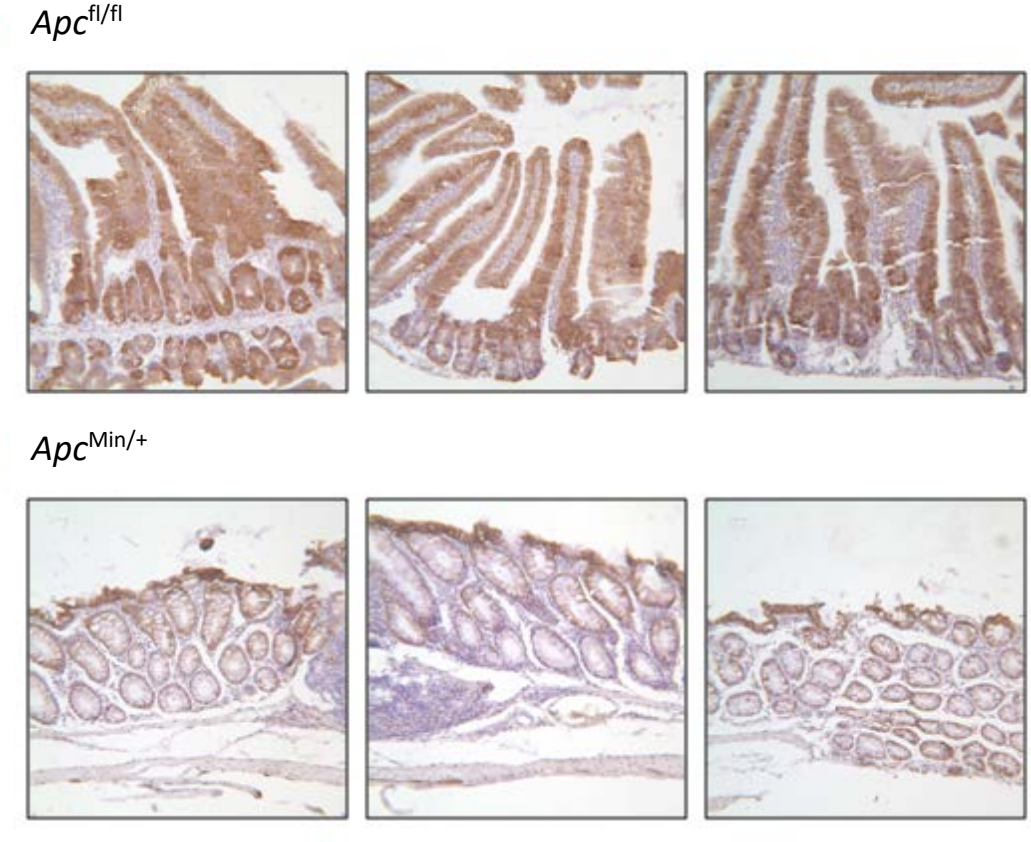

Figure 6.5.1.3. β-catenin expression in *Apc* mutant mice. Images show intestinal tissue sections taken from AhCre+ *Apc*$^{fl/fl}$ and *Apc*$^{Min/+}$ mice (N=1); with β-catenin protein detected by IHC with specific antibody and diaminobenzene (DAB) stain and cell nucleus staining with haematoxylin, respectively. Sections of intestinal tissue were incubated with a 1:50 dilution of anti-mouse β-catenin antibody, with sections (n=3 sections for each strain) imaged at 25x magnification. AhCre+ *Apc*$^{fl/fl}$ small intestinal tissue shows high levels of DAB staining, with lower levels seen in the *Apc*$^{Min/+}$ colonic tissue (3 random image fields per section).

6.5.2 Optimisation of tissue IHC imaging of germ-free *Il10*$^{-/-}$ mice using ImageJ

Germ-free *Il10*$^{-/-}$ mice on a 129SvEv background were colonised with *E. coli* HM44 by Dr Janelle Arthur at the gnotobiotic facility at NC State University using methods previously described (Arthur *et al.*, 2012). Mice were colonised with *E. coli* HM44 on 8/2/2012 in order of mouse number (see Chapter 4.12; Table 4.12.2). It was noted on 2/3/2012 that the majority of mice had ruffled fur and irregular stool was found in all cages. On 16/3/2012, two of the colonised mice were found dead with mouse #2 appearing to be of ill health (possibly linked to the large abscesses); subsequently, all other mice

were sacrificed on 3/19/12. Microtome-sectioned bundled gut tissue from these mice was kindly donated for IHC use in the current study.

Following IHC, images were taken at 4x, 10x, 25x and 40x magnification on a light microscope (Leica). Images were scrutinised optically to determine the extent of total staining, as well as the localisation of nuclear and cytoplasmic staining (**Figure 6.5.2.1**). Using anti mouse COX-2 antibody stained tissue (1:400 dilution), it was concluded that the 25x magnification should be used for quantification of immuno-staining. Optical visualisation at lower 4x and 10x magnifications did not allow for clear distinction between individual cells, nor clear distinction of absence or presence of nuclear staining, and moreover seemed to show greater variation in light intensity both across and between images; the latter of these issues was likely a problem caused by microscope or the image acquisition software at the time of testing. Imaging at 25x and 40x both gave better consistency in light intensity, avoiding light rings seen at lower magnification, and ability to distinguish localisation of staining. As the 25x magnification gave a better coverage of tissue, allowing more cells to be incorporated into the scoring, it was decided that the 25x magnification would be used going forward.

The process of quantifying or scoring within ImageJ required the removal of any possible contaminants that might influence results; an example of this would be cell debris stained by DAB that could be misinterpreted as tissue specific staining within the automated scoring system; these edits can be performed within ImageJ by selecting and clearing unwanted sections of tissue or debris (**Figure 6.5.2.2**).

Following optimisation of tissue processing and imaging, it was necessary to be able to validate the automated method of scoring; as tissue from the optimisation step had already been processed and imaging completed, it was decided that these images be used for validation.

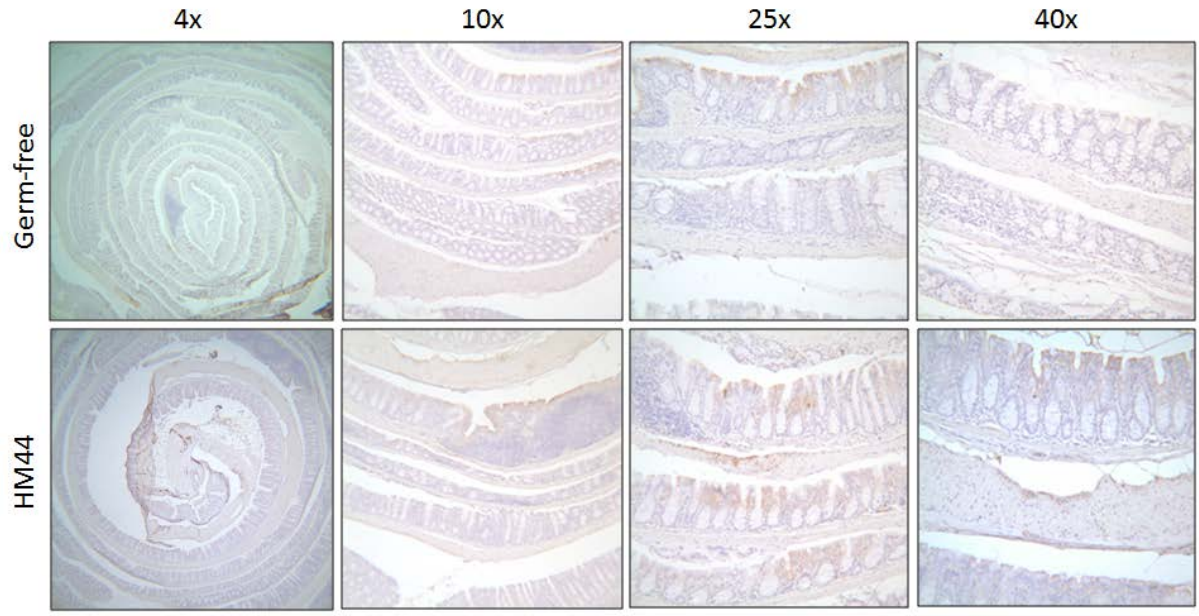

Figure 6.5.2.1. Cyclooxygenase-2 (COX-2) colonic tissue protein expression in germ-free and HM44 mono-associated *Il10*$^{-/-}$ 129SvEv mice. Images show germ-free and HM44 mono-associated *Il10*$^{-/-}$ 129SvEv mouse colonic tissue with COX-2 protein detected by IHC with specific antibody and diaminobenzene (DAB) stain and cell nucleus staining with haematoxylin, respectively. Tissue sections were imaged at 4x, 10x, 25x and 40x magnification.

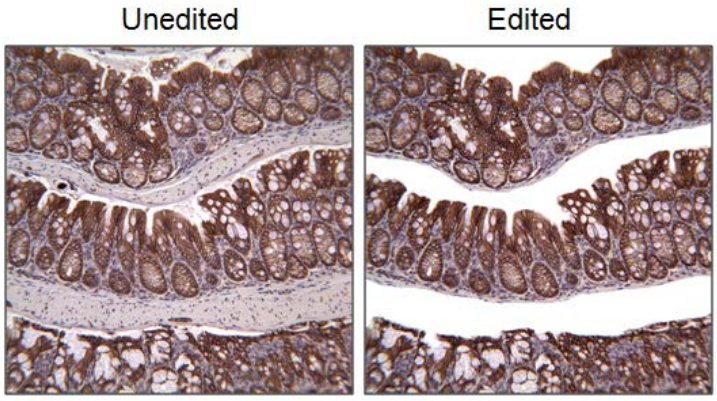

Figure 6.5.2.2. Image editing within ImageJ (version 1.48). Unedited and edited image of a gut tissue section taken from a HM44 mono-associated *Il10*$^{-/-}$ mouse (mouse #3, image 4). Tissue had been immuno-stained to show β-catenin expression, i.e. with antibody specific staining of protein detected using diaminobenzene (DAB), and cell nucleus staining with haematoxylin, respectively. Tissue was imaged at 40x magnification.

6.5.3 Validation of the Modified HSCORE quantification method using ImageJ

The ImageJ plugin IHC Profiler was used to analyse tissue immuno-staining. IHC Profiler allows scoring of DAB detection staining on an arbitrary scale using staining categorised by percentage of positive and negative staining. Following splitting of the image into haematoxylin and DAB detection stain recognition, we were able to clear either the empty and/or unwanted areas, such as non-epithelial cells for β-catenin scoring and/or cell debris, to prepare the image for scoring. IHC Profiler was then used to analyse images based on both the intensity and distribution of DAB detection reagent staining. The IHC localisation was scored in a semi-quantitative fashion; each image was processed using the IHC Profiler, with staining automatically recorded as percentages of positively stained target cells in each of five intensity categories; these were denoted as negative (no staining), low positive (weak but detectable above control), positive (distinct staining) and high positive (strong staining). For each tissue, a value designated as the HSCORE was derived by summing the percentages of cells staining at each intensity multiplied by the weighted intensity of staining:

Modified HSCORE calculation

HSCORE value = (%Negative x 0) + (%Low Positive x 1) + (%Positive x 2) + (%High Positive x 3)

Using this calculation, the scale of Modified HSCORE value would be between 0–300, with a score of 0 achieved where 100% of the tissue staining for one image was categorised as negative and a score of 300 achieved where 100% of the tissue staining was categorised as high positive. This system was validated using images of COX-2 and β-catenin immuno-stained tissue from the DSS-induced colitis and the AhCre+ *Apc*$^{fl/fl}$ mouse models, respectively. Images of DSS-induced colitis mouse model tissue at days 7 and 11, along with *Apc*$^{fl/fl}$ and *Apc*$^{Min/+}$ intestinal tissues, were processed as described by Varghese *et al.* (2014) and a score obtained for each image (Varghese *et al.*, 2014). Following imaging and automated processing of COX-2 IHC processed intestinal tissue, DSS-induced colitis mice at day 7 following DSS treatment achieved a modified HSCORE of 38.5 ± 5.6, whereas tissue from day 11 achieved a lower score of 17.9 ± 6.5 (N=1, n=3 sections; 3 images per slide). Following imaging of

β-catenin IHC processed tissue, the AhCre+ *Apc*$^{fl/fl}$ small intestinal tissue achieved a score of 113.4 ± 3.0, compared to 47.4±2.9 for *Apc*$^{Min/+}$ colon tissue; N=1, n=3 sections; 3 images per slide (**Figure 6.5.3**).

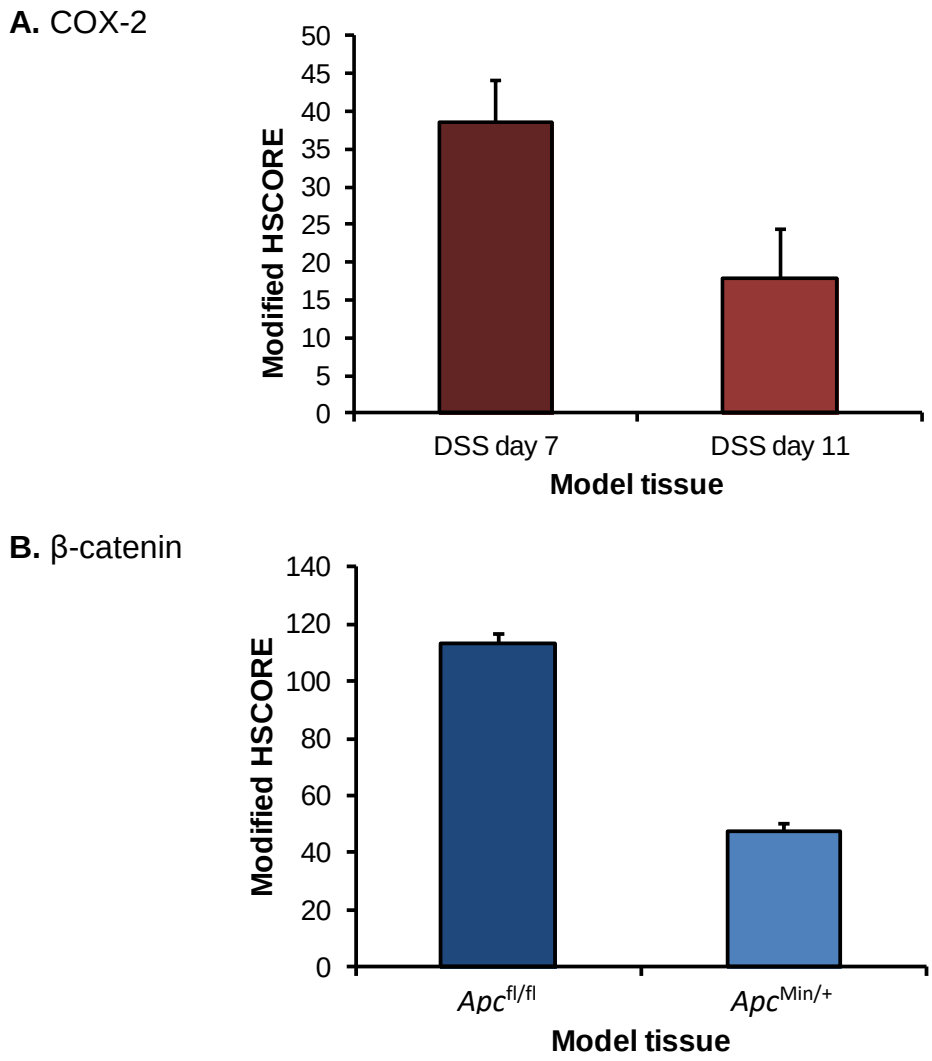

Figure 6.5.3. Modified HSCORE validation for quantification of cyclooxygenase-2 (COX-2) and β-catenin expression in mouse intestinal tissue. Graphs show modified HSCORE quantification of (A) COX-2 stained intestinal tissue from C57BL/6 DSS-induced colitis model and (B) β-catenin stained intestinal tissue from *Apc* mutant mice; higher scores were achieved by small intestinal tissue from mice at day 7 following 2% w/v DSS treatment and the AhCre+ *Apc*$^{fl/fl}$ model for COX-2 and β-catenin, respectively, with lower scores for small intestinal tissue from mice at day 11 following DSS colitis induction and in the colon of *Apc*$^{Min/+}$ model. Quantification was completed using images of immuno-stained tissue sections at 25x magnification, with protein expression determined by IHC and detection using diaminobenzene (DAB) stain and cell nucleus staining with haematoxylin, respectively (N=1, n=3; 3 images per slide).

6.5.4 Validation of the ImmunoRatio ImageJ plugin for nuclear protein quantification

Following validation of the modified HSCORE method, *Apc* mutant mouse gut tissue was used to validate the ImmunoRatio scoring system. This has been previously used to assess nuclear localisation in tissue sections, and was applied here to assess the extent of β-catenin nuclear localisation. In this case, an image of AhCre+ *Apc*$^{fl/fl}$ tissue at 25x magnification was used to determine threshold cut-offs for DAB and haematoxylin staining (**Figure 6.5.4**), set as -20 for DAB staining and 5 for haematoxylin staining. These thresholds were kept consistent for all tissue types in the study.

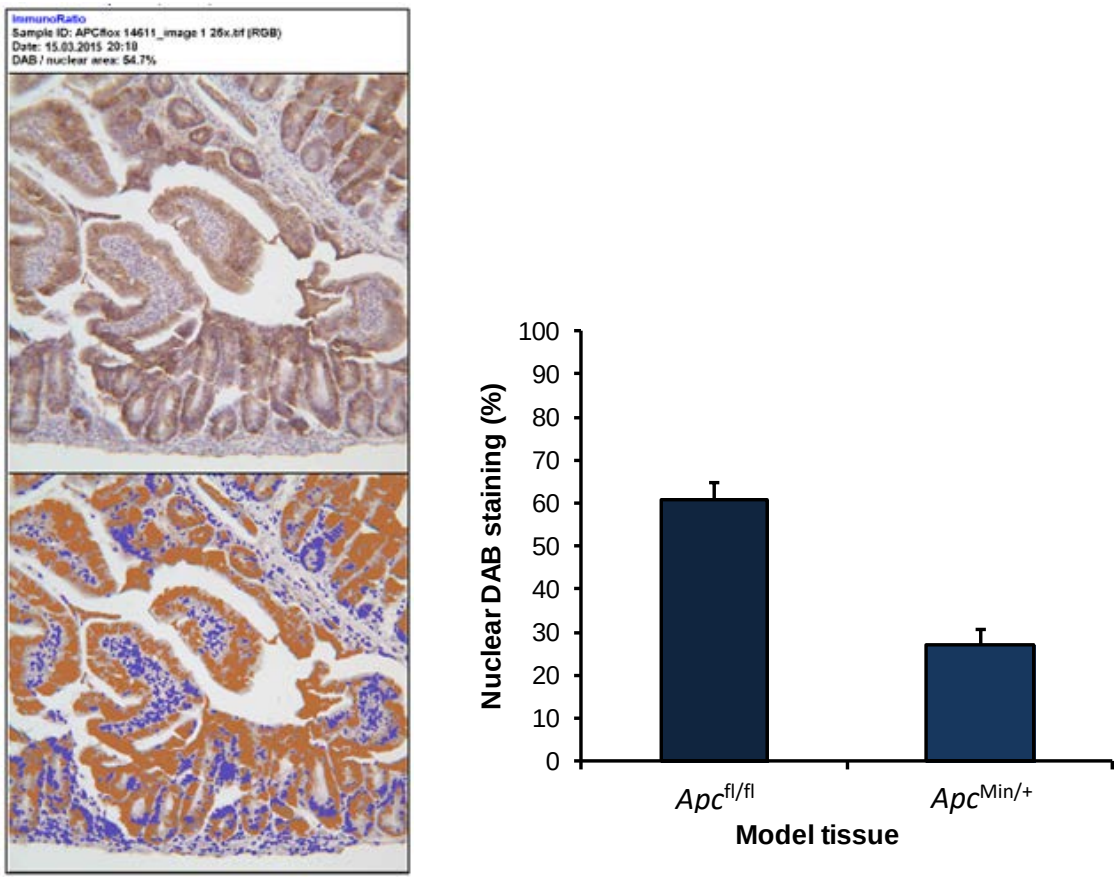

Figure 6.5.4. ImmunoRatio validation for quantification of nuclear DAB staining to indicate β-catenin expression in mouse tissue. The image was produced by ImageJ as a montage of the quantification of DAB staining of AhCre+ *Apc*$^{fl/fl}$ small intestinal tissue following processing using the ImmunoRatio plugin. The graph shows the results of quantification of nuclear DAB staining for both AhCre+ *Apc*$^{fl/fl}$ and *Apc*$^{Min/+}$ gut tissue. Quantification was completed using images of immuno-stained tissue sections at 25x magnification, with protein expression detected by IHC with specific antibody and diaminobenzene (DAB) stain and cell nucleus stained using haematoxylin, respectively (N=1, n=3; 3 images per slide).

By applying set cut-offs for DAB and haematoxylin staining for all images, it was established that *Apc*$^{fl/fl}$ small intestinal tissue had 60.9 ± 3.9 % of β-catenin showing nuclear localisation. This was around a 2-fold increase that seen in *Apc*$^{Min/+}$ colonic tissue, which had 26.9 ± 3.7 % nuclear β-catenin localisation (**Figure 6.5.4**). These results suggested that the ImmunoRatio plugin is a suitable automated system to be able to show differences in nuclear β-catenin localisation in murine intestinal tissue. Following optimisation/confirmation of the COX-2 and β-catenin antibody dilutions, imaging magnification and validation of the automated modified HSCORE and ImmunoRatio scoring systems, we implemented these processes to the germ-free *Il10*$^{-/-}$ mouse tissues with the aim of establishing effect of mono-association of these mice with the human CRC mucosa-associated *E. coli* isolate HM44.

6.5.5 Increased COX-2 and β-catenin expression in colonic epithelial tissue from HM44 mono-associated mice

Germ-free *Il10*$^{-/-}$ 129/SvEv mice were mono-associated with human mucosa-associated *E. coli* isolate HM44 for 6 weeks (infected, n=15; germ free (GF), n=5). IHC of fixed paraffin wax embedded colonic tissue revealed significant increases in mucosal COX-2 protein levels and significant increased total β-catenin protein levels in the intestinal epithelium, as well as increased nuclear localisation of β-catenin.

The median HSCORE for COX-2 staining was 32.2 (IQR 15.6, 56.6) in germ-free control *Il10*$^{-/-}$ mouse intestinal tissue, with a significant increase to 89.9 (IQR 66.0, 100.9) in tissue from *E. coli* HM44 mono-associated mice (**Figure 6.5.5.1**; Mann-Whitney U, P<0.001). Epithelial staining for β-catenin showed a median HSCORE of 44.1 (IQR 28.8, 126.0) in germ-free control tissue and 177.2 (IQR 98.8, 184.9) in the *E. coli* HM44 colonised intestinal tissue (**Figure 6.5.5.2**; P<0.001), while median nuclear localisation of β-catenin within the epithelium was scored at 16.7% (IQR 11.5, 45.3) and 62.4% (IQR 42.4, 67.1) respectively (**Figure 6.5.5.2**; P<0.001).

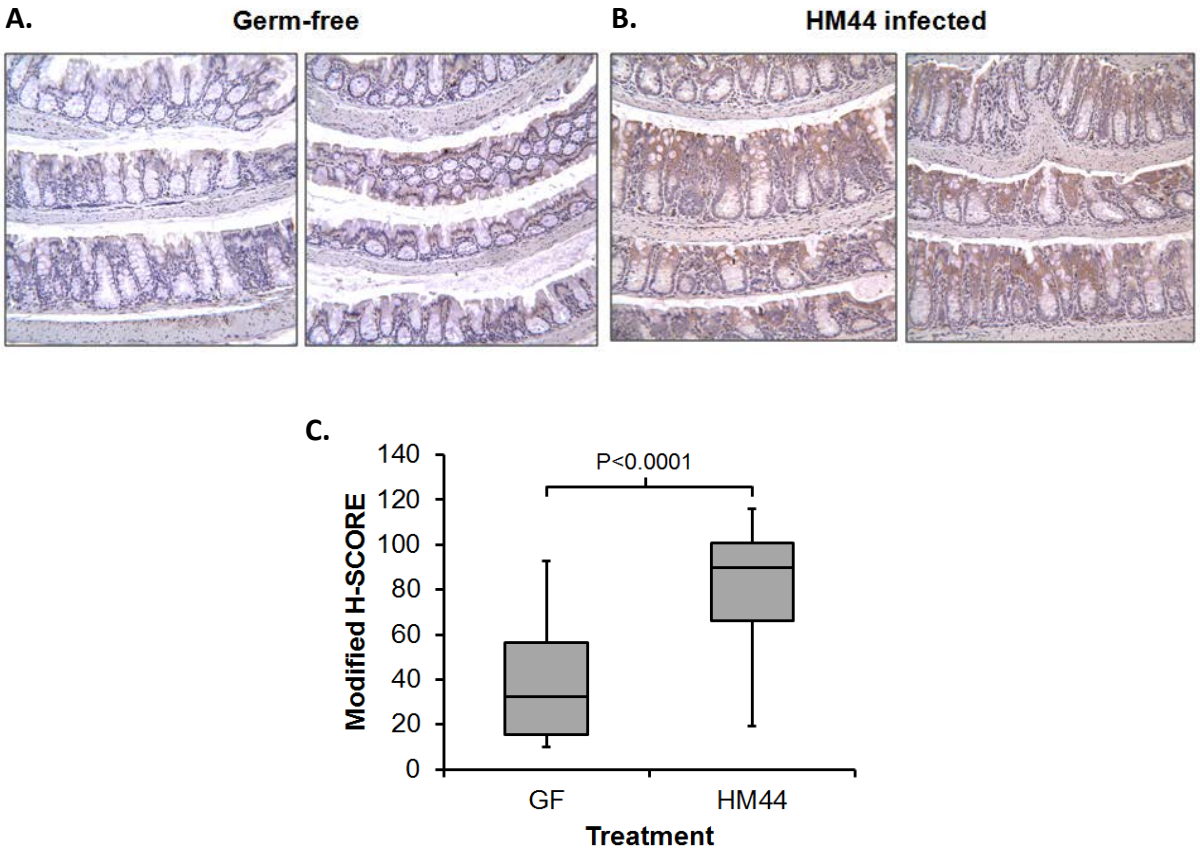

Figure 6.5.5.1. Significant increases in cyclooxygenase-2 (COX-2) expression quantification in intestinal tissue following *in vivo* mono-association of germ-free *Il10*$^{-/-}$ mice with a CRC mucosa-associated *E. coli*. IHC images show COX-2 protein expression detected using diaminobenzene (DAB) stain and cell nucleus staining with haematoxylin respectively, in **(A)** germ-free *Il10*$^{-/-}$ mice and **(B)** mice mono-associated *E. coli* HM44. **(C)** Graph shows modified HSCORE quantification of total COX-2 protein levels in intestinal tissue, with significantly higher scores observed in mice mono-associated with HM44 (P<0.001; Mann-Whitney U). Image quantification was completed on sections from N=5 germ free mice, and N=15 HM44 mono-associated mice (with n=5 images per section) at 25x magnification.

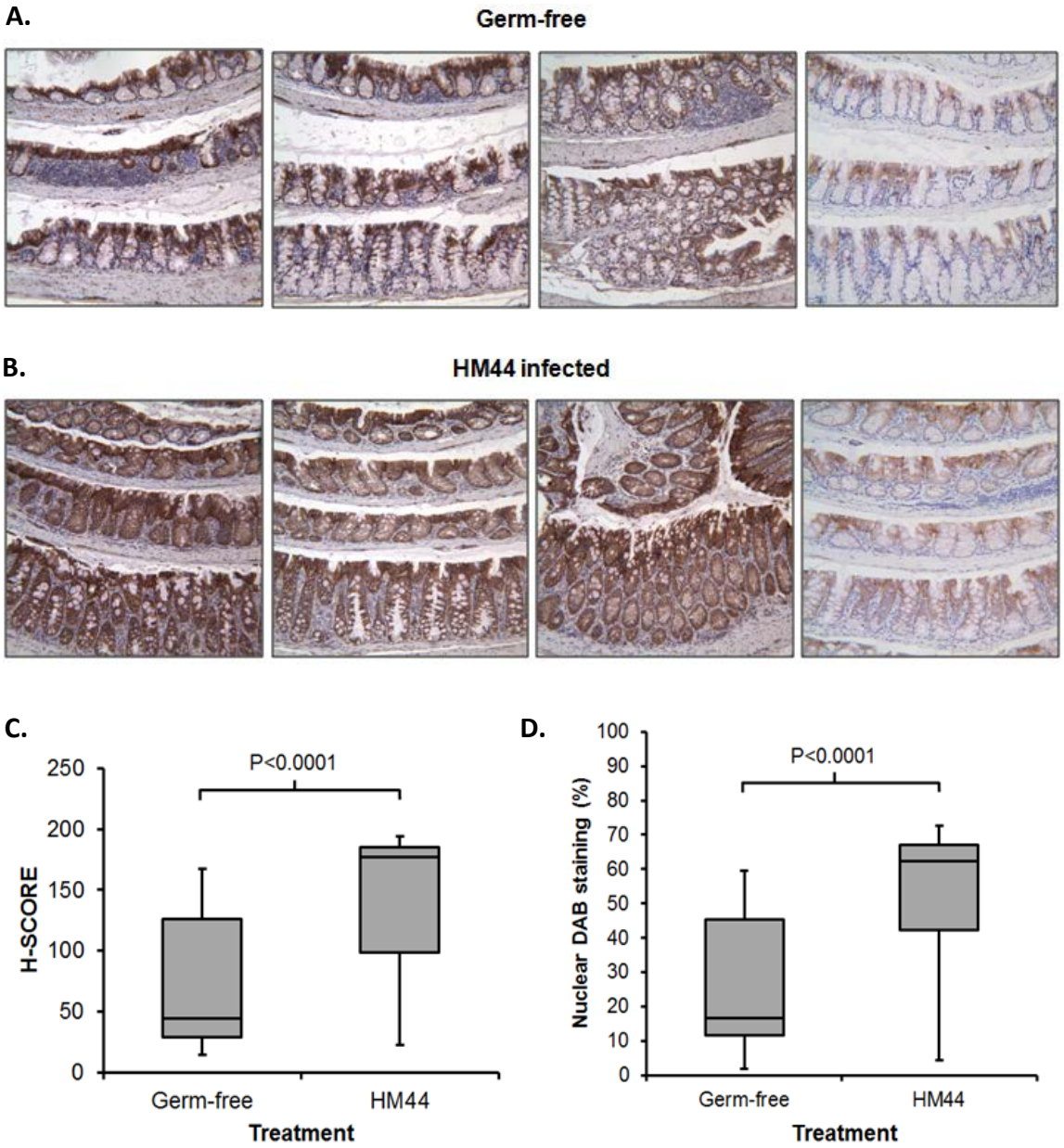

Figure 6.5.5.2. Significant increases in β-catenin expression and nuclear localisation quantification in intestinal tissue following *in vivo* mono-association of germ-free *Il10*$^{-/-}$ mice with a CRC mucosa-associated *E. coli*. IHC images show β-catenin protein expression detected using diaminobenzene (DAB) stain and cell nucleus staining with haematoxylin respectively, in in **(A)** germ-free *Il10*$^{-/-}$ mice and **(B)** mice mono-associated *E. coli* HM44. Graphs show modified HSCORE and % nuclear DAB staining quantification for **(C)** total β-catenin expression and **(D)** nuclear localisation in intestinal tissue. Significantly higher scores/staining were seen in tissue taken from HM44 mono-associated mice (both P<0.001; Mann-Whitney U). Image quantification was completed on sections from N=5 germ free mice, and N=15 HM44 mono-associated mice (with n=5 images per section) at 25x magnification.

Mean and confidence interval data show an approximate 2-fold significant increase (P<0.001) in COX-2 staining *E. coli* HM44 colonised intestinal tissue (mean 78.7; 95%CI 71.0, 86.4) compared to germ-free control *Il10*$^{-/-}$ mice (mean 38.6; 95%CI 27.4, 49.8). A similar 2-fold significant increase (P<0.001) was also observed for total β-catenin staining in *E. coli* HM44 colonised tissue (mean 146.0; 95%CI 130.4, 161.5) compared to germ-free tissue (mean 71.8; 95%CI 50.9, 92.7). Nuclear localisation of β-catenin was also shown to significantly elevated, again around 2-fold (P<0.001) in *E. coli* HM44 colonised tissue (mean 51.6%; 95%CI 45.4, 57.8) compared to controls (mean 25.8; 95%CI 18.1, 33.6).

The staining intensity, along with the final HSCORE values, for both COX-2 and β-catenin, in intestinal tissue sections from the murine model systems used (DSS-induced colitis and *Apc* mutants) were assessed and confirmed by two independent experimenters, Dr Carrie Duckworth and Dr John Jenkins (University of Liverpool), both with vast experience of murine and human histopathology (and specifically IHC for COX-2 and β-catenin). A random selection of images were also confirmed to correlate with automated HSCORE values attributed to tissues from both germ-free and HM44 mono-associated *Il10*$^{-/-}$ mice.

Haematoxylin and eosin staining was also processed by Dr Janelle Arthur and reviewed by animal pathology expert, Dr Jonathan Williams, University of Liverpool (now at Department of Pathology and Pathogen Biology, Royal Veterinary College, North Mymms AL9 7TA, UK). Imaging of germ-free mice showed normal colonic folds of proximal colon with relatively few goblet cells, with thin mucosa seen in some small areas (**Figure 6.5.5.3**). In comparison, *E. coli* HM44 mono-associated mice showed infiltration of neutrophils, lymphocytes and plasma cells in the lamina propria, areas of crypt mitosis, and extravasated erythrocytes indicating possible minimal haemorrhage. Some images also showed thinning of the crypts, neutrophils undergoing epithelial exocytosis, and single cell apoptosis/necrosis, with possible micro-erosions.

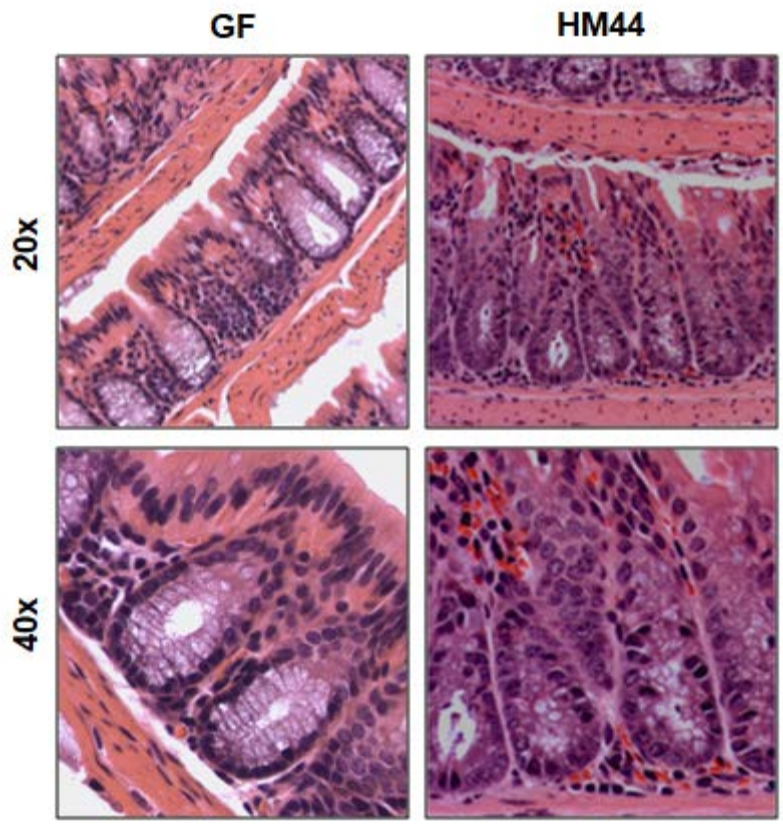

Figure 6.5.5.3. H&E imaging of intestinal tissue following *in vivo* mono-association of germ-free *Il10*$^{-/-}$ mice with a CRC mucosa-associated *E. coli*. H&E histology of germ-free *Il10*$^{-/-}$ mice and mice mono-associated with *E. coli* HM44 was completed by Dr Janelle Arthur (University of North Carolina Chapel Hill, USA) and reviewed by Dr Jonathan Williams (University of Liverpool). Images shown were captured at 20x and 40x magnification.

In summary, automated quantification of IHC processed intestinal tissue suggests that HM44 mono-association of germ-free *Il10*$^{-/-}$ mice caused an approximate 2-fold increase in both COX-2 and Wnt pathway activation (i.e. nuclear localisation of β-catenin), and these increases were seen to be highly significant. Further work remains to fully determine phenotypic changes and development of hyperplasia and/or tumours, with early observations of the gut epithelial environment showing inflammatory infiltrate and crypt mitosis, suggesting a proliferative state of crypt cells. This remains to be quantified.

6.5.6 Discussion

Following mono-association of germ-free *Il10*$^{-/-}$ mice with a CRC mucosa-associated *E. coli* isolate, there were significant increases observed in intestinal tissue expression of both COX-2 and β-catenin protein, with the latter showing increased levels of nuclear localisation. Nuclear translocation of beta catenin leads to significant potential for activation of TCF/Lef Wnt pathway signalling, a key early step in colorectal carcinogenesis (Behrens *et al*., 1996, Morin *et al*., 1997, Kobayashi *et al*., 2000). This result obtained *in vivo* validates data obtained *in vitro* following infection of CRC cell-lines SW480 and DLD-1 with CRC and IBD mucosa-associated *E. coli* (see Chapter 5).

Microbial composition has been found to influence the development of colitis-associated colorectal cancer. Studies using germ-free mouse models have revealed a key role for the microbiota in driving colorectal cancer with mice raised in germ-free conditions typically devoid of intestinal inflammation and tumours (Arthur and Jobin, 2011). Gut bacteria interaction with Toll-like receptors (TLRs) on the luminal surface of intestinal epithelial cells (with consequent signalling via MyD88) is a key step in experimental CRC pathogenesis (Rakoff-Nahoum and Medzhitov, 2009). Moreover, *MyD88*$^{-/-}$ mice cross-bred onto either *Apc*$^{Min/+}$ mice resulted in marked reduction in tumours and mortality (Rakoff-Nahoum and Medzhitov, 2007). In other susceptible mouse models, the presence of commensal and other bacteria facilitates CRC development in comparison with germ-free animals. Examples include, the spontaneous CRC that develops in TCR-βchain-p53 double-knockout mice, which does not develop if animals are kept under germ-free conditions (Kado *et al*., 2001), and colonisation of germ-free rats with *E. coli* or *Bacteroides* spp. increases the number of carcinogen-induced aberrant crypt foci, a precursor for CRC (Onoue *et al*., 1997).

The IL-10 family of cytokines have been established as playing an essential role in anti-inflammatory immune response, with a particular role in defence against infections within epithelial cells (Ouyang *et al.*, 2011, Iyer and Cheng, 2012, Couper *et al.*, 2008). The germ-free *Il10*$^{-/-}$ murine model used in the present study has been highlighted by Scheinin *et al.* (2003) to be important in advancing our

understanding of pathogenesis in inflammation-associated bowel diseases and in supporting development of new therapeutics for conditions such as Crohn's disease, a bowel disease with significant increased risk of CRC, and where mucosa-associated *E. coli* likely play a key role in this condition (Martin *et al*., 2004, Prorok-Hamon *et al*., 2014). The removal of this innate defence mechanism allows a direct look at the effect of CRC (and IBD) mucosa-associated *E. coli* infection of an otherwise germ-free gut. Using microscopic evaluation of the immuno-stained mouse intestinal tissue, we were able to see an increase in both COX-2 and β-catenin protein levels following infection solely with an adherent, invasive *E. coli* HM44 isolated from a patient with CRC (Martin *et al.*, 2004).

Il10$^{-/-}$ mice that develop colitis in the presence of normal enteric microbiota, do not develop inflammation if kept in a germ-free environment, and when given the carcinogen azoxymethane, only develop CRC when acquiring a normal gut microbiota following transfer from germ-free conditions, with modulation of the microbiota also altering CRC susceptibility (Uronis *et al*., 2009).

Germ-free *Il10*$^{-/-}$ mice have previously been shown to develop colitis after being colonized with other specific bacteria, such as *Enterococcus faecalis* (*E. faecalis*) (Balish and Warner, 2002). *E. faecalis* not only induced inflammation, primarily in the colon and rectum, but rectal dysplasia and adenocarcinoma were also observed in the infected mice (Balish and Warner, 2002). In addition, conventional housed *Il10*$^{-/-}$ mice with a complex-intestinal microbiota actually developed *E. faecalis*-induced colitis within 10 to 15 weeks of age and showed more pathology in the caecum (typhlitis) than observed with *E. faecalis*-induced colitis in germ-free *Il10*$^{-/-}$ mice. In contrast, neither germ-free *Il10*$^{-/-}$ mice nor *Il10*$^{-/-}$ mice colonized with a pure culture of *Candida albicans*, *E. coli*, *Lactobacillus casei*, *L. reuteri*, *L. acidophilus*, a *Bifidobacterium* spp., *Lactococcus lactis* or a *Bacillus* spp. developed colitis during the 25-30 week study. The authors concluded here that *E. faecalis* could specifically trigger colitis, dysplasia, and carcinoma in a genetically susceptible murine host (Balish and Warner, 2002). *E. faecalis* is also known to produce superoxide, which results in genomic instability, severe inflammation and CRC in *Il10*$^{-/-}$ mice (Wang and Huycke, 2007, Wang *et al*., 2012c).

Mono-association of germ-free *Il10*$^{-/-}$ mice with a murine AIEC isolate, influenced by intestinal inflammation, appears to drive CRC progression in carcinogen-treated mice through the *pks* pathogenicity island (Arthur *et al*., 2012) encoding for colibactin, a genotoxin shown to induce enterocyte DNA damage and promote tumour growth (Cuevas-Ramos *et al*., 2010, Cougnoux *et al*., 2014). An increased prevalence of *pks*-positive *E. coli* isolates in colorectal tissue implies a similar cancer-promoting role in human CRC (Arthur *et al*., 2012, Prorok-Hamon *et al*., 2014).

However, the CRC mucosa-associated *E. coli* strain used in this study, HM44, does not harbour the *pks* pathogenicity island encoding for colibactin (Arthur *et al.*, 2012; Prorok-Hamon *et al.*, 2014) but does harbour the *afa* operon, more characteristic of diffuse adherent *E. coli* (DAEC) isolates (Servin, 2005). It has been recently observed that there is increased prevalence of *afa*-expressing mucosa-associated *E. coli* in CRC, with these isolates showing significant ability to upregulate angiogenic *VEGF* mRNA (Prorok-Hamon *et al.*, 2014). DAEC have also been observed to both increase activity of AKT serine/threonine kinase, a molecular link to Wnt signalling, and to enhance nuclear localization of β-catenin (Anderson and Wong, 2010, Cane *et al*., 2007). DAEC afimbrial adhesins (Afa/Dr) are also known to promote secretion of pro-angiogenic VEGF from epithelial cells and to induce epithelial-mesenchymal transition (Cane *et al*., 2010), a potential mechanism for carcinoma progression (Thiery *et al*., 2009). Moreover, VEGF/VEGFR2 signaling is a key molecular link between inflammation and CRC promoting epithelial cell proliferation and tumour growth *in vivo* (Waldner *et al*., 2010).

Our ability to quantify the changes in COX-2 and β-catenin protein expression following as little as 6-weeks of colonisation *in vivo* in this study could be seen as an important step towards linking mucosa-associated *E. coli* infections to an increased risk of CRC development and progression. This is a key finding, further supporting showing that inflammation signals and increase in Wnt signalling, could be an early event in bacteria-induced colon carcinogenesis.

For this part of the study, immunohistochemical staining was a powerful tool in being able to visualise the changes in expression of COX-2 and β-catenin. The use of DAB staining for nuclear localisation was

also important to assess β-catenin nuclear localisation. However, even with the use of negative controls and blocking, absolute quantification using DAB staining intensities can be difficult to interpret, comparatively (Rizzardi *et al.*, 2012, de Matos *et al.*, 2010). Other robust techniques such as qPCR and immunoblotting can be used alongside IHC to allow more comparisons to be drawn and to confirm changes in gene and protein expression. Future analysis using techniques such as these may help to strengthen and confirm our findings of COX-2 and β-catenin protein expression changes.

This use of an automated scoring system to detect levels of COX-2 and β-catenin allowed for a higher throughput image quantification in this study, where experimenter bias was also significantly reduced. With a pre-determined number of images taken per immuno-stained tissue section and microscopy light settings consistent for imaging of both germ-free and HM44 mono-associated *Il10*$^{-/-}$ murine tissues, automating the process of categorising the DAB staining intensity ruled out the maximum number of variables that could affect the outcome of this scoring method. High quality results were achieved by adapting the HSCORE method – an early approach reported in a breast cancer model (McCarty *et al.*, 1986). Due to the limited availability of colonic tissue from the *in vivo* mono-association study, we decided first to optimise and validate the HSCORE method of quantification before submitting the germ-free *Il10*$^{-/-}$ model tissue for immunohistochemistry (IHC). Intestinal tissues tissue from a wild-type C57BL/6 mouse treated with 2% w/v DSS, typically used to model the development of DSS-induced colitis, and with observed upregulation of COX-2 (Singh *et al*., 2010) was first used to validate the HSCORE system for COX-2 staining. The original study utilising this scoring technique evaluated the immunohistochemical staining of human tumour tissue using a monoclonal anti-oestrogen receptor antibody (McCarty *et al.*, 1986). Immunohistochemical localisation was scored in a semi-quantitative fashion incorporating both the intensity and the distribution of specific staining (McCarty *et al.*, 1986). Evaluation of staining in our study, was recorded as percentages of positively stained target cells in five intensity categories; these were denoted as 0 (no staining), 1+ (weak but detectable above control), 2+ (distinct), 3+ (strong), and 4+ (minimal light transmission through stained nucleus). These percentages were used to designate a HSCORE value derived by

summing the percentages of cells staining at each intensity multiplied by the weighted intensity of staining (McCarty *et al.*, 1986). The method of achieving a final HSCORE value described in the original study is similar to that incorporated into the IHC Profiler values of negative, low positive, positive and high positive. The IHC Profiler is a plugin for ImageJ, and was also used in our study. This method is typically used for scoring protein targets with cytoplasmic and/or nuclear expression (Varghese *et al.*, 2014), making it suitable for scoring total epithelial levels of COX-2 and β-catenin expression. As mentioned previously, the ability to deconvolute the cell nuclear blue haematoxylin stain and the brown diaminobenzidine (DAB) stain used to detect COX-2 and β-catenin antibody binding, allowed for a more sensitive method of quantification. If such a tissue scoring technique was to be utilised as a marker for COX-2 or β-catenin in future studies, it would benefit from a compared to an established scoring system using tissue pathology. One such system has been developed for visual analogue scoring in order to quantifying immunohistochemical staining, and has been used to compare untreated and *H. felis*-infected C57BL/6 mice (Duckworth *et al.*, 2015). This would enable the experimenter to further confirm the suitability of the automated scoring technique. In order to further minimise the risk of bias with more valuable tissue, for example limited biopsy tissue being used to determine CRC cancer risk, it would be beneficial to introduce an image blinding system, where the person evaluating the staining intensity of each image was blinded as to the origin of the tissue. Nevertheless, the way in which this scoring system is automated should remove any interference with the final scoring outcome.

Following the validation of the COX-2 protocol, we sought to optimise and validate the HSCORE system for β-catenin staining. As previously mentioned, gut tissue obtained from loxP-flanked *Apc* mutant ($Apc^{fl/fl}$) AhCre mice (Sansom *et al.*, 2004, Su *et al.*, 1992), recommended for modelling CRC (Karim and Huso, 2013, Newman *et al.*, 2001), was used to validate the scoring system for β-catenin, but also to validate the ImmunoRatio scoring system (described above), which has been previously used to assess nuclear localisation in tissue sections (Tuominen *et al.*, 2010, Sundara Rajan *et al.*, 2014).

The *APC* gene codes for the functional tumour-suppressor protein adenomatous polyposis coli, with inactivation recognised as a key early event in the development of sporadic colorectal cancers (Sansom *et al.*, 2004). APC protein is responsible for targeting β-catenin for degradation; therefore, loss of conventional Apc function in these mouse models gives rise to unregulated Wnt signalling, leading to increased cell adhesion and migration, loss of cell cycle control, reduced apoptosis and chromosomal stability (Bienz and Clevers, 2000, Nathke *et al.*, 1996, Fodde *et al.*, 2001). The loss of *Apc* function in this mouse model meant that gut tissue would be highly valuable for the optimisation and validation of the scoring technique that was to be used to assess β-catenin localisation in the HM44 mono-association model.

The $Apc^{fl/fl}$ mutant mouse model, a novel inducible transgenic line in conjunction with a loxP-flanked *Apc* allele, was created by Sansom *et al.* (2004) using Cre/loxP technology (Sansom *et al.*, 2004) and adopted by Dr John Jenkins and Dr Cleberson Quieroz, who kindly donated gut tissue for use in our study. Cre recombinase is a tyrosine recombinase enzyme responsible for the excision of any region of DNA placed between two loxP sites, with the loxP site genetically targeted around an essential exon in a gene, in this case *Apc*. The resulting mice contain the floxed (flanked by loxP sites) allele in all tissues but are phenotypically wildtype. These floxed mice are then bred to Cre expressing transgenic animals, where an inducer is required to drive Cre expression in order for gene deletion to occur (Hall *et al.*, 2009). In this case, the Cre $Apc^{fl/fl}$ was induced by beta-napthoflavone injectons (Sansom *et al.*, 2004).

The multiple intestinal neoplasia mouse model is typically used as a model for familial adenomatous polyposis coli (FAP). Mice in this model harbour one wild-type *Apc* allele and one *Apc* allele mutated at codon 850 ($Apc^{Min/+}$). Due to the mutation, this model displays *Apc*-driven tumourigenesis in the intestine, and investigation of adenomas from both FAP patients and $Apc^{Min/+}$ mice has shown either mutation or loss of the wild-type *Apc* allele in most adenomas (Luo *et al.*, 2009). Adenomas found in this mouse model are predominantly localised to the small intestine and are generally benign, meaning a lack of progression to invasive colon cancer (Young *et al.*, 2013).

Summary

Significant increases in both COX-2 and β-catenin expression, and in nuclear localisation of β-catenin, was shown in murine intestinal tissue mono-associated with a human CRC mucosa-associated *E. coli* isolate HM44. This demonstrates translation of findings seen *in vitro*, where COX-2 and Wnt signalling pathway activation was observed in laboratory cultures CRC cell-lines infected by the same isolate (and other similar CRC and IBD mucosa-associated *E. coli* isolates), into a disease-relevant *in vivo* system. These increases in β-catenin/Wnt pathway activation could impact cell adhesion and migration, loss of cell cycle control, reduced apoptosis and chromosomal stability as previously reported. Further work remains to fully determine phenotypic changes and development of hyperplasia and/or tumours, but early observations of the gut epithelial environment showed inflammatory infiltrate and crypt mitosis, suggesting a proliferative state of crypt cells infected with CRC-associated *E. coli* HM44. With a number of factors, both genetic and environmental, causing a shift towards increased numbers of these pathogenic bacteria, influenced by intestinal inflammation, this could be seen as a possible early driving event in the development and/or progression of colorectal cancers. Additional study of other chronic mucosa-associated *E. coli* infections would be beneficial, and could help to build a convincing argument towards the involvement of these specific Wnt-activating bacteria in IBD-associated and sporadic CRC.

Chapter 7:

Identification of genomic elements responsible for COX-2 up-regulation using a fosmid clone library generated from CRC mucosa-associated *E. coli* HM358

7.1 Introduction

With a wide role of cyclooxygenase-2 (COX-2) in CRC development and progression, and a cascade suggested for the role of COX-2 and prostaglandin-E_2 (PGE_2) in stimulating cancer cell growth via Wnt activation (Castellone *et al*., 2005), it is highly possible that COX-2 induction following chronic bacterial infection of colonic cells could lead to sustained increases in Wnt signalling *in vivo*.

COX-2-driven PGE_2 increases are believed to activate the G protein–coupled receptor EP2 leading to phosphoinositide 3-kinase (PI3K) activation of the Wnt signalling pathway via the inactivation of glycogen synthase kinase 3β (GSK3β). The subsequent accumulation of β-catenin in the cytoplasm and its nuclear translocation following infection of colonic cells with mucosa-associated *E. coli* could support cancer cell proliferation, migration and metastasis. With gut inflammation able to alter the composition of the microbiota in favour of the adherent, invasive *E. coli* pathovar (Darfeuille-Michaud *et al.*, 1998, Swidsinski *et al.*, 1998, Martin *et al.*, 2004), this could create an environment that also favours tumour development and progression, by resultant expansion of, and contact with, these mucosa-associated bacteria. In addition, as CRC mucosa-associated *E. coli* strains can also survive and replicate within human mucosal macrophages, leading to further increases in mucosal COX-2 expression and subsequent PGE_2 secretion (Raisch *et al.*, 2015).

We have so far been able to characterise upregulation of Wnt signalling target genes alongside increases in COX-2 and β-catenin at both mRNA and protein level following *in vitro* infection of CRC cell lines with mucosa-associated *E. coli* isolates, including HM44 and HM358 both isolated from CRC patient biopsy tissues. We have also been able to show translation of increased CRC *E. coli*-induced COX-2 and β-catenin protein expression to that observed *in vivo* in an infection model using germ-free *Il10*$^{-/-}$ mice mono-associated with the CRC mucosa-associated *E. coli* HM44.

These results suggest that inflammation-associated and CRC mucosa-associated adherent, invasive *E. coli* may harbour a key virulence factor(s) that support increased COX-2 and Wnt signalling, important as possible drivers in the development and/or progression of CRC. Therefore, we aimed to

establish whether specific genomic elements could be identified as being responsible for or contributing towards these effects in colonic cell lines. To support this, we were fortunate to have access to a screening library of 968 clones prepared using sheared gDNA fragments isolated from CRC mucosa-associated *E. coli* HM358, shown to increase COX2 in CRC cell lines *in vitro* (See Chapter 5) randomly inserted into the pCC1Fos fosmid vector transformed to non-pathogenic *E. coli* EPI300-T1 (see Figure 7.4). This approach had already successfully been used to identify the afimbrial adhesin *afa* operon, more common to diffusely adherent *E. coli* (DAEC) (Servin, 2005), showing its role in adhesion to, and invasion of epithelial cells, increased VEGF expression (i.e. angiogenic potential), and increased prevalence and presence in *E. coli* isolates from the colorectal mucosae of patients with Crohn's disease and CRC (Prorok-Hamon *et al.*, 2014).

With these mucosa-associated *E. coli* found in increased numbers within intestinal tissue taken from patients with IBD and CRC, a considerable impact could be made by identifying a bacterial gene cluster/gene encoding a key virulence factor(s) responsible for, or contributing towards, increased mucosal COX-2 and Wnt signal pathway activation, characteristic of inflammation-associated and sporadic CRC.

7.2 Hypothesis

Increases in COX-2 following mucosa-associated *E. coli* infection of colonocytes, observed *in vitro* and *in vivo*, are driven by specific genomic elements encoding key virulence factors likely specific to mucosa-associated *E. coli*.

7.3 Aims

- To investigate *PTGS2* (COX-2) gene expression by RT-PCR following infection of SW480 CRC cells with 968 library clones each containing a fosmid harbouring a functional fragment of gDNA from the CRC mucosa-associated *E. coli* HM358 (known *in vitro* to upregulate COX2).
- To sequence all confirmed *PTGS2*-inducing fosmid clones to find any common genes/operons and identify genomic elements responsible for or contributing towards mucosal COX-2 expression changes.

7.4 Methods

To identify potential genomic elements involved in activation of COX-2 by CRC mucosa-associated *E. coli*, we used a 968 fosmid clone library previously prepared in *E. coli* EPI300-T1 using sheared large functional fragments of genomic DNA from *E. coli* HM358, a haemagglutination-positive, adherent, invasive CRC isolate (Prorok-Hamon *et al.*, 2014). Briefly, genomic DNA from this isolate was extracted using the Genomix Cell/Tissue kit (Talent; Italy) and randomly sheared to create a non-biased fosmid library using the CopyControl fosmid library kit (Epicentre; USA). DNA fragments were ligated into the pCC1Fos vector and introduced into phage T1-resistant *E. coli* K-12 derivate EPI300-T1, with subsequent clones selected on chloramphenicol (12.5 µg/mL) containing LB agar.

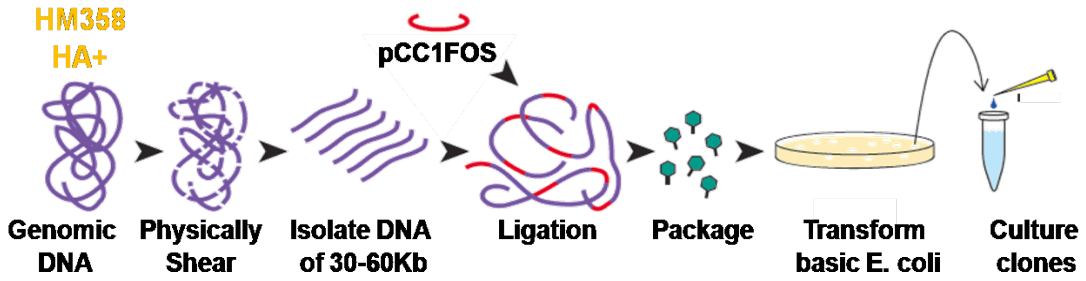

Figure 7.4. Production of fosmid library and subsequent induction of clones using haemagglutinnating positive (HA+) CRC mucosa-associated *E. coli* isolate HM358. Adapted from Epicentre CopyControl™ Fosmid Library Production (http://www.epibio.com/docs/default-source/protocols/copycontrol-fosmid-library-production-kit-with-pcc1fos-vector.pdf).

For our study, each of the 968 fosmid library clones were sub-cultured from -80°C stored Protect bead stocks, and glycerol stocks generated for long-term storage and SW480 CRC cell infections in a 96 well format. Briefly, liquid LB broth was prepared (5g sodium chloride, 5g tryptone, 2.5g yeast extract and 500 mL Elga-purified dionised water), with 500 µL added to each well of a deep 96-well plate (Sigma Aldrich; UK). Using a sterile loop, a single Protect bead was added to individual wells of the 96 deep well liquid LB plate. The 96-well cultures were covered using a slotted rubber plate lid (Sigma Aldrich)

and incubated at 37 °C overnight in a shacking incubator (140 rpm). Culture growth was characterized by a cloudy haze in the media and confirmed by conducting optical density (OD_{600nm}) measurement using samples from 3 randomly selected wells, before using the same sample to grow clones on LB agar; a negative control using LB media supplemented with 500 µg/mL gentamicin (Sigma Aldrich) with and without bacteria was used to confirm lack of growth in these cultures. Following growth, 500 µL of 50% glycerol (100% glycerol in Elga-purified deionised water) was added to each well of bacterial culture and gently mixed. Glycerol stocks were stored at -80°C. To recover bacteria from frozen glycerol stocks, a sterile loop was used to streak onto LB agar plates and grown overnight.

For infection studies using SW480 CRC cells, cells of a low passage number (below 20 passages) were cultured as monolayers and maintained in DMEM supplemented with 10% FBS at 37˚C. Trypsinised cells were diluted to a cell suspension containing 250,000 cells/mL, with 2 mL of culture added to each well of clear 12-well cell culture plates (Corning; UK) and incubated overnight at 37 ˚C. Cells were infected with each of the 968 fosmid library clones for 4 hours at 37˚C (MOI: 10) for consistency with previous *in vitro* infection studies. Following infection, bacteria-containing media was removed and cells washed three times using sterile PBS (pH7.4) before lysis. Lysates were processed for extraction of RNA using the Zymo ZR-96 Quick-RNA kit (R1052; Zymo Research, US) following the manufacturers protocol. Briefly, each lysate was transferred to the 96-well Silicon-A Plate (supplied) and centrifuged at 4500 x g for 5 min. Lysate was then mixed with RNA lysis buffer and washed in Prep and Wash buffers (supplied), centrifuged at 4500 x g for 5 min. RNA was then eluted using DNase/RNase free water. Eluted RNA was used to synthesise cDNA and stored at -80 ˚C.

RT-PCR using the cDNA was then used to assess expression of the *PTGS2* gene encoding for COX-2 protein, as in previous *in vitro* infection studies (see Chapter 5). Results were normalised to the expression of β actin gene, *ACTB*. Positive and negative controls using parent CRC mucosa-associated *E. coli* HM358 infected SW480 cells and non-infected cells respectively, were included in each run, with the same RT-PCR and amplification/quantification conditions optimised previously for use in the LightCycler 480 (Roche). Analysis of Ct values was then completed.

Fosmid library clones up-regulating *PTGS2* expression were screened again to confirm activity, this time by RT-PCR using cDNA reverse transcribed from extracted total RNA from each infected culture using the same RT-PCR conditions. Following confirmation, fosmid DNA from positive clones and the parent HM358 strain were each extracted using the QIAfilter Midi kit (Qiagen) following the manufacturer's instructions and DNA quantified using Qubit (Thermo) fluorometric quantification according to manufacturer's instructions. Extracted fosmid DNA was kindly sequenced using Illumina MiSeq technology (Illumina Inc., USA) by Dr Matthew Bull and Professor Julian Marchesi (School of Biosciences, Cardiff University). As only 12 fosmids were to be sequenced in this study, a single-index approach was used, where only one end of each fragment was indexed.

Briefly, extracted fosmid DNA was fragmented using dsDNA fragmentase (#M0348L, New England BioLabs Inc., USA), and resulting fragments size-selected to approximately 400 bp using Ampure XP SPRI beads (Beckman Coulter). Illumina sequencing libraries were prepared using a NEBNext Ultra DNA Library Prep Kit (#E7645L, New England BioLabs Inc.), following the manufacturer's instructions. Resulting libraries were quantified using Qubit (Life Technologies) and combined at equimolar concentrations for sequencing. Libraries were sequenced on a MiSeq (Illumina Inc.) using a 2x150 Nano sequencing kit (Illumina Inc.) following manufacturer's instructions, with sequence analysis tasks carried out virtually, hosted by the Cloud Infrastructure for Microbial Bioinformatics (CLIMB; http://www.climb.ac.uk/) according to established protocols (Esson *et al.*, 2016, McNally *et al.*, 2016). The reads from each fosmid were assembled into contigs using the plasmidSPAdes function of SPAdes Genome Assembler software (version 3.8.0; http://bioinf.spbau.ru/spades) as previously reported (Antipov *et al.*, 2016). Contigs denoting overlapping sequence data were screened for genomic DNA based on sequencing coverage and ordered based on fosmid backbone positioning. Subsequent fosmid-only assemblies were then annotated using Prokka annotation software (version 1.11; https://github.com/tseemann/prokka) as previously reported (Seemann, 2014).

7.5 Results

7.5.1 Initial screening of fragmented *E. coli* HM358 fosmid library clones

Following infection of SW480 cells with each of 968 fosmid library clones of fragmented *E. coli* HM358 genome, and subsequent cellular lysis, RNA extraction and cDNA synthesis (4 hours post-infection), RT-PCR was completed using primers for COX-2 (*PTGS2*), as well as β-actin (*ACTB*) as a house-keeping gene, to calculate changes in COX-2 gene expression for each clone of the fosmid library. RNA extraction was successful for 842 clone infections (87.0%).

A cut-off threshold of ≥2-fold change in *PTGS2* expression was set to be consistent with previous cut-off threshold set for the Wnt signalling RT^2 PCR array data sets (Chapter 5). Initial screening of fosmid clones revealed ≥2-fold up-regulation of COX-2 gene expression caused by 45 clones (5.3%) and ≥2-fold down-regulation caused by 34 clones (4.0%), with the remaining 763 clones (90.6%) resulting in ≤2-fold up- or down-regulation considered to have caused no change (**Figure 7.5.1**); expression change s for clones causing ≥2-fold up-regulation is shown in **Table 7.5.1** (n=1).

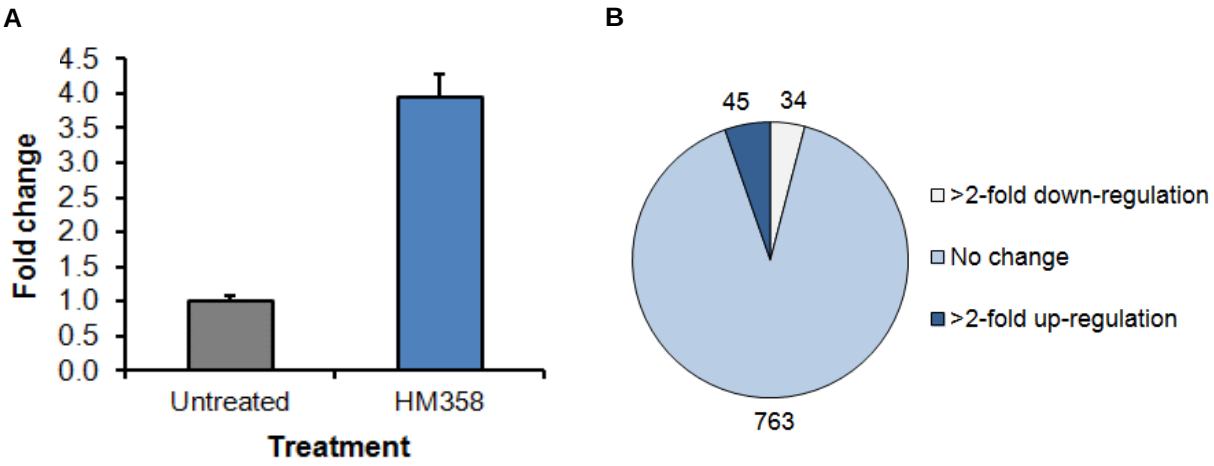

Figure 7.5.1. Changes in COX-2 gene expression following infection of SW480 cells with *E. coli* EPI300T1 fosmid library clones from a fragmented *E. coli* HM358 fosmid library. Graphs show fold change data for (A) untreated and HM358 treated controls (n=10) and (B) clones from a fragmented *E. coli* HM358 fosmid library (n=1). Fold change data for the fosmid clones was segregated into those that caused ≥2-fold up-regulation and ≥2-fold down-regulation, with changes of <2 fold up- or down-regulation designated as no change.

Table 7.5.1. Fold change in COX-2 (*PTGS2*) gene expression for positive clones.

Clone	Fold Change	Clone	Fold Change	Clone	Fold Change
1C5	29.17*	3E10	2.08	6E8	2.57
1E9	2.02	4E5	2.55	6G6	2.03
1F1	2.39	4G11	2.55	6G8	2.30
1F5	2.09	5F8	5821.89*	7B5	2.36
1F7	2.17	6A1	2.22	7B12	2.08
2B8	33.86*	6A2	2.27	7D11	2.18
2C4	13.15*	6A9	2.05	7F11	1.60
2E4	2.13	6A12	2.24	7G6	3.09
2E12	2.4	6B4	4.35	7G11	2.10
2F9	3.71	6B8	2.05	8B11	2.07
2G8	172.65*	6C7	2.27	9E6	153986.42*
3D1	3.02	6C9	2.03	9E12	26846.45**
3D2	2	6C12	2.16	9G7	2821.89*
3E2	2.19	6E2	2.07	9G8	15962.99*
3E6	2.23	6E6	2.03	10E1	2.14

*****High Ct value (>30) for *ACTB* housekeeping gene with no notable change in Ct value for *PTGS2* compared to untreated controls

**Low Ct value (<10) for *PTGS2* with no notable change in Ct value for *ACTB* housekeeping gene compared to untreated controls

7.5.2 Confirmation RT-PCR of positive clones causing up-regulation of *PTGS2*

Initial screening of the 968 fosmid library of clones measured changes in *PTGS2* gene expression following single infections (n=1); therefore, it was necessary to confirm these findings using a secondary screen. This was done by RT-PCR of cDNA reverse-transcribed from extracted total RNA of SW480 cells infected with each of the 36 clones showing ≥2-fold up-regulation of *PTGS2* and 3 randomly selected clones showing ≥2-fold down-regulation or no change (n=3). A decision was made to not include 9 clones showing ≥2-fold up-regulation in the initial screen due to abnormally high or low Ct values for either *ACTB* or *PTGS2*; again, this was to ensure consistency with results obtained in the Wnt signalling RT^2 PCR array data sets.

The secondary screen revealed only 12 clones (33.3%) were confirmed to show ≥2-fold up-regulation of *PTGS2* expression, with 14 clones (38.9%) showing ≥2-fold down-regulation and 10 clones (27.8%) considered to have caused no change (**Figure 7.5.2; Table 7.5.2**); expression changes for clones confirmed to show ≥2-fold up-regulation has been shown in **Table 7.5.2** (n=3).

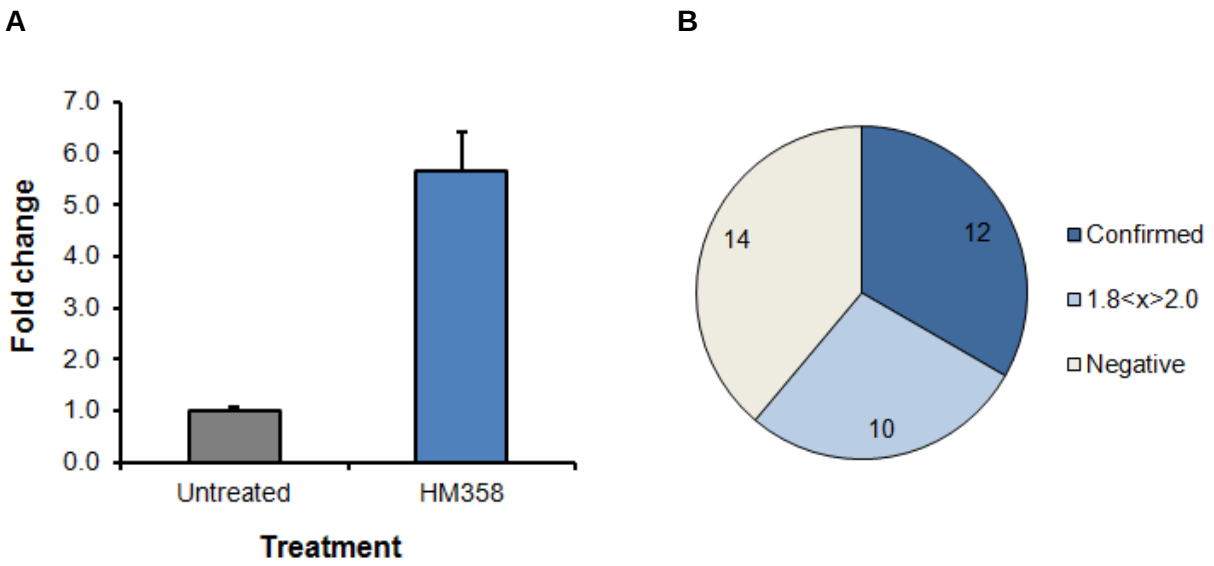

Figure 7.5.2. Confirmation of COX-2 (*PTGS2*) gene up-regulation caused by CRC mucosa-associated *E. coli* HM358 and *E. coli* EPI300T1 fosmid library clones generated from 30-60Kb gDNA fragments of *E. coli* HM358 genome. Graphs show fold change data for (A) uninfected and parent *E. coli* isolate HM358-infected controls (n=6) and (B) clones from a fragmented *E. coli* HM358 fosmid library initially identified as *PTGS2* up-regulating (n=3). Confirmation results for the fosmid clones were segregated into those that again caused >2-fold up-regulation (Confirmed), those that caused between 1.8 to 2.0 fold up-regulation (1.8<x>2.0) and those that caused less than 1.8-fold change (Negative).

Table 7.5.2. Fold change in COX-2 (*PTGS2*) gene expression for fosmid clones screened in confirmation studies.

Confirmed	Fold Change	1.8<x>2.0	Fold Change	Negative	Fold Change
1F7	2.00	3D1	1.85	1E9	1.30
2E4	2.76	6A1	1.88	1F1	1.19
2E12	2.02	6A9	1.95	1F5	1.47
3D2	2.65	6A11	1.87	2B5	1.63
3E10	2.24	6A12	1.94	2F9	1.60
6C7	3.69	6B8	1.76	3E2	1.52
6E2	2.58	6C9	3.69	3E6	1.46
6E8	3.81	6C12	1.91	4E5	1.33
6B4	2.20	7G3	1.49	4G11	1.15
7B12	2.45	8B11	1.87	6A2	1.24
7D11	2.62			6E6	1.52
10E11	2.80			7B5	1.49
				7G6	1.40
				7G11	1.42

These results showed that 12 clones from the HM358 fosmid library were confirmed to up-regulate *PTGS2* gene expression more than 2-fold; this would suggest that these clones may contain specific genomic elements inserted within the fosmid that are responsible for the increase observed in COX-2 following HM358 infection and perhaps as a consequence, Wnt signal pathway activation. To identify the genomic elements, we undertook sequence analysis of fosmid DNA isolated from the 12 clones confirmed in the secondary screen to up-regulate *PTGS2* gene expression.

7.5.3 Illumina MiSeq sequencing of fosmid DNA from fosmid library clones generated from DNA fragments of *E. coli* HM358 confirmed to up-regulate *PTGS2* gene expression

Following confirmation of fosmid library clones showing >2-fold up-regulation of *PTGS2* expression in both the primary screen and secondary confirmatory screen, fosmid DNA was extracted from 12 positive clones. Fosmid DNA was extracted using QIAfilter Midi kit following the manufacturer's instructions, with fosmid DNA from the parent CRC mucosa-associated *E. coli* HM358 isolate also extracted for sequencing. Each sample was then submitted for Qubit fluorimetric quantification of DNA content (**Table 7.5.3**).

Table 7.5.3. Qubit quantification of fosmid DNA from confirmed *PTGS2* up-regulating library clones and DNA from HM358.

Clones	DNA (µg/mL)
1F7	4.29
2E4	15.20
2E12	3.15
3D2	6.76
3E10	3.87
6B4	3.12
6C7	2.65
6E2	7.00
6E8	8.40
7B12	3.96
7D11	20.20
10E11	11.00
HM358	19.70

Following DNA extraction and quantification, samples were sent to Cardiff University for sequencing using the Illumina MiSeq (Illumina Inc., USA). As only 12 fosmids were to be sequenced in this study, a single-index approach was used, where only one end of each fragment was indexed. Following

sequencing, SPAdes Genome Assembler software (version 3.10.1; http://bioinf.spbau.ru/spades) was used for fosmid assembly and Prokka software (version 1.11; https://github.com/tseemann/prokka) for rapid prokaryotic genome annotation. Annotation comparisons were then completed using the Artemis Comparison Tool (http://www.sanger.ac.uk/science/tools/artemis-comparison-tool-act). Here, regions of sequence homology are linked with vertical red (forward match) or blue (reverse match) lines (not shown). In all cases, the fosmid operon sequences are shown at the top of the image, with the reference backbone sequence at the bottom.

Of the 12 confirmed positive clones sequenced, some appeared to have common homology. All but one clone contained the fosmid vector sequence comprised of the *repE*, *soj* and *virB* operons, which were found as a cluster (**Figure 7.5.3.2**).

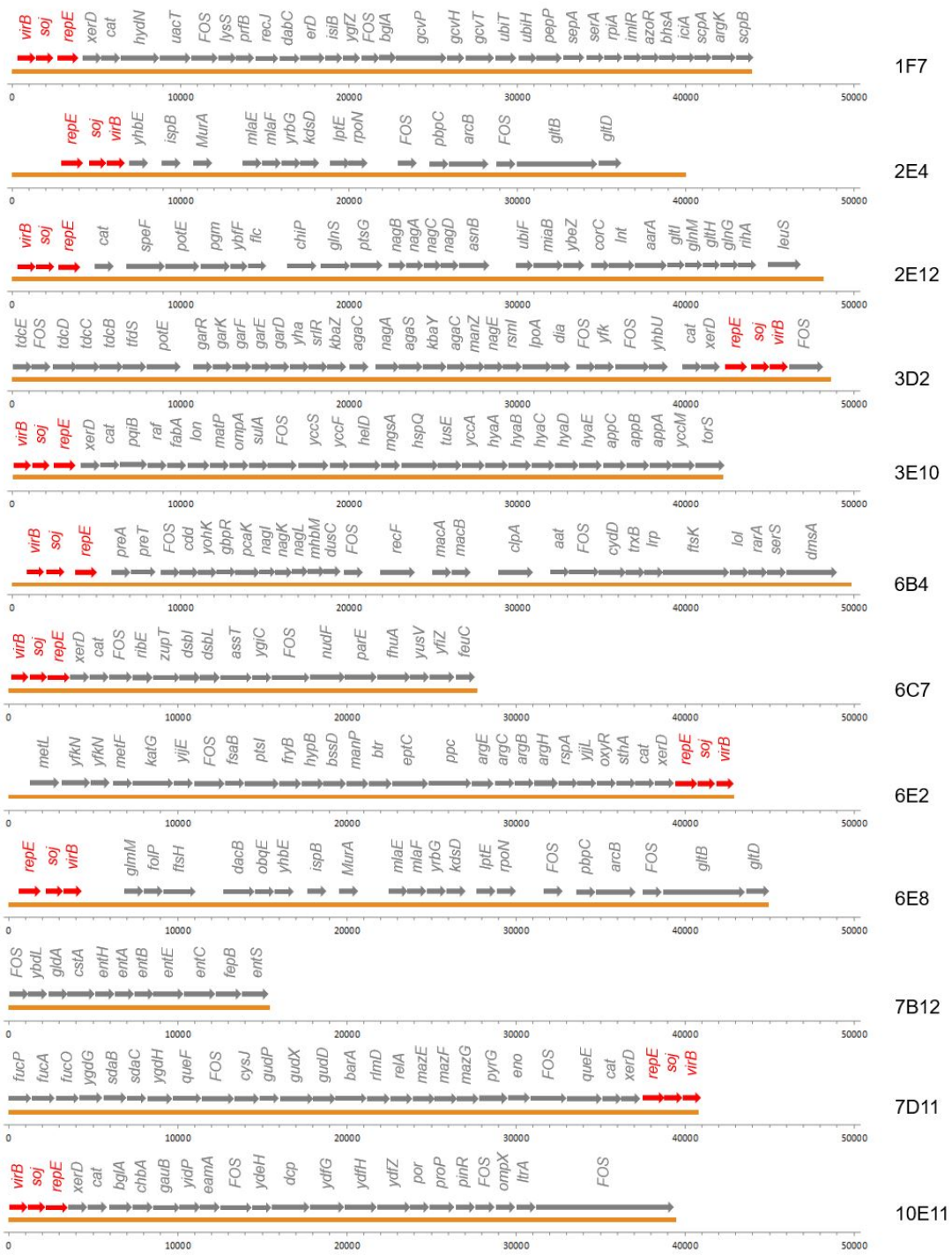

Figure 7.5.3.2. Sequence alignment of 12 fosmid clones positive for *PTGS2* up-regulation. The fosmid vector reference sequence of *repE*, *soj* and *virB* operons (red arrows) was identified in 11 of 12 fosmid clones. Sequences were between 30-50 kDa in 10 of 12 fosmid clones.

Fosmid clone 7B12 was found to be around 15 kDa and did not contain the fosmid vector reference sequence, suggesting this was an incomplete sequence. Interestingly, clones 2E4 and 6E8 contained sequence homology for 15 genomic elements/operons, including *yrb*, *kds*, *lpt*, *rpo*, *pts* and *glt* (**Figure 7.5.3.3**). Some of these genomic elements/operons were also found in other *PTGS2* up-regulating clones, and may be of interest for future studies.

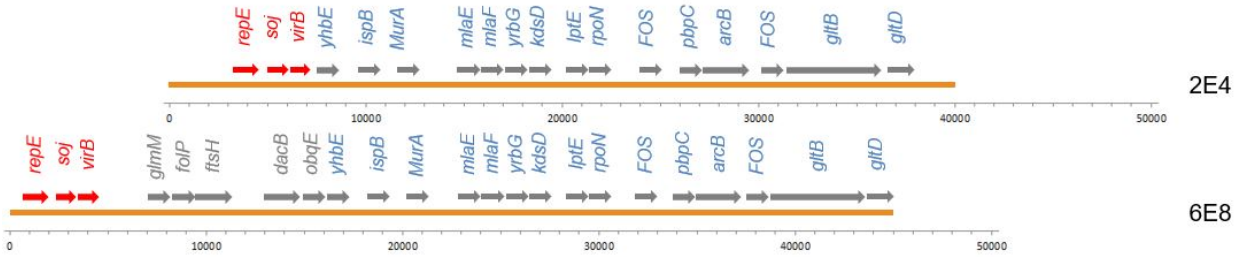

Figure 7.5.3.3. Sequence alignment of fosmid clones 2E4 and 6E8 positive for *PTGS2* up-regulation. The fosmid vector reference sequence of *repE*, *soj* and *virB* operons (red arrows) was identified, with the majority of other operons common in both clones (blue arrows) and only 5 additional operons in clone 6E8 (grey arrows). The order sequence of the common operons was identical.

7.6 Discussion

By screening clones from the fragmented *E. coli* HM358 fosmid library using RNA extractions from infected CRC cells *in vitro*, we were unable to identify a common factor associated with increased *PTGS2* (COX-2) expression. Initial and confirmation screening efforts appeared to identify 12 fosmid clones showing increased *PTGS2* expression. Subsequent sequencing of these clones using Illumina MiSeq showed similarities in DNA content, with particularly common homology in two of these fosmid DNA inserts. The fosmid vector sequence of *repE*, *soj* and *virB* operons were used to identify the coding region in each clone, with *repE* and *soj* encoding replication initiator proteins (Wada *et al.*, 1987, Ogura *et al.*, 2003) and *virB* required for survival and replication (Schmiederer *et al.*, 2001). The operons identified following on from the vector sequence were almost identical for the 2E4 and 6E8 clones. The following sections highlight their known functions.

The *ispB* gene codes for the octaprenyl diphosphate synthase enzyme involved in quinone synthesis (Maouche *et al.*, 2016). This gene is essential for normal growth of *E. coli* (Okada *et al.*, 1997), but to date is not known to be associated with virulence. The *yrbG* gene is believed to play a protective role against the lethal action of quinolones (a family of synthetic broad-spectrum antibiotics), with *yrbB* mutations making *E. coli* more susceptible to quinolone-mediated lethality (Han *et al.*, 2011). YrbB is a component of an ABC transport system that maintains lipid asymmetry in the outer membrane of Gram-negative bacteria, by preventing surface exposure of phospholipids. It has been suggested that these genes may be implicated in cell envelope integrity (Sperandeo *et al.*, 2006). A role for *yrbB* in supporting survival of *E. coli* in high-stress environments has been shown, with y*rbB* mutation associated with a greater susceptibility to stress-induced killing (including stressors such as UV and oxidative damage) than wild-type *E. coli*, although no difference were seen in response to heat-induced death (Han *et al.*, 2011).

The *kdsD* gene codes for d-Arabinose 5-phosphate isomerase (API), the first enzyme in the biosynthetic pathway of 3-deoxy-d-manno-octulosonate (KDO), a unique 8-carbon sugar component

of lipopolysaccharides located in the outer leaflet of the outer membrane of Gram-negative bacteria. However, presence of the *kdsD* gene and encoding of API has been reported in *E. coli* K-12 (Meredith and Woodard, 2005), an isolate which was shown to have no impact on *PTGS2* expression throughout our study. Therefore, the *kdsD* gene is unlikely to have an important role in driving increased *PTGS2* expression.

The *lpt* operon in *E. coli* codes for the Lpt protein machinery, seven essential proteins (A, B, C, D, E, F, and G) which form a complex that constitutes a transporter for lipopolysaccharide (LPS), one of the most powerful proinflammatory bacterial virulence factors, engaging transport of LPS from the cytoplasm to the outer membrane (Martorana *et al.*, 2014, Bollati *et al.*, 2015). As these are considered essential for LPS transport in Gram-negative bacteria, changes in expression (i.e. up-regulation) in *E. coli* may affect their ability to survive, which may then enhance their ability to infect host cells. This could be a driving factor for *PTGS2* expression, but would need to be confirmed either by functional studies of insertion of a plasmid containing the *lpt* operon into a non-*PTGS2* inducing *E. coli* (gain of function study) or through use of transposon mutagenesis (Goryshin *et al*., 2000) to create insertional knockout of *lpt* operon genes in the parent CRC mucosa-associated *PTGS2*-inducing *E. coli* HM358 (loss of function study). This could then be followed up by mono-association of germ free mice with HM358 and the isogenic knockout strain

In *E. coli*, the phosphoenolpyruvate-carbohydrate phosphotransferase system (PTS), coded for by the *pts* gene family, is responsible for the transport and phosphorylation of sugars, such as glucose. PTS is believed to play an important role in controlling the preferential utilisation of glucose (Escalante *et al*., 2012, Plumbridge, 2002). Earlier studies also reported PTS as being a well characterized system mediating information transfer from the external medium to multiple targets inside the cell (De Reuse *et al*., 1989). Again, this growth and survival mechanism may be enhanced in clones shown to up-regulate *PTGS2* expression, and may aid COX-2 signalling changes.

The *gltB* and *gltD* operons are responsible for the synthesis of glutamate synthase enzyme. Under nitrogen-rich conditions, this can be used to form glutamate and glutamine (Kumar and Shimizu, 2010). Some *E. coli* mutants that are deficient in glutamate synthase activity have difficulty growing with nitrogen sources other than ammonia, suggesting this enzyme is important in bacterial growth in nitrogen-rich conditions. Increases in nitrogen metabolism have been shown in IBD, where the microbiome begins to respond and compensate to gut inflammation driven oxidative stress (Morgan *et al.*, 2012). The Morgan *et al*. study reported an increase in glutathione transport gene abundance in UC and CD and an increase in glutathione metabolism gene abundance in UC. Inflammatory cascades aid the production of highly reactive oxygen and nitrogen metabolites, which have been found greatly increased in active IBD. Monocytes in the lamina propia also release homocysteine during inflammation, which further contributes to oxidative stress (Morgan *et al*., 2012). These may reflect a mechanism by which the gut microbiome addresses the oxidative stress caused by inflammation, where changes in expression of genes responsible for controlling bacterial survival under these conditions may become important.

The Morgan *et al*. study also highlighted that this type of stress allows entero-haemorrhagic *E. coli* to use nitrogen sources as a competitive advantage under these conditions. The possibility that *E. coli* may be highly represented in IBD because they gain a competitive advantage from inflammation-induced oxidative and/or acid stress, and that they appear better able to compensate for this through metabolism of glutathione has been raised previously (Morgan *et al.*, 2012), and may make presence of this genomic element in several of the positive fosmid library clones (from the parent isolate HM358) in our study of more interest.

An additional study has also indicated the elevated expression of *rpo* genes in response to increased *gltB* and *gltD* expression (Kumar and Shimizu, 2010). Alternative sigma factor 54 (RpoN), coded for by *rpo*, is an important regulator of stress resistance and virulence genes in many bacterial species. RpoN plays a major role in the response of *E. coli* to nitrogen-limiting conditions. Under such conditions, RpoN directs the transcription of several operons/regulators in the nitrogen regulatory response in *E.*

coli (Riordan *et al.*, 2010). With the *rpoN* operon found in our study in both the 2E4 and 6E8 fosmid library clones, and where *gltB* and *gltD* were also identified, this perhaps establishes a further association between their presence/expression, and may link further to the impact of nitrogen sources in intestinal inflammatory conditions as with the *gltB* and *gltD* operons.

As bacteria have to adapt quickly and efficiently to multiply in response to changes in their environment, membrane-linked transport systems, such as those eluded to here, are designed to recognise and translocate specific molecules across the cell membrane in order to survive, grow and persist. The PTS is a good example of a system specifically designed to transport a large number of carbohydrates, and is also one of the best characterized systems mediating information transfer from the external medium to multiple targets inside the cell (De Reuse *et al*., 1989). If mucosa-associated *E. coli* do harness these features for growth and survival better than non-pathogenic strains, particularly in higher stress conditions such as inflammation, their ability to infect host cells may be improved and may have contributed to the COX-2 and Wnt signaling changes observed both *in vitro* and *in vivo*.

Going forwards, it would be interesting to look deeper into those operons/genes shared by *PTGS2* up-regulating fosmid library clones more closely. Once key operons/genes have been identified, it would be useful to screen all clones for the presence of this operon using RT-PCR. This was done in the study of Prorok-Hamon *et al.*, (2014) where sequence analysis of *E. coli* HM358 and haemagglutination-positive fosmid clones were subsequently screened by PCR for a conserved element of the 454-sequencing identified afimbrial adhesin *afa-1* operon (i.e. *afaC,* encoding an usher protein). Subsequent insertion of the identified *afa-1* operon into a plasmid and transformation of the non-pathogenic *E. coli* EPI300-T1 (K-12) base clone strain, demonstrated that presence of this genomic element to confer ability to adhere to, and invade, HEp-2 and I-407 epithelial cells (Prorok-Hamon *et al.*, 2014). In the same study, the wild-type strain HM358 showed a greater ability to adhere to, and invade into, these cells compared to the *afa-1*-transfected *E. coli* K-12 strain, implying that other adhesins/invasins might also be involved, as invasion into I-407 cells was seen some *afaC*-negative

mucosa-associated *E. coli* isolates. This means that any leads stemming from our study may not be the only factors involved in inducing COX-2 and Wnt signalling, and could mean a role for several genes/proteins working in tandem to elicit these effects. It would also be useful to be able to compare the sequence of HM358 (data not available) and other mucosa-associated *E. coli* isolates from CRC and IBD patients and to that of *E. coli* K12 genome (accession number: U00096.2), with the potential to insert any genes/operons of interest from data from our study into a wild-type control, such as *E. coli* K12, to investigate effects on *PTGS2* expression in SW480 cells.

The similarities seen in only two of the fosmid clones was an unexpected result, especially given that such similarities were not seen in the use of the fosmid library successfully identifying the afimbrial adhesin (*afa-1*) operon, but also that that the *afa-1* operon was seen in 7/8 positive clones (one not having sequenced) in the Prorok-Hamon study (Prorok-Hamon *et al.*, 2014).

Given the COX-2 increases are already shown *in vitro* (see Chapter 5) and *in vivo* (see Chapter 6) data accumulated in our project, measurement of *PTGS2* gene expression changes appeared a logical way to screen the fosmid library or clones. However, few assays measuring COX-2 activation on a high-throughput scale would have been suitable for obtaining a robust signal window in order to efficiently identify fosmid clones that up-regulate COX-2.

Readouts using the stable transfected HeLa TCF/LEF luciferase reporter assay (Signosis, USA), which yielded reliable and robust data when characterising the *in vitro* effects of mucosa-associated *E. coli* (see Chapter 5), was trial screened following infection with the same fosmid library clones identified to up-regulate *PTGS2* gene expression. The assay readout did not produce any reproducible data sets to identify TCF/LEF signalling changes following infection with fosmid clones showing COX-2 gene changes (n=3, data not shown); this was despite showing reproducible increases in TCF/LEF signalling using several mucosa-associated *E. coli*, including HM358, as positive controls. However, this could again be due to limitations of the primary screen in identifying suitable fosmids. Instead, it may be possible to examine the effects on Wnt signalling using qPCR to identify changes in expression of

specific Wnt-relevant genes such as Axin2, known to be rapidly induced by the activation of Wnt signalling (Jho *et al*., 2002). Another possibility could be to utilise a PGE_2 ELISA (such as that shown in the *in vitro* monocyte-derived macrophage infection assays in Chapter 5) as a screening tool, where cells inoculated with each fosmid library clones are lysed and used to quantify host cell production of PGE_2 released to cell supernatants. Measurement of PGE_2 would be a downstream reporter of COX-2 activity. Use of an ELISA readout for COX-2 has also been used with success in a high-throughput screening format (Cuendet *et al.*, 2006).

Summary

Future work using this data could identify one or even several genes or operons that establish an active factor, or factors, that contribute to the induction of COX-2 and Wnt signalling observed *in vitro* and *in vivo* experiments described earlier in the project. If mucosa-associated *E. coli* are to be shown to harness any of the operons identified here for growth and survival, particularly in higher stress conditions such as inflammation, increase their ability to infect host cells and contribute to COX-2 and Wnt signalling changes, these could become potential therapeutic targets.

Chapter 8:

Development of a three-dimensional (3D) cell culture method to investigate the effects of mucosa-associated *E. coli* infections

8.1 Introduction

Mucosa-associated *E. coli* have been found in high numbers within intestinal tissue taken from IBD and CRC patients (Martin *et al*., 2004, Hold *et al*., 2014, Swidsinski *et al*., 1998). Results obtained so far suggest that colonic mucosa-associated *E. coli* support increased intestinal COX-2 expression and Wnt signalling as a possible early event in the development and/or progression of colorectal cancers. We have been able to characterise changes in both COX-2 gene and protein expression and Wnt signalling, including increased nuclear translocation of β-catenin, following *in vitro* infection of CRC cell lines with mucosa-associated *E. coli*, as well as showing the translation of these effects in an *in vivo* infection model using germ-free *Il10* knock-out mice mono-associated with HM44, a mucosa-associated *E. coli* isolated from a CRC patient.

With gut inflammation already shown to alter composition of the gut microbiota in favour of pathobiont mucosa-associated *E. coli* (Darfeuille-Michaud *et al*., 1998, Swidsinski *et al*., 1998, Martin *et al*., 2004), the resultant expansion of these bacteria would likely increase their interactions with gut mucosa. With few studies looking to mimic the intricacies of the parent colonic tissue, opportunities to effectively show the translational effects of these interactions *in vitro* have so far been limited. One method of modelling better these interactions is by utilising three-dimensional (3D) organotypic cell cultures. Previous development of 3D culture models to study host-pathogen interactions has allowed a better platform for studying these interactions as these cultures tend to better replicate the growth of cells and tissues *in vivo* compared to 2D monolayer cultures, particularly in the case of tumour formation. One study in particular reported successful use of CRC cell lines formed as 3D organotypic cultures to study host interaction with pathogens such as enteropathogenic *E. coli* (EPEC) and enterohaemorrhagic *E. coli* (EHEC) ((Carvalho *et al*., 2005). The authors made use of a rotating cell culture system (RCCS; Synthecon, USA), originally designed and used by the National Aeronautics and Space Administration (NASA) to provide a simulated microgravity environment during certain phases of the Shuttle missions, before being made commercially available for the production of 3D cell

structures (Jessup *et al.*, 1993). This system has been used extensively to characterise cell behaviour and neoplastic transformation in 3D culture using a host of different cell types, including cancer cells (Vidyasekar *et al.*, 2015), skeletal muscle cells (Klement *et al.*, 2004) and bacteria (Bergmann and Steinert, 2015).

The RCCS generates low-shear stress and microgravity conditions provide unique advantages for the cultivation of mammalian tissues (Jessup *et al.*, 1993). A lack of gravity-induced sedimentation supports 3D growth in culture and permits human epithelial cells to grow to high densities. The system also allows the use of cell micro-carriers, where cells can adhere to, and undergo cell division on, these micro-carriers whilst remaining as aggregates in suspension. This culture method is especially useful for allowing natural cell-cell interaction, with growth in the RCCS shown to support morphological differentiation of human colon carcinoma cells, particularly in co-culture with human stromal cells to create a foundation layer for the neoplastic cells to grow on (Jessup *et al.*, 1993, Jessup *et al.*, 2000).

With several CRC cell lines, such as HT-29 (Goodwin *et al.*, 1992), Caco-2 (Kaeffer *et al.*, 2002) and HCT-8 (Carvalho *et al.*, 2005), already having been shown to be suitable for use in this system, our aim was to create 3D cultures suitable for infection with mucosa-associated *E. coli*. For this project, porous Cytodex micro-carrier beads were examined for their use as a support for CRC cell growth in the RCCS system. Two types of micro-carrier beads coated with collagen and *diethylaminoethyl* (DEAE) cellulose, a positively charged resin, were used to simulate the supportive environment provided to epithelial colon cells *in vivo*.

Here, RCCS culture was initially developed using the SW480 CRC cell line (successfully used in *in vitro* studies demonstrating mucosa-associated *E. coli*-induced COX-2 expression and Wnt pathway activation – Chapter 5) and then expanded to investigate a late-stage adenoma cell line AA/C1 and adenocarcinoma cell line AA/C1/SB, both experimentally-transformed from an epithelial adenoma cell line PC/AA (Williams *et al.*, 1990, Paraskeva *et al.*, 1992). By using these cell-lines, we would gain insight into the impact of colonic mucosa-associated *E. coli* infection on cells at key stages of

transformation in the colorectal adenoma-carcinoma sequence (Armaghany *et al*., 2012). Development of a 3D organotypic cell culture method using this array of colorectal cell lines would also afford us opportunity to investigate the effects of mucosa-associated *E. coli* infection in a system that better mimics chronic pathogenic bacterial infection in patients. With a fully validated culture procedure, we would then have an efficient and reliable culture platform available for use in future studies.

8.2 Hypothesis

Three-dimensional organotypic cell cultures will allow us to investigate the effects of colonic mucosa-associated *E. coli* infection in a system that better mimics the intricacies of bacteria-host interactions *in vivo*.

8.3 Aims

- To develop a 3D organotypic cell culture using a series of colorectal cell-lines at different stages of malignant transformation in the adenoma-carcinoma pathway.
- To investigate the action of colonic mucosa-associated *E. coli* infection of 3D organotypic cell cultures on COX-2 expression and Wnt pathway activation.

8.4 Methods

The adherent human colonic epithelial cell lines SW480 and DLD-1, derived from male patients with Duke's type B (Leibovitz *et al.*, 1976) and type C (Dexter *et al.*, 1981) colorectal adenocarcinomas, respectively, were initially grown as monolayer cultures as previously described (see Section 4.1). Cells were maintained in complete Dulbecco's Modified Eagle's Medium (DMEM, Sigma Aldrich) supplemented with 10% (v/v) fetal bovine serum (FBS) (Invitrogen; Paisley, UK), 100 U/mL penicillin and 100 µg/mL streptomycin (Sigma Aldrich, UK) at 37°C in a humidified atmosphere of 5% CO_2, 95% air until they reached confluency. The epithelial cell line PC/AA and experimentally-transformed AA/C1 and AA/C1/SB cells were originally established from a pre-malignant adenoma taken from a patient with familial adenomatous polyposis and kindly donated by Professor Chris Paraskeva, University of Bristol, UK (Williams *et al.*, 1990, Paraskeva *et al.*, 1992). The AA/C1 and AA/C1/SB cell lines were grown and maintained under the same conditions as SW480 and DLD-1 cells, excepting that complete DMEM was additionally supplemented with 2 mM L-glutamine (Sigma Aldrich), 1 µg/mL hydrocortisone sodium succinate (Sigma Aldrich) and 0.2 U/mL human insulin (Sigma Aldrich).

Once cell lines had reached around 90% confluency, colonic cell lines were each seeded at the required density, for example 1 x 10^6 cells/vessel, directly into 10 mL and 50 mL vessels and added to the Synthecon Rotary Cell Culture System (RCCS) following manufacturer recommendations (**Figure 8.4**). Initiation and maintenance technique, as well as cell density and rotation speed were optimised for individual cell lines and culture volumes (see Chapter 8.5). Briefly, cells were maintained in complete DMEM, with appropriate supplementary reagents required for specific cell lines, at 37°C in a humidified atmosphere of 5% CO_2, 95% air. Media was changed 72-96 hours after seeding, then every 48 hours until cell aggregates were harvested. Periodic sampling of cell aggregates following media changes allowed monitoring of cell aggregation and viability using light microscopy. Following culture in the RCCS for up to 4 weeks, cell aggregates were harvested and plated for *E. coli* treatment. Assays used the same multiplicity of infection (MOI: 10) as used in earlier 2D monolayer studies; this MOI was

estimated based on the initial cell density at the beginning of RCCS culture and rate of replication of cells seen in 2D monolayer studies.

Figure 8.4. Rotary cell culture system (RCCS). The annotated image shows a typical RCCS setup using a 50 mL disposable culture vessel. The RCCS culture system (left) would be placed inside the incubator, with the control box (right) placed outside and linked via cable.

Cultures were also created using extracellular-matrix-coated (ECM) micro-carrier beads, where cells grown in monolayer cultures were trypsinised and incubated with the coated beads before being added to a rotary cell culture vessel. In this case, Cytodex beads coated in with *diethylaminoethyl* (DEAE) cellulose (Cytodex-1) and collagen (Cytodex-3) were used (Sigma Aldrich); micro-carrier beads were prepared and used following the manufacturer's recommendations. Briefly, Cytodex beads were sterilized in 100% ethanol before swelling in excess sterile phosphate-buffered saline (PBS; pH7.4), using 50 mL/g of Cytodex beads, for a minimum of 2 hours. The cell-bead suspension was then left to settle for 10 minutes; the supernatant PBS was decanted and replaced with 70 % (v/v) ethanol in distilled water; the beads were washed twice in this solution and then incubated overnight in 70 % (v/v) ethanol in distilled water, using 70–100 mL/g Cytodex beads. Following incubation, the 70% (v/v) ethanol solution was removed, with the Cytodex beads then washed three times in sterile PBS (50 mL/g Cytodex beads). The supernatant PBS was again removed and the beads washed once in the

appropriate cell culture medium (20–50 mL/g Cytodex beads) before use. Immediately prior to use, the supernatant was decanted and the beads briefly rinsed in warm 37 °C cell culture medium (20–50 mL/g Cytodex beads) before being transferred to the culture vessel via sterile syringe. Periodic sampling of cell aggregates following media changes every 2-4 days also allowed monitoring of cell growth development on the micro-carrier beads (see Chapter 8.5).

Following culture and subsequent *E. coli* treatment, cell aggregates were harvested and fixed using 4% (w/v) paraformaldehyde (Sigma Aldrich) before being washed and stored in sterile PBS (approximately 10 ml) overnight. Cell aggregates from each vessel were then suspended in 500µL heated Histogel (Thermo; Paisley, UK) until set, before being placed in histological processing cassettes. Cell aggregates were then processed overnight using a Shandon 2LE tissue processor, and embedded within the histological processing cassettes using Surgipath Formula R Paraffin (Leica, Milton Keynes, UK) in a Shandon Histocentre embedder (Thermo Shandon, Paisley, UK) as previously described. For sectioning of the cell aggregates, the embedded wax blocks containing the aggregates were cooled for 30 minutes on ice, microtome-sectioned to 4 µm, and floated in a 37°C heated water bath before adhering to glass slides; for immunohistochemistry, 3-aminoprpyltriethoxylsilane (APTS) coated slides were used (Fisher Scientific). Slide-mounted sections were then air-dried in an oven at 37 °C overnight.

Cell aggregates treated with mucosa-associated *E. coli* (MOI: 10) were assessed by RT-PCR for COX-2 and β-catenin, as well as by haematoxylin and eosin (H&E) staining and immunohistochemistry (IHC). For RT-PCR analysis, RNA was extracted and purified using the RNeasy Kit (Qiagen, Manchester, UK), with cDNA subsequently synthesised using the Transcriptor First Strand Kit (Roche, Welwyn Garden City, UK). RT-PCR was run with primers designed using the ProbeFinder (Roche) and matched to the correct probe (see Table 4.6.4) in the human Universal ProbeLibrary (Roche). RT-PCR was run in 96-well format using TaqMan detection (LightCycler 480 Probes Master; Roche) using the LightCycler 480 (Roche) and analysis completed in Microsoft Excel.

For H&E staining (see Section 4.12.4), microtome slides were placed in Gill no.1 haematoxylin (Sigma-Aldrich) for 3 minutes before running under tap water for 10 minutes. Slides were then placed in eosin (Sigma-Aldrich) for 3 minutes, and then put immediately in water for 2 minutes before dehydration (20 dips sequentially in 70%, 90% and 100% ethanol). For immunohistochemistry (see Section 4.12.4), COX-2 (#ab15191; Abcam, UK) and β-catenin (#610154; BD Biosciences) antibodies were used at 1:400 and 1:50 dilutions, respectively. Heat-induced antigen retrieval was performed in citric acid buffer (pH 6.4). Slides were mounted onto glass coverslips (22 x 50mm) using DPX Mountant (Sigma Aldrich). Images were captured using SPOT Image Capture Software (SPOT Imaging Solutions) on a light microscope (Leica; Germany).

8.5 Results

8.5.1 Method development and optimising cell aggregation

The rotating cell culture system (RCCS) was set up in a suitable CO_2 incubator set at 37˚C, 5% CO_2 and 95% air, as recommended by the manufacturer, keeping culture conditions consistent with monolayer cultures, with the control box sat above the incubator. Once cells in monolayer culture had reached 90% confluence, cells were trypsinised and placed in either a 10 mL or 50mL disposable culture vessel. During culture initiation and maintenance, additional steps were incorporated to improve ease-of-use.

To stabilise the disposable culture vessels, they were placed in a sterile 6-well plate in sterile laminar flow conditions. Once in the 6-well plate, the large stopper was removed and small ports opened. Tilting the culture vessel at a 45-degree angle for initiation was improved upon by adding a small amount of culture medium via the large port, 1 ml to a 10 mL vessel and 5 mL to a 50 mL vessel, before adding cells; this stopped the cells accumulating in one area of the vessel. Cell cultures using micro-carrier beads appeared to have a better distribution of cells and fewer disrupted beads (appearing popped or broken under microscopy at day 2) with a pre-incubated of cells and beads for 10-15 minutes, using approximately 5 mg beads per 1 mL cells, before adding to the vessel. All subsequent maintenance steps and sampling was done using the same 6-well plate stabilisation and sterile technique.

It was found that the attachment of 3 mL syringes, containing the appropriate cell medium, to both small ports was most suitable for both removing bubbles and sampling. As noted by the manufacturer, bubbles tended to develop during maintenance of cultures due to evaporation. These bubbles noticeably disrupted the rotation of cultures causing abnormal movement and collision of cell aggregates, and this had to be corrected roughly every 2 days. Removal of bubbles was aided by rotating the vessel by hand until the bubbles were aligned with one of the small ports, with bubbles then removed by introducing new culture medium into the opposite port; approximately 1 mL and 2-

3 mL of culture was removed for sampling from 10 mL and 50 mL vessels, respectively, to visualise the development of cell aggregates. During method development, it was found that rotation speed generally had to be increased by around 0.5 rpm following each sampling/maintenance step, with an initial rotation speed of approximately 15 rpm found to be most suitable to prevent cell sediment; the speed increases were likely required due to the increasing sizes of cell aggregates causing them to settle more quickly.

Several resources had suggested initiating cultures with at least 1 x 10^6 cells per vessel (Goodwin *et al.*, 1992, Carvalho *et al.*, 2005, Kaeffer *et al.*, 1999); 1 x 10^7 cells were initially added to 50 mL vessels due to the larger size. Following several rounds of testing, including initial cell seeding densities of 1 x 10^5, 5 x 10^5, 1 x 10^6 and 1 x 10^7 cells per 10 mL vessel and up to a larger density of 1 x 10^8 cells per 50 mL vessel, it was found that an initial density of >1 x 10^6 cells per 10 mL vessel and 1 x 10^7 cells per 50 mL vessel produced acceptable levels of aggregation with CRC cell lines. From observation during microscopy, lower densities appeared to delay the formation of aggregates and caused higher levels of cell anoikis/apoptosis, with higher densities causing the formation of larger clumps of multiple aggregates; this was not quantified. Larger clumps may have limited the adherence and invasion of capable bacteria during infection due to a smaller accessible surface area.

Upon harvesting the cell aggregates, the large port was found to cause less disruption of aggregates. The vessel was removed from the RCCS and tilted to allow the cells to drop to the bottom of the vessel. The smaller ports were then opened (no syringes added), followed by removal of the large stopper, with the culture then slowly emptied into a sterile centrifuge tube via the large port. The cell aggregates were then allowed to settle, with the supernatant used to wash the vessel to maximise yield.

8.5.2 Case study: SW480 colonocyte 3D aggregation over 21 days of culture in the RCCS

8.5.2.1 Aggregation without micro-carrier beads

Following optimisation of the culture method, two cultures of SW480 cells were maintained over 21 days to assess growth of aggregates, initially in the absence of micro-carrier beads (**Figure 8.5.2.1**). Three-dimensional (3D) culture was first tested in 10 mL and 50 mL vessels using 1 x 10^7 cells in both vessels; initiation of rotating culture was considered as day 0. On sampling and media replenishment on day 2, SW480 cells remained viable upon evaluation by microscopy (see Figure 8.5.2). Most cells at this stage were not yet aggregated in either 10 mL or 50 mL vessel, with only few cells aggregating to form small clumps.

At day 4, cells began to form larger clusters in both 10 mL and 50 mL vessels. Interestingly, most, if not all, cells began to show signs of spikes/projections from cell membrane. Cells remained viable at day 6, with many beginning to incorporate into larger aggregates in 10 mL or 50 mL vessels. The spikes/projections noted at day 4 became more pronounced, until around day 10 where they were no longer visible, suggesting cells had become more accustomed to the rotational conditions. Samples from day 8 and day 10 showed the cells forming multiple clusters in both vessels, with what appeared to be growing clusters that had combined to aggregate into numerous, much larger, spherical clusters.

Large clusters remained in both vessels at day 13 and day 15, with a lower number of large clusters obtained from the 10 mL vessel; this could have been due to the settling of these larger clusters in the 50 mL vessel, and possibly the removal of a higher proportion of cells from the 10 mL vessel during earlier sampling. A higher number of smaller spheroids had formed by this point in the 10 mL vessels, presumably from small clusters of cells. Cell debris became increasingly noticeable at day 15 with some cell rounding observed, mainly in those cells yet to aggregate but this was difficult to see within clusters. Between day 15 and day 21, the larger clusters appeared to have darkened areas; at this stage, it was presumed that cells were either at a high density or necrotic cell death was beginning to occur; cell viability was not quantified. Culture maintenance was ended at day 21.

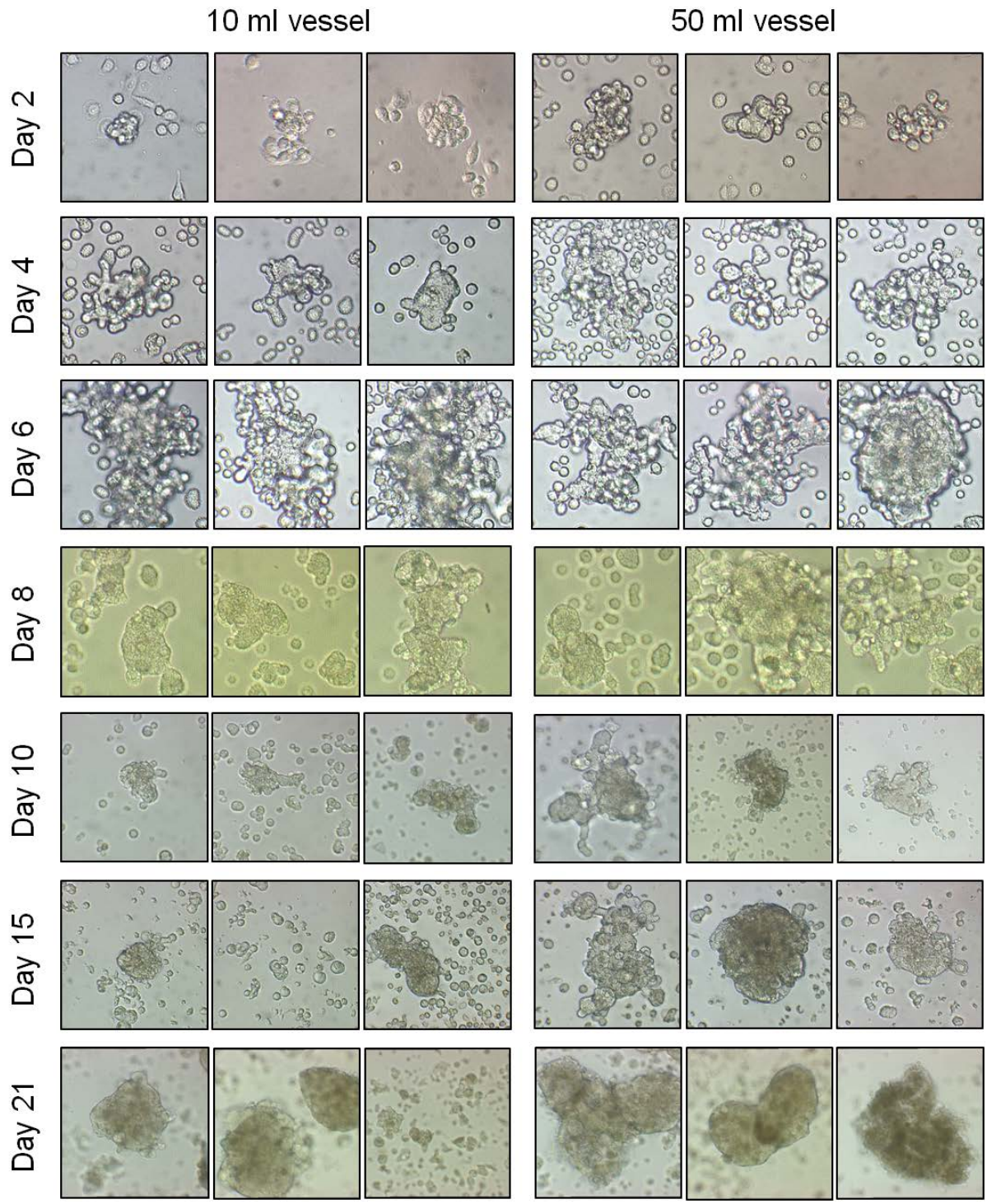

Figure 8.5.2.1. SW480 cell aggregate development from day 0 to day 21. Three representative images for each sampling point show the development of SW480 cell aggregates in 3D culture using the rotating cell culture system (RCCS). Cell aggregates were grown for 21 days in 10 mL and 50 mL vessels, with images captured at 25x (day 2-8) and 10x (day 10-21) magnification upon sampling and media replenishment.

8.5.2.2 Aggregation with micro-carrier beads

SW480 cultures were also maintained for 21 days in combination with Cytodex-1 and Cytodex-3 micro-carrier beads coated with *diethylaminoethyl* (DEAE) cellulose and collagen, respectively, using 10 mL vessels at a cell density of 1 x 10^7 cells per vessel (**Figure 8.5.2.2**). Cells appeared to remain viable in 10 mL vessels in combination with both micro-carriers; although this was not quantified.

At day 2, most cells remained unattached, but with some cells already noticeably interacting with both Cytodex-1 and Cytodex-3 micro-carrier beads. Cell coverage of beads began to improve by day 5, with some aggregates beginning to form individually but with most cells still remaining in suspension. From day 5 onwards, attached cells appear to spread across the surface of micro-carrier beads; this was seen to be more pronounced on Cytodex-1 beads (see **Figure 8.5.2.2**). Cells also began showing signs of elongation or spikes/projections from the cell membrane, but this was not as pronounced as without the use of micro-carrier beads.

From day 7, samples obtained from the cultures were observed to contain cell debris, possibly due to damage following impact with rotating beads. Cell projections between attached cells began to spread across the Cytodex-1 beads, a phenomenon observed to a lesser extent using Cytodex-3 beads. From day 9, beads began to form bonds with neighbouring beads via cells attached to DEAE or collagen surfaces, creating considerably larger clustering of micro-carriers; these were readily obtained upon sampling from day 12 (see **Figure 8.5.2.2**).

Little difference was observed between days 14 and 21 cultures in terms of cell coverage of micro-carriers, with the appearance of greater levels of gathering cell debris seen from day 14 onwards. Cells appeared to project and spread more readily across Cytodex-1 beads coated with DEAE, with up to 20 cells observed attached to one bead. There was considerable variation in cell coverage between beads within the same cultures, with bead size also seen to vary.

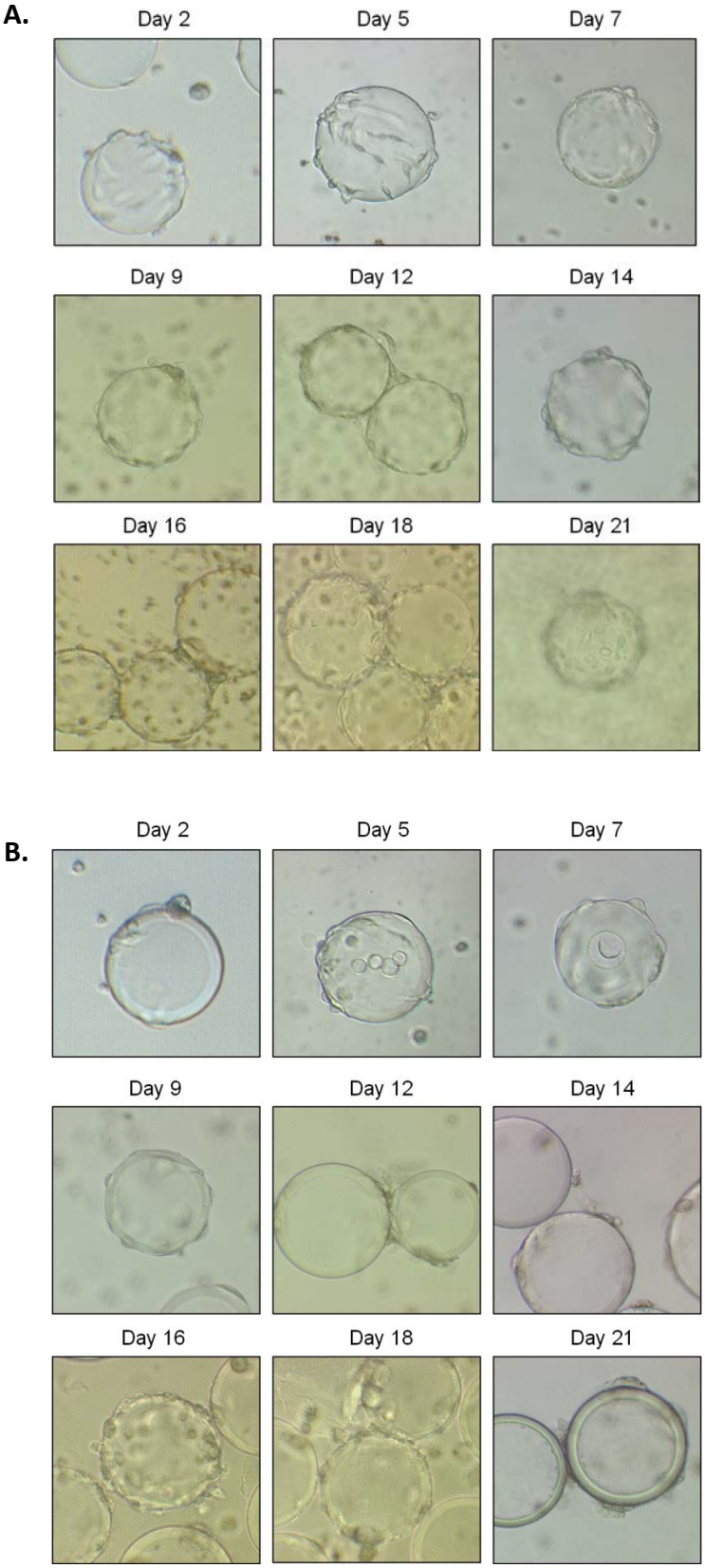

Figure 8.5.2.2. SW480 CRC cells grown as 3D organotypic cultures using micro-carriers. One representative image for each sampling point showing development of SW480 cells growing on (A) Cytodex-1 and (B) Cytodex-3 micro-carrier beads coated with diethylaminoethyl (DEAE) cellulose and collagen, respectively; images taken at 10x magnification throughout.

8.5.2.3 H&E staining of 3D SW480 aggregates without micro-carrier beads

Samples of 3D SW480 cultures, alone and in combination with micro-carriers, were also submitted for haematoxylin and eosin (H&E) staining. Unfortunately, it was not possible to retain samples at day 2 of RCCS culture during histological processing due to the small size of the aggregates. H&E staining of sample sections allowed insight into the development of 3D cell aggregates (**Figure 8.5.2.3**). The early stages of 3D cell aggregation (up to day 10) showed most cells intact within the developing aggregate, which would suggest growth of a spheroid. This is opposed to the situation observed in the later stages of culture (beyond day 10), where most cells at the centre of the aggregate had undergone cell death. Cell debris was seen to increasingly accumulate, with only a few layers of cells remaining intact.

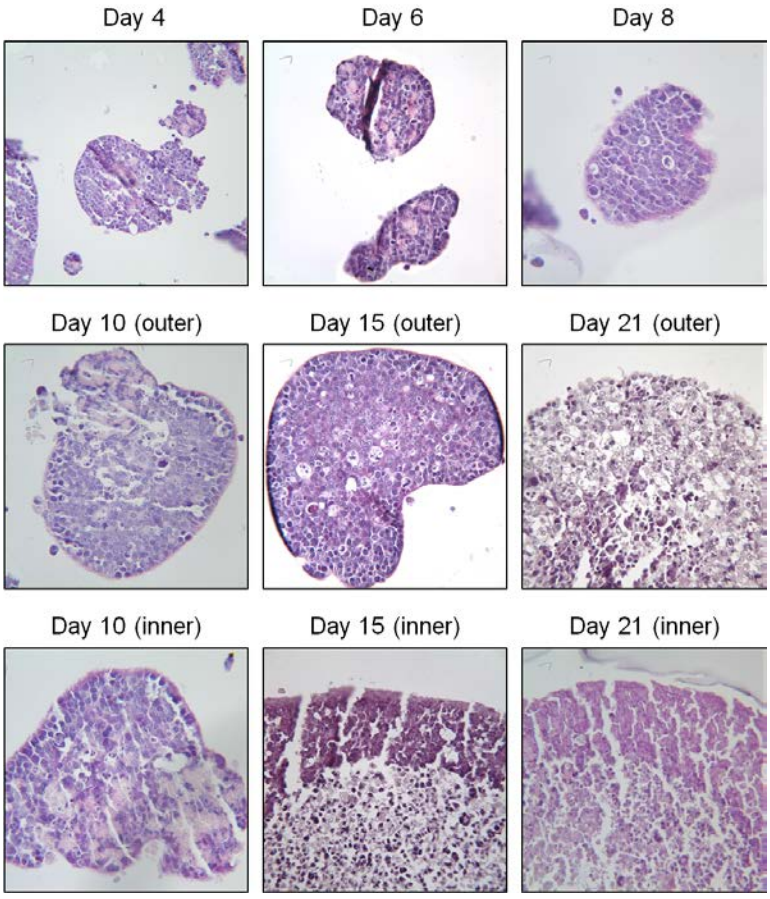

Figure 8.5.2.3. H&E staining of SW480 cells in 3D culture without micro-carrier beads. Representative images show H&E staining of SW480 3D cell aggregates grown over 21 days; development of aggregates from day 4 to day 21 are depicted for sections of the outer edges of aggregates, as well as central sections of aggregates at day 10 to day 21 of culture. Images were taken at 40x magnification.

8.5.2.4 H&E staining of 3D SW480 aggregates with micro-carrier beads

H&E staining was also completed for cells grown on micro-carrier beads, Cytodex-1 and Cytodex-3 (**Figure 8.5.2.4**). However, due to the eosinophilic coatings of the micro-carrier beads H&E staining was not compatible, with difficulties in distinguishing cells from micro-carrier coatings observed from sample taken at day 4 of culture.

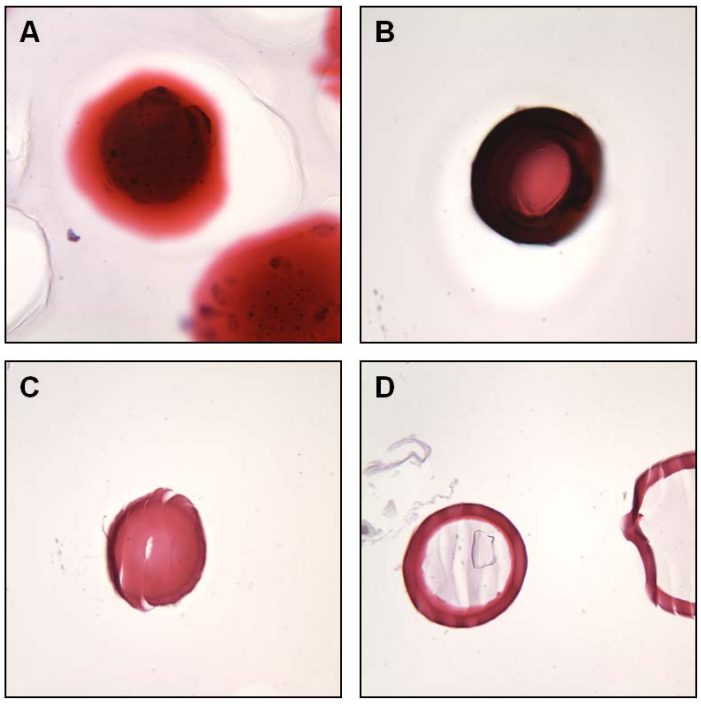

Figure 8.5.2.4. H&E staining of SW480 cells in 3D culture with micro-carrier beads. Representative images show H&E staining of SW480 cells grown for 4 days on (A) Cytodex-1 and (B) Cytodex-3 micro-carrier beads, with (C) outer surface and (D) cross-sectional views of Cytodex-3 beads also shown, with strong eosin staining of both Cytodex-1 and Cytodex-3 beads. Images taken at 40x magnification.

Following successful formation of 3D cell aggregates using SW480 cells, both with and without micro-carriers, the RCCS culture method was then applied to other colonic cells, with the aim of replicating and confirming the suitability of this technique to number of different colonic cell lines; this included DLD-1 cells and the transformed colorectal adenoma-carcinoma cell lines AA/C1 and AA/C1/SB.

8.5.3 DLD-1 colonocyte 3D organotypic aggregation in the RCCS

DLD-1 cells show a high basal level of Wnt pathway activation due to an *APC* gene truncation. Using the RCCS conditions determined for SW480 cells, development of DLD-1 cell aggregates was seen to occur at a much faster rate (see **Figure 8.5.3**). Many of the aggregates observed under microscopy appeared to contain large dark areas, suggesting greater intra-aggregate cell death and resultant cellular debris.

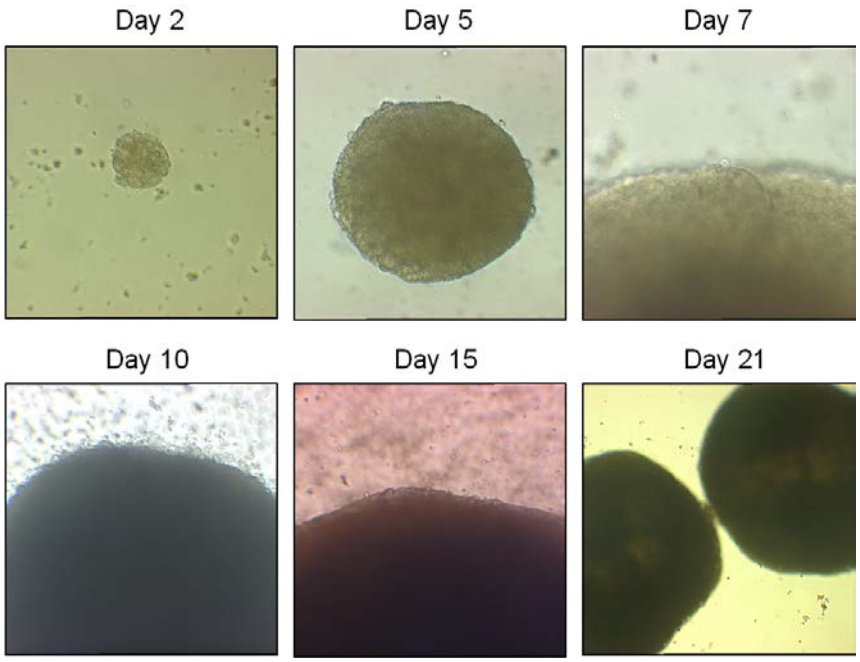

Figure 8.5.3. DLD-1 cell aggregate development from day 0 to day 21 without micro-carriers. Representative images show the development of DLD-1 3D cell aggregates using RCCS culture. Cell aggregates were grown for 21 days in 50 mL vessels, with images captured at 10x (day 2-15) and 5x (day 21) magnification upon sampling and media replenishment.

8.5.4 Transformed adenoma-carcinoma cell 3D organotypic aggregation in the RCCS

Following success of generating functional aggregates up to day 10 of culture with SW480 and DLD-1 cells, two experimentally transformed cell lines representative within the adenoma-carcinoma sequence, AA/C1 and AA/C1/SB, were similarly grown as organotypic 3D cultures for 10 days using the

RCCS (**Figure 8.5.4**). AA/C1 cells were found not to be compatible with the RCCS, with substantial cell rounding, accumulation of large quantities of cellular debris and lack of aggregation seen by day 6 of culture; the AA/C1 3D cultures were therefore terminated early. Conversely, AA/C1/SB cells were seen to be compatible with culture in the RCCS, with the appearance of large aggregates observed by microscopy (see Figure 8.5.4).

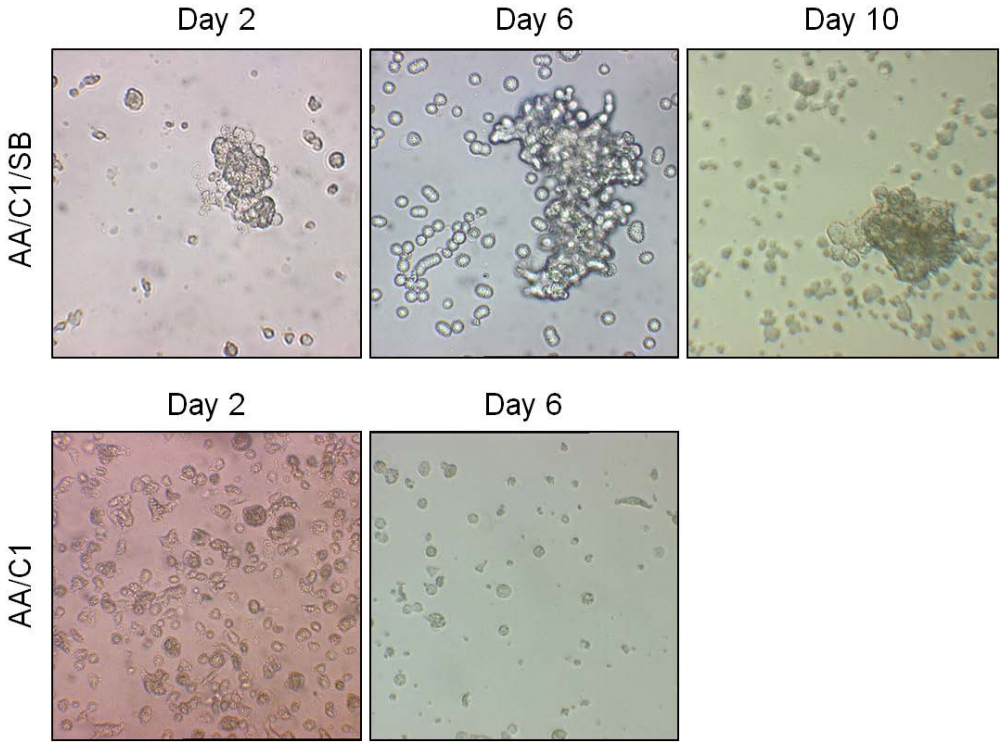

Figure 8.5.4. Cell aggregate development testing using AA/C1 and AA/C1/SB cell lines. Representative images show the development of AA/C1 and AA/C1/SB cell aggregates in 3D RCCS culture. AA/C1 cell aggregate development was terminated after 6 days due to cell rounding and appearance of cell debris; AA/C1/SB cells were maintained in culture for 10 days. Images were captured at 25x (day 2-6) and 10x (day 10) magnification upon sampling and media replenishment.

Due to the successful compatibility of AA/C1/SB cells in 3D aggregate cultures in the RCCS, these cells, along with 3D SW480 aggregates, were used in infection assays using mucosa-associated *E. coli*. Infection of non-tumorigenic human AA/C1/SB colonic cells (derived from the colonic PC/AA adenoma

cell-line) grown as 3D aggregates, allowed us to investigate the impact of these bacteria on Wnt activation earlier in the adenoma-carcinoma sequence.

8.5.5 Infection of 3D organotypic colonic cell aggregates to determine COX-2 expression and Wnt activation

Following the successful development of 3D organotypic aggregates using both SW480 and AA/C1/SB cells in the RCCS, these cultures were utilised for infection assays. At this point, we were unaware how quickly these 3D aggregates expanded under RCCS conditions, and along with the inevitable loss of smaller cell aggregates during media replenishment, it was not possible to establish an accurate multiplicity of infection (MOI). For this reason, the initial cell density (1×10^7 cells/vessel) was used to establish a MOI of 10. Both the SW480 and AA/C1/SB 3D organotypic cultures were maintained for 10 days in 10 mL vessels before harvesting for infection with mucosa-associated *E. coli* for 4 hours in 6-well plates. Following infection of 3D organotypic aggregates, extraction of cellular RNA allowed for synthesis of cDNA, which was then subjected to RT-PCR to quantify COX-2 (*PTGS2*) and β-catenin (*CTNNB1*) gene expression.

Mucosa-associated *E. coli* treatment of SW480 3D organotypic cell aggregates at day 10 for 4 hours showed a significant increase in *PTGS2* expression, with isolates HM44, HM358 and HM605 giving 2.82 ± 0.27 ($P<0.01$; Unpaired T-test), 6.17 ± 0.76 ($P<0.01$) and 102 ± 3.53 ($P<0.001$) fold changes, respectively (N=2, n=3; **Figure 8.5.5.1**). Cells treated with non-pathogenic *E. coli* K12 gave Ct values above 40 cycles (as per non-template controls) on all occasions during RT-PCR, thus a fold change value could not be given, and other *E. coli* treatment data were compared to untreated controls. Infection of SW480 3D aggregates with the same isolates produced similar results when quantifying *CTNNB1* expression, with increases from 2.1 to 12.6 fold observed following treatment with HM44 ($P<0.01$), HM358 ($P<0.001$) and HM605 ($P=0.1428$) compared with non-pathogenic *E. coli* K12 treatment (N=2, n=3; **Figure 8.5.5.2**).

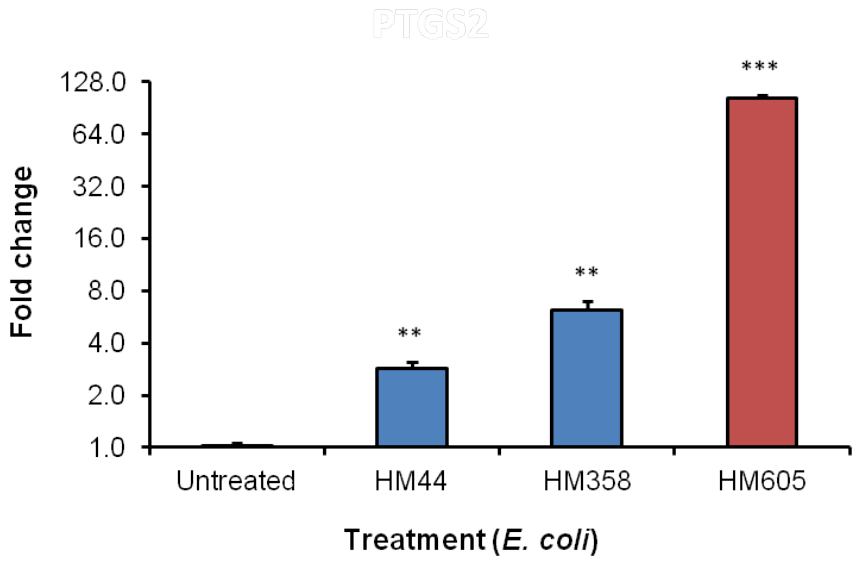

Figure 8.5.5.1. Changes in COX-2 (*PTGS2*) gene expression in SW480 colonic cells grown as 3D aggregates without micro-carrier beads. Graph shows mean ± SEM fold change data for SW480 cells treated with mucosa-associated *E. coli* isolates HM44, HM358, HM545 and HM605, and untreated controls (MOI: 10 based on original cell seeding density of $1x10^7$ cells/vessel). Fold change data normalised to untreated controls due to lack of *E. coli* K12 data (N=2, n=3; **P<0.01, ***P<0.001, Unpaired T-test).

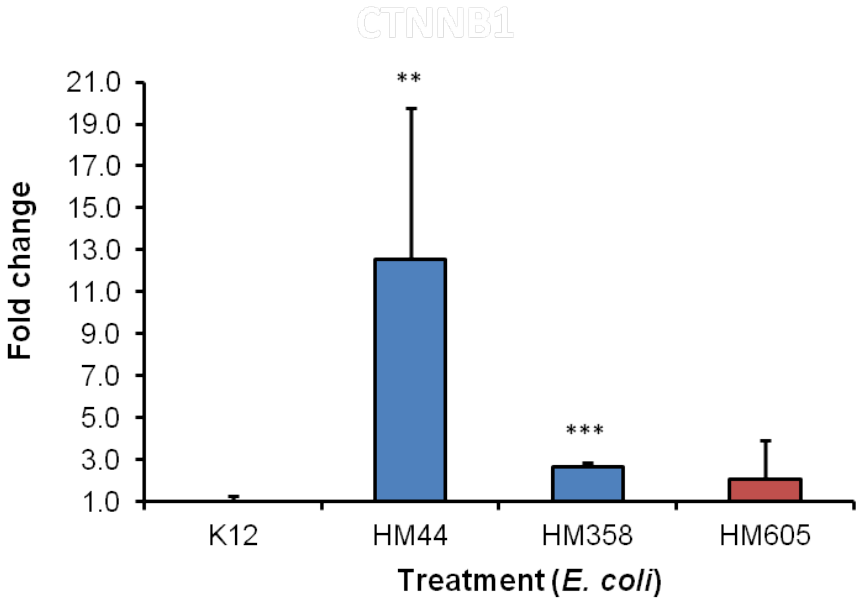

Figure 8.5.5.2. Changes in β-catenin (*CTNNB1*) gene expression in SW480 colonic cells grown as 3D aggregates without micro-carrier beads. Graph shows mean ± SEM fold change data for SW480 cells treated with mucosa-associated *E. coli* isolates HM44, HM358, HM545 and HM605, and non-pathogenic *E. coli* K12 (MOI: 10 based on original cell seeding density of $1x10^7$ cells/vessel). Fold change data normalised to *E. coli* K12 treatment (N=2, n=3; **P<0.01, ***P<0.001, Unpaired T-test).

Following the successful observation of significant increases in COX-2 and β-catenin gene expression following mucosa-associated *E. coli* infection of SW480 3D aggregate cultures, AA/C1/SB 3D aggregates grown in the RCCS for 10 days were treated with the same *E. coli* isolates, and compared to *E. coli* K12 treatments or untreated controls. Results from non-pathogenic *E. coli* K12 treated aggregates were only obtained for *CTNNB1* expression. However, as no data were obtained for *PTGS2* expression in response to *E. coli* K12 due to a lack of Ct values during RT-PCR, untreated controls were used for data comparisons.

Mucosa-associated *E. coli* treatment of AA/C1/SB 3D cell aggregates showed significant increases in *PTGS2* (**Figure 8.5.5.3**) and *CTNNB1* (**Figure 8.5.5.4**) expression using CRC mucosa-associated isolates HM44 and HM358, showing 19.19 ± 1.42 ($P<0.001$) and 7.56 ± 1.36 ($P<0.001$) fold changes in *PTGS2* expression, and smaller 1.52 ± 0.11 ($P=0.0162$) and 1.19 ± 0.11 ($P=0.3491$) fold changes in *CTNNB1* expression, respectively. Conversely, treatment with another CRC mucosa-associated *E. coli* isolate HM545 and CD mucosa-associated *E. coli* isolate HM605 effected little/no increase in *PTGS2* expression, but significantly increased *CTNNB1* expression, with 1.58 ± 0.05 fold ($P<0.001$) and 1.37 ± 0.11 fold ($P=0.0622$) changes confirmed, respectively.

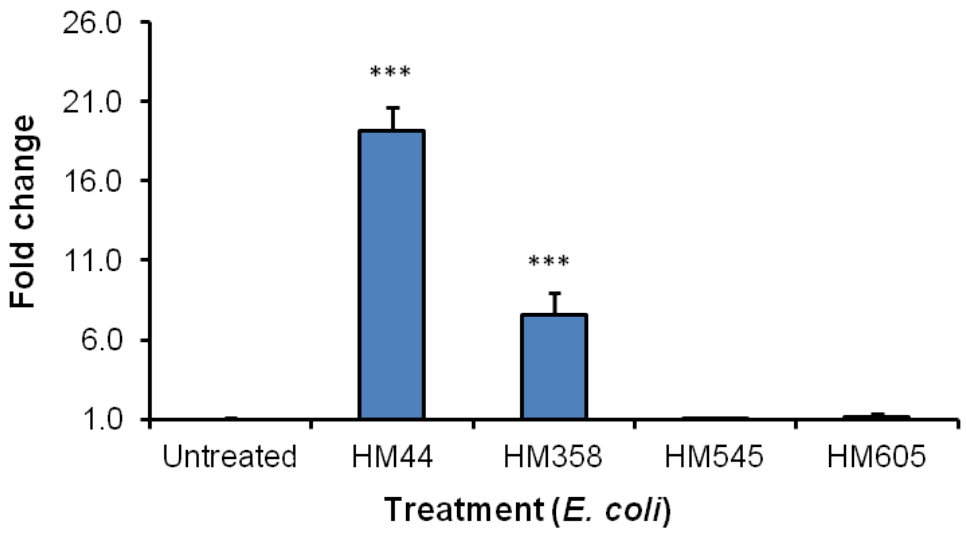

Figure 8.5.5.3. Changes in COX-2 (*PTGS2*) gene expression in AA/C1/SB colonic cells grown as 3D aggregates without micro-carrier beads. Graph shows mean ± SEM fold change data for AA/C1/SB cells treated with mucosa-associated *E. coli* isolates HM44, HM358, HM545 and HM605 (MOI: 10 based on original cell seeding density of $1x10^7$ cells/vessel). Fold change data normalised to untreated 3D aggregates due to lack of *E. coli* K12 data (N=2, n=3; *P<0.05, Unpaired T-test).

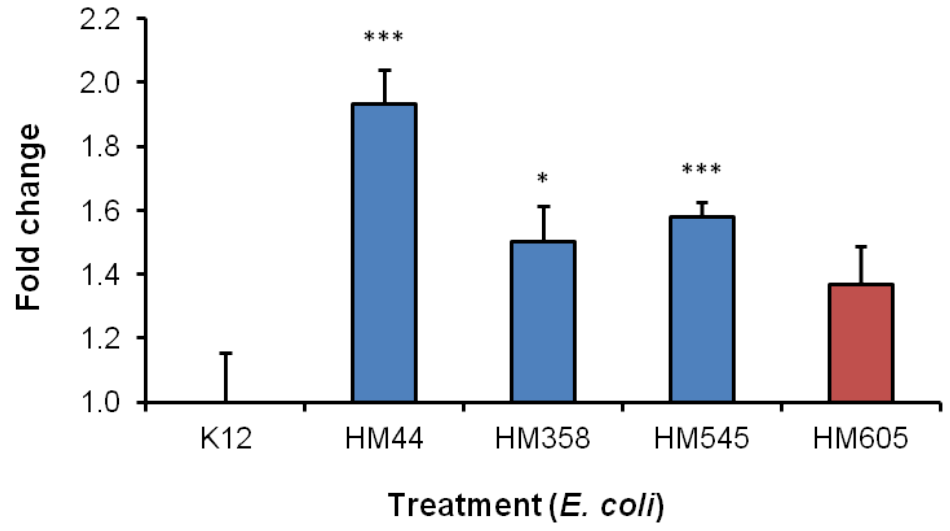

Figure 8.5.5.4. Changes in β-catenin (*CTNNB1*) gene expression in AA/C1/SB colonic cells grown as 3D aggregates without micro-carrier beads. Graph shows mean ± SEM fold change data for AA/C1/SB cells treated with mucosa-associated *E. coli* isolates HM44, HM358, HM545 and HM605, and non-pathogenic *E. coli* K12 (MOI: 10 based on original cell seeding density of $1x10^7$ cells/vessel). Fold change data was normalised to *E. coli* K12 treatment data (N=2, n=3; *P<0.05, Unpaired T-test).

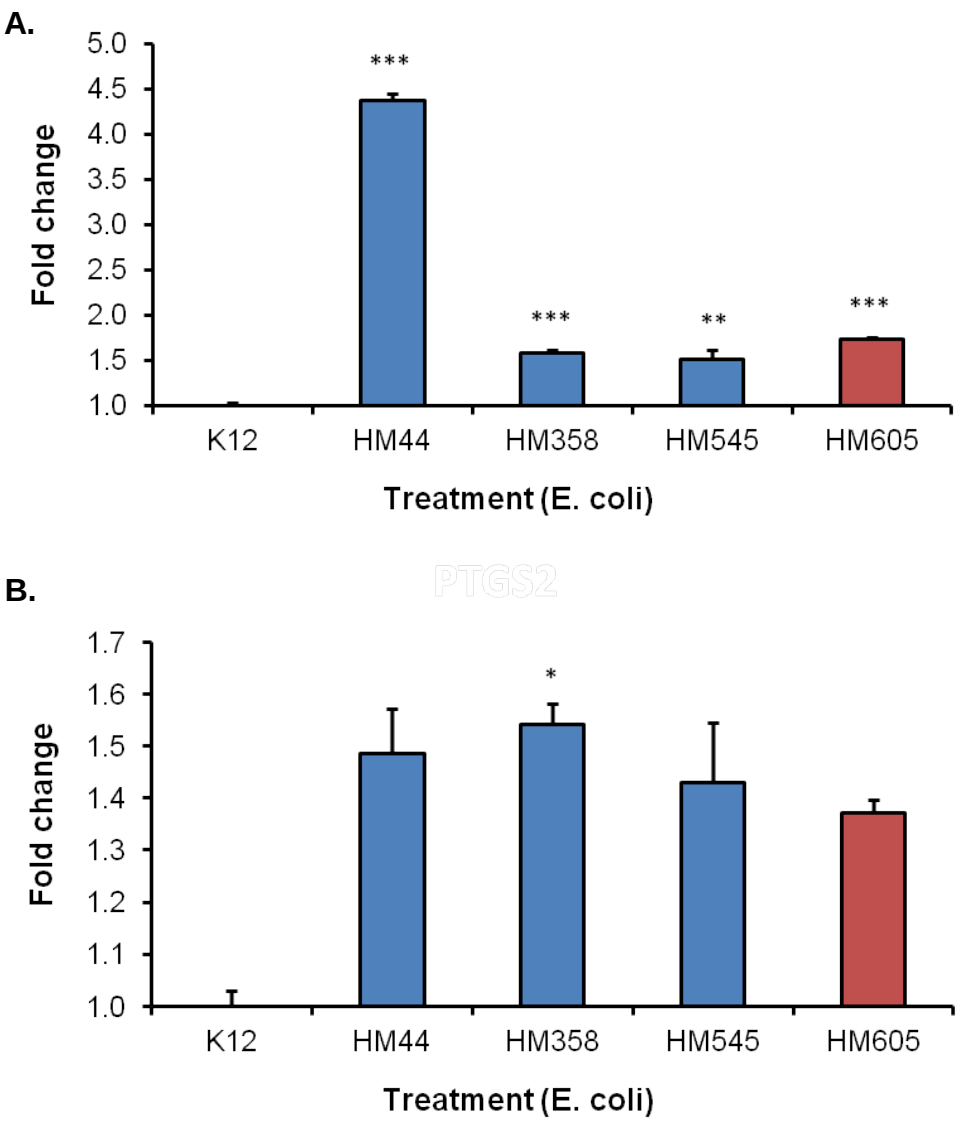

Figure 8.5.5.5. Changes in COX-2 (*PTGS2*) and β-catenin (*CTNNB1*) gene expression in AA/C1/SB colonic cells grown in 2D monolayer culture. Graph shows mean ± SEM fold change data for (A) *PTGS2* and (B) *CTNNB1* gene expression in AA/C1/SB cells treated with mucosa-associated *E. coli* isolates HM44, HM358, HM545 and HM605, and non-pathogenic *E. coli* K12 (MOI: 10). Fold change data was normalised to cell left untreated (N=2, n=3; *P<0.05, **P<0.01, ***P<0.001, Unpaired T-test).

Data for infection of AA/C1/SB cells in 2D monolayer culture was gathered concurrently to enable comparison of RT-PCR data obtained from 3D aggregates (**Figure 8.5.5.5**). These infection assays confirmed data obtained from 3D aggregate infections, with similar patterns of increase in *PTGS2* and *CTNNB1* expression for all mucosa-associated *E. coli* isolates tested. All mucosa-associated *E. coli* infection data was compared to that from non-pathogenic *E. coli* K12 treatments.

8.6 Discussion

Successful 3D aggregate culture of SW480 and DLD-1 CRC cell lines was achieved using a rotating cell culture system (RCCS), alone and using micro-carrier bead supports. Following development, with respect to structure and formation of 3D organotypic CRC cell aggregates, as observed by microscopy and H&E staining, we decided to follow the example of the Carvalho *et al.* (2005) in using 3D aggregates formed following 10 days of culture in the RCCS for subsequent infection assays. This cut-off (day 10), limited appearance of large dark areas within SW480 cell aggregates at later stages of development (>15 days), shown to be a collection of cellular damage/debris. However, this cut-off (day 10), meant that DLD-1 3D cell aggregates were not considered suitable for infection studies as appearance of dark centres were seen in these particular 3D cell aggregates before day 10 and likely would affect their viability and potential for use in infection studies. Production of more viable of 3D organotypic aggregates using DLD-1 cells therefore requires further development/investigation.

Study of mucosa-associated *E. coli* infection-induced COX2 and β-catenin gene expression in an organotypic system was conducted using the adenocarcinoma SW480 cells and in non-tumorigenic, anchorage dependent AA/C1/SB colonic cells (Williams *et al.*, 1990) derived from human colonic adenoma cell-line PC/AA (Paraskeva *et al*., 1988). The early data obtained from infecting these 3D organotypic aggregates would suggest that this method of culture is suitable for studying mucosa-associated *E. coli*-host epithelium interactions, and confirmed/complemented data previously obtained by infection of 2D monolayer CRC cell cultures and those responses seen in an *in vivo* gut infection model (see Chapters 5 and 6, respectively). The RT-PCR data obtained from infection assays using SW480 3D cell aggregates showed considerably different fold-change results to those observed in monolayer cultures, but exhibited the same trend of increasing COX-2 (*PTGS2*) and β-catenin (*CTNNB1*) gene expression following treatment with mucosa-associated *E. coli.* Unfortunately, a lack of data for *PTGS2* expression induced by infection with *E. coli* K12 meant that we could not corroborate the lack of change in expression of this gene using this non-pathogenic strain observed in 2D SW480

cell monolayer cultures. We are unable to explain the inability to obtain a Ct value in the range of 40 cycles, set as the maximum number of cycles during RT-PCR, using *E. coli* K12 treatments. It is possible that this was due to reagent handling given that results were obtained for *CTNNB1* expression using the same samples, but the fact that this occurred using N=2 could point elsewhere; this may have also contributed to the lack of change in *PTGS2* expression following HM545 and HM605 treatment of AA/C1/SB cell aggregates.

The data obtained from non-tumorigenic colonic AA/C1/SB 3D organotypic aggregates was particularly interesting. Results suggest that CRC mucosa-associated *E. coli* treatment can increase epithelial COX-2 expression and Wnt/β-catenin pathway activation at the later adenoma stage. Judging by review of available literature, this is the first time that changes in these surrogate early markers of cancer development have been seen in an anchorage dependant, non-tumorigenic adenoma cell line, and points towards the effects of these bacteria earlier in the adenoma-carcinoma sequence than originally realised. However, as these are only changes in gene expression, it would benefit from showing the impact of these infections on protein expression in these 3D aggregates. The studies conducted here would also be supported better from availability of data from cells at even earlier stages of the adenoma-carcinoma sequence, such as early passages of the PC/AA adenoma cell line (Paraskeva *et al*., 1988), unfortunately not available for these studies, as well as using primary cells or organoid-derived colonocytes from human tissue with no disease association to be able to model the impact of these bacteria throughout the development and progression of colonic disease. As discussed in the *in vitro* studies (see Chapter 5), we encountered slow growth of non-tumorigenic AA/C1 cells in 2D monolayer culture in preparation for adding to the RCCS for 3D culture. As these cells mimic the properties of a later stages of adenoma, this is not a surprising find; but the fact that these cells grow slowly in monolayer culture may contribute to the incompatibility of these cells when they were eventually added to the RCCS. AA/C1 is described as a late passage clonogenic variant of pre-malignant epithelial adenoma cell line PC/AA (Paraskeva *et al*., 1988), likely representing a later stage in tumour progression, i.e. still retaining characteristics of the early adenoma cells but acquiring

certain characteristics of cancer cells. AA/C1 had a higher colony forming efficiency than its parent, but a lower efficiency than that of subsequent AA/C1/SB variants (Williams *et al.*, 1990, Paraskeva *et al.*, 1992). The lower colony forming efficiency and higher anchorage dependency may have contributed to the slow growth in monolayer culture, as well as their downfall in 3D aggregate culture within the RCCS.

In contrast, the sodium butyrate transformed AA/C1/SB cells seemed to be much more compatible. This was the first time AA/C1/SB 3D cell aggregates have successfully been used to quantify COX-2 and β-catenin gene expression. The AA/C1/SB cells obtained from Professor Paraskeva's group for this study were non-tumourigenic. It would also be beneficial to investigate the compatibility of the subsequent tumorigenic AA/C1/SB10 cell line, generated following treatment of AA/C1/SB cells with N-methyl-N'-nitro-N-nitrosoguanidine (MNNG), a chemical *carcinogen* widely used for to develop *carcinogenesis in cell and animal* models (Lee *et al.*, 2007). This treatment was shown to allow anchorage independence and increase tumourigenicity (Williams *et al.*, 1990), and these attributes may help the cells to grow quicker and adapt better to culture within the RCCS.

To be consistent with the earlier *in vitro* CRC 2D monolayer cell-line studies (see Chapter 5), it would be important to confirm the impact of mucosa-associated *E. coli* on COX-2 and β-catenin protein expression in both SW480 and AA/C1/SB 3D cell aggregates. Techniques such as immunoblotting, immunofluorescence and IHC could be used to order to confirm the translation of increased gene expression in infected aggregates. Considering the RT-PCR data showing increased gene expression in 3D cell aggregates, it is possible that higher levels of DAB staining in IHC might be seen in these cultures treated with mucosa-associated *E. coli,* particularly in the outer cell layers where bacteria would have easier access. The IHC protocol for detecting protein expression, more specifically here for COX-2 and β-catenin, would likely have to be optimised for use with 3D organotypic aggregates.

There are an array of published techniques available to develop 3D organoid and organotypic spheroid cultures (Achilli *et al.*, 2012), from the more simplistic and better established low-adherence poly-

hema cultures through to the less well established, more expensive and convoluted stem-cell derived organoid cultures used to model human organ development and human disease (Clevers, 2016). Each of these options were considered for use in this study; each system has merits, but the choice of 3D organotypic culture using RCCS technique for this particular project was an easy one and allowed us to utilise/examine cells at stages within the adenoma-carcinoma sequence.

There are only a small number of studies that have evaluated the use of the RCCS using colonocytes (Goodwin *et al.*, 1992, Carvalho *et al.*, 2005, Kaeffer *et al.*, 1999), but the study by Carvalho *et al.* (2005) was a key study, previously utilising the system to investigate pathogenic *E. coli* interactions using colonic cells. This study used human intestinal epithelial HCT-8 cells within the RCCS, with layered cell aggregates developing after only 10 days in culture (Carvalho *et al.*, 2005). This aggregation was replicated using the colorectal cell lines in our study. The authors noted that the aggregates created in this system expressed normal intestinal tissue markers in patterns that suggested greater cellular differentiation than conventionally grown monolayers, produced higher levels of disaccharidases and alkaline phosphatase, typical of the normal intestine. Cells also developed microvilli and desmosomes, more than that seen when grown as 2D monolayers, again representative of normal intestinal tissue. This is an important consideration for this work, and is something that still needs to be confirmed using the SW480, DLD-1 and transformed adenoma cell lines. However, due to limitations in time, examination of markers of cellular differentiation were not undertaken in our project, thus we cannot confirm/add to these findings. Future studies may also be further expanded to examining differentiation following co-cultures with micro-carrier beads. The use of micro-carrier beads here was seen to be a fast and efficient way of mimicking the basement layers known to support epithelial growth without having to develop more complicated systems of co-cultures. The use of the beads within the culture was a technique to enable a higher yield of anchorage-dependent cell aggregates, with Cytodex beads used in this study developed specifically for the culture of a wide range of cell types and culture volumes; these were shown to work well with

the CRC cell lines used in this study, and further study may show these micro-carriers, to be of significant value in modelling the infection of colonic cells.

The low-shear microgravity conditions created by the RCCS also more closely mimic low-shear conditions in the intestine, as created by microvilli (Carvalho *et al.*, 2005), and was an important consideration for our study. An additional factor supporting use of the RCCS in our project was that there was no observable effect of rotation culture on the bacteria inoculum, with Carvalho *et al*. having previously noted that microgravity culture had no influence on pathogenic *E. coli* growth nor on virulence gene expression as compared with normal gravity conditions, with the exception of intimin expression by EHEC, which was found to be elevated. The authors also showed that the response of cell aggregates to infection with *E. coli* under RCCS conditions was similar to infection of intact colonic tissue, demonstrated by the appearance of the resultant attaching and effacing lesions seen *in vivo* (Carvalho *et al.*, 2005). Due to limitations in time, we did not examine microgravity effects of known adhesion/invasion virulence factors of mucosa-associated *E. coli* (Prorok-Hamon *et al*., 2014) but this would be an interesting future study to be undertaken.

Even some of the earliest reports on the use of the RCCS suggested that cells grown in bioreactors that simulate aspects of microgravity, or that use actual microgravity conditions, could produce tissues in sufficient quantity and quality to simulate *in vivo* tissues (Jessup *et al.*, 1993). With the right conditions, certain cultures could also promote differentiation and neoplastic transformation, and that a microgravity environment would not alter the ability of epithelial cells to recognize and associate with not only each other but also with constituents of basement membrane and extracellular matrix (Jessup *et al.*, 1993). A study by (Laguinge *et al*., 2004) used Annexin V staining to detect cells that may have experienced apoptotic death within 3D cultures, with propidium iodide-Annexin-V used alongside FITC to dual-stain these cells. Caspase-3 activity was also assessed by labelling cells with a fluorescent probe. Given the appearance of what seemed to be necrotic/apoptotic cell debris in the centre of cell aggregates in the absence of micro-carrier beads in our project, it would be interesting to investigate the exact nature of cell death and composition of debris within these 3D cultures.

The use of 3D organotypic cultures is becoming more prominent and relevant to study infectious diseases, especially as monolayer cell line cultures tend to exhibit altered properties due to immortalization and two-dimensional growth (Barrila *et al*., 2010, Herbst-Kralovetz *et al*., 2013, McGowin *et al*., 2013). A 3-D organotypic model of human intestinal epithelium has been successfully used to elucidate the role of key invasion and intracellular replication factors of *Salmonella enterica*, showing similar actions to those seen in infection *in vivo* (Radtke *et al*., 2010). Thus, the development of 3D organotypic culture models as part of this study, using two CRC cell-lines (SW480 and DLD-1) and the non-tumorigenic adenoma cell-line (AA/C1/SB), to study Wnt pathway activation, was another important step in building better platforms for the study of the interactions between *E. coli* and colorectal cells in a more parent tissue-like and disease-relevant context. With a limited number of representative small animal models available to effectively study these interactions, an organotypic culture using colonic cell lines allows fast and efficient development of multi-cellular tissue-like structures that mimic human tissues. Human tissue explants can be grown using *in vitro* organ cultures (IVOC), which has been done previously, and provides a complex multicellular environment for the study of host–pathogen interactions. However, these culture systems require a laboratory facility that has quick access to the collection of biopsy materials and suitable laboratories for the culture of these *in vitro*. IVOC studies are also limited to bacterial-host interactions during the relatively short lifespan of the collected biopsy material, whereas the use of human cell lines in a 3D organotypic culture have an indefinite lifespan (Carvalho *et al.*, 2005). Use of stem-cell derived organoids offers an alternative solution (Clevers, 2016), but would require micro-injection of bacteria into the lumen of cultured organoids; this is not required in 3D organotypic culture (Carvalho *et al*., 2005).

It is clear that more work remains to be done to test the suitability and compatibility of the 3D organotypic cultures tested in this project to study pathogen-host intestinal epithelial interactions and signalling. The opportunities to improve upon the technique developed here are exciting, both with and without use of different extracellular matrix bearing micro-carrier beads, and co-culture with stromal cells (Jessup *et al.*, 1993), including myofibroblasts and macrophages, key players of the

surrounding micro-environment driving colonic inflammation and neoplasia (Jessup *et al*., 1993, Crotti *et al*., 2017).

Additionally, investigating the effects on Wnt protein expression using immunoblotting would strengthen these results further. In the event of recent reports showing other pathways such as gp130/Stat3 signalling being rate-limiting, even with increased β-catenin nuclear localisation, (Phesse *et al*., 2015), other assays confirming cell proliferation and migration, as well as assessing cell viability and metabolism, during 3D development would be beneficial in confirming increased Wnt signalling driving malignant development. Due to the potential killing effect of bacterial infections of human cells for longer than 4 hours, development of these assays could include gentamicin treatment after 4 hours of infection in order to allow a longer window to assess phenotypic changes.

Summary

The initial work completed here has allowed further insight into the development of colonic cells using a 3D RCCS culture method, but more importantly has hinted towards the impact of mucosa-associated *E. coli* during the adenoma-carcinoma sequence. We have been able to show increases in both COX-2 and β-catenin gene expression, and future use of this RCCS culture method may show changes in COX2 protein levels and Wnt pathway activation (changes β-catenin protein expression/nuclear localisation). While the application of this 3D infection model has not, as yet, been shown to be suitable for all colonic cell types, the development of this culture method using the RCCS brings us a step closer to modelling mucosa-associated *E. coli* infection using a system that *in vitro* model epithelium that better mimics/recapitulates the *in vivo* complex architecture and biochemical intricacies of the parent tissue.

Chapter 9:

General Discussion

9.1 Summary of findings and advances in links between *E. coli* and colorectal cancer

Increasing evidence suggests that constituents in the gut microbiota and chronic inflammation are involved in colorectal cancer (CRC) development, with CRC associated with increased numbers of mucosal bacteria, particularly *E. coli* (Swidsinski *et al*., 1998, Martin *et al*., 2004). This likely contributes to promotion and progression of cancer by virulence factors that disrupt cellular signalling pathways controlling inflammation and tumorigenesis (Prorok-Hamon *et al*., 2014). Our study provides further data supporting the notion that mucosa-associated *E. coli* isolates can upregulate epithelial pro-inflammatory COX-2 and PGE_2 release, suggested to consistently contribute towards increased Wnt activation as measured by numerous methods both *in vitro* and *in vivo*. This suggests translational effects that might be seen in patients, which indicates a role for mucosa-associated *E. coli*, in the development and progression of colorectal cancer via increased Wnt signalling.

The aim of the project was to investigate whether specific *E. coli* isolates taken from IBD and CRC patients possess ability to activate key cancer-promoting proteins within epithelial cells lining the bowel, including those known to help development, growth and spread of tumours. The main pathway under investigation was the canonical Wnt pathway signals through β-catenin. Wnt signalling helps to regulate cell cycle and cell growth, whilst also playing a crucial role in colorectal tumorigenesis.

As described in chapter 5, data obtained early in the project pointed towards Wnt activation following infection of human colorectal cell-lines with *E. coli* isolates taken from CRC patients. CRC-associated *E. coli* HM44 and HM358 were selected for use in initial studies as they had been previously shown to have strong cancer-related activity, such as increases in pro-angiogenic VEGF (Prorok-Hamon *et al*., 2014). The Wnt gene array panel allowed us to get an insight into where these infections may be impacting any Wnt activity in these epithelial cells. We observed the expression of a number of genes being upregulated >2 fold, as well as some typically inhibitory genes downregulated >2-fold following infection. The expression of genes associated with angiogenic factors (*VEGFA* and *JAG1*), cell cycle regulators (*PTGS2*, *FOSL1* and *MYC*) and connective tissue growth factors (*WISP1*) were all seen to be

increased by varying levels following infection with these bacteria, with very noticeable increases seen in *PTGS2* and *VEGFA* expression. Given that no significant changes were seen with the non-pathogenic *E. coli* K12, this was seen as a potentially specific effects seen only with CRC bacteria capable of adhering to an invading the gut mucosa.

The *PTGS2* gene was commonly up-regulated in CRC cell lines SW480 and DLD-1 throughout the study following infection with both HM44 and HM358 strains alongside expression of the gene encoding β-catenin, *CTNNB1*, and has been previously linked to increases in Wnt signalling (Castellone *et al*., 2005). Immunoblots confirmed increased gene expression of *PTGS2* and *CTNNB1* translated into changes in protein levels of COX-2 and β-catenin, respectively. Results show that CRC mucosa-associated *E. coli* infection increases expression of β-catenin in a time-dependent manner, and that this correlated with increased expression of COX-2 protein in CRC cell lines.

Another CRC mucosa-associated isolate, HM545, an isolate taken from a Crohn's Disease (CD) patient, HM605, and the non-pathogenic *E. coli* K12 were then used to infect SW480 and DLD1 cells alongside HM44 and HM358. Assessment of nuclear localisation of β-catenin following mucosa-associated *E. coli* infection suggested that increased gene and protein expression seen previously translated to increased nuclear translocation. Downstream activation of Wnt transcription via TCF/LEF activity induces transcription of Wnt target genes by binding promoters of downstream target genes involved in cell proliferation, survival, and migration (Morin *et al*., 1997, van de Wetering *et al*., 2002).

We were able to observe significant increases in luciferase activity coupled to TCF/LEF transcription following treatment with CRC, CD and UC mucosa-associated *E. coli* isolates, with no change following non-pathogenic *E. coli* K12 infection. Diclofenac at a concentration of 100 μM showed consistent, significant inhibition of mucosa-associated *E. coli*-induced TCF/LEF transcription. This would suggest that Wnt transcription induced by mucosa-associated *E. coli* treatment translates from increased nuclear β-catenin localisation, and that cyclooxygenase activity contributes significantly to increased Wnt transcription.

The existing link between COX-2 and β-catenin suggested translation of these results into an *in vivo* infection model. In chapter 6, we investigated this using a germ-free *Il10*$^{-/-}$ mouse model mono-associated with the CRC mucosa-associated *E. coli* HM44 isolated from a CRC patient. Germ-free *Il10*$^{-/-}$ 129SvEv strain mice were mono-associated with *E. coli* HM44 for 6 weeks (n=15) or left untreated (n=5) at the gnotobiotic facility at NC State University by Dr Janelle Arthur *et al*. at the as previously described (Arthur *et al*., 2012). Immunohistochemistry for cyclooxygenase-2 and β-catenin showed highly significant increases in both COX-2 and β-catenin expression, as well as β-catenin nuclear localisation, indicating significant increases in Wnt signalling following mucosa-associated *E. coli* mono-association *in vivo*. This suggests translational effects into a more disease-relevant model.

Macrophages resident in the gut epithelium *in vivo* help to guide an immune response towards infection. Upon chronic infection, additional macrophages can be recruited in the form of blood monocytes that differentiate into macrophages. A recently published study showed CRC-associated *E. coli* promoting COX-2 and PGE_2 expression in human macrophages (Raisch *et al*., 2015). The authors reported significant with CRC-associated *E. coli* but not with commensal or non-pathogenic *E. coli* strains, with this induction requiring live bacteria; the changes were not associated with colibactin production. The study used human blood monocytes differentiated into macrophages, replicating the *in vivo* immune response.

In chapter 5, we were able to show significantly increased concentrations of PGE_2 in the supernatant of monocyte-derived macrophage cells infected with CRC mucosa-associated *E. coli* isolates HM44 and HM545, as well as CD mucosa-associated isolate HM605, using the same method of differentiation. These results were similar to those reported in the Raisch *et al.* (2015) study, with both CRC and CD associated *E. coli* isolates inducing significantly higher levels of PGE_2 secretion. CRC-associated *E. coli* strains can survive and replicate within human macrophages, as well as increase COX-2 expression and subsequent PGE_2 secretion (Raisch *et al*., 2015). Our results support these findings, and expand upon them by suggesting that mucosa-associated *E. coli* from IBD patients also enhance PGE_2 secretion following infection, which may implicate these *E. coli* in IBD-associated CRC risk.

Significant increases in COX-2 expression and activity, and subsequent PGE_2 synthesis, have now been observed in numerous studies where cancer-associated *E. coli* have been studied in the context of CRC (Raisch *et al*., 2014, Abdallah Hajj Hussein *et al*., 2012, Lew *et al*., 2002). Both human and animal models of CRC have shown a long-standing association with increased PGE_2 synthesis, and investigation of PGE_2 synthesis in the gut mucosa using mucosal biopsy specimens obtained during diagnostic colonoscopies show its role in the adenoma-carcinoma sequence (Pugh and Thomas, 1994). These results suggested colorectal carcinogenesis via the adenoma-carcinoma sequence could be associated with a progressive increase in PGE_2 synthesis. As COX-2 and PGE_2 have been shown to stimulate colon cancer cell growth via activation of the canonical Wnt signalling pathway (Castellone *et al*., 2005), this provides a molecular framework for further evaluation of mucosa-associated *E. coli* infection in inflammation-associated colorectal cancer.

The use of a non-pathogenic *E. coli* throughout the study was an important control in being able to establish a link between the necessary mucosa-association of *E. coli* strains and the observed changes in Wnt signalling. In this case, *E. coli* K-12 was used as a control in each assay. This wild-type strain of *E. coli* was isolated from the faeces of a convalescent diphtheria patient and is now frequently used as a host strain in gene cloning experiments (Kuhnert *et al*., 1995). Given the lack of COX-2 and Wnt activation *in vitro* following infection with *E. coli* K12, it is important to consider whether there may be specific bacterial factors prevalent in mucosa-associated strains responsible for these changes.

The adherent and invasive nature of the mucosa-associated *E. coli* HM44 and HM358 strains suggests it is possible that increased Wnt signalling comes from the increased intracellular survival of these strains when compared to non-invasive strains such as *E. coli* K12. A better understanding of phenotypic AIEC characteristics associated with increased Wnt signalling could allow a targeted inhibition of the effects of AIEC infection in the activation of COX-2 and/or Wnt signalling. Following results *in vitro* and *in vivo* showing significant increases in COX-2, we were able to confirm up-regulated COX-2 gene expression in a number of fosmid clones using the fragmented HM358 fosmid

library screen (see chapter 7). Fosmid clones created previously (Prorok-Hamon *et al*., 2014) were screened for changes in COX-2 gene expression using RT-PCR following infection of CRC cells.

Initial and confirmation screening efforts identified 12 fosmid clones showing common *PTGS2* expression increases. Subsequent sequencing of these clones showed similarities in DNA content, with particularly common homology in two of these fosmids. The operons identified following the vector sequence were almost identical for the 2E4 and 6E8 clones. A number of genes involved in the growth and survival of *E. coli*, particularly under high-stress inflammatory conditions, were identified, including the *ispB* gene that codes for the octaprenyl diphosphate synthase enzyme involved in quinone synthesis (Maouche *et al*., 2016), and the *gltB* and *gltD* operons responsible for the synthesis of glutamate synthase (Kumar and Shimizu, 2010).

If the mucosa-associated *E. coli* do harness these features for growth and survival better than non-pathogenic strains, particularly in higher stress conditions such as inflammation, their ability to infect host cells may be improved and may have contributed to the signaling changes observed both *in vitro* and *in vivo*. With further infection modelling and continued identification of key operons/genes, it may be possible to confirm the presence of existing and/or novel genes/operons involved in the adhesion and invasion of mucosa-associated *E. coli* and subsequent impact of increased COX-2 and Wnt signalling.

9.2 A new model to investigate the interactions between *E. coli* and the gut epithelium

The higher presence of *E. coli* in the gut microbiota under inflammatory conditions, including strains possessing an ability to become opportunistic pathogens that adhere to and invade intestinal epithelial cells, implicates them as a risk factors for gastrointestinal cancers via chronic infection and inflammation. With inflammatory pathways triggering downstream signalling events, we suggested that the ability to model or mimic these interactions *in vitro* would go some way to being able to understand the risks posed by bacteria such as mucosa-associated *E. coli* in colorectal disease.

One of our aims was to mimic these interactions utilising 3D cell cultures. Previous development of 3D culture models to study host-pathogen interactions by different groups has allowed a better platform for studying these interactions, with one study in particular having already reported successful use of CRC cell lines to study host-pathogen interactions with *E. coli* (Carvalho *et al*., 2005). As this study made use of the rotating cell culture system (RCCS), we were able to use this information as a template for our own 3D model.

As described in chapter 8, three-dimensional cultures were created suitable for infection with mucosa-associated *E. coli*, including the use of porous micro-carrier beads coated with collagen and diethylaminoether (DEAE) as a support for CRC cell growth in the RCCS system, simulating the supportive environment *in vivo*. The RT-PCR data obtained from infection assays using SW480 cell aggregates showed considerably different fold-change results to those observed in monolayer cultures, but exhibited the same trend of significant increases in COX-2 and β-catenin gene expression following treatment with mucosa-associated *E. coli.*

Unfortunately, a lack of K12 data for COX-2 gene expression means that we cannot confirm the lack of change in expression using this non-pathogenic strain as expected. We are so far unable to explain the inability to obtain a Ct value in the range of 40 cycles set in the RT-PCR, considering that this was achievable following all other treatments and in previous monolayer treatments using K12. It is possible that this was due to reagent handling given that results were obtained for *CTNNB1* expression using the same samples, but the fact that this occurred using N=2 could point elsewhere; this may have also contributed to the lack of change in COX-2 gene expression following HM545 and HM605 treatment of AA/C1/SB cell aggregates.

RCCS culture was also attempted using late-stage adenoma cell line AA/C1 and completed using the adenocarcinoma cell line AA/C1/SB, experimentally-transformed from epithelial adenoma cell line PC/AA (Williams *et al*., 1990, Paraskeva *et al*., 1992). The AA/C1/SB aggregates were also successfully used in RT-PCR studies, with significant increases in COX-2 and β-catenin gene expression shown

following CRC mucosa-associated *E. coli* infections. This was particularly interesting, as it was the first time we had seen the impact of mucosa-associated *E. coli* infections in these cells when grown as 3D aggregates; this may also be the first time these results have been seen in an adenocarcinoma cell line, and points towards the effects of these bacteria earlier in the adenoma-carcinoma sequence than originally realised. This work allowed further insight into the development of 3D RCCS colonic cell cultures, but more importantly hinted towards the impact of mucosa-associated *E. coli* during the adenoma-carcinoma sequence.

While the application of this 3D infection model hasn't yet been shown to be suitable for all colonic cell types, the development of this technique brings us a step closer to modelling mucosa-associated *E. coli* infections *in vitro* using a system that better mimics growth in the *in vivo* state. Several groups have been able to establish stem-cell derived gastric organoid systems suitable for infection studies, using microinjection of *H. pylori* (Burkitt *et al*., 2017, Bartfeld *et al*., 2015, Schlaermann *et al*., 2016). Future use of organoid cultures for *E. coli* infection studies would further build on our work, allowing a system that better reflects key structural and functional properties of the gut and the impact of bacterial infections (Clevers, 2016).

9.3 Expanding on the relationship between infection, inflammation and cancer

The inflammatory response is already known to involve a number of signalling pathways responsible for regulating the expression of inflammatory mediators. Pro-inflammatory cytokines such as interleukins, tumour necrosis factor (TNF)-α, nitric oxide and COX-2, commonly implicated in inflammatory disease, are released upon tissue damage or following infection (Bartchewsky *et al*., 2009, Anderson *et al*., 1996, Laflamme *et al*., 1999, Tak and Firestein, 2001). Both TNF-α and COX-2 have come into focus in recent years as driving forces for the recruitment and activation of inflammatory cells (Karin *et al*., 2006). By blocking key inflammatory mediators associated with TNF-α and COX-2 release, it is possible to attenuate the inflammatory response, hence these inflammatory cytokines now being established as important therapeutic targets in chronic inflammatory diseases

(Karin *et al*., 2006, Nakamura *et al*., 2009). Under chronic inflammatory conditions such as in IBD in both Crohn's disease and ulcerative colitis, the faecal microbiota commonly shows reduced bacterial diversity. This is most pronounced in Crohn's disease where a reduction in Firmicutes can be observed alongside an increase in Proteobacteria such as *E. coli* (Hold *et al*., 2014). Animal models of IBD and gastroenteritis have been found to result in similar changes in the microbiota, particularly reduced diversity. In a mouse model of colitis, induced by dextran sodium sulphate, there is marked disturbance of the mucosal barrier including loss of colonic adherent mucus, where the faecal microbiota shows a reduction in diversity and an increase in *Enterobacteriaceae* such as *E. coli* (Nagalingam and Lynch, 2012). Similar changes are seen in mouse models of infective gastroenteritis using *Citrobacter rodentium* and *Campylobacter jejuni* infections, as well as chemically and genetically induced models of intestinal inflammation to demonstrate that host-mediated inflammation in response to an infecting agent, a chemical trigger, or genetic predisposition markedly alters the colonic microbial community (Lupp *et al*., 2007). Our study has shown a consistent increase in inflammatory COX-2 signalling both *in vitro* and *in vivo* following mucosa-associated *E. coli* infections, which could be contributing to the chronic inflammation seen in colonic disease.

Other studies focussing on the mucosa-associated microbiota have generated more dramatic differences than study of faecal microbiota between health and IBD, particularly in Crohn's disease. This is the case for the mucosa-associated *E. coli* that have been found more commonly in mucosal biopsies from the ileum and colon of patients with Crohn's disease (Darfeuille-Michaud *et al*., 1998, Martin *et al*., 2004). In colonic biopsies, many of these bacteria are present within the adherent mucus (Swidsinski *et al*., 2002), although there is also evidence of intracellular *E. coli* from study of gentamicin-treated and subsequently lysed mucosal samples (Martin *et al*., 2004). The increased abundance of *E. coli* in the gut has long been linked to carcinogenesis. A study detected bacteria in 90% and 93% of adenoma and carcinoma biopsy specimens, respectively. In addition, partially intracellular *E. coli* were found in 87% of patients with adenoma and carcinoma compared to none in control samples. It was therefore concluded that the colonic mucosa of patients with colorectal

carcinoma but not normal colonic mucosa was colonised by intracellular *E. coli* (Swidsinski *et al*., 1998). It is now believed that many of the changes in microbiota composition seen in IBD, including an increase in *E. coli*, may be secondary to the inflammation. Mucosa-associated *E. coli* in colon cancers also show some of the adherent, invasive phenotypic features of Crohn's associated *E. coli* (Martin *et al*., 2004). The isolates from the Martin *et al*. study are the same isolates tested throughout this study.

The microbiota has previously been linked to innate (Clarke *et al*., 2010) and adaptive immunity (Chervonsky, 2010), gastrointestinal development (Hooper, 2004), invasion and angiogenesis (Stappenbeck *et al*., 2002). Due to gut bacteria being implicated in a number of steps of disease progression in CRC, it is easy to see the varying ways in which bacteria can influence colorectal disease. The major route in which bacterial infection can aid progression of CRC is via inflammatory pathway. TLR signalling plays an important role in inflammation and tissue regeneration via the myeloid differentiation primary response gene 88 (MyD88). Activation of TLR signalling results in the expression of antimicrobial peptides and the production of prostaglandins and cytokines as a protective mechanism to stop bacterial colonization of IECs. This includes the induction of cyclooxygenase expression, which can promote epithelial cell proliferation. Dysregulation of protective mechanisms such as TLR signalling helps to explain how bacterial infections of the gut could promote colorectal cancer. It is possible that COX-2 increases shown throughout our study could be brought on via these pathways.

Infection-induced hyper-proliferation of epithelial cells, either via inflammatory cytokines or independent of them, seems to be a common theme in most gut-associated cancers. One aspect that seems to stand out is the impact of bacterial composition in carcinogenesis, with dysbiosis being a consistency. With evidence of *E. coli* found within gut tissues in Crohn's disease and colon cancer, the characteristics responsible for their ability to adhere to and invade these tissues have been recently investigated (Prorok-Hamon *et al*., 2014). Increased presence of *E. coli* correlated with increased adherence to and invasion of intestinal epithelial cells, as well as increased VEGF expression known to

aid angiogenesis and, therefore, development and progression of cancer. As mentioned earlier, colonic mucosal *E. coli* from IBD and CRC patients more commonly express the pks pathogenicity island responsible for the formation of colibactin (Prorok-Hamon *et al*., 2014, Arthur *et al*., 2012). The presence of the *pks* pathogenicity island likely contributes to CRC development, but is unlikely to be the sole determinant, and adherence and invasion characteristics may contribute to carcinogenesis.

To reduce the inflammatory effects of *E. coli* within the gut mucosa it would beneficial to be able to remove or kill these bacteria. However, mucosa-associated AIEC have been shown to be resistant to killing by mucosal macrophages, which has shown to be important in disease pathogenesis (Tawfik *et al*., 2014) and virulence, adherence and invasive factors associated with mucosa-associated *E. coli* are believed to be responsible. Further investigation to identify and characterise virulence, adherence and invasive factors supporting mucosa-associated *E. coli* survival could give insights into novel and targeted AIEC treatments (Tawfik *et al*., 2014).

9.4 Mucosa-associated *E. coli* increase Wnt signalling similar to other pathogenic bacteria

Disrupted Wnt signalling is currently considered as a major risk factor for colorectal cancer, but it is not the only contributor or requirement for tumour initiation and progression (Coste *et al*., 2007). Many studies have since focused on epigenetic changes in colorectal cancer and how environmental factors such as diet can influence colorectal cancer via changes in gene-expression. Evaluation of mucosa-associated *E. coli* in this study has revealed further links between bacteria and Wnt signalling. An interruption of normal Wnt signalling has previously been confirmed following *H. pylori* infection, with β-catenin identified as a specific host molecule influencing gastric carcinogenesis in conjunction with *H. pylori* infection (Polk and Peek, 2010). Nuclear accumulation of β-catenin has been shown to be increased in gastric adenomas compared with non-transformed gastric mucosa, which suggests that irregular Wnt-signalling precedes the development of gastric cancer. Increased Wnt signalling has also been identified in intestinal cells following infection with *S. typhimurium* (Liu *et al*., 2010).

Important mechanisms by which bacterial agents may induce carcinogenesis include chronic infection, immune evasion and immune suppression. Bacterial infections can induce the release of cytokines such as reactive oxygen species, interleukins and cyclooxygenases from inflammatory cells, which can contribute to carcinogenic and mutagenic changes. Chronic stimulation of these substances has been shown to contribute to carcinogenesis (Mager, 2006). With a substantial body of evidence supporting the role of bacteria, particularly *E. coli*, in inflammation and intestinal disease, the inclusion of standard IBD and cancer therapies based on bacterial infections seems almost inevitable.

9.5 Potential future impact on CRC treatment

9.5.1 The need for novel and personalised CRC treatment

The next step forward for adjuvant therapy for CRC is treatment focussed on smaller patient groups and individualised therapies using a more translational approach where diagnosis and treatment regimens take into account novel molecular staging as well as traditional pathological and clinical staging. Our understanding of the underlying molecular biology of CRC is leading to the development of novel and better-targeted therapies. Antibodies against the vascular endothelial growth factor (VEGF) such as bevacizumab, and anti-EGFR antibodies such as cetuximab and panitumumab are now being successfully investigated as adjuvant therapies (Arnold and Schmoll, 2005, Van Cutsem *et al*., 2009b). Treatments using non-steroidal anti-inflammatory drugs (NSAIDs) such as sulindac are now considered for post-surgery chemoprevention. in high-risk patients (Kim *et al*., 2014) following studies in human colorectal cancer cell lines (Liggett *et al*., 2014, Williams *et al*., 1999a, Flis and Splwinski, 2009) and *in vivo* models (Chiu *et al*., 1997).

An early study helped to identify adenomas as the starting point for most colorectal carcinomas, outlined some common genetic alterations and loss of functions at various stages of cancer development (Vogelstein *et al*., 1988). The 'Big Bang' model now suggests that colorectal tumours grow predominantly as a single expansion populated by numerous intermixed sub-clones, with

alterations arising early during growth and increasing numbers of mutations and gene copy numbers over time. This model allows a quantitative framework to interpret tumour growth dynamics and predict early malignant potential with significant clinical implications (Sottoriva *et al*., 2015). With compounding mutations found in both primary and advanced CRC and differences in mutation sequences in different forms and stages of CRC (Rhodes and Campbell, 2002), there is a severe lack of effective treatments, which highlights the need for more innovative approaches for diagnosis and therapy.

Specific features and molecular/genetic markers are becoming more of a focus due to our improved understanding of the molecular biology of CRC, and it is hoped this will obtain maximal benefit for each therapeutic option available to smaller patient groups and individualised therapies in the future. The main area of therapeutic potential is arguably to target common changes in molecular biology seen in colorectal cancers. The impact of mucosa-associated *E. coli* on cancer-associated signalling warrants attention as a therapeutic target.

9.5.2 Targeting mucosa-associated *E. coli* in colorectal disease

One particular focus has been on antibiotic treatment of mucosa-associated *E. coli*. There is evidence of metronidazole with azathioprine and ornidazole treatment as prophylaxis limiting the postoperative recurrence of Crohn's disease, which could be beneficial in preventing disease progression into CRC (D'Haens *et al*., 2008, Rutgeerts *et al*., 2005). Quinolone-based antibiotic regimens have also been effective in targeting intra-macrophage *E. coli* isolates *in vitro* (Subramanian *et al*., 2008), and antibiotic combination therapies such as ciprofloxacin, tetracycline, and trimethoprim could prove clinically relevant and reduce the risk of drug resistance, a problem that has been previously highlighted using mucosa-associated *E. coli* isolates from CD patients (Dogan *et al*., 2013). Nitroimidazole compounds have shown efficacy in Crohn's disease, decreasing recurrence rates in operated patients. However, one major problem has been the appearance of adverse systemic effects limiting the long-term use of antibiotics as a preventative Crohn's disease therapy. Rifaximin,

a semi-synthetic derivative of rifamycin, has given some promising results in inducing remission of CD with an excellent safety profile (Scribano and Prantera, 2013).

9.5.3 Targeting inflammatory cyclooxygenases and prostaglandin production

Studies suggest that targeting prostaglandin production can reduce the incidence of colorectal adenomas, colorectal cancer, and deaths from colorectal cancer. Recent results are now being used to help explain the beneficial effects of non-steroidal anti-inflammatory drugs (NSAIDs) in animal models and human disease. With bacterial infections causing increased cyclooxygenase/prostaglandin production, such as those modelled in this study with mucosa-associated *E. coli*, the impact of infections in CRC could be minimised by preventing inflammatory signalling.

Long-term intake of compounds inhibiting cyclooxygenases has been shown to reduce the overall relative risk for developing colorectal cancer (Gupta and Dubois, 2001), with selective COX-2 inhibitors now approved for use as therapy in patients with familial polyposis (Brown and DuBois, 2005). Animal and human studies suggest that regular use of aspirin may also decrease the risk of colorectal adenomas, the precursors to most colorectal cancers (Baron *et al*., 2003). Daily use of aspirin is associated with significant reduction in the incidence of colorectal adenomas in patients with previous colorectal cancer (Sandler *et al*., 2003).

Another method of reducing the downstream effects of prostaglandins would be to limit interactions with receptors. The predominant prostaglandin species in benign and malignant colorectal tumours is PGE_2, which is known to acts via four EP receptors, termed EP1 to EP4 (Hull *et al*., 2004). EP receptors have been identified as potential targets for prevention of a variety of cancers, including skin (Rundhaug *et al*., 2011), breast (Reader *et al*., 2011) and non-small cell lung cancer (NSCLC) (Gray *et al*., 2009). Signalling through EP receptors has been linked to several cancer signalling pathways. EP2 receptor activation leads to GSK-3 phosphorylation, and subsequent inactivation (Fang *et al*., 2000), which has been linked to increased β-catenin/TCF transcriptional activity.

The importance of the prostaglandin synthesis pathway and in particular the rate-limiting step involving cyclooxygenases in colorectal carcinogenesis is important in the development of novel colorectal cancer therapies aimed at bacterial infection. Sustained use of other NSAIDs such as celecoxib could permit increased surveillance intervals in the expectation of reduced risks of colorectal cancer (Baron *et al*., 2006). However, the potential toxicities of non-aspirin NSAIDs would need to be weighed against their benefits in the context of the risk reduction already provided by periodic surveillance colonoscopy and polypectomy, meaning that even proven efficacy of these drugs would not automatically justify their wide use for chemoprevention (Baron *et al*., 2006).

Prostaglandin production is fast becoming a key focus in CRC diagnosis and treatment. Increased expression of COX-2 leads to an increase in prostaglandin E2 (PGE2) production, promoting cancer cell growth via EP2 receptor-mediated signalling (Castellone *et al*., 2005). COX-2 targeted inhibition using NSAIDs such as aspirin reduces CRC incidence and improves clinical outcome following CRC surgery (Tougeron *et al*., 2014), and may be beneficial in reducing the downstream effects of mucosa-associated *E. coli* infection.

9.5.4 Targeted inhibition of canonical Wnt signalling

Since Wnt signalling results in diverse downstream intracellular events including proliferation, invasion and angiogenesis, targeted inhibition of Wnt/beta-catenin signalling would be a rational new approach for CRC therapy (Qi and Zhu, 2008). The added implications of mucosa-associated *E. coli* and several other bacteria inducing Wnt signalling mean that Wnt targeted therapies could reduce the burden brought about by pathogenic bacteria.

There has been an increase in interest in developing therapeutics targeting Wnt-mediated transcription and inactivating Wnt target genes (McDonald and Silver, 2011). Destruxin B (DB) isolated from fungus (*Metarhizium anisopliae*) has been identified for pre-clinical evaluation as a Wnt signalling target suppressing progression of colorectal cancer. It has been shown to suppress the proliferation of and induced cell cycle arrest in HT29, SW480 and HCT116 cells (Yeh *et al*., 2012) causing down-

regulation of β-catenin/Tcf4 transcriptional activity leading to decreased expression of target genes and inducing apoptosis in HT29 cells. DB-treated mice consistently demonstrated suppressed β-catenin expression and increased caspase-3 expression, supports destruxin B as an inhibitor of Wnt pathway that may be beneficial in CRC treatment (Yeh *et al*., 2012).

An extensive review of small molecule inhibitors reveals the importance of targeting Wnt signalling in the future of cancer treatment. A number of compounds are able to inhibit Wnt signalling, such as sulindac targeting the Wnt protein Dishevelled, bosutinib targeting Src kinase, ethacrynic acid derivatives targeting Lef-1 and a number of compounds targeting β-catenin directly (Voronkov and Krauss, 2013). The leucine-rich repeat-containing G protein-coupled receptor 5 (LGR5) has also been identified as a surface marker of colorectal cancer stem cells. LGR5 expression is known to be frequently elevated in human CRC, which has been demonstrated to be associated with CRC initiation and progression, and recent findings suggest that LGR5 plays a vital role in CRC pathogenesis and has the potential to serve as a diagnostic marker and a therapeutic target for CRC patients (Hsu *et al*., 2014). Targeting individual components of the Wnt pathway could be one way of eliminating the impact of *E. coli*-induced Wnt signalling in CRC. However, as Wnt signalling through β-catenin is required for homeostasis and regeneration of the adult intestinal epithelium, therapeutic targeting of this pathway could be challenging (Phesse *et al*., 2014).

Advancements in targeting ligand/receptor interactions in Wnt signalling have also shown promise in colorectal cancer. Frizzled 7 (FZD_7) is a Wnt receptor commonly up-regulated in a variety of cancers, including colorectal cancer, and has been targeted using small molecule inhibitors and antibodies. Secreted Frizzled-related proteins (sFRPs) have also been in focus as targets for cancer therapy, with peptide fragments of Wnt ligands binding FZD receptors also proposed as potential therapeutic agents (Zhang and Hao, 2015, Blagodatski *et al*., 2014). However, it has been stated that further clinical studies of these therapeutic agents targeting ligand/receptor interactions are required to confirm their safety in patients (Zhang and Hao, 2015).

9.5.5 Targeting downstream of Wnt signalling

As described in chapter 5, the expression of a number of other downstream Wnt targets were found to be increased. For example, the expression of VEGF was found to be increased consistently across both SW480 and DLD-1 cell lines. By targeting downstream of Wnt signalling, this would likely be a last resort therapy. However, with some already established treatment currently in clinical trials for this is a possibility.

Antibodies against VEGF protein are now being successfully investigated in advanced and metastatic colorectal cancer trials as adjuvant therapies, and with VEGF being induced by *E. coli* invasion in epithelial cells (Prorok-Hamon *et al*., 2014) this could reduce the impact of bacteria-induced CRC pathogenesis. Both VEGF and microvessel density (MVD) have been associated with greater incidence of CRC metastases and decreased survival. Meta-analysis was performed on twenty studies focussing on VEGF and MVD. Increased levels of VEGF were associated with unfavourable survival, with a 4-fold increase in the rate of distant metastases. Similar analysis on studies for MVD showed that patients with high MVD expression in tumours again had poorer overall survival and disease prognosis. Results from this study demonstrate a strong indication of using VEGF and MVD as future prognostic biomarkers for CRC patients (Wang *et al*., 2014).

Increased VEGF expression has recently been associated with the presence of the afimbrial adhesin operon in mucosa-associated *E. coli* in CD and colon cancer, correlating with diffuse adherence to and invasion of intestinal epithelial cells (Prorok-Hamon *et al*., 2014). The specific identification of VEGF expression in this case also supports the inclusion of VEGF as a future biomarker and a potential target for reducing the effects of mucosa-associated *E. coli* in CD and colon cancer.

9.5.6 Enhancing the defences of the intestinal epithelium

An important part of the host-bacterial interactions is the limit of interactions between the two, so it is then important that the intestinal microbiota is kept at a distance from intestinal epithelial cells to

minimise the likelihood of bacterial invasion (Brown *et al*., 2013). Innate immune strategies are in place to keep much of the microbial community within the lumen of the intestinal tract and limit invasion of pathogenic bacteria. Specialised functional cells such as goblet cells are responsible for the production of mucins and Paneth cells producing bactericidal compounds help protect the epithelial barrier from commensal and pathogenic bacteria. The mucus layer, antimicrobial peptides (AMPs) and innate lymphoid cells (ILCs) functioning together help to avoid bacterial invasion whilst promoting mutualistic interactions. Microbial signals can also induce the production of interleukins such as IL-22, and immunoglobulins such as IgA to aid in barrier function (Brown *et al*., 2013).

Where obesity, excessive alcohol consumption and high-calorie diets can promote cancer, there is evidence indicating that di*et al*so be used a form of preventative therapy. Foods containing folates, selenium, vitamin D, dietary fibre, garlic, milk, calcium, spices, vegetables, and fruits are now known to be protective against CRC (Aggarwal *et al*., 2013). Numerous natural agents termed 'nutraceuticals' have potential to both prevent and treat CRC. Evidence suggests that food-based compounds could be used to suppress growth of CRC. Use in cell culture and animal models has given insights into modulation of multiple targets, including transcription factors, growth factors, inflammatory pathways, invasion and angiogenesis (Aggarwal *et al*., 2013).

Bacterial adherence to intestinal epithelial cells can be inhibited using complex oligosaccharides such as those present in bovine submaxillary mucin and soluble edible plant fibres (Martin *et al*., 2004), which therefore have therapeutic potential. Elevated risk of colon cancer has been associated with the suppression of microbial fermentation and butyrate production, as butyrate provides fuel for the mucosa and is anti-inflammatory and anti-proliferative (Greer and O'Keefe, 2011). A significant reduction of butyrate-producing bacteria was found in the gut microbiota of CRC patients, and the subsequent increase of opportunistic pathogens was suggested to constitute a major structural imbalance of gut microbiota in CRC patients (Wang *et al*., 2012b).

Dietary fibres have been shown to produce butyrate by fermentation in the colon. Like other short-chain fatty acids, such as propionate, butyrate has anti-cancer properties against colorectal cancer cells. Soluble plant fibres have been extensively studied using *in vitro* and *ex vivo* human intestinal mucosa and animal models. Plantain bananas in particular are able to block the adherence of *E. coli* to gut epithelial cells and block translocation across cultured M cells and Peyer's patches (Roberts *et al*., 2010, Roberts *et al*., 2013). This effect has since been termed 'contrabiotic' to distinguish it from the prebiotic effects of dietary fibres. Clinical trials are now beginning to test natural food-based agents for efficacy in human disease, and due to their relative safety and affordability in comparison to pharmaceutical drugs, this could provide a novel opportunity for early treatment and even help prevent human CRC. The major nutraceuticals and functional foods used to modulate the composition of intestinal microbiota are represented by prebiotics, probiotics, polyunsaturated fatty acids, amino acids and polyphenols (Magrone and Jirillo, 2013). The cellular and molecular effects of these natural products in terms of modulation of the intestinal microbiota and mostly attenuation of the inflammatory pathway should not be overlooked in CRC treatment.

There is now a consistent and convincing body of evidence supporting the protective role of dietary fibre against colorectal cancer (Norat *et al*., 2014). CRC prevention methods now include a fibre-rich and meat products poor diet (Perez-Cueto and Verbeke, 2012). With soluble plantain fibres blocking the adhesion of intestinal bacteria such as *E. coli* to the intestinal mucosa and preventing M-cell translocation of intestinal pathogens (Roberts *et al*., 2013), this could represent an important novel mechanism by which soluble dietary fibres can promote intestinal health. Dietary fibre taken from the medicinal plant *Plantago ovato* was used in a study to treat patients resected for colorectal cancer (Nordgaard *et al*., 1996). Following increased intake of *Plantago ovato* dietary fibre, the colonic flora was adapted to increase the production of butyrate and increased faecal concentrations of butyrate in patients resected for colonic cancer.

Flavonoids such as isorhamnetin have been shown to aid prevention of CRC. Tumorigenesis studies using an inbred FVB/N strain of mice treated with the chemical carcinogen azoxymethane and

subsequently exposed to colonic irritant dextran sodium sulphate (DSS) showed dietary isorhamnetin decreases mortality, tumour number and tumour burden (Saud *et al*., 2013). An interesting finding in this study was the reduction of DSS-induced inflammation, as well as inhibition of AOM/DSS–induced oncogenic c-Src activation and β-catenin nuclear translocation. These observations suggest the chemoprotective effects of isorhamnetin in colon cancer are linked to its anti-inflammatory activities and an inhibition of oncogenic Src activity and Wnt signalling (Saud *et al*., 2013).

Vitamin D supplementation also enhances killing of intracellular AIEC in both murine and human macrophages, where it stimulates immune response via cellular production of antimicrobial peptides and defensins, making it a good supplement for Crohn's disease patients. A significant reduction in risk of requiring surgery was seen for vitamin D deficient Crohn's disease patients who normalised their vitamin D levels with supplementation (Ananthakrishnan *et al*., 2013), which could help to reduce IBD-associated CRC cases in particular.

Adherent and invasive *E. coli* adhesion is believed to be dependent, at least in part, on expression of type 1 pili on the bacterial surface and carcinoembryonic antigen-related cell adhesion molecule 6 (CEACAM6) glycoprotein on the apical surface of intestinal epithelial cells (Barnich *et al*., 2007). With both CEACAM5 and CEACAM6 overexpressed in many cancers associated with adhesion and invasion, it has been identified as a therapeutic target. Monoclonal antibodies have been evaluated in migration, invasion and adhesion assays *in vitro* using a panel of human pancreatic, breast, and colonic cancer cell lines, and in an *in vivo* model for human colonic micrometastasis (Blumenthal *et al*., 2005). These antibodies were effective at inhibiting cell migration, invasion and cell penetration through an extracellular matrix (ECM). Antibodies and/or inhibitors targeting either CEACAM5 or CEACAM6 could reduce cell migration, cell invasion, and cell adhesion, and have anti-metastatic effects. Targeting CEACAM6 to reduce the influence of bacterial invasion on colorectal carcinogenesis warrants further investigation as a novel therapeutic target.

With adverse systemic effects limiting the long-term use of antibiotics as a preventative therapy, it would be beneficial to consider targeting the effects of bacterial interactions and limiting interactions of mucosa-associated *E. coli* with the gut mucosa. As mucosa-associated *E. coli* produce an array of effects associated with both inflammatory and cancer pathways, it may be difficult to show successful treatment by targeting only one of these mechanisms, meaning combination therapies could be a reasonable future approach.

9.5.7 Targeting the effects of mucosa-associated *E. coli* infections using immunotherapy

Immunotherapy is becoming an increasing focus in cancer treatment, and is beginning to be targeted in other diseases such as diabetes and infectious diseases. Immunotherapy is used to focus the immune response towards particular antigens presented on the surface of specific cells, such as tumour cells or infected cells. Increased antigen presentation by these cells can mean a more targeted effect at these cells, limiting adverse effects.

Immune responses typically involve signalling between T cells and antigen presenting cells (APCs) and between B cells and T cells. Other accessory signals are necessary, such as the secretion of cytokines functioning to further enhance, modify, and skew the responding effector cells. T-cell priming and B-cell activation can occur in absence of CD40 signals, but many cellular and immune functions are defective in the absence of this interaction, showing the importance of this ligand/receptor pair in the development of adaptive immunity (Elgueta *et al*., 2009).

Macrophages are considered the key type of APC involved in fighting bacterial infections, with phagocytosis and destruction of bacteria and presentation of bacteria-derived antigens to T cells. However, dendritic cells (DCs) are also capable of phagocytosing particulate antigens, including bacteria, so DCs may also be important in initiating an immune response to these mucosa-associated *E. coli* infections. Studies have shown stimulation of immune responses by *E. coli* and *Salmonella* typhi, with T cell stimulation also shown *in vivo*. These cells are normally able to process *E. coli* and *Salmonella* typhi for antigen presentation on the major histocompatibility complex (MHC), which is

involved in the control of the adaptive immune response. Data shows that these infections can up-regulate MHC expression, as well as several co-stimulatory molecules and secretion of cytokines. DCs are now believed to contribute to the immune response to *Salmonella* infections (Yrlid *et al*., 2000). With mucosa-associated *E. coli* able to survive within macrophages, it may be possible to try to improve the immune response to these bacteria by stimulating DC responses.

Antigen processing and recognition is a key feature of antibacterial immune responses to intracellular bacteria, with both conventional and unconventional T cells known to participate in antibacterial protection. We are now beginning to understand the broad spectrum of antigen recognition and stimulation of distinct T-cell populations that recognize proteins, lipids and carbohydrates from bacterial pathogens to strengthen protective immunity (Kaufmann and Schaible, 2005). Pathogens able to exploit antigen presentation may be able to evade immune responses, but so far few mechanisms for this have been described in bacterial infections. A new focus on the recognition of bacterial infections, particularly for those capable of surviving and replicating within immune cells, may help to improve natural immune responses to infection before chronic inflammation is able to affect cancer development.

Another important factor could be the role of bacterial DNA in modulating responses from epithelial and antigen-presenting cells. One study has shown *in vitro* and *in vivo* treatment with bacterial DNA from *Bifidobacterium breve* and *Salmonella enterica* can enhance the secretion of cytokines from epithelial cells and underlying APCs, as well as inducing cytokine secretion from T cells (Campeau *et al*., 2012). If the bacterial DNA is able to induce a cytokine response in these cells, it is possible that certain genes or virulence factors could be found and targeted, either by immunotherapy or a more directly targeted drug therapy.

In conclusion, if mucosa-associated *E. coli* can survive and replicate within epithelial and macrophage cell within the gut mucosa, it seems feasible to try to target these infected cells. As infection of various cells with different bacteria has been shown to alter antigen presentation, improved targeting of the

immune response towards antigens presented by infected epithelial cells could limit the cancer-related impact of chronic infections. Immunotherapies using the same antigens to activate a targeted response from T and B cells could help to reduce the impact of these infections, and may be worth investigating.

9.6 Implications for future investigation

While data obtained from our study points towards a clear impact of mucosa-associated *E. coli* infections on inflammatory COX-2 signalling and cancer-related Wnt signalling, further investigation is required. The impact of a number of factors involved in our *in vitro* and *in vivo* work could be improved with more data from additional sources.

SW480 and DLD-1 cells were selected for use throughout our study, both of which are known to have high basal levels of Wnt signalling (Yang *et al*., 2006). Whilst high basal levels of Wnt signalling makes these cell lines a useful model for this study, larger increases in Wnt signalling could be masked in comparison to other CRC cell lines such as HT-29. There is potential for mucosa-associated *E. coli* isolates to have a similar impact in intestinal epithelial cells with lower levels of basal Wnt activity and those earlier in the intestinal adenoma-carcinoma sequence. Our current *in vitro* data has focussed predominantly on the impact of mucosa-associated *E. coli* infections of CRC cell lines. Use of cell lines earlier in the the adenoma-carcinoma sequence, such as the early-stage adenoma PC/AA and later-stage adenoma AA/C1 cell lines (Williams *et al*., 1990, Paraskeva *et al*., 1992) in monolayer infection studies would allow further insight into the impact of mucosa-associated *E. coli* infections on COX-2 and β-catenin gene and protein expression earlier in the adenoma-carcinoma sequence. Our results demonstrating that Wnt pathway activation by mucosa-associated *E. coli* can be attenuated with the use of COX inhibitors such as diclofenac could also be of high scientific interest, and warrants further investigation.

We have shown significant increases in intestinal tissue expression of both COX-2 and β-catenin protein, with the latter showing increased levels of nuclear localisation following mono-association of

germ-free *Il10*$^{-/-}$ mice with CRC mucosa-associated *E. coli* isolate HM44. It has been reported that germ-free *Il10*$^{-/-}$ mice nor *Il10*$^{-/-}$ mice colonized with pure cultures of non-pathogenic *E. coli*, as well as other bacteria such as a *Bifidobacterium* spp. and a *Bacillus* spp. developed colitis did not develop colitis, dysplasia or carcinoma (Balish and Warner, 2002). It would therefore be beneficial to investigate changes in COX-2 and β-catenin protein expression following mono-association of the same germ-free *Il10*$^{-/-}$ mice used in our study with other mucosa-associate *E. coli* as well as non-pathogenic *E. coli* K12, to confirm the effect is specific to mucosa-associated *E. coli*.

The IHC Profiler was used in our study to achieve a final HSCORE value to quantify expression of both COX-2 and β-catenin protein. As this method is typically used for scoring protein targets with cytoplasmic and/or nuclear expression (Varghese *et al.*, 2014), it was deemed suitable for scoring total epithelial levels of COX-2 and β-catenin expression. If such a tissue scoring technique was to be utilised as a marker for COX-2 or β-catenin in future studies, it would benefit from a comparison to an established scoring system using tissue pathology. One such system has been developed for visual analogue scoring in order to quantifying IHC staining, and has been used to compare untreated and *H. felis*-infected C57BL/6 mice (Duckworth *et al.*, 2015). This would enable the experimenter to further confirm the suitability of the automated scoring technique. In order to further minimise the risk of bias with more valuable tissue, for example limited biopsy tissue being used to determine CRC cancer risk, it would be beneficial to introduce an image blinding system, where the person evaluating the staining intensity of each image was blinded as to the origin of the tissue.

It remains clear that more works is yet to be done to test the suitability and compatibility of different CRC cell lines for 3D culture using the RCCS, with micro-carrier beads as well as in co-cultures with other supportive cells, such as human fibroblasts and stromal cells. With a fully validated culture procedure, we would then have an efficient and reliable culture platform available for use in future studies. In chapter 8, we show changes in COX-2 and β-catenin gene expression. However, we would benefit from showing the impact of these infections on protein expression, as well as nuclear translocation. We would also benefit from data using cells at an earlier stage of the adenoma-

carcinoma sequence in the RCCS, as well as regular colonic cells with no disease association to model the impact of these bacteria throughout the development and progression of colonic disease.

Following initial results from sequencing the fosmids confirmed to up-regulate COX-2 gene expression, it would be interesting to look into the genes/operons shared by fosmid clones up-regulating COX-2 gene expression more closely. Once key genes/operons have been identified, it would be useful to screen all clones for the presence of this operon. Similar to the Prorok-Hamon *et al*. (2014) study, where sequence analysis of *E. coli* HM358 and haemagglutination-positive fosmid clones revealed afa-1 as an adhesion and invasion factor (Prorok-Hamon *et al*., 2014), further investigation may confirm the presence of existing and/or novel genes/operons involved in the adhesion and invasion of mucosa-associated *E. coli* and subsequent impact of increased COX-2 and Wnt signalling.

Our study has focussed on the impact of mucosa-associated *E. coli* infections on COX-2 and Wnt signalling due to existing links between these *E. coli* strains and gut infections (Martin *et al*., 2004, Darfeuille-Michaud *et al*., 1998), and links between inflammatory signalling and Wnt signalling (Castellone *et al*., 2005). However, other signalling pathways are likely to be involved in disease pathogenesis implicated with mucosa-associated *E. coli* infections. Chronic inflammatory signalling as a result of tissue damage and/or infection is often implicated in altering key cancer signalling pathways. One example of this is chronic TNF-α and COX-2 release mediating response via NF-κB signalling (Paik *et al*., 2002, Lawrence, 2009). Activation of the canonical NF-κB pathway in response to inflammatory cytokines has shown to be important in the pathogenesis of chronic inflammatory diseases such as rheumatoid arthritis and IBD (Tak and Firestein, 2001). The NF-κB pathway is also believed to be important in intestinal innate immunity within intestinal epithelial cells and underlying macrophages rapidly available to keep potential pathogens under control, as well as in maintaining mucosal homeostasis (Jarry *et al*., 2014). NF-κB is known to be involved in the increased expression of many genes of inflammatory and immune responses and can be upregulated in response to microorganisms and lipopolysaccharides and is considered a crucial factor in maintaining chronic inflammation (La Ferla *et al*., 2004). Normally, NF-κB-containing complexes are sequestered in the

cytosol in inactive form due to their association with inhibitory proteins. Activation of the canonical pathway causes nuclear translocation of NF-κB (Scheidereit, 2006) where it induces target gene transcription including pro-inflammatory cytokines such as TNF-α (Jarry *et al*., 2014).

Activation of NF-κB has also been demonstrated *in situ* in macrophages and in intestinal epithelial cells in the inflamed mucosa from IBD patients (Rogler *et al*., 1998). With the activation of NF-κB seen in enterocytes in response to various *E. coli*, its role in the response of intestinal epithelial cells to bacterial infections, particularly *E. coli*, could be crucial (Savkovic *et al*., 1997, Elewaut *et al*., 1999). Increased TNF-α promoter activity in cells stimulated with bacterial isolates from IBD patients suggests TNF-α plays an important role in inflammation caused by *E. coli* strains associated with inflammatory disease (La Ferla *et al*., 2004, Wang and Hardwidge, 2012). In addition, inhibition of NF-κB in both colon and mammary carcinoma cells converts the LPS-induced growth response to LPS-induced tumour regression (Luo *et al*., 2004).

Molecular mechanisms that link bacterial infections, inflammation and cancer, indicate that certain strains of *E. coli* as a risk factor for patients with colon cancer following the acquisition of virulence factors. One of these factors is a protein toxin named cytotoxic necrotizing factor 1 (CNF1) (Travaglione *et al*., 2008), which is reported to induce a long-lasting activation of the transcription factor NF-kB and COX2 expression, as well as protect epithelial cells from apoptosis and promote cellular motility. As cancer may arise through dysfunction of similar regulatory systems, it seems likely that other *E. coli* infections associated with virulence factors could contribute to tumour development in a similar fashion.

It would also be beneficial to investigate similar effects of other pathogenic bacteria found in increased numbers in inflammatory gut conditions. Several studies implicate microbial dysbiosis in the development of colorectal adenomas and CRC (Wu *et al*., 2013, Zhu *et al*., 2014, Chen *et al*., 2012, Sobhani *et al*., 2011). Another recent study characterising the gut microbiome in healthy, adenoma,

and carcinoma patients representing various stages of colorectal cancer development has added extra weight to this theory (Zackular *et al*., 2014).

Alterations in bacterial community composition associated with adenomas may be a contributory cause of CRC, and these findings could lead to strategies to manipulate the microbiota to prevent colorectal adenomas and cancer as well as to identify individuals at high risk (Shen *et al*., 2010, Dulal and Keku, 2014). Study of the mucosa-associated microbiota has revealed changes including increases in mucosa-associated *E. coli* as well as *Fusobacterium nucleatum* (*F. nucleatum*). Infection with *F. nucleatum* is associated with colorectal cancer (CRC) and linked to adherence, invasion and induction of oncogenic and inflammatory responses to stimulate growth of CRC cells. *F. nucleatum* infection is believed to occur through its unique FadA adhesin, which has been shown to bind to E-cadherin, activating β-catenin signalling (Rubinstein *et al*., 2013). With similar traits to mucosa-associated *E. coli*, it is possible that similar virulence factors could influence Wnt signalling in a similar manner. This suggests further investigation into other similar bacteria would be beneficial, and could be key in identifying other mechanisms by which bacteria can drive Wnt signalling and CRC.

These additions to current *in vitro* and *in vivo* data could be important in identifying virulence factors and other driving forces affecting cancer-associated signalling, particularly Wnt signalling, and could be a potential diagnostic and therapeutic CRC target. Further investigation into the ability of mucosa-associated *E. coli* to activate cancer-promoting proteins within intestinal epithelial cells will improve our understanding of the potential impact of development, growth and spread of colonic tumours. Recent reports of a rate-limiting effect of gp130/Stat3 on Wnt signalling, even where β-catenin nuclear localisation is increased (Phesse *et al*., 2015), would suggest other assays confirming proliferation and migration using colorectal cells and tissue, as well as assessing cell viability and metabolism, would be beneficial in confirming increased Wnt signalling driving phenotypic changes and impacting malignant development.

9.7 Final conclusions

The aim of this project was to investigate whether specific mucosa-associated *E. coli* isolates taken from IBD and CRC patients possess ability to activate key cancer-promoting proteins within epithelial cells lining the bowel, including those known to help development, growth and spread of tumours. The main pathway under investigation was the canonical Wnt pathway signalling through β-catenin, which helps to regulate cell cycle and cell growth, whilst also playing a crucial role in colorectal tumorigenesis.

Data obtained throughout the project has pointed towards Wnt activation through β-catenin following infection of human colorectal cell-lines with mucosa-associated *E. coli* isolates taken from IBD and CRC patients. This has been shown consistently alongside increases in COX-2 signalling following infection of cell lines *in vitro* and germ-free *Il10*$^{-/-}$ mice. Importantly, these changes have not been replicated following non-pathogenic *E. coli* K12 infection, which suggests that this impact if conserved for mucosa-associated isolates. The use of a fosmid clone library has allowed us to sequence fosmid clones confirmed to up-regulate COX-2 gene expression, which leads us closer to the identification the factors that might be contributing towards these changes. We have also sought to establish a novel infection model making use of 3D cell aggregates, and have confirmed changes in COX-2 and β-catenin gene expression in mucosa-associated *E. coli* infected aggregates.

The data obtained from this project adds expands on the relationship between bacterial infection, inflammation and cancer, with a focus on mucosa-associated *E. coli* that are already shown to be more prevalent under colorectal disease conditions. This project has shown that mucosa-associated *E. coli* can increase Wnt signalling similar to other pathogenic bacteria, and that this could have future impact on CRC treatment focussed on limiting the inflammatory and cancer-promoting effects of mucosa-associated *E. coli* infection.

References

ABDALLAH HAJJ HUSSEIN, I., FREUND, J. N., REIMUND, J. M., SHAMS, A., YAMINE, M., LEONE, A. & JURJUS, A. R. 2012. Enteropathogenic e.coli sustains iodoacetamide-induced ulcerative colitis-like colitis in rats: modulation of IL-1beta, IL-6, TNF-alpha, COX-2, and apoptosisi. *J Biol Regul Homeost Agents,* 26**,** 515-26.

ACHILLI, T. M., MEYER, J. & MORGAN, J. R. 2012. Advances in the formation, use and understanding of multi-cellular spheroids. *Expert Opin Biol Ther,* 12**,** 1347-60.

AGGARWAL, B., PRASAD, S., SUNG, B., KRISHNAN, S. & GUHA, S. 2013. Prevention and Treatment of Colorectal Cancer by Natural Agents From Mother Nature. *Curr Colorectal Cancer Rep,* 9**,** 37-56.

AHMED, D., EIDE, P. W., EILERTSEN, I. A., DANIELSEN, S. A., EKNAES, M., HEKTOEN, M., LIND, G. E. & LOTHE, R. A. 2013. Epigenetic and genetic features of 24 colon cancer cell lines. *Oncogenesis,* 2**,** e71.

ALBENBERG, L. G. & WU, G. D. 2014. Diet and the intestinal microbiome: associations, functions, and implications for health and disease. *Gastroenterology,* 146**,** 1564-72.

ANANTHAKRISHNAN, A. N., CAGAN, A., GAINER, V. S., CAI, T., CHENG, S. C., SAVOVA, G., CHEN, P., SZOLOVITS, P., XIA, Z., DE JAGER, P. L., SHAW, S. Y., CHURCHILL, S., KARLSON, E. W., KOHANE, I., PLENGE, R. M., MURPHY, S. N. & LIAO, K. P. 2013. Normalization of plasma 25-hydroxy vitamin D is associated with reduced risk of surgery in Crohn's disease. *Inflamm Bowel Dis,* 19**,** 1921-7.

ANDERSON, E. C. & WONG, M. H. 2010. Caught in the Akt: regulation of Wnt signaling in the intestine. *Gastroenterology,* 139**,** 718-22.

ANDERSON, G. D., HAUSER, S. D., MCGARITY, K. L., BREMER, M. E., ISAKSON, P. C. & GREGORY, S. A. 1996. Selective inhibition of cyclooxygenase (COX)-2 reverses inflammation and expression of COX-2 and interleukin 6 in rat adjuvant arthritis. *J Clin Invest,* 97**,** 2672-9.

ANTIPOV, D., HARTWICK, N., SHEN, M., RAIKO, M., LAPIDUS, A. & PEVZNER, P. A. 2016. plasmidSPAdes: assembling plasmids from whole genome sequencing data. *Bioinformatics,* 32**,** 3380-3387.

ARMAGHANY, T., WILSON, J. D., CHU, Q. & MILLS, G. 2012. Genetic alterations in colorectal cancer. *Gastrointest Cancer Res,* 5**,** 19-27.

ARNOLD, D. & SCHMOLL, H. J. 2005. (Neo-)adjuvant treatments in colorectal cancer. *Ann Oncol,* 16 Suppl 2**,** ii133-40.

ARNOLD, M., SIERRA, M. S., LAVERSANNE, M., SOERJOMATARAM, I., JEMAL, A. & BRAY, F. 2017. Global patterns and trends in colorectal cancer incidence and mortality. *Gut*, 66, 683-91.

ARTHUR, J. C. & JOBIN, C. 2011. The struggle within: Microbial influences on colorectal cancer. *Inflammatory Bowel Diseases,* 17**,** 396-409 10.1002/ibd.21354.

ARTHUR, J. C., PEREZ-CHANONA, E., MÜHLBAUER, M., TOMKOVICH, S., URONIS, J. M., FAN, T.-J., CAMPBELL, B. J., ABUJAMEL, T., DOGAN, B., ROGERS, A. B., RHODES, J. M., STINTZI, A., SIMPSON, K. W., HANSEN, J. J., KEKU, T. O., FODOR, A. A. & JOBIN, C. 2012. Intestinal Inflammation Targets Cancer-Inducing Activity of the Microbiota. *Science,* 338**,** 120-123.

BACHMANN, B. J. 1972. Pedigrees of some mutant strains of Escherichia coli K-12. *Bacteriol Rev,* 36**,** 525-57.

BALISH, E. & WARNER, T. 2002. Enterococcus faecalis induces inflammatory bowel disease in interleukin-10 knockout mice. *Am J Pathol,* 160**,** 2253-7.

BALMANA, J., BALAGUER, F., CERVANTES, A., ARNOLD, D. & GROUP, E. G. W. 2013. Familial risk-colorectal cancer: ESMO Clinical Practice Guidelines. *Ann Oncol,* 24 Suppl 6**,** vi73-80.

BARBAZAN, J., VIEITO, M., ABALO, A., ALONSO-ALCONADA, L., MUINELO-ROMAY, L., ALONSO-NOCELO, M., LEON, L., CANDAMIO, S., GALLARDO, E., ANIDO, U., DOLL, A., DE LOS ANGELES CASARES, M., GOMEZ-TATO, A., ABAL, M. & LOPEZ-LOPEZ, R. 2012. A logistic model for the detection of circulating tumour cells in human metastatic colorectal cancer. *J Cell Mol Med,* 16**,** 2342-9.

BARNICH, N., CARVALHO, F. A., GLASSER, A. L., DARCHA, C., JANTSCHEFF, P., ALLEZ, M., PEETERS, H., BOMMELAER, G., DESREUMAUX, P., COLOMBEL, J. F. & DARFEUILLE-MICHAUD, A. 2007. CEACAM6 acts as a receptor for adherent-invasive *E. coli*, supporting ileal mucosa colonization in Crohn disease. *J Clin Invest,* 117**,** 1566-74.

BARON, J. A., COLE, B. F., SANDLER, R. S., HAILE, R. W., AHNEN, D., BRESALIER, R., MCKEOWN-EYSSEN, G., SUMMERS, R. W., ROTHSTEIN, R., BURKE, C. A., SNOVER, D. C., CHURCH, T. R., ALLEN, J. I., BEACH, M., BECK, G. J., BOND, J. H., BYERS, T., GREENBERG, E. R., MANDEL, J. S., MARCON, N., MOTT, L. A., PEARSON, L., SAIBIL, F. & VAN STOLK, R. U. 2003. A randomized trial of aspirin to prevent colorectal adenomas. *N Engl J Med,* 348**,** 891-9.

BARON, J. A., SANDLER, R. S., BRESALIER, R. S., QUAN, H., RIDDELL, R., LANAS, A., BOLOGNESE, J. A., OXENIUS, B., HORGAN, K., LOFTUS, S., MORTON, D. G. & INVESTIGATORS, A. P. T. 2006. A randomized trial of rofecoxib for the chemoprevention of colorectal adenomas. *Gastroenterology,* 131**,** 1674-82.

BARRILA, J., RADTKE, A. L., CRABBE, A., SARKER, S. F., HERBST-KRALOVETZ, M. M., OTT, C. M. & NICKERSON, C. A. 2010. Organotypic 3D cell culture models: using the rotating wall vessel to study host-pathogen interactions. *Nat Rev Microbiol,* 8**,** 791-801.

BARTCHEWSKY, W., JR., MARTINI, M. R., MASIERO, M., SQUASSONI, A. C., ALVAREZ, M. C., LADEIRA, M. S., SALVATORE, D., TREVISAN, M., PEDRAZZOLI, J., JR. & RIBEIRO, M. L. 2009. Effect of Helicobacter pylori infection on IL-8, IL-1beta and COX-2 expression in patients with chronic gastritis and gastric cancer. *Scand J Gastroenterol,* 44**,** 153-61.

BAUER, T. W. & SPITZ, F. R. 1998. Adjuvant and neoadjuvant chemoradiation therapy for primary colorectal cancer. *Surg Oncol,* 7**,** 175-81.

BEHRENS, J., VON KRIES, J. P., KUHL, M., BRUHN, L., WEDLICH, D., GROSSCHEDL, R. & BIRCHMEIER, W. 1996. Functional interaction of beta-catenin with the transcription factor LEF-1. *Nature,* 382**,** 638-42.

BELLAMY, C. O., MALCOMSON, R. D., HARRISON, D. J. & WYLLIE, A. H. 1995. Cell death in health and disease: the biology and regulation of apoptosis. *Semin Cancer Biol,* 6**,** 3-16.

BERGMANN, S. & STEINERT, M. 2015. From Single Cells to Engineered and Explanted Tissues: New Perspectives in Bacterial Infection Biology. *Int Rev Cell Mol Biol,* 319**,** 1-44.

BERSCHNEIDER, B. & KONIGSHOFF, M. 2011. WNT1 inducible signaling pathway protein 1 (WISP1): a novel mediator linking development and disease. *Int J Biochem Cell Biol,* 43**,** 306-9.

BERTAGNOLLI, M. M., EAGLE, C. J., ZAUBER, A. G., REDSTON, M., SOLOMON, S. D., KIM, K., TANG, J., ROSENSTEIN, R. B., WITTES, J., CORLE, D., HESS, T. M., WOLOJ, G. M., BOISSERIE, F., ANDERSON, W. F., VINER, J. L., BAGHERI, D., BURN, J., CHUNG, D. C., DEWAR, T., FOLEY, T. R., HOFFMAN, N., MACRAE, F., PRUITT, R. E., SALTZMAN, J. R., SALZBERG, B., SYLWESTROWICZ, T., GORDON, G. B., HAWK, E. T. & INVESTIGATORS, A. P. C. S. 2006. Celecoxib for the prevention of sporadic colorectal adenomas. *N Engl J Med,* 355**,** 873-84.

BIENZ, M. & CLEVERS, H. 2000. Linking colorectal cancer to Wnt signaling. *Cell,* 103**,** 311-20.

BLAGODATSKI, A., POTERYAEV, D. & KATANAEV, V. L. 2015. Targeting the Wnt pathway for therapies. *Mol Cell Ther*, 2, 28.

BLUMENTHAL, R. D., HANSEN, H. J. & GOLDENBERG, D. M. 2005. Inhibition of adhesion, invasion, and metastasis by antibodies targeting CEACAM6 (NCA-90) and CEACAM5 (Carcinoembryonic Antigen). *Cancer Res,* 65**,** 8809-17.

BOLLATI, M., VILLA, R., GOURLAY, L. J., BENEDET, M., DEHO, G., POLISSI, A., BARBIROLI, A., MARTORANA, A. M., SPERANDEO, P., BOLOGNESI, M. & NARDINI, M. 2015. Crystal structure of LptH, the periplasmic component of the lipopolysaccharide transport machinery from Pseudomonas aeruginosa. *FEBS J,* 282**,** 1980-97.

BONGERS, G., PACER, M. E., GERALDINO, T. H., CHEN, L., HE, Z., HASHIMOTO, D., FURTADO, G. C., OCHANDO, J., KELLEY, K. A., CLEMENTE, J. C., MERAD, M., VAN BAKEL, H. & LIRA, S. A. 2014. Interplay of host microbiota, genetic perturbations, and inflammation promotes local development of intestinal neoplasms in mice. *J Exp Med,* 211**,** 457-72.

BOTTING, R. M. 2006. Inhibitors of cyclooxygenases: mechanisms, selectivity and uses. *J Physiol Pharmacol,* 57 Suppl 5**,** 113-24.

BRINGER, M.-A., BARNICH, N., GLASSER, A.-L., BARDOT, O. & DARFEUILLE-MICHAUD, A. 2005. HtrA Stress Protein Is Involved in Intramacrophagic Replication of Adherent and Invasive Escherichia coli Strain LF82 Isolated from a Patient with Crohn's Disease. *Infection and Immunity,* 73**,** 712-721.

BRINGER, M.-A., ROLHION, N., GLASSER, A.-L. & DARFEUILLE-MICHAUD, A. 2007. The Oxidoreductase DsbA Plays a Key Role in the Ability of the Crohn's Disease-Associated Adherent-Invasive Escherichia coli Strain LF82 To Resist Macrophage Killing. *Journal of Bacteriology,* 189**,** 4860-4871.

BROWN, E. M., SADARANGANI, M. & FINLAY, B. B. 2013. The role of the immune system in governing host-microbe interactions in the intestine. *Nat Immunol,* 14**,** 660-667.

BROWN, J. R. & DUBOIS, R. N. 2005. COX-2: a molecular target for colorectal cancer prevention. *J Clin Oncol,* 23**,** 2840-55.

BURKITT, M. D., DUCKWORTH, C. A., WILLIAMS, J. M. & PRITCHARD, D. M. 2017. *Helicobacter pylori*-induced gastric pathology: insights from in vivo and ex vivo models. *Dis Model Mech*, 10, 89-104.

BURKITT, M. D., HANEDI, A. F., DUCKWORTH, C. A., WILLIAMS, J. M., TANG, J. M., O'REILLY, L. A., PUTOCZKI, T. L., GERONDAKIS, S., DIMALINE, R., CAAMANO, J. H. & PRITCHARD, D. M. 2015. NF-kappaB1, NF-kappaB2 and c-Rel differentially regulate susceptibility to colitis-associated adenoma development in C57BL/6 mice. *J Pathol,* 236**,** 326-36.

BUTLER, W. J. & ROBERTS-THOMSON, I. C. 2004. Polymorphisms and risk for sporadic colorectal cancer. *J Gastroenterol Hepatol,* 19**,** 1215-6.

CAMPEAU, J. L., SALIM, S. Y., ALBERT, E. J., HOTTE, N. & MADSEN, K. L. 2012. Intestinal epithelial cells modulate antigen-presenting cell responses to bacterial DNA. *Infect Immun,* 80**,** 2632-44.

CANE, G., GINOUVES, A., MARCHETTI, S., BUSCA, R., POUYSSEGUR, J., BERRA, E., HOFMAN, P. & VOURET-CRAVIARI, V. 2010. HIF-1alpha mediates the induction of IL-8 and VEGF expression on infection with Afa/Dr diffusely adhering *E. coli* and promotes EMT-like behaviour. *Cell Microbiol,* 12**,** 640-53.

CANE, G., MOAL, V. L., PAGES, G., SERVIN, A. L., HOFMAN, P. & VOURET-CRAVIARI, V. 2007. Up-regulation of intestinal vascular endothelial growth factor by Afa/Dr diffusely adhering Escherichia coli. *PLoS One,* 2**,** e1359.

CARVALHO, H. M., TEEL, L. D., GOPING, G. & O'BRIEN, A. D. 2005. A three-dimensional tissue culture model for the study of attach and efface lesion formation by enteropathogenic and enterohaemorrhagic Escherichia coli. *Cell Microbiol,* 7**,** 1771-81.

CASSIDY, J., CLARKE, S., DIAZ-RUBIO, E., SCHEITHAUER, W., FIGER, A., WONG, R., KOSKI, S., RITTWEGER, K., GILBERG, F. & SALTZ, L. 2011. XELOX vs FOLFOX-4 as first-line therapy for metastatic colorectal cancer: NO16966 updated results. *Br J Cancer,* 105**,** 58-64.

CASSIDY, J., TABERNERO, J., TWELVES, C., BRUNET, R., BUTTS, C., CONROY, T., DEBRAUD, F., FIGER, A., GROSSMANN, J., SAWADA, N., SCHOFFSKI, P., SOBRERO, A., VAN CUTSEM, E. & DIAZ-RUBIO, E. 2004. XELOX (capecitabine plus oxaliplatin): active first-line therapy for patients with metastatic colorectal cancer. *J Clin Oncol,* 22**,** 2084-91.

CASTELLONE, M. D., TERAMOTO, H., WILLIAMS, B. O., DRUEY, K. M. & GUTKIND, J. S. 2005. Prostaglandin E2 promotes colon cancer cell growth through a Gs-axin-beta-catenin signaling axis. *Science,* 310**,** 1504-10.

CHASSAING, B. & DARFEUILLE–MICHAUD, A. 2011. The Commensal Microbiota and Enteropathogens in the Pathogenesis of Inflammatory Bowel Diseases. *Gastroenterology,* 140**,** 1720-1728.e3.

CHASSAING, B., ROLHION, N., VALL, XE, E, A., XE, LIE, D., SALIM, S., X, AD, Y., PROROK-HAMON, M., NEUT, C., CAMPBELL, B. J., XF, DERHOLM, J. D., HUGOT, J.-P., COLOMBEL, J.-F., XE, XE, RIC & DARFEUILLE-MICHAUD, A. 2011. Crohn disease–associated adherent-invasive *E. coli* bacteria

target mouse and human Peyer's patches via long polar fimbriae. *The Journal of Clinical Investigation,* 121**,** 966-975.
CHEN, W., LIU, F., LING, Z., TONG, X. & XIANG, C. 2012. Human intestinal lumen and mucosa-associated microbiota in patients with colorectal cancer. *PLoS One,* 7**,** e39743.
CHERVONSKY, A. V. 2010. Influence of microbial environment on autoimmunity. *Nat Immunol,* 11**,** 28-35.
CHIU, C. H., MCENTEE, M. F. & WHELAN, J. 1997. Sulindac causes rapid regression of preexisting tumors in Min/+ mice independent of prostaglandin biosynthesis. *Cancer Res,* 57**,** 4267-73.
CHO, M., GWAK, J., PARK, S., WON, J., KIM, D. E., YEA, S. S., CHA, I. J., KIM, T. K., SHIN, J. G. & OH, S. 2005. Diclofenac attenuates Wnt/beta-catenin signaling in colon cancer cells by activation of NF-kappaB. *FEBS Lett,* 579**,** 4213-8.
CHOI, P. M. & ZELIG, M. P. 1994. Similarity of colorectal cancer in Crohn's disease and ulcerative colitis: implications for carcinogenesis and prevention. *Gut,* 35**,** 950-4.
CLARKE, T. B., DAVIS, K. M., LYSENKO, E. S., ZHOU, A. Y., YU, Y. & WEISER, J. N. 2010. Recognition of peptidoglycan from the microbiota by Nod1 enhances systemic innate immunity. *Nat Med,* 16**,** 228-31.
CLEVERS, H. 2016. Modeling Development and Disease with Organoids. *Cell,* 165**,** 1586-97.
COLLIER, P. E., TUROWSKI, P. & DIAMOND, D. L. 1985. Small intestinal adenocarcinoma complicating regional enteritis. *Cancer,* 55**,** 516-21.
COMPARE, D. & NARDONE, G. 2011. Contribution of Gut Microbiota to Colonic and Extracolonic Cancer Development. *Digestive Diseases,* 29**,** 554-561.
COSTE, I., FREUND, J. N., SPADERNA, S., BRABLETZ, T. & RENNO, T. 2007. Precancerous Lesions Upon Sporadic Activation of β-Catenin in Mice. *Gastroenterology,* 132**,** 1299-1308.
COTILLARD, A., KENNEDY, S. P., KONG, L. C., PRIFTI, E., PONS, N., LE CHATELIER, E., ALMEIDA, M., QUINQUIS, B., LEVENEZ, F., GALLERON, N., GOUGIS, S., RIZKALLA, S., BATTO, J. M., RENAULT, P., CONSORTIUM, A. N. R. M., DORE, J., ZUCKER, J. D., CLEMENT, K. & EHRLICH, S. D. 2013. Dietary intervention impact on gut microbial gene richness. *Nature,* 500**,** 585-8.
COUGNOUX, A., DALMASSO, G., MARTINEZ, R., BUC, E., DELMAS, J., GIBOLD, L., SAUVANET, P., DARCHA, C., DECHELOTTE, P., BONNET, M., PEZET, D., WODRICH, H., DARFEUILLE-MICHAUD, A. & BONNET, R. 2014. Bacterial genotoxin colibactin promotes colon tumour growth by inducing a senescence-associated secretory phenotype. *Gut,* 63**,** 1932-42.
COUGNOUX, A., GIBOLD, L., ROBIN, F., DUBOIS, D., PRADEL, N., DARFEUILLE-MICHAUD, A., DALMASSO, G., DELMAS, J. & BONNET, R. 2012. Analysis of structure-function relationships in the colibactin-maturating enzyme ClbP. *J Mol Biol,* 424**,** 203-14.
COUPER, K. N., BLOUNT, D. G. & RILEY, E. M. 2008. IL-10: the master regulator of immunity to infection. *J Immunol,* 180**,** 5771-7.
CROTTI, S., PICCOLI, M., RIZZOLIO, F., GIORDANO, A., NITTI, D. & AGOSTINI, M. 2017. Extracellular Matrix and Colorectal Cancer: How Surrounding Microenvironment Affects Cancer Cell Behavior? *J Cell Physiol,* 232**,** 967-975.
CUENDET, M., MESECAR, A. D., DEWITT, D. L. & PEZZUTO, J. M. 2006. An ELISA method to measure inhibition of the COX enzymes. *Nat Protoc,* 1**,** 1915-21.
CUEVAS-RAMOS, G., PETIT, C. R., MARCQ, I., BOURY, M., OSWALD, E. & NOUGAYREDE, J. P. 2010. Escherichia coli induces DNA damage in vivo and triggers genomic instability in mammalian cells. *Proc Natl Acad Sci U S A,* 107**,** 11537-42.
D'HAENS, G. R., VERMEIRE, S., VAN ASSCHE, G., NOMAN, M., AERDEN, I., VAN OLMEN, G. & RUTGEERTS, P. 2008. Therapy of metronidazole with azathioprine to prevent postoperative recurrence of Crohn's disease: a controlled randomized trial. *Gastroenterology,* 135**,** 1123-9.
DAIGNEAULT, M., PRESTON, J. A., MARRIOTT, H. M., WHYTE, M. K. & DOCKRELL, D. H. 2010. The identification of markers of macrophage differentiation in PMA-stimulated THP-1 cells and monocyte-derived macrophages. *PLoS One,* 5**,** e8668.

DALMASSO, G., COUGNOUX, A., DELMAS, J., DARFEUILLE-MICHAUD, A. & BONNET, R. 2014. The bacterial genotoxin colibactin promotes colon tumor growth by modifying the tumor microenvironment. *Gut Microbes*, 00-00.

DANNENBERG, A. J., ALTORKI, N. K., BOYLE, J. O., DANG, C., HOWE, L. R., WEKSLER, B. B. & SUBBARAMAIAH, K. 2001. Cyclo-oxygenase 2: a pharmacological target for the prevention of cancer. *Lancet Oncol,* 2**,** 544-51.

DARFEUILLE-MICHAUD, A. & COLOMBEL, J. F. 2008. Pathogenic Escherichia coli in inflammatory bowel diseases Proceedings of the 1st International Meeting on *E. coli* and IBD, June 2007, Lille, France. *J Crohns Colitis,* 2**,** 255-62.

DARFEUILLE-MICHAUD, A., NEUT, C., BARNICH, N., LEDERMAN, E., DI MARTINO, P., DESREUMAUX, P., GAMBIEZ, L., JOLY, B., CORTOT, A. & COLOMBEL, J.-F. 1998. Presence of adherent Escherichia coli strains in ileal mucosa of patients with Crohn's disease. *Gastroenterology,* 115**,** 1405-1413.

DAVIES, S. R., DAVIES, M. L., SANDERS, A., PARR, C., TORKINGTON, J. & JIANG, W. G. 2010. Differential expression of the CCN family member WISP-1, WISP-2 and WISP-3 in human colorectal cancer and the prognostic implications. *Int J Oncol,* 36**,** 1129-36.

DE MATOS, L.L., TRUFELLI, D.C., DE MATOD, M.G.L. & PINHAL, M.A.D.S. 2010. Immunohistochemistry as an important tool in biomarker detection and clinical practice. *Biomark Insights*, 5, 9-20.

DE REUSE, H., LEVY, S., ZENG, G. & DANCHIN, A. 1989. Genetics of the PTS components in Escherichia coli K-12. *FEMS Microbiol Rev,* 5**,** 61-7.

DEXTER, D. L., SPREMULLI, E. N., FLIGIEL, Z., BARBOSA, J. A., VOGEL, R., VANVOORHEES, A. & CALABRESI, P. 1981. Heterogeneity of cancer cells from a single human colon carcinoma. *Am J Med,* 71**,** 949-56.

DIN, F. V., DUNLOP, M. G. & STARK, L. A. 2004. Evidence for colorectal cancer cell specificity of aspirin effects on NF kappa B signalling and apoptosis. *Br J Cancer,* 91**,** 381-8.

DOGAN, B., SCHERL, E., BOSWORTH, B., YANTISS, R., ALTIER, C., MCDONOUGH, P. L., JIANG, Z. D., DUPONT, H. L., GARNEAU, P., HAREL, J., RISHNIW, M. & SIMPSON, K. W. 2013. Multidrug resistance is common in Escherichia coli associated with ileal Crohn's disease. *Inflamm Bowel Dis,* 19**,** 141-50.

DUBOIS, R. N. 2014. Role of inflammation and inflammatory mediators in colorectal cancer. *Transactions of the American Clinical and Climatological Association,* 125**,** 358-373.

DUCKWORTH, C. A., ABUDERMAN, A. A., BURKITT, M. D., WILLIAMS, J. M., O'REILLY, L. A. & PRITCHARD, D. M. 2015. bak deletion stimulates gastric epithelial proliferation and enhances Helicobacter felis-induced gastric atrophy and dysplasia in mice. *Am J Physiol Gastrointest Liver Physiol,* 309**,** G420-30.

DULAL, S. & KEKU, T. O. 2014. Gut microbiome and colorectal adenomas. *Cancer J,* 20**,** 225-31.

DUNLOP, M. G., BRITISH SOCIETY FOR, G., ASSOCIATION OF COLOPROCTOLOGY FOR GREAT, B. & IRELAND 2002. Guidance on gastrointestinal surveillance for hereditary non-polyposis colorectal cancer, familial adenomatous polypolis, juvenile polyposis, and Peutz-Jeghers syndrome. *Gut,* 51 Suppl 5**,** V21-7.

DUXBURY, M. S., ITO, H., ZINNER, M. J., ASHLEY, S. W. & WHANG, E. E. 2004. CEACAM6 gene silencing impairs anoikis resistance and in vivo metastatic ability of pancreatic adenocarcinoma cells. *Oncogene,* 23**,** 465-73.

EADEN, J. A., ABRAMS, K. R. & MAYBERRY, J. F. 2001. The risk of colorectal cancer in ulcerative colitis: a meta-analysis. *Gut,* 48**,** 526-35.

EADEN, J. A., MAYBERRY, J. F., BRITISH SOCIETY FOR, G., ASSOCIATION OF COLOPROCTOLOGY FOR GREAT, B. & IRELAND 2002. Guidelines for screening and surveillance of asymptomatic colorectal cancer in patients with inflammatory bowel disease. *Gut,* 51 Suppl 5**,** V10-2.

EKBOM, A., HELMICK, C., ZACK, M. & ADAMI, H. O. 1990a. Increased risk of large-bowel cancer in Crohn's disease with colonic involvement. *Lancet,* 336**,** 357-9.

EKBOM, A., HELMICK, C., ZACK, M. & ADAMI, H. O. 1990b. Ulcerative colitis and colorectal cancer. A population-based study. *N Engl J Med,* 323**,** 1228-33.

ELEWAUT, D., DIDONATO, J. A., KIM, J. M., TRUONG, F., ECKMANN, L. & KAGNOFF, M. F. 1999. NF-kappa B is a central regulator of the intestinal epithelial cell innate immune response induced by infection with enteroinvasive bacteria. *J Immunol,* 163**,** 1457-66.

ELGUETA, R., BENSON, M. J., DE VRIES, V. C., WASIUK, A., GUO, Y. & NOELLE, R. J. 2009. Molecular mechanism and function of CD40/CD40L engagement in the immune system. *Immunol Rev,* 229**,** 152-72.

ELLIOTT, N., LEE, T., YOU, L. & YUAN, F. 2011. Proliferation behavior of *E. coli* in a three-dimensional in vitro tumor model. *Integrative Biology,* 3**,** 696-705.

ESCALANTE, A., SALINAS CERVANTES, A., GOSSET, G. & BOLIVAR, F. 2012. Current knowledge of the Escherichia coli phosphoenolpyruvate-carbohydrate phosphotransferase system: peculiarities of regulation and impact on growth and product formation. *Appl Microbiol Biotechnol,* 94**,** 1483-94.

ESCHRICH, S., YANG, I., BLOOM, G., KWONG, K. Y., BOULWARE, D., CANTOR, A., COPPOLA, D., KRUHØFFER, M., AALTONEN, L., ORNTOFT, T. F., QUACKENBUSH, J. & YEATMAN, T. J. 2005. Molecular Staging for Survival Prediction of Colorectal Cancer Patients. *Journal of Clinical Oncology,* 23**,** 3526-3535.

ESSON, D., MATHER, A. E., SCANLAN, E., GUPTA, S., DE VRIES, S. P., BAILEY, D., HARRIS, S. R., MCKINLEY, T. J., MERIC, G., BERRY, S. K., MASTROENI, P., SHEPPARD, S. K., CHRISTIE, G., THOMSON, N. R., PARKHILL, J., MASKELL, D. J. & GRANT, A. J. 2016. Genomic variations leading to alterations in cell morphology of Campylobacter spp. *Sci Rep,* 6**,** 38303.

FANG, X., YU, S. X., LU, Y., BAST, R. C., JR., WOODGETT, J. R. & MILLS, G. B. 2000. Phosphorylation and inactivation of glycogen synthase kinase 3 by protein kinase A. *Proc Natl Acad Sci U S A,* 97**,** 11960-5.

FEARON, E. R. 1995. Molecular genetics of colorectal cancer. *Ann N Y Acad Sci,* 768**,** 101-10.

FERLAY, J., SHIN, H. R., BRAY, F., FORMAN, D., MATHERS, C. & PARKIN, D. M. 2010. Estimates of worldwide burden of cancer in 2008: GLOBOCAN 2008. *Int J Cancer,* 127**,** 2893-917.

FLANAGAN, D. J., PHESSE, T. J., BARKER, N., SCHWAB, R. H., AMIN, N., MALATERRE, J., STANGE, D. E., NOWELL, C. J., CURRIE, S. A., SAW, J. T., BEUCHERT, E., RAMSAY, R. G., SANSOM, O. J., ERNST, M., CLEVERS, H. & VINCAN, E. 2015a. Frizzled7 functions as a Wnt receptor in intestinal epithelial Lgr5(+) stem cells. *Stem Cell Reports,* 4**,** 759-67.

FLANAGAN, P. K., CHIEWCHENGCHOL, D., WRIGHT, H. L., EDWARDS, S. W., ALSWIED, A., SATSANGI, J., SUBRAMANIAN, S., RHODES, J. M. & CAMPBELL, B. J. 2015b. Killing of Escherichia coli by Crohn's Disease Monocyte-derived Macrophages and Its Enhancement by Hydroxychloroquine and Vitamin D. *Inflamm Bowel Dis,* 21**,** 1499-510.

FLIS, S. & SPLWINSKI, J. 2009. Inhibitory effects of 5-fluorouracil and oxaliplatin on human colorectal cancer cell survival are synergistically enhanced by sulindac sulfide. *Anticancer Res,* 29**,** 435-41.

FODDE, R., KUIPERS, J., ROSENBERG, C., SMITS, R., KIELMAN, M., GASPAR, C., VAN ES, J. H., BREUKEL, C., WIEGANT, J., GILES, R. H. & CLEVERS, H. 2001. Mutations in the APC tumour suppressor gene cause chromosomal instability. *Nat Cell Biol,* 3**,** 433-8.

FREWER, K. A., SANDERS, A. J., OWEN, S., FREWER, N. C., HARGEST, R. & JIANG, W. G. 2013. A role for WISP2 in colorectal cancer cell invasion and motility. *Cancer Genomics Proteomics,* 10**,** 187-96.

GALAMB, O., KALMAR, A., PETERFIA, B., CSABAI, I., BODOR, A., RIBLI, D., KRENACS, T., PATAI, A.D., WICHMANN, B., BARTAK, B.K., TOTH, K., VALCZ, G., SPISAK, S., TULASSAY, Z. & MOLNAR, B. 2016. *Epigenetics*, 11, 588-602.

GELLAD, Z. F. & PROVENZALE, D. 2010. Colorectal cancer: national and international perspective on the burden of disease and public health impact. *Gastroenterology,* 138**,** 2177-90.

GEVERS, D., KUGATHASAN, S., DENSON, L. A., VAZQUEZ-BAEZA, Y., VAN TREUREN, W., REN, B., SCHWAGER, E., KNIGHTS, D., SONG, S. J., YASSOUR, M., MORGAN, X. C., KOSTIC, A. D., LUO, C., GONZALEZ, A., MCDONALD, D., HABERMAN, Y., WALTERS, T., BAKER, S., ROSH, J., STEPHENS, M., HEYMAN, M., MARKOWITZ, J., BALDASSANO, R., GRIFFITHS, A., SYLVESTER, F., MACK, D., KIM, S., CRANDALL, W., HYAMS, J., HUTTENHOWER, C., KNIGHT, R. & XAVIER, R. J. 2014. The treatment-naive microbiome in new-onset Crohn's disease. *Cell Host Microbe,* 15**,** 382-92.

GOH, T. K., ZHANG, Z. Y., CHEN, A. K., REUVENY, S., CHOOLANI, M., CHAN, J. K. & OH, S. K. 2013. Microcarrier culture for efficient expansion and osteogenic differentiation of human fetal mesenchymal stem cells. *Biores Open Access,* 2**,** 84-97.

GOODWIN, T. J., JESSUP, J. M. & WOLF, D. A. 1992. Morphologic differentiation of colon carcinoma cell lines HT-29 and HT-29KM in rotating-wall vessels. *In Vitro Cell Dev Biol,* 28A**,** 47-60.

GORYSHIN, I. Y., JENDRISAK, J., HOFFMAN, L. M., MEIS, R. & REZNIKOFF, W. S. 2000. Insertional transposon mutagenesis by electroporation of released Tn5 transposition complexes. *Nat Biotechnol,* 18**,** 97-100.

GRAY, S. G., AL-SARRAF, N., BAIRD, A. M., CATHCART, M. C., MCGOVERN, E. & O'BYRNE, K. J. 2009. Regulation of EP receptors in non-small cell lung cancer by epigenetic modifications. *Eur J Cancer,* 45**,** 3087-97.

GREER, J. B. & O'KEEFE, S. J. 2011. Microbial induction of immunity, inflammation, and cancer. *Front Physiol,* 1**,** 168.

GREGORIEFF, A. & CLEVERS, H. 2005. Wnt signaling in the intestinal epithelium: from endoderm to cancer. *Genes & Development,* 19**,** 877-890.

GUPTA, R. A. & DUBOIS, R. N. 2001. Colorectal cancer prevention and treatment by inhibition of cyclooxygenase-2. *Nat Rev Cancer,* 1**,** 11-21.

HALL, B., LIMAYE, A. & KULKARNI, A. B. 2009. Overview: generation of gene knockout mice. *Curr Protoc Cell Biol,* Chapter 19**,** Unit 19 12 19 12 1-17.

HAN, X., GENG, J., ZHANG, L. & LU, T. 2011. The role of Escherichia coli YrbB in the lethal action of quinolones. *J Antimicrob Chemother,* 66**,** 323-31.

HANAHAN, D. & WEINBER, R. A. 2011. Hallmarks of cancer: the next generation. *Cell*, 144, 646-74.

HANNEMANN, S., GAO, B. & GALAN, J. E. 2013. Salmonella modulation of host cell gene expression promotes its intracellular growth. *PLoS Pathog,* 9**,** e1003668.

HERBST-KRALOVETZ, M. M., RADTKE, A. L., LAY, M. K., HJELM, B. E., BOLICK, A. N., SARKER, S. S., ATMAR, R. L., KINGSLEY, D. H., ARNTZEN, C. J., ESTES, M. K. & NICKERSON, C. A. 2013. Lack of norovirus replication and histo-blood group antigen expression in 3-dimensional intestinal epithelial cells. *Emerg Infect Dis,* 19**,** 431-8.

HIRABAYASHI, K., YASUDA, M., KAJIWARA, H., ITOH, J., MIYAZAWA, M., HIRASAWA, T., MURAMATSU, T., MURAKAMI, M., MIKAMI, M. & OSAMURA, R. Y. 2008. Alterations in mucin expression in ovarian mucinous tumors: immunohistochemical analysis of MUC2, MUC5AC, MUC6, and CD10 expression. *Acta Histochem Cytochem,* 41**,** 15-21.

HIRATA, A., UTIKAL, J., YAMASHITA, S., AOKI, H., WATANABE, A., YAMAMOTO, T., OKANO, H., BARDEESY, N., KUNISADA, T., USHIJIMA, T., HARA, A., JAENISCH, R., HOCHEDLINGER, K. & YAMADA, Y. 2013. Dose-dependent roles for canonical Wnt signalling in de novo crypt formation and cell cycle properties of the colonic epithelium. *Development,* 140**,** 66-75.

HOESEL, B. & SCHMID, J. A. 2013. The complexity of NF-kappaB signaling in inflammation and cancer. *Mol Cancer,* 12**,** 86.

HOLD, G. L., SMITH, M., GRANGE, C., WATT, E. R., EL-OMAR, E. M. & MUKHOPADHYA, I. 2014. Role of the gut microbiota in inflammatory bowel disease pathogenesis: what have we learnt in the past 10 years? *World J Gastroenterol,* 20**,** 1192-210.

HOOPER, L. V. 2004. Bacterial contributions to mammalian gut development. *Trends Microbiol,* 12**,** 129-34.

HOOPER, L. V., XU, J., FALK, P. G., MIDTVEDT, T. & GORDON, J. I. 1999. A molecular sensor that allows a gut commensal to control its nutrient foundation in a competitive ecosystem. *Proc Natl Acad Sci U S A,* 96**,** 9833-8.

HOUSSEAU, F. & SEARS, C. L. 2010. Enterotoxigenic Bacteroides fragilis (ETBF)-mediated colitis in Min (Apc+/-) mice: a human commensal-based murine model of colon carcinogenesis. *Cell Cycle,* 9**,** 3-5.

HSU, H. C., LIU, Y. S., TSENG, K. C., TAN, B. C., CHEN, S. J. & CHEN, H. C. 2014. LGR5 regulates survival through mitochondria-mediated apoptosis and by targeting the Wnt/beta-catenin signaling pathway in colorectal cancer cells. *Cell Signal,* 26**,** 2333-42.

HULL, M. A., KO, S. C. & HAWCROFT, G. 2004. Prostaglandin EP receptors: targets for treatment and prevention of colorectal cancer? *Mol Cancer Ther,* 3**,** 1031-9.

INOUE, T., ANAI, S., ONISHI, S., MIYAKE, M., TANAKA, N., HIRAYAMA, A., FUJIMOTO, K. & HIRAO, Y. 2013. Inhibition of COX-2 expression by topical diclofenac enhanced radiation sensitivity via enhancement of TRAIL in human prostate adenocarcinoma xenograft model. *BMC Urol,* 13**,** 1.

IYER, S. S. & CHENG, G. 2012. Role of interleukin 10 transcriptional regulation in inflammation and autoimmune disease. *Crit Rev Immunol,* 32**,** 23-63.

JACKSTADT, R., SANSOM, O.J 2016. Mouse models of intestinal cancer. *J Pathol*, 238, 141-151.

JARRY, A., CREMET, L., CAROFF, N., BOU-HANNA, C., MUSSINI, J. M., REYNAUD, A., SERVIN, A. L., MOSNIER, J. F., LIEVIN-LE MOAL, V. & LABOISSE, C. L. 2014. Subversion of human intestinal mucosa innate immunity by a Crohn's disease-associated *E. coli*. *Mucosal Immunol*.

JESS, T., GAMBORG, M., MATZEN, P., MUNKHOLM, P. & SORENSEN, T. I. 2005. Increased risk of intestinal cancer in Crohn's disease: a meta-analysis of population-based cohort studies. *Am J Gastroenterol,* 100**,** 2724-9.

JESSUP, J. M., FRANTZ, M., SONMEZ-ALPAN, E., LOCKER, J., SKENA, K., WALLER, H., BATTLE, P., NACHMAN, A., WEBER, M., THOMAS, D., CURBEAM, R., JR., BAKER, T. & GOODWIN, T. 2000. Microgravity culture reduces apoptosis and increases the differentiation of a human colorectal carcinoma cell line. *In Vitro Cellular & Developmental Biology - Animal,* 36**,** 367-373.

JESSUP, J. M., GOODWIN, T. J. & SPAULDING, G. 1993. Prospects for use of microgravity-based bioreactors to study three-dimensional host-tumor interactions in human neoplasia. *J Cell Biochem,* 51**,** 290-300.

JHO, E.H., ZHANG, T., DOMON, C., JOO, C.K., FREUND, J.N. & COSTANTINI, F. 2002. Wnt/beta-catenin/Tcf signaling induces the transcription of Axin2, a negative regulator of the signaling pathway. *Mol Cell Biol*, 22, 1172-83.

JOHANSSON, M. E., PHILLIPSON, M., PETERSSON, J., VELCICH, A., HOLM, L. & HANSSON, G. C. 2008. The inner of the two Muc2 mucin-dependent mucus layers in colon is devoid of bacteria. *Proc Natl Acad Sci U S A,* 105**,** 15064-9.

KADO, S., UCHIDA, K., FUNABASHI, H., IWATA, S., NAGATA, Y., ANDO, M., ONOUE, M., MATSUOKA, Y., OHWAKI, M. & MOROTOMI, M. 2001. Intestinal microflora are necessary for development of spontaneous adenocarcinoma of the large intestine in T-cell receptor beta chain and p53 double-knockout mice. *Cancer Res,* 61**,** 2395-8.

KAEFFER, B., BENARD, C., LAHAYE, M., BLOTTIERE, H. M. & CHERBUT, C. 1999. Biological properties of ulvan, a new source of green seaweed sulfated polysaccharides, on cultured normal and cancerous colonic epithelial cells. *Planta Med,* 65**,** 527-31.

KAEFFER, B., TRUBUIL, A., KERVRANN, C., PARDINI, L. & CHERBUT, C. 2002. Three-dimensional binding of epidermal growth factor peptides in colonic tissues produced from rotating bioreactor. *In Vitro Cell Dev Biol Anim,* 38**,** 436-9.

KALER, P., AUGENLICHT, L. & KLAMPFER, L. 2012. Activating Mutations in β-Catenin in Colon Cancer Cells Alter Their Interaction with Macrophages; the Role of Snail. *PLoS ONE,* 7**,** e45462.

KAMADA, N., SEO, S. U., CHEN, G. Y. & NUNEZ, G. 2013. Role of the gut microbiota in immunity and inflammatory disease. *Nat Rev Immunol,* 13**,** 321-35.
KAPITANOVIC, S., CACEV, T., ANTICA, M., KRALJ, M., CAVRIC, G., PAVELIC, K. & SPAVENTI, R. 2006. Effect of indomethacin on E-cadherin and beta-catenin expression in HT-29 colon cancer cells. *Exp Mol Pathol,* 80**,** 91-6.
KARIM, B. O. & HUSO, D. L. 2013. Mouse models for colorectal cancer. *Am J Cancer Res,* 3**,** 240-50.
KARIN, M., LAWRENCE, T. & NIZET, V. 2006. Innate Immunity Gone Awry: Linking Microbial Infections to Chronic Inflammation and Cancer. *Cell,* 124**,** 823-835.
KARIN, M., YAMAMOTO, Y. & WANG, Q. M. 2004. The IKK NF-[kappa]B system: a treasure trove for drug development. *Nat Rev Drug Discov,* 3**,** 17-26.
KAUFMANN, S. H. & SCHAIBLE, U. E. 2005. Antigen presentation and recognition in bacterial infections. *Curr Opin Immunol,* 17**,** 79-87.
KAUR, J. & SANYAL, S. N. 2010. Modulation of inflammatory changes in early stages of colon cancer through activation of PPARgamma by diclofenac. *Eur J Cancer Prev,* 19**,** 319-27.
KAUR SAINI, M. & NATH SANYAL, S. 2010. Evaluation of chemopreventive response of two cycloxygenase-2 inhibitors, etoricoxib and diclofenac in rat colon cancer using FTIR and NMR spectroscopic techniques. *Nutr Hosp,* 25**,** 577-85.
KIM, K. Y., JEON, S. W., PARK, J. G., YU, C. H., JANG, S. Y., LEE, J. K. & HWANG, H. Y. 2014. Regression of Colonic Adenomas After Treatment With Sulindac in Familial Adenomatous Polyposis: A Case With a 2-Year Follow-up Without a Prophylactic Colectomy. *Ann Coloproctol,* 30**,** 201-4.
KIM, S. S., RUIZ, V. E., CARROLL, J. D. & MOSS, S. F. 2011. Helicobacter pylori in the pathogenesis of gastric cancer and gastric lymphoma. *Cancer Letters,* 305**,** 228-238.
KLEMENT, B. J., YOUNG, Q. M., GEORGE, B. J. & NOKKAEW, M. 2004. Skeletal tissue growth, differentiation and mineralization in the NASA rotating wall vessel. *Bone,* 34**,** 487-98.
KOBAYASHI, M., HONMA, T., MATSUDA, Y., SUZUKI, Y., NARISAWA, R., AJIOKA, Y. & ASAKURA, H. 2000. Nuclear translocation of beta-catenin in colorectal cancer. *Br J Cancer,* 82**,** 1689-93.
KUFE, D. W. 2009. Mucins in cancer: function, prognosis and therapy. *Nat Rev Cancer,* 9**,** 874-85.
KUHNERT, P., NICOLET, J. & FREY, J. 1995. Rapid and accurate identification of Escherichia coli K-12 strains. *Appl Environ Microbiol,* 61**,** 4135-9.
KUMAR, R. & SHIMIZU, K. 2010. Metabolic regulation of Escherichia coli and its gdhA, glnL, gltB, D mutants under different carbon and nitrogen limitations in the continuous culture. *Microb Cell Fact,* 9**,** 8.
LA FERLA, K., SEEGERT, D. & SCHREIBER, S. 2004. Activation of NF-kappaB in intestinal epithelial cells by *E. coli* strains isolated from the colonic mucosa of IBD patients. *Int J Colorectal Dis,* 19**,** 334-42.
LAFLAMME, N., LACROIX, S. & RIVEST, S. 1999. An essential role of interleukin-1beta in mediating NF-kappaB activity and COX-2 transcription in cells of the blood-brain barrier in response to a systemic and localized inflammation but not during endotoxemia. *J Neurosci,* 19**,** 10923-30.
LAGUINGE, L. M., LIN, S., SAMARA, R. N., SALESIOTIS, A. N. & JESSUP, J. M. 2004. Nitrosative stress in rotated three-dimensional colorectal carcinoma cell cultures induces microtubule depolymerization and apoptosis. *Cancer Res,* 64**,** 2643-8.
LAWRENCE, T. 2009. The nuclear factor NF-kappaB pathway in inflammation. *Cold Spring Harb Perspect Biol,* 1**,** a001651.
LE NEGRATE, G. 2012. Subversion of innate immune responses by bacterial hindrance of NF-kappaB pathway. *Cell Microbiol,* 14**,** 155-67.
LEE, S. H., LEE, S. J., KIM, J. H. & PARK, B. J. 2007. Chemical carcinogen, N-methyl-N'-nitro-N-nitrosoguanidine, is a specific activator of oncogenic Ras. *Cell Cycle,* 6**,** 1257-64.
LEE, S. H., NAM, J. K., PARK, J. K., LEE, J. H., MIN DO, S. & KUH, H. J. 2014. Differential protein expression and novel biomarkers related to 5-FU resistance in a 3D colorectal adenocarcinoma model. *Oncol Rep,* 32**,** 1427-34.

LEIBOVITZ, A., STINSON, J. C., MCCOMBS, W. B., 3RD, MCCOY, C. E., MAZUR, K. C. & MABRY, N. D. 1976. Classification of human colorectal adenocarcinoma cell lines. *Cancer Res,* 36**,** 4562-9.

LETEURTRE, E., ZERIMECH, F., PIESSEN, G., WACRENIER, A., LEROY, X., COPIN, M. C., MARIETTE, C., AUBERT, J. P., PORCHET, N. & BUISINE, M. P. 2006. Relationships between mucinous gastric carcinoma, MUC2 expression and survival. *World J Gastroenterol,* 12**,** 3324-31.

LEW, J. I., GUO, Y., KIM, R. K., VARGISH, L., MICHELASSI, F. & ARENAS, R. B. 2002. Reduction of intestinal neoplasia with adenomatous polyposis coli gene replacement and COX-2 inhibition is additive. *J Gastrointest Surg,* 6**,** 563-8.

LIAO, X., LOCHHEAD, P., NISHIHARA, R., MORIKAWA, T., KUCHIBA, A., YAMAUCHI, M., IMAMURA, Y., QIAN, Z. R., BABA, Y., SHIMA, K., SUN, R., NOSHO, K., MEYERHARDT, J. A., GIOVANNUCCI, E., FUCHS, C. S., CHAN, A. T. & OGINO, S. 2012. Aspirin use, tumor PIK3CA mutation, and colorectal-cancer survival. *N Engl J Med,* 367**,** 1596-606.

LIGGETT, J. L., CHOI, C. K., DONNELL, R. L., KIHM, K. D., KIM, J. S., MIN, K. W., NOEGEL, A. A. & BAEK, S. J. 2014. Nonsteroidal anti-inflammatory drug sulindac sulfide suppresses structural protein Nesprin-2 expression in colorectal cancer cells. *Biochim Biophys Acta,* 1840**,** 322-31.

LIU, X., LU, R., WU, S. & SUN, J. 2010. Salmonella regulation of intestinal stem cells through the Wnt/β-catenin pathway. *FEBS Letters,* 584**,** 911-916.

LU, J., YE, X., FAN, F., XIA, L., BHATTACHARYA, R., BELLISTER, S., TOZZI, F., SCEUSI, E., ZHOU, Y., TACHIBANA, I., MARU, D. M., HAWKE, D. H., RAK, J., MANI, S. A., ZWEIDLER-MCKAY, P. & ELLIS, L. M. 2013. Endothelial cells promote the colorectal cancer stem cell phenotype through a soluble form of Jagged-1. *Cancer Cell,* 23**,** 171-85.

LUCEY, B. P., NELSON-REES, W. A. & HUTCHINS, G. M. 2009. Henrietta Lacks, HeLa cells, and cell culture contamination. *Arch Pathol Lab Med,* 133**,** 1463-7.

LUO, F., BROOKS, D. G., YE, H., HAMOUDI, R., POULOGIANNIS, G., PATEK, C. E., WINTON, D. J. & ARENDS, M. J. 2009. Mutated K-ras(Asp12) promotes tumourigenesis in Apc(Min) mice more in the large than the small intestines, with synergistic effects between K-ras and Wnt pathways. *Int J Exp Pathol,* 90**,** 558-74.

LUO, J. L., MAEDA, S., HSU, L. C., YAGITA, H. & KARIN, M. 2004. Inhibition of NF-kappaB in cancer cells converts inflammation- induced tumor growth mediated by TNFalpha to TRAIL-mediated tumor regression. *Cancer Cell,* 6**,** 297-305.

LUPP, C., ROBERTSON, M. L., WICKHAM, M. E., SEKIROV, I., CHAMPION, O. L., GAYNOR, E. C. & FINLAY, B. B. 2007. Host-mediated inflammation disrupts the intestinal microbiota and promotes the overgrowth of Enterobacteriaceae. *Cell Host Microbe,* 2**,** 204.

LYSENKO, E. S., CLARKE, T. B., SHCHEPETOV, M., RATNER, A. J., ROPER, D. I., DOWSON, C. G. & WEISER, J. N. 2007. Nod1 signaling overcomes resistance of S. pneumoniae to opsonophagocytic killing. *PLoS Pathog,* 3**,** e118.

MACDONALD, B. T., TAMAI, K. & HE, X. 2009. Wnt/beta-catenin signaling: components, mechanisms, and diseases. *Dev Cell,* 17**,** 9-26.

MAGER, D. L. 2006. Bacteria and cancer: cause, coincidence or cure? A review. *Journal of Translational Medicine,* 4**,** 1-18.

MAGRONE, T. & JIRILLO, E. 2013. The interplay between the gut immune system and microbiota in health and disease: nutraceutical intervention for restoring intestinal homeostasis. *Curr Pharm Des,* 19**,** 1329-42.

MAOUCHE, R., BURGOS, H. L., MY, L., VIALA, J. P., GOURSE, R. L. & BOUVERET, E. 2016. Coexpression of Escherichia coli obgE, Encoding the Evolutionarily Conserved Obg GTPase, with Ribosomal Proteins L21 and L27. *J Bacteriol,* 198**,** 1857-67.

MARSHMAN, E., BOOTH, C. & POTTEN, C. S. 2002. The intestinal epithelial stem cell. *Bioessays,* 24**,** 91-8.

MARTIN, H. M., CAMPBELL, B. J., HART, C. A., MPOFU, C., NAYAR, M., SINGH, R., ENGLYST, H., WILLIAMS, H. F. & RHODES, J. M. 2004. Enhanced Escherichia coli adherence and invasion in Crohn's disease and colon cancer. *Gastroenterology,* 127**,** 80-93.

MARTORANA, A. M., MOTTA, S., DI SILVESTRE, D., FALCHI, F., DEHO, G., MAURI, P., SPERANDEO, P. & POLISSI, A. 2014. Dissecting Escherichia coli outer membrane biogenesis using differential proteomics. *PLoS One,* 9**,** e100941.

MAY, M. J. & GHOSH, S. 1997. Rel/NF-kappa B and I kappa B proteins: an overview. *Semin Cancer Biol,* 8**,** 63-73.

MCCARTY, K. S., JR., SZABO, E., FLOWERS, J. L., COX, E. B., LEIGHT, G. S., MILLER, L., KONRATH, J., SOPER, J. T., BUDWIT, D. A., CREASMAN, W. T. & *ET AL*. 1986. Use of a monoclonal anti-estrogen receptor antibody in the immunohistochemical evaluation of human tumors. *Cancer Res,* 46**,** 4244s-4248s.

MCDONALD, S. L. & SILVER, A. R. 2011. On target? Strategies and progress in the development of therapies for colorectal cancer targeted against WNT signalling. *Colorectal Dis,* 13**,** 360-9.

MCGOWIN, C. L., RADTKE, A. L., ABRAHAM, K., MARTIN, D. H. & HERBST-KRALOVETZ, M. 2013. Mycoplasma genitalium infection activates cellular host defense and inflammation pathways in a 3-dimensional human endocervical epithelial cell model. *J Infect Dis,* 207**,** 1857-68.

MCNALLY, A., OREN, Y., KELLY, D., PASCOE, B., DUNN, S., SREECHARAN, T., VEHKALA, M., VALIMAKI, N., PRENTICE, M. B., ASHOUR, A., AVRAM, O., PUPKO, T., DOBRINDT, U., LITERAK, I., GUENTHER, S., SCHAUFLER, K., WIELER, L. H., ZHIYONG, Z., SHEPPARD, S. K., MCINERNEY, J. O. & CORANDER, J. 2016. Combined Analysis of Variation in Core, Accessory and Regulatory Genome Regions Provides a Super-Resolution View into the Evolution of Bacterial Populations. *PLoS Genet,* 12**,** e1006280.

MELGAR, S., KARLSSON, A. & MICHAELSSON, E. 2005. Acute colitis induced by dextran sulfate sodium progresses to chronicity in C57BL/6 but not in BALB/c mice: correlation between symptoms and inflammation. *Am J Physiol Gastrointest Liver Physiol,* 288**,** G1328-38.

MENZEL, T., SCHAUBER, J., KRETH, F., KUDLICH, T., MELCHER, R., GOSTNER, A., SCHEPPACH, W. & LUHRS, H. 2002. Butyrate and aspirin in combination have an enhanced effect on apoptosis in human colorectal cancer cells. *Eur J Cancer Prev,* 11**,** 271-81.

MEREDITH, T. C. & WOODARD, R. W. 2005. Identification of GutQ from Escherichia coli as a D-arabinose 5-phosphate isomerase. *J Bacteriol,* 187**,** 6936-42.

MERLOS-SUÁREZ, A., BARRIGA, FRANCISCO M., JUNG, P., IGLESIAS, M., CÉSPEDES, MARÍA V., ROSSELL, D., SEVILLANO, M., HERNANDO-MOMBLONA, X., DA SILVA-DIZ, V., MUÑOZ, P., CLEVERS, H., SANCHO, E., MANGUES, R. & BATLLE, E. The Intestinal Stem Cell Signature Identifies Colorectal Cancer Stem Cells and Predicts Disease Relapse. *Cell Stem Cell,* 8**,** 511-524.

MIYOSHI, J., YAJIMA, T., SHIMAMURA, K., MATSUOKA, K., OKAMOTO, S., HIGUCHI, H., FUNAKOSHI, S., TAKAISHI, H. & HIBI, T. 2012. 5-aminosalicylic acid mediates expression of cyclooxygenase-2 and 15-hydroxyprostaglandin dehydrogenase to suppress colorectal tumorigenesis. *Anticancer Res,* 32**,** 1193-202.

MORGAN, X. C., TICKLE, T. L., SOKOL, H., GEVERS, D., DEVANEY, K. L., WARD, D. V., REYES, J. A., SHAH, S. A., LELEIKO, N., SNAPPER, S. B., BOUSVAROS, A., KORZENIK, J., SANDS, B. E., XAVIER, R. J. & HUTTENHOWER, C. 2012. Dysfunction of the intestinal microbiome in inflammatory bowel disease and treatment. *Genome Biol,* 13**,** R79.

MORIN, P. J., SPARKS, A. B., KORINEK, V., BARKER, N., CLEVERS, H., VOGELSTEIN, B. & KINZLER, K. W. 1997. Activation of β-Catenin-Tcf Signaling in Colon Cancer by Mutations in β-Catenin or APC. *Science,* 275**,** 1787-1790.

MPOFU, C. M., CAMPBELL, B. J., SUBRAMANIAN, S., MARSHALL-CLARKE, S., HART, C. A., CROSS, A., ROBERTS, C. L., MCGOLDRICK, A., EDWARDS, S. W. & RHODES, J. M. 2007. Microbial mannan inhibits bacterial killing by macrophages: a possible pathogenic mechanism for Crohn's disease. *Gastroenterology,* 133**,** 1487-98.

NAGALINGAM, N. A. & LYNCH, S. V. 2012. Role of the microbiota in inflammatory bowel diseases. *Inflamm Bowel Dis,* 18**,** 968-84.

NAKAMURA, T., KODAMA, N., ARAI, Y., KUMAMOTO, T., HIGUCHI, Y., CHAICHANTIPYUTH, C., ISHIKAWA, T., UENO, K. & YANO, S. 2009. Inhibitory effect of oxycoumarins isolated from the Thai medicinal plant Clausena guillauminii on the inflammation mediators, iNOS, TNF-alpha, and COX-2 expression in mouse macrophage RAW 264.7. *J Nat Med,* 63**,** 21-7.

NATHKE, I. S., ADAMS, C. L., POLAKIS, P., SELLIN, J. H. & NELSON, W. J. 1996. The adenomatous polyposis coli tumor suppressor protein localizes to plasma membrane sites involved in active cell migration. *J Cell Biol,* 134**,** 165-79.

NEWCOMB, P. A., NORFLEET, R. G., STORER, B. E., SURAWICZ, T. S. & MARCUS, P. M. 1992. Screening sigmoidoscopy and colorectal cancer mortality. *J Natl Cancer Inst,* 84**,** 1572-5.

NEWMAN, J. V., KOSAKA, T., SHEPPARD, B. J., FOX, J. G. & SCHAUER, D. B. 2001. Bacterial infection promotes colon tumorigenesis in Apc(Min/+) mice. *J Infect Dis,* 184**,** 227-30.

NG, K., MEYERHARDT, J. A., CHAN, A. T., SATO, K., CHAN, J. A., NIEDZWIECKI, D., SALTZ, L. B., MAYER, R. J., BENSON, A. B., 3RD, SCHAEFER, P. L., WHITTOM, R., HANTEL, A., GOLDBERG, R. M., VENOOK, A. P., OGINO, S., GIOVANNUCCI, E. L. & FUCHS, C. S. 2015. Aspirin and COX-2 inhibitor use in patients with stage III colon cancer. *J Natl Cancer Inst,* 107**,** 345.

NILSSON, L., MADSEN, K., TOPCU, S. O., JENSEN, B. L., FROKIAER, J. & NORREGAARD, R. 2012. Disruption of cyclooxygenase-2 prevents downregulation of cortical AQP2 and AQP3 in response to bilateral ureteral obstruction in the mouse. *Am J Physiol Renal Physiol,* 302**,** F1430-9.

NORAT, T., AUNE, D., CHAN, D. & ROMAGUERA, D. 2014. Fruits and vegetables: updating the epidemiologic evidence for the WCRF/AICR lifestyle recommendations for cancer prevention. *Cancer Treat Res,* 159**,** 35-50.

NORDGAARD, I., HOVE, H., CLAUSEN, M. R. & MORTENSEN, P. B. 1996. Colonic production of butyrate in patients with previous colonic cancer during long-term treatment with dietary fibre (Plantago ovata seeds). *Scand J Gastroenterol,* 31**,** 1011-20.

NOURSADEGHI, M., TSANG, J., HAUSTEIN, T., MILLER, R. F., CHAIN, B. M. & KATZ, D. R. 2008. Quantitative imaging assay for NF-kappaB nuclear translocation in primary human macrophages. *J Immunol Methods,* 329**,** 194-200.

OGINO, S., KIRKNER, G. J., NOSHO, K., IRAHARA, N., KURE, S., SHIMA, K., HAZRA, A., CHAN, A. T., DEHARI, R., GIOVANNUCCI, E. L. & FUCHS, C. S. 2008. Cyclooxygenase-2 expression is an independent predictor of poor prognosis in colon cancer. *Clin Cancer Res,* 14**,** 8221-7.

OGUMA, K., OSHIMA, H., AOKI, M., UCHIO, R., NAKA, K., NAKAMURA, S., HIRAO, A., SAYA, H., TAKETO, M. M. & OSHIMA, M. 2008. Activated macrophages promote Wnt signalling through tumour necrosis factor-alpha in gastric tumour cells. *EMBO J,* 27**,** 1671-81.

OGURA, Y., OGASAWARA, N., HARRY, E. J. & MORIYA, S. 2003. Increasing the ratio of Soj to Spo0J promotes replication initiation in Bacillus subtilis. *J Bacteriol,* 185**,** 6316-24.

OHMAN, U. 1982. Colorectal carcinoma in patients with ulcerative colitis. *Am J Surg,* 144**,** 344-9.

OKADA, K., MINEHIRA, M., ZHU, X., SUZUKI, K., NAKAGAWA, T., MATSUDA, H. & KAWAMUKAI, M. 1997. The ispB gene encoding octaprenyl diphosphate synthase is essential for growth of Escherichia coli. *J Bacteriol,* 179**,** 3058-60.

ONOUE, M., KADO, S., SAKAITANI, Y., UCHIDA, K. & MOROTOMI, M. 1997. Specific species of intestinal bacteria influence the induction of aberrant crypt foci by 1,2-dimethylhydrazine in rats. *Cancer Lett,* 113**,** 179-86.

OSHIMA, H. & OSHIMA, M. 2010. Mouse models of gastric tumors: Wnt activation and PGE2 induction. *Pathol Int,* 60**,** 599-607.

OUYANG, W., RUTZ, S., CRELLIN, N. K., VALDEZ, P. A. & HYMOWITZ, S. G. 2011. Regulation and functions of the IL-10 family of cytokines in inflammation and disease. *Annu Rev Immunol,* 29**,** 71-109.

PAIK, J., LEE, J. Y. & HWANG, D. 2002. Signaling pathways for TNFa-induced COX-2 expression: mediation through MAP kinases and NFkB, and inhibition by certain nonsteroidal anti-inflammatory drugs. *Adv Exp Med Biol,* 507**,** 503-8.

PARASKEVA, C., FINERTY, S. & POWELL, S. 1988. Immortalization of a human colorectal adenoma cell line by continuous in vitro passage: possible involvement of chromosome 1 in tumour progression. *Int J Cancer,* 41**,** 908-12.

PARASKEVA, C., HAGUE, A., ROONEY, N., WILLIAMS, A. C., HARPER, S. J., HANLON, K. A., ATKINSON, R. J. & CORFIELD, A. P. 1992. A single human colonic adenoma cell line can be converted in vitro to both a colorectal adenocarcinoma and a mucinous carcinoma. *Int J Cancer,* 51**,** 661-4.

PENNICA, D., SWANSON, T. A., WELSH, J. W., ROY, M. A., LAWRENCE, D. A., LEE, J., BRUSH, J., TANEYHILL, L. A., DEUEL, B., LEW, M., WATANABE, C., COHEN, R. L., MELHEM, M. F., FINLEY, G. G., QUIRKE, P., GODDARD, A. D., HILLAN, K. J., GURNEY, A. L., BOTSTEIN, D. & LEVINE, A. J. 1998. WISP genes are members of the connective tissue growth factor family that are up-regulated in wnt-1-transformed cells and aberrantly expressed in human colon tumors. *Proc Natl Acad Sci U S A,* 95**,** 14717-22.

PEREZ-CHANONA, E. & JOBIN, C. 2014. From promotion to management: the wide impact of bacteria on cancer and its treatment. *Bioessays,* 36**,** 658-64.

PEREZ-CUETO, F. J. & VERBEKE, W. 2012. Consumer implications of the WCRF's permanent update on colorectal cancer. *Meat Sci,* 90**,** 977-8.

PETERSON, D. A., FRANK, D. N., PACE, N. R. & GORDON, J. I. 2008. Metagenomic approaches for defining the pathogenesis of inflammatory bowel diseases. *Cell Host Microbe,* 3**,** 417-27.

PHESSE, T. J., BUCHERT, M., STUART, E., FLANAGAN, D. J., FAUX, M., AFSHAR-STERLE, S., WALKER, F., ZHANG, H. H., NOWELL, C. J., JORISSEN, R., TAN, C. W., HIROKAWA, Y., EISSMANN, M. F., POH, A. R., MALATERRE, J., PEARSON, H. B., KIRSCH, D. G., PROVERO, P., POLI, V., RAMSAY, R. G., SIEBER, O., BURGESS, A. W., HUSZAR, D., VINCAN, E. & ERNST, M. 2014. Partial inhibition of gp130-Jak-Stat3 signaling prevents Wnt-beta-catenin-mediated intestinal tumor growth and regeneration. *Sci Signal,* 7**,** ra92.

PHESSE, T.J., DURBAN, V.M. & SANSOM, O.J. 2017. Defining key concepts of intestinal and epithelial cancer biology through the use of mouse models. *Carcinogenesis*, bgx080.

PLUMBRIDGE, J. 2002. Regulation of gene expression in the PTS in Escherichia coli: the role and interactions of Mlc. *Curr Opin Microbiol,* 5**,** 187-93.

POLK, D. B. & PEEK, R. M. 2010. Helicobacter Pylori: gastric cancer and beyond. *Nat Rev Cancer,* 10**,** 593-593.

POTTEN, C. S. & LOEFFLER, M. 1990. Stem cells: attributes, cycles, spirals, pitfalls and uncertainties. Lessons for and from the crypt. *Development,* 110**,** 1001-20.

PRADERE, J. P., DAPITO, D. H. & SCHWABE, R. F. 2014. The Yin and Yang of Toll-like receptors in cancer. *Oncogene,* 33**,** 3485-95.

PROROK-HAMON, M., FRISWELL, M. K., ALSWIED, A., ROBERTS, C. L., SONG, F., FLANAGAN, P. K., KNIGHT, P., CODLING, C., MARCHESI, J. R., WINSTANLEY, C., HALL, N., RHODES, J. M. & CAMPBELL, B. J. 2014. Colonic mucosa-associated diffusely adherent afaC+ Escherichia coli expressing lpfA and pks are increased in inflammatory bowel disease and colon cancer. *Gut,* 63**,** 761-770.

PUGH, S. & THOMAS, G. A. 1994. Patients with adenomatous polyps and carcinomas have increased colonic mucosal prostaglandin E2. *Gut,* 35**,** 675-8.

PUTZE, J., HENNEQUIN, C., NOUGAYREDE, J. P., ZHANG, W., HOMBURG, S., KARCH, H., BRINGER, M. A., FAYOLLE, C., CARNIEL, E., RABSCH, W., OELSCHLAEGER, T. A., OSWALD, E., FORESTIER, C., HACKER, J. & DOBRINDT, U. 2009. Genetic structure and distribution of the colibactin genomic island among members of the family Enterobacteriaceae. *Infect Immun,* 77**,** 4696-703.

QASIM, B. J., ALI, H. H. & HUSSEIN, A. G. 2013. Immunohistochemical expression of matrix metalloproteinase-7 in human colorectal adenomas using specified automated cellular image analysis system: a clinicopathological study. *Saudi J Gastroenterol,* 19**,** 23-7.

QI, J. & ZHU, Y. Q. 2008. Targeting the most upstream site of Wnt signaling pathway provides a strategic advantage for therapy in colorectal cancer. *Curr Drug Targets,* 9**,** 548-57.

QIN, J., LI, R., RAES, J., ARUMUGAM, M., BURGDORF, K. S., MANICHANH, C., NIELSEN, T., PONS, N., LEVENEZ, F., YAMADA, T., MENDE, D. R., LI, J., XU, J., LI, S., LI, D., CAO, J., WANG, B., LIANG, H., ZHENG, H., XIE, Y., TAP, J., LEPAGE, P., BERTALAN, M., BATTO, J. M., HANSEN, T., LE PASLIER, D., LINNEBERG, A., NIELSEN, H. B., PELLETIER, E., RENAULT, P., SICHERITZ-PONTEN, T., TURNER, K., ZHU, H., YU, C., LI, S., JIAN, M., ZHOU, Y., LI, Y., ZHANG, X., LI, S., QIN, N., YANG, H., WANG, J., BRUNAK, S., DORE, J., GUARNER, F., KRISTIANSEN, K., PEDERSEN, O., PARKHILL, J., WEISSENBACH, J., META, H. I. T. C., BORK, P., EHRLICH, S. D. & WANG, J. 2010. A human gut microbial gene catalogue established by metagenomic sequencing. *Nature,* 464**,** 59-65.

RADTKE, A. L., WILSON, J. W., SARKER, S. & NICKERSON, C. A. 2010. Analysis of interactions of Salmonella type three secretion mutants with 3-D intestinal epithelial cells. *PLoS One,* 5**,** e15750.

RAHMAN, M. M. & MCFADDEN, G. 2011. Modulation of NF-kappaB signalling by microbial pathogens. *Nat Rev Microbiol,* 9**,** 291-306.

RAISCH, J., ROLHION, N., DUBOIS, A., DARFEUILLE-MICHAUD, A. & BRINGER, M. A. 2014. Intracellular colon cancer-associated Escherichia coli promote protumoral activities of human macrophages by inducing sustained COX-2 expression. *Lab Invest*.

RAISCH, J., ROLHION, N., DUBOIS, A., DARFEUILLE-MICHAUD, A. & BRINGER, M. A. 2015. Intracellular colon cancer-associated Escherichia coli promote protumoral activities of human macrophages by inducing sustained COX-2 expression. *Lab Invest,* 95**,** 296-307.

RAKOFF-NAHOUM, S. & MEDZHITOV, R. 2007. Regulation of spontaneous intestinal tumorigenesis through the adaptor protein MyD88. *Science,* 317**,** 124-7.

RAKOFF-NAHOUM, S. & MEDZHITOV, R. 2009. Toll-like receptors and cancer. *Nat Rev Cancer,* 9**,** 57-63.

RAWLS, J. F., MAHOWALD, M. A., LEY, R. E. & GORDON, J. I. 2006. Reciprocal gut microbiota transplants from zebrafish and mice to germ-free recipients reveal host habitat selection. *Cell,* 127**,** 423-33.

READER, J., HOLT, D. & FULTON, A. 2011. Prostaglandin E2 EP receptors as therapeutic targets in breast cancer. *Cancer Metastasis Rev,* 30**,** 449-63.

RECONDO, G. J., DIAZ-CANTON, E., DE LA VEGA, M., GRECO, M., RECONDO, G. S. & VALSECCHI, M. E. 2014. Advances and new perspectives in the treatment of metastatic colon cancer. *World J Gastrointest Oncol*, 6, 211-24.

RENZ, B. W., THASLER, W. E., PREISSLER, G., HEIDE, T., KHALIL, P. N., MIKHAILOV, M., JAUCH, K. W., KREIS, M. E., RENTSCH, M. & KLEESPIES, A. 2013. Clinical outcome of IBD-associated versus sporadic colorectal cancer: a matched-pair analysis. *J Gastrointest Surg,* 17**,** 981-90.

RHEE, K. J., WU, S., WU, X., HUSO, D. L., KARIM, B., FRANCO, A. A., RABIZADEH, S., GOLUB, J. E., MATHEWS, L. E., SHIN, J., SARTOR, R. B., GOLENBOCK, D., HAMAD, A. R., GAN, C. M., HOUSSEAU, F. & SEARS, C. L. 2009. Induction of persistent colitis by a human commensal, enterotoxigenic Bacteroides fragilis, in wild-type C57BL/6 mice. *Infect Immun,* 77**,** 1708-18.

RHODES, J. M. & CAMPBELL, B. J. 2002. Inflammation and colorectal cancer: IBD-associated and sporadic cancer compared. *Trends Mol Med,* 8**,** 10-6.

RIORDAN, J. T., TIETJEN, J. A., WALSH, C. W., GUSTAFSON, J. E. & WHITTAM, T. S. 2010. Inactivation of alternative sigma factor 54 (RpoN) leads to increased acid resistance, and alters locus of enterocyte effacement (LEE) expression in Escherichia coli O157 : H7. *Microbiology,* 156**,** 719-30.

RIZZARDI, A.E., JONSON, A.T., VOGEL, R.I., PAMBUCCIAN, S.E., HENRIKSEN, J., SKUBITZ, A.P.N., METZGER, G.J. & SCHMECHEL, S.C. 2012. Quantitative comparison of immunohistochemical staining measured by digital image analysis versus pathologist visual scoring. *Diag Pathol*, 7, 42.

ROBERTS, C. L., KEITA, A. V., DUNCAN, S. H., O'KENNEDY, N., SODERHOLM, J. D., RHODES, J. M. & CAMPBELL, B. J. 2010. Translocation of Crohn's disease Escherichia coli across M-cells: contrasting effects of soluble plant fibres and emulsifiers. *Gut,* 59**,** 1331-9.

ROBERTS, C. L., KEITA, A. V., PARSONS, B. N., PROROK-HAMON, M., KNIGHT, P., WINSTANLEY, C., N, O. K., SODERHOLM, J. D., RHODES, J. M. & CAMPBELL, B. J. 2013. Soluble plantain fibre blocks adhesion and M-cell translocation of intestinal pathogens. *J Nutr Biochem,* 24**,** 97-103.

ROCHETTE, P. J., BASTIEN, N., LAVOIE, J., GUERIN, S. L. & DROUIN, R. 2005. SW480, a p53 double-mutant cell line retains proficiency for some p53 functions. *J Mol Biol,* 352**,** 44-57.

ROGLER, G., BRAND, K., VOGL, D., PAGE, S., HOFMEISTER, R., ANDUS, T., KNUECHEL, R., BAEUERLE, P. A., SCHOLMERICH, J. & GROSS, V. 1998. Nuclear factor kappaB is activated in macrophages and epithelial cells of inflamed intestinal mucosa. *Gastroenterology,* 115**,** 357-69.

RUBINSTEIN, M. R., WANG, X., LIU, W., HAO, Y., CAI, G. & HAN, Y. W. 2013. Fusobacterium nucleatum promotes colorectal carcinogenesis by modulating E-cadherin/beta-catenin signaling via its FadA adhesin. *Cell Host Microbe,* 14**,** 195-206.

RUNDHAUG, J. E., SIMPER, M. S., SURH, I. & FISCHER, S. M. 2011. The role of the EP receptors for prostaglandin E2 in skin and skin cancer. *Cancer Metastasis Rev,* 30**,** 465-80.

RUTGEERTS, P., VAN ASSCHE, G., VERMEIRE, S., D'HAENS, G., BAERT, F., NOMAN, M., AERDEN, I., DE HERTOGH, G., GEBOES, K., HIELE, M., D'HOORE, A. & PENNINCKX, F. 2005. Ornidazole for prophylaxis of postoperative Crohn's disease recurrence: a randomized, double-blind, placebo-controlled trial. *Gastroenterology,* 128**,** 856-61.

SADOT, E., CONACCI-SORRELL, M., ZHURINSKY, J., SHNIZER, D., LANDO, Z., ZHARHARY, D., KAM, Z., BEN-ZE'EV, A. & GEIGER, B. 2002. Regulation of S33/S37 phosphorylated beta-catenin in normal and transformed cells. *J Cell Sci,* 115**,** 2771-80.

SAMUELS, Y., WANG, Z., BARDELLI, A., SILLIMAN, N., PTAK, J., SZABO, S., YAN, H., GAZDAR, A., POWELL, S. M., RIGGINS, G. J., WILLSON, J. K., MARKOWITZ, S., KINZLER, K. W., VOGELSTEIN, B. & VELCULESCU, V. E. 2004. High frequency of mutations of the PIK3CA gene in human cancers. *Science,* 304**,** 554.

SANDLER, R. S., HALABI, S., BARON, J. A., BUDINGER, S., PASKETT, E., KERESZTES, R., PETRELLI, N., PIPAS, J. M., KARP, D. D., LOPRINZI, C. L., STEINBACH, G. & SCHILSKY, R. 2003. A randomized trial of aspirin to prevent colorectal adenomas in patients with previous colorectal cancer. *N Engl J Med,* 348**,** 883-90.

SANSOM, O. J., REED, K. R., HAYES, A. J., IRELAND, H., BRINKMANN, H., NEWTON, I. P., BATLLE, E., SIMON-ASSMANN, P., CLEVERS, H., NATHKE, I. S., CLARKE, A. R. & WINTON, D. J. 2004. Loss of Apc in vivo immediately perturbs Wnt signaling, differentiation, and migration. *Genes Dev,* 18**,** 1385-90.

SANTIAGO, A., LI, D., ZHAO, L. Y., GODSEY, A. & LIAO, D. 2013. p53 SUMOylation promotes its nuclear export by facilitating its release from the nuclear export receptor CRM1. *Mol Biol Cell,* 24**,** 2739-52.

SAUD, S. M., YOUNG, M. R., JONES-HALL, Y. L., ILEVA, L., EVBUOMWAN, M. O., WISE, J., COLBURN, N. H., KIM, Y. S. & BOBE, G. 2013. Chemopreventive activity of plant flavonoid isorhamnetin in colorectal cancer is mediated by oncogenic Src and beta-catenin. *Cancer Res,* 73**,** 5473-84.

SAVKOVIC, S. D., KOUTSOURIS, A. & HECHT, G. 1997. Activation of NF-kappaB in intestinal epithelial cells by enteropathogenic Escherichia coli. *Am J Physiol,* 273**,** C1160-7.

SCHLAERMANN P., TOELLE B., BERGER H., SCHMIDT S. C., GLANEMANN M., ORDEMANN J., BARTFELD S., MOLLENKOPF H. J.& MEYER T.F. 2016. A novel human gastric primary cell culture system for modelling Helicobacter pylori infection in vitro. *Gut*. 65, 202-13.

SCHEIDEREIT, C. 2006. IkappaB kinase complexes: gateways to NF-kappaB activation and transcription. *Oncogene,* 25**,** 6685-705.

SCHMIEDERER, M., ARCENAS, R., WIDEN, R., VALKOV, N. & ANDERSON, B. 2001. Intracellular induction of the Bartonella henselae virB operon by human endothelial cells. *Infect Immun,* 69**,** 6495-502.

SCRIBANO, M. L. & PRANTERA, C. 2013. Use of antibiotics in the treatment of Crohn's disease. *World J Gastroenterol,* 19**,** 648-53.

SEEMANN, T. 2014. Prokka: rapid prokaryotic genome annotation. *Bioinformatics,* 30**,** 2068-9.

SERAFINO, A., MORONI, N., ZONFRILLO, M., ANDREOLA, F., MERCURI, L., NICOTERA, G., NUNZIATA, J., RICCI, R., ANTINORI, A., RASI, G. & PIERIMARCHI, P. 2014. WNT-pathway components as predictive markers useful for diagnosis, prevention and therapy in inflammatory bowel disease and sporadic colorectal cancer. *Oncotarget,* 5**,** 978-92.

SERMAN, L., MARTIC, T.N., SERMAN, A. & VRANIC, S. 2014. *Bosn J Basic Med Sci*, 14, 191-4.

SERVIN, A. L. 2005. Pathogenesis of Afa/Dr diffusely adhering Escherichia coli. *Clin Microbiol Rev,* 18**,** 264-92.

SHANAHAN, F. 2001. Inflammatory bowel disease: immunodiagnostics, immunotherapeutics, and ecotherapeutics. *Gastroenterology,* 120**,** 622-35.

SHEN, X. J., RAWLS, J. F., RANDALL, T., BURCAL, L., MPANDE, C. N., JENKINS, N., JOVOV, B., ABDO, Z., SANDLER, R. S. & KEKU, T. O. 2010. Molecular characterization of mucosal adherent bacteria and associations with colorectal adenomas. *Gut Microbes,* 1**,** 138-47.

SIEZEN, R. J. & KLEEREBEZEM, M. 2011. The human gut microbiome: are we our enterotypes? *Microb Biotechnol,* 4**,** 550-3.

SINGH, U. P., SINGH, N. P., SINGH, B., HOFSETH, L. J., PRICE, R. L., NAGARKATTI, M. & NAGARKATTI, P. S. 2010. Resveratrol (trans-3,5,4'-trihydroxystilbene) induces silent mating type information regulation-1 and down-regulates nuclear transcription factor-kappaB activation to abrogate dextran sulfate sodium-induced colitis. *J Pharmacol Exp Ther,* 332**,** 829-39.

SIRIWARDANA, P. N., PATHMESWARAN, A., HEWAVISENTHI, J. & DEEN, K. I. 2009. Histopathology reporting in colorectal cancer: a proforma improves quality. *Colorectal Dis,* 11**,** 849-53.

SOBHANI, I., TAP, J., ROUDOT-THORAVAL, F., ROPERCH, J. P., LETULLE, S., LANGELLA, P., CORTHIER, G., TRAN VAN NHIEU, J. & FURET, J. P. 2011. Microbial dysbiosis in colorectal cancer (CRC) patients. *PLoS One,* 6**,** e16393.

SONNENBURG, J. L., XU, J., LEIP, D. D., CHEN, C. H., WESTOVER, B. P., WEATHERFORD, J., BUHLER, J. D. & GORDON, J. I. 2005. Glycan foraging in vivo by an intestine-adapted bacterial symbiont. *Science,* 307**,** 1955-9.

SOTTORIVA, A., KANG, H., MA, Z., GRAHAM, T.A., SALOMON, M.P., ZHAO, J., MARJORAM, P., SIEGMNUD, K., PRESS, M., F., SHIBATA, D. & CURTIS, C. 2015. A Big Bang model of human colorectal tumor growth. *Nat Genet*, 47, 209-16.

SPERANDEO, P., POZZI, C., DEHO, G. & POLISSI, A. 2006. Non-essential KDO biosynthesis and new essential cell envelope biogenesis genes in the Escherichia coli yrbG-yhbG locus. *Res Microbiol,* 157**,** 547-58.

STAPPENBECK, T. S., HOOPER, L. V. & GORDON, J. I. 2002. Developmental regulation of intestinal angiogenesis by indigenous microbes via Paneth cells. *Proc Natl Acad Sci U S A,* 99**,** 15451-5.

SU, L. K., KINZLER, K. W., VOGELSTEIN, B., PREISINGER, A. C., MOSER, A. R., LUONGO, C., GOULD, K. A. & DOVE, W. F. 1992. Multiple intestinal neoplasia caused by a mutation in the murine homolog of the APC gene. *Science,* 256**,** 668-70.

SUBRAMANIAN, S., ROBERTS, C. L., HART, C. A., MARTIN, H. M., EDWARDS, S. W., RHODES, J. M. & CAMPBELL, B. J. 2008. Replication of Colonic Crohn's Disease Mucosal Escherichia coli Isolates within Macrophages and Their Susceptibility to Antibiotics. *Antimicrob Agents Chemother,* 52**,** 427-34.

SUNDARA RAJAN, S., HORGAN, K., SPEIRS, V. & HANBY, A. M. 2014. External validation of the ImmunoRatio image analysis application for ERalpha determination in breast cancer. *J Clin Pathol,* 67**,** 72-5.

SWIDSINSKI, A., KHILKIN, M., KERJASCHKI, D., SCHREIBER, S., ORTNER, M., WEBER, J. & LOCHS, H. 1998. Association between intraepithelial Escherichia coli and colorectal cancer. *Gastroenterology,* 115**,** 281-6.

SWIDSINSKI, A., LADHOFF, A., PERNTHALER, A., SWIDSINSKI, S., LOENING-BAUCKE, V., ORTNER, M., WEBER, J., HOFFMANN, U., SCHREIBER, S., DIETEL, M. & LOCHS, H. 2002. Mucosal flora in inflammatory bowel disease. *Gastroenterology,* 122**,** 44-54.

TAK, P. P. & FIRESTEIN, G. S. 2001. NF-κB: a key role in inflammatory diseases. *The Journal of Clinical Investigation,* 107**,** 7-11.

TAKIKITA, M., ALTEKRUSE, S., LYNCH, C. F., GOODMAN, M. T., HERNANDEZ, B. Y., GREEN, M., COZEN, W., COCKBURN, M., SIBUG SABER, M., TOPOR, M., ZERUTO, C., ABEDI-ARDEKANI, B., REICHMAN, M. E. & HEWITT, S. M. 2009. Associations between selected biomarkers and prognosis in a population-based pancreatic cancer tissue microarray. *Cancer Res,* 69**,** 2950-5.

TAO, L., ZHANG, J., MERANER, P., TOVAGLIERI, A., WU, X., GERHARD, R., ZHANG, X., STALLCUP, W.B., MIAO, J., HE, X., HURDLE, J.G., BREAULT, D.T., BRASS, A.L. & DONG, M. 2016. Frizzled proteins are colonic epithelial receptors for *C. difficile* toxin B. *Nature*, 538, 350-5.

TAWFIK, A., FLANAGAN, P. K. & CAMPBELL, B. J. 2014. Escherichia coli-host macrophage interactions in the pathogenesis of inflammatory bowel disease. *World J Gastroenterol,* 20**,** 8751-63.

THIERY, J. P., ACLOQUE, H., HUANG, R. Y. & NIETO, M. A. 2009. Epithelial-mesenchymal transitions in development and disease. *Cell,* 139**,** 871-90.

TOUGERON, D., SHA, D., MANTHRAVADI, S. & SINICROPE, F. A. 2014. Aspirin and colorectal cancer: back to the future. *Clin Cancer Res,* 20**,** 1087-94.

TRAVAGLIONE, S., FABBRI, A. & FIORENTINI, C. 2008. The Rho-activating CNF1 toxin from pathogenic *E. coli*: a risk factor for human cancer development? *Infect Agent Cancer,* 3**,** 4.

TSUCHIYA, S., YAMABE, M., YAMAGUCHI, Y., KOBAYASHI, Y., KONNO, T. & TADA, K. 1980. Establishment and characterization of a human acute monocytic leukemia cell line (THP-1). *Int J Cancer,* 26**,** 171-6.

TUOMINEN, V. J., RUOTOISTENMAKI, S., VIITANEN, A., JUMPPANEN, M. & ISOLA, J. 2010. ImmunoRatio: a publicly available web application for quantitative image analysis of estrogen receptor (ER), progesterone receptor (PR), and Ki-67. *Breast Cancer Res,* 12**,** R56.

TYE, H., KENNED, C.L., NAJDOVSKA, M., MCLEOD, L., MCCORMACK, W., HUGHES, N., DEV, A., SIEVERT, W., OOI, C.H., ISHIKAWA, T.O., OSHIMA, H., BHATHAL, P.S., PARKER, A.E., OSIMA, M., TAN, P. & JENKINS, B.J. 2012. STAT3-driven upregulation of TLR2 promotes gastric tumorigenesis independent of tumor inflammation. *Cancer Cell*, 22, 466-78.

URONIS, J. M., MUHLBAUER, M., HERFARTH, H. H., RUBINAS, T. C., JONES, G. S. & JOBIN, C. 2009. Modulation of the intestinal microbiota alters colitis-associated colorectal cancer susceptibility. *PLoS One,* 4**,** e6026.

URSELL, L. K., METCALF, J. L., PARFREY, L. W. & KNIGHT, R. 2012. Defining the human microbiome. *Nutr Rev,* 70 Suppl 1**,** S38-44.

VAN CUTSEM, E., OLIVEIRA, J. & GROUP, E. G. W. 2009a. Advanced colorectal cancer: ESMO clinical recommendations for diagnosis, treatment and follow-up. *Ann Oncol,* 20 Suppl 4**,** 61-3.

VAN CUTSEM, E., OLIVEIRA, J. & GROUP, E. G. W. 2009b. Primary colon cancer: ESMO clinical recommendations for diagnosis, adjuvant treatment and follow-up. *Ann Oncol,* 20 Suppl 4**,** 49-50.

VAN DE WETERING, M., SANCHO, E., VERWEIJ, C., DE LAU, W., OVING, I., HURLSTONE, A., VAN DER HORN, K., BATLLE, E., COUDREUSE, D., HARAMIS, A. P., TJON-PON-FONG, M., MOERER, P., VAN DEN BORN, M., SOETE, G., PALS, S., EILERS, M., MEDEMA, R. & CLEVERS, H. 2002. The beta-catenin/TCF-4 complex imposes a crypt progenitor phenotype on colorectal cancer cells. *Cell,* 111**,** 241-50.

VAN DER FLIER, L. G., SABATES–BELLVER, J., OVING, I., HAEGEBARTH, A., DE PALO, M., ANTI, M., VAN GIJN, M. E., SUIJKERBUIJK, S., VAN DE WETERING, M., MARRA, G. & CLEVERS, H. 2007. The Intestinal Wnt/TCF Signature. *Gastroenterology,* 132**,** 628-632.

VARGHESE, F., BUKHARI, A. B., MALHOTRA, R. & DE, A. 2014. IHC Profiler: an open source plugin for the quantitative evaluation and automated scoring of immunohistochemistry images of human tissue samples. *PLoS One,* 9**,** e96801.

VERDE, P., CASALINO, L., TALOTTA, F., YANIV, M. & WEITZMAN, J. B. 2007. Deciphering AP-1 function in tumorigenesis: fra-ternizing on target promoters. *Cell Cycle,* 6**,** 2633-9.

VIDYASEKAR, P., SHYAMSUNDER, P., ARUN, R., SANTHAKUMAR, R., KAPADIA, N. K., KUMAR, R. & VERMA, R. S. 2015. Genome Wide Expression Profiling of Cancer Cell Lines Cultured in Microgravity Reveals Significant Dysregulation of Cell Cycle and MicroRNA Gene Networks. *PLoS One,* 10**,** e0135958.

VILJOEN, K. S., DAKSHINAMURTHY, A., GOLDBERG, P. & BLACKBURN, J. M. 2015. Quantitative profiling of colorectal cancer-associated bacteria reveals associations between fusobacterium spp., enterotoxigenic Bacteroides fragilis (ETBF) and clinicopathological features of colorectal cancer. *PLoS One,* 10**,** e0119462.

VOGELSTEIN, B., FEARON, E. R., HAMILTON, S. R., KERN, S. E., PREISINGER, A. C., LEPPERT, M., NAKAMURA, Y., WHITE, R., SMITS, A. M. & BOS, J. L. 1988. Genetic alterations during colorectal-tumor development. *N Engl J Med,* 319**,** 525-32.

VORONKOV, A. & KRAUSS, S. 2013. Wnt/beta-catenin signaling and small molecule inhibitors. *Curr Pharm Des,* 19**,** 634-64.

WADA, C., IMAI, M. & YURA, T. 1987. Host control of plasmid replication: requirement for the sigma factor sigma 32 in transcription of mini-F replication initiator gene. *Proc Natl Acad Sci U S A,* 84**,** 8849-53.

WALDNER, M. J., WIRTZ, S., JEFREMOW, A., WARNTJEN, M., NEUFERT, C., ATREYA, R., BECKER, C., WEIGMANN, B., VIETH, M., ROSE-JOHN, S. & NEURATH, M. F. 2010. VEGF receptor signaling links inflammation and tumorigenesis in colitis-associated cancer. *J Exp Med,* 207**,** 2855-68.

WANG, H. M. & ZHANG, G. Y. 2005. Indomethacin suppresses growth of colon cancer via inhibition of angiogenesis in vivo. *World J Gastroenterol,* 11**,** 340-3.

WANG, P., ZHANG, L., JIANG, J. M., MA, D., TAO, H. X., YUAN, S. L., WANG, Y. C., WANG, L. C., LIANG, H., ZHANG, Z. S. & LIU, C. J. 2012a. Association of NOD1 and NOD2 genes polymorphisms with Helicobacter pylori related gastric cancer in a Chinese population. *World J Gastroenterol,* 18**,** 2112-20.

WANG, T., CAI, G., QIU, Y., FEI, N., ZHANG, M., PANG, X., JIA, W., CAI, S. & ZHAO, L. 2012b. Structural segregation of gut microbiota between colorectal cancer patients and healthy volunteers. *ISME J,* 6**,** 320-9.

WANG, X. & HARDWIDGE, P. R. 2012. Enterotoxigenic Escherichia coli prevents host NF-kappaB activation by targeting IkappaBalpha polyubiquitination. *Infect Immun,* 80**,** 4417-25.

WANG, X. & HUYCKE, M. M. 2007. Extracellular superoxide production by Enterococcus faecalis promotes chromosomal instability in mammalian cells. *Gastroenterology,* 132**,** 551-61.

WANG, X., YANG, Y., MOORE, D. R., NIMMO, S. L., LIGHTFOOT, S. A. & HUYCKE, M. M. 2012c. 4-hydroxy-2-nonenal mediates genotoxicity and bystander effects caused by Enterococcus faecalis-infected macrophages. *Gastroenterology,* 142**,** 543-551 e7.

WANG, Y., YAO, X., GE, J., HU, F. & ZHAO, Y. 2014. Can Vascular Endothelial Growth Factor and Microvessel Density Be Used as Prognostic Biomarkers for Colorectal Cancer? A Systematic Review and Meta-Analysis. *ScientificWorldJournal,* 2014**,** 102736.

WILLIAMS, A. C., HARPER, S. J. & PARASKEVA, C. 1990. Neoplastic transformation of a human colonic epithelial cell line: in vitro evidence for the adenoma to carcinoma sequence. *Cancer Res,* 50**,** 4724-30.

WILLIAMS, A. R., BALASOORIYA, B. A. & DAY, D. W. 1982. Polyps and cancer of the large bowel: a necropsy study in Liverpool. *Gut,* 23**,** 835-42.

WILLIAMS, C. S., GOLDMAN, A. P., SHENG, H., MORROW, J. D. & DUBOIS, R. N. 1999a. Sulindac sulfide, but not sulindac sulfone, inhibits colorectal cancer growth. *Neoplasia,* 1**,** 170-6.

WILLIAMS, C. S., MANN, M. & DUBOIS, R. N. 1999b. The role of cyclooxygenases in inflammation, cancer, and development. *Oncogene,* 18**,** 7908-16.

WILLIAMS, J. G., PULLAN, R. D., HILL, J., HORGAN, P. G., SALMO, E., BUCHANAN, G. N., RASHEED, S., MCGEE, S. G., HABOUBI, N., ASSOCIATION OF COLOPROCTOLOGY OF GREAT, B. & IRELAND 2013. Management of the malignant colorectal polyp: ACPGBI position statement. *Colorectal Dis,* 15 Suppl 2**,** 1-38.

WILLIAMS, J. M., DUCKWORTH, C. A., VOWELL, K., BURKITT, M. D. & PRITCHARD, D. M. 2016. Intestinal Preparation Techniques for Histological Analysis in the Mouse. *Curr Protoc Mouse Biol,* 6**,** 148-68.

WINAWER, S., FLETCHER, R., REX, D., BOND, J., BURT, R., FERRUCCI, J., GANIATS, T., LEVIN, T., WOOLF, S., JOHNSON, D., KIRK, L., LITIN, S., SIMMANG, C. & GASTROINTESTINAL CONSORTIUM, P. 2003. Colorectal cancer screening and surveillance: clinical guidelines and rationale-Update based on new evidence. *Gastroenterology,* 124**,** 544-60.

WINAWER, S. J., FLETCHER, R. H., MILLER, L., GODLEE, F., STOLAR, M. H., MULROW, C. D., WOOLF, S. H., GLICK, S. N., GANIATS, T. G., BOND, J. H., ROSEN, L., ZAPKA, J. G., OLSEN, S. J., GIARDIELLO, F. M., SISK, J. E., VAN ANTWERP, R., BROWN-DAVIS, C., MARCINIAK, D. A. & MAYER, R. J. 1997. Colorectal cancer screening: Clinical guidelines and rationale. *Gastroenterology,* 112**,** 594-642.

WIRTZ, S., NEUFERT, C., WEIGMANN, B. & NEURATH, M. F. 2007. Chemically induced mouse models of intestinal inflammation. *Nat Protoc,* 2**,** 541-6.

WU, G. D., CHEN, J., HOFFMANN, C., BITTINGER, K., CHEN, Y. Y., KEILBAUGH, S. A., BEWTRA, M., KNIGHTS, D., WALTERS, W. A., KNIGHT, R., SINHA, R., GILROY, E., GUPTA, K., BALDASSANO, R., NESSEL, L., LI, H., BUSHMAN, F. D. & LEWIS, J. D. 2011. Linking long-term dietary patterns with gut microbial enterotypes. *Science,* 334**,** 105-8.

WU, N., YANG, X., ZHANG, R., LI, J., XIAO, X., HU, Y., CHEN, Y., YANG, F., LU, N., WANG, Z., LUAN, C., LIU, Y., WANG, B., XIANG, C., WANG, Y., ZHAO, F., GAO, G. F., WANG, S., LI, L., ZHANG, H. & ZHU, B. 2013. Dysbiosis signature of fecal microbiota in colorectal cancer patients. *Microb Ecol,* 66**,** 462-70.

WU, S., MORIN, P. J., MAOUYO, D. & SEARS, C. L. 2003. Bacteroides fragilis enterotoxin induces c-Myc expression and cellular proliferation. *Gastroenterology,* 124**,** 392-400.

XU, M. H. & ZHANG, G. Y. 2005. Effect of indomethacin on cell cycle proteins in colon cancer cell lines. *World J Gastroenterol,* 11**,** 1693-6.

XU, Q., DONG, Q. G., SUN, L. P., HE, C. Y. & YUAN, Y. 2013. Expression of serum miR-20a-5p, let-7a, and miR-320a and their correlations with pepsinogen in atrophic gastritis and gastric cancer: a case-control study. *BMC Clin Pathol,* 13**,** 11.

YANG, J., ZHANG, W., EVANS, P. M., CHEN, X., HE, X. & LIU, C. 2006. Adenomatous polyposis coli (APC) differentially regulates beta-catenin phosphorylation and ubiquitination in colon cancer cells. *J Biol Chem,* 281**,** 17751-7.

YANG, V. W., SHIELDS, J. M., HAMILTON, S. R., SPANNHAKE, E. W., HUBBARD, W. C., HYLIND, L. M., ROBINSON, C. R. & GIARDIELLO, F. M. 1998. Size-dependent increase in prostanoid levels in adenomas of patients with familial adenomatous polyposis. *Cancer Res,* 58**,** 1750-3.

YEH, C. T., RAO, Y. K., YE, M., WU, W. S., CHANG, T. C., WANG, L. S., WU, C. H., WU, A. T. & TZENG, Y. M. 2012. Preclinical evaluation of destruxin B as a novel Wnt signaling target suppressing proliferation and metastasis of colorectal cancer using non-invasive bioluminescence imaging. *Toxicol Appl Pharmacol,* 261**,** 31-41.

YONEZAWA, S., GOTO, M., YAMADA, N., HIGASHI, M. & NOMOTO, M. 2008. Expression profiles of MUC1, MUC2, and MUC4 mucins in human neoplasms and their relationship with biological behavior. *Proteomics,* 8**,** 3329-41.

YOUNG, M., ORDONEZ, L. & CLARKE, A. R. 2013. What are the best routes to effectively model human colorectal cancer? *Mol Oncol,* 7**,** 178-89.

YRLID, U., SVENSSON, M., JOHANSSON, C. & WICK, M. J. 2000. Salmonella infection of bone marrow-derived macrophages and dendritic cells: influence on antigen presentation and initiating an immune response. *FEMS Immunol Med Microbiol,* 27**,** 313-20.

ZACKULAR, J. P., ROGERS, M. A., RUFFIN, M. T. T. & SCHLOSS, P. D. 2014. The Human Gut Microbiome as a Screening Tool for Colorectal Cancer. *Cancer Prev Res (Phila)*.

ZHANG, X. & HAO, J. 2015. Development of anticancer agents targeting the Wnt/beta-catenin signaling. *Am J Cancer Res*, 5, 2344-60.

ZHU, Q., JIN, Z., WU, W., GAO, R., GUO, B., GAO, Z., YANG, Y. & QIN, H. 2014. Analysis of the intestinal lumen microbiota in an animal model of colorectal cancer. *PLoS One,* 9**,** e90849.

Appendices

Appendix 1: Nuclear localisation analysis using ImageJ for DAPI/FITC Fluorescence

Prepare image channels

1. Download and open ImageJ software
2. Open image containing DAPI/FITC overlay
3. Split channels into red/green/blue channels: Image > Color > Split Channels. Channel images should now be in greyscale.
4. Retain blue (DAPI) and green (FITC) channels, discard red channel
5. Subtract background fluorescence for both image channels: Process > Subtract Background. Pixel radius of 50.0 used; ensure all tick options are not selected.

Define nuclear regions of interest (ROIs)

6. Duplicate the DAPI image: hover mouse over image > right click > Duplicate
7. Following background subtraction, use blue (DAPI) channel to define max/min greyscale thresholds: Image > Adjust > Thresholds. Image background will default to red; match DAPI-stained cell nuclei (grey) to those of the unaltered duplicate. Click 'Apply' and close Threshold adjuster.
8. Define nuclear regions of interest (ROIs): Edit > Selection > Create Mask
9. Remove mask outliers: Process > Noise > Remove Outliers. Pixel radius of 2.0, and threshold of 10 used to remove dark outliers.
10. Analyse mask particles: Analyze > Analyze Particles. For dark stained nuclei, use maximum pixel size minus 'Infinity' (250-Infinity), and include any measure of circularity (0.00-1.00); ensure 'Add to manager' option is ticked to add nuclear ROIs to 'ROI manager' (opens automatically). Image mask should now contain numbered nuclear ROIs corresponding to ROIs in ROI manager.

Define cytoplasmic region of interest

11. Duplicate the FITC image: hover mouse over image > right click > Duplicate
12. Threshold the FITC image: Image > Adjust > Thresholds. Image background will default to red; match FITC-staining (grey) to that of the unaltered duplicate. Click 'Apply' and close Threshold adjuster.
13. Define cytoplasmic region of interest (ROIs): Edit > Selection > Create Mask
14. Invert image mask: Edit > Invert. FITC staining should now be white.
15. Remove nuclear staining: Process > Image Calculator. Use this to add (Operation: Add) nuclear mask (Image 1: mask) to cytoplasmic mask (Image 2: mask). Create a new window for the mask result; any nuclear staining should have been removed in the new window.
16. Invert result: Edit > Invert. FITC staining should now be black with white background.
17. Select all cytoplasmic staining: Edit > Selection > Create Selection. This will outline all FITC staining in the cytoplasmic mask.
18. Add cytoplasmic ROI to manager: Edit > Selection > Add to Manager. Cytoplasmic ROI should have been added to the bottom of the ROI manager. Rename this ROI as 'Cytoplasmic'.

Quantify ROIs

19. Set required measurements: Analyze > Set Measurements. Set measurements to give a 'Mean gray value', plus any other measurement you may require (e.g. Standard deviation). Select to 'Display label' alongside you result to distinguish the cytoplasmic ROI. Do not redirect measurements (select 'None'). Select decimal places required. Click 'OK'.
20. Select the unaltered FITC image (duplicated in step 11).
21. Select all the ROIs from ROI manager ('Show all'). Nuclei and cytoplasm should be outlined.
22. Quantify staining within ROI Manager: More > Multi Measure. Deselect options for 'One Row Per Slice' and 'Append results'. Click 'OK'. Results table should appear automatically.

NOTE: If only one result appears, close this results tab. Highlight all ROIs (nuclear and cytoplasmic), deselect and then re-select ‘Show all’ and repeat step 22.

23. Copy measurements into an Excel file: Edit > Copy.
24. Save the quantified ROIs.

Analyse nuclear localisation

25. Average nuclear ROI data to get a mean nuclear stain.
26. Obtain a ratio for ‘nuclear:cytoplasmic’ staining by dividing your mean nuclear stain by the mean cytoplasmic stain (use result from defined ‘Cytoplasmic’ ROI).
27. Compare ratios between control and treated cells. Normalise to negative/untreated controls. Use an appropriate positive control.